NRSC REPORT

NATIONAL RADIO SYSTEMS COMMITTEE

NRSC-R13
AM Technical Assignment Criteria: An Examination of Issues Raised in MM Docket No. 87-267
June 17, 1988

NAB: 1771 N Street, N.W.
Washington, DC 20036
Tel: (202) 429-5356 Fax: (202) 775-4981

CEA: 1919 South Eads Street
Arlington, VA 22202
Tel: (703) 907-7660 Fax: (703) 907-8113

Co-sponsored by the Consumer Electronics Association and the National Association of Broadcasters
http://www.nrscstandards.org

NOTICE

NRSC Standards, Guidelines, Reports and other technical publications are designed to serve the public interest through eliminating misunderstandings between manufacturers and purchasers, facilitating interchangeability and improvement of products, and assisting the purchaser in selecting and obtaining with minimum delay the proper product for his particular need. Existence of such Standards, Guidelines, Reports and other technical publications shall not in any respect preclude any member or nonmember of the Consumer Electronics Association (CEA) or the National Association of Broadcasters (NAB) from manufacturing or selling products not conforming to such Standards, Guidelines, Reports and other technical publications, nor shall the existence of such Standards, Guidelines, Reports and other technical publications preclude their voluntary use by those other than CEA or NAB members, whether to be used either domestically or internationally.

Standards, Guidelines, Reports and other technical publications are adopted by the NRSC in accordance with the NRSC patent policy. By such action, CEA and NAB do not assume any liability to any patent owner, nor do they assume any obligation whatever to parties adopting the Standard, Guideline, Report or other technical publication.

This Guideline does not purport to address all safety problems associated with its use or all applicable regulatory requirements. It is the responsibility of the user of this Guideline to establish appropriate safety and health practices and to determine the applicability of regulatory limitations before its use.

Published by
CONSUMER ELECTRONICS ASSOCIATION
Technology & Standards Department
1919 S. Eads St.
Arlington, VA 22202

NATIONAL ASSOCIATION OF BROADCASTERS
Science and Technology Department
1771 N Street, NW
Washington, DC 20036

FOREWORD

NRSC-R13, AM Technical Assignment Criteria: An Examination of Issues Raised in MM Docket No. 87-267 ("Review of the Technical Assignment Criteria for the AM Broadcast Service"), was prepared for the National Association of Broadcasters and addresses four issues raised in Docket 87-267:

- Atmospheric and man-made noise;
- Minimum usable field strength;
- Adjacent-channel protection ratios;
- Root-Sum-Square (RSS) calculations and adjacent-channel skywave interference.

The NRSC is jointly sponsored by the Consumer Electronics Association and the National Association of Broadcasters. It serves as an industry-wide standards-setting body for technical aspects of terrestrial over-the-air radio broadcasting systems in the United States.

AM Technical Assignment Criteria

An Examination of Issues Raised in MM Docket No. 87–267

An AM Improvement Report
from the
National Association of Broadcasters

June 17, 1988

Harrison J. Klein, P.E.
Hammett & Edison, Inc.
Consulting Engineers
San Francisco, California

on behalf of the
AM Improvement Committee
Michael C. Rau, Staff Liaison
National Association of Broadcasters
1771 N Street, N.W.
Washington, DC 20036

NAB BROADCASTERS

AM Technical Assignment Criteria

An Examination of Issues Raised in MM Docket No. 87-267

HARRISON J. KLEIN, P.E.

TABLE OF CONTENTS

APPENDICES

FIGURES

AM Technical Assignment Criteria

An Examination of Issues Raised in MM Docket No. 87–267

HARRISON J. KLEIN, P.E.[1]

I. EXECUTIVE SUMMARY

This technical report addresses four issues in the FCC's Notice of Inquiry in MM Docket No. 87–267:

1. Atmospheric and man-made noise
2. Minimum usable field strength
3. Adjacent-channel protection ratios
4. RSS (root-sum-square) calculations and adjacent-channel skywave interference.

Here are the principal conclusions of this report:

1. Minimum usable field strength can vary widely depending on atmospheric and man-made noise environment and on required system performance. No single protected contour is appropriate for all circumstances. Differing requirements should be accommodated by the Commission's allocation scheme.
2. Existing protection ratios are entirely inadequate to prevent adjacent-channel interference, even with today's narrowband receivers. New protection ratios can be calculated that will reflect present and future technical parameters such as the National Radio Systems Committee (NRSC) audio standard.
3. The existing RSS calculation method using 50% exclusion results in unrealistic predictions of nighttime service and, over the years, has permitted widespread increases in interference. Use of a 25% exclusion method would more accurately portray nighttime service contours and would minimize future increases in interference.
4. The existing RSS calculation method produces correct estimates of total 10%-time interference even though the 10%-time values of the interferers are individually specified prior to calculating the RSS.
5. RSS calculations should include the effects of adjacent-channel skywave interference by weighting each RSS contributor by the appropriate protection ratio.

Finally, and most importantly, this report contains PC-compatible computer programs that permit an AM engineer to calculate the values of appropriate technical assignment criteria using user-supplied input parameters. Sample calculations are provided.

II. INTRODUCTION

This report, which was prepared on behalf of the National Association of Broadcasters (NAB), contains the results of a broad examination of AM technical assignment criteria. NAB's efforts were prompted by the August 17, 1987, release by the Federal Communications Commission of a Notice of Inquiry in MM Docket No. 87–267 ("Notice"). The Notice initiated a review of the many technical assignment criteria that collectively represent the technical framework for the AM broadcast service. Among the issues raised by the Commission are whether existing protected contours and protection ratios for the various classes of AM stations are appropriate in light of past and potential changes in transmission technology, AM receiver design, and listener habits. Related issues include the effects of atmospheric and man-made noise, and whether current FCC calculation methods adequately describe AM groundwave and skywave propagation and the effects of multiple interfering signals.

This report collects and analyzes available technical information and provides computer tools useful in developing recommendations for FCC action. The report considers the geographical dependence of atmospheric and man-made noise, and provides sources that contain estimates for their values. It analyzes each component required to determine the minimum usable field strength, E_{min}. It describes the factors that affect radio frequency protection ratios and describes the methods that have been developed to calculate protection ratios. The matters of RSS calculations and adjacent-channel skywave interference are thoroughly discussed; in particular, the report describes the proper method for calculating the effects of multiple interfering skywave signals.

Computer programs are provided for calculating E_{min}, adjacent-channel protection ratios, and signal-to-interference ratios for multiple skywave signals. The algorithms are explained in some detail and are available for the Commission and others to use in their deliberations.

A specific set of technical standards is not proposed by this report. Rather, interested parties are encouraged to use the information contained in this report to formulate suitable technical criteria they believe to be appropriate for the present and future AM broadcasting environment. This study was conducted because NAB wished to ensure that the Commission's technical standards are as accurate and objective as possible.

---

[1] Mr. Klein is with Hammett & Edison, Inc., Consulting Engineers, Box 280068, San Francisco, CA 94128-0068, (415) 342-5200.

III. ATMOSPHERIC AND MAN-MADE NOISE

The ambient noise level is a determining factor in the minimum usable field strength, E_{min}, which in turn is the basis for defining protected contours. A knowledge of the ambient atmospheric and man-made noise throughout the United States is essential to the development of more appropriate technical standards for the AM band. Stations must have an appropriate RF signal-to-noise ratio (SNR) in order to provide listeners with the quality of sound they demand.

A. Atmospheric Noise

Knowledge about atmospheric noise levels has improved significantly in the years since the present FCC allocation standards were developed. Extensive research has been conducted into the distribution of atmospheric noise throughout the world. The results are summarized in reports of the International Radio Consultative Committee (CCIR); the most recent is CCIR Report 322–3, "Characteristics and Applications of Atmospheric Radio Noise Data," which is dated 1986 and is included with this report as Appendix A. Report 322–3 is based principally on research performed by Spaulding and Washburn of the U.S. National Telecommunications and Information Administration [1].

Report 322–3 presents atmospheric noise data in the form of maps and graphs. Each map and its two associated graphs cover a specified season (winter, spring, summer, autumn) and four-hour time period (e.g., 0000–0400 local time). The map shows the expected value of atmospheric radio noise throughout the world, for a frequency of 1 MHz. Consistent with conventional technical discussions of noise, this report defines noise in terms of an effective antenna noise figure, F_a, and describes how F_a can be converted to an equivalent noise field strength in millivolts per meter. In the United States, F_{am}[2] ranges from a low of approximately 30 dB (Pacific Northwest, winter, 0800–1200) to a high of approximately 90 dB (Midwest, summer, 2000–2400).

One of the graphs associated with each map shows the variation of radio noise with frequency. Noise levels are highest at low frequencies and generally decrease with increasing frequency at the rate of approximately 30–70 dB per decade. Above about 30 MHz, atmospheric noise levels are beneath the level of galactic noise.

The other graph associated with each map shows, as a function of frequency, the remaining parameters necessary for a complete statistical description of the noise. V_d is the ratio, in dB, of the rms noise envelope voltage to the mean noise envelope voltage.[3] The higher the value of V_d, the more impulsive or "spiky" the noise. D_l and D_u are the lower and upper deciles, respectively, of the average noise power. The lower decile is the value exceeded for 90% of the hours within a time block; the upper decile is the value exceeded for 10% of the hours. D_l and D_u are measures of the deviation of F_a from its median value. The graph also shows the standard deviations of the various statistical quantities.

B. Man-made Noise

Man-made noise has become a much more serious allocation consideration as its level has increased due to the proliferation of power lines, industrial machinery, and noise-generating appliances, but less data is available on this topic than on atmospheric noise. CCIR Report 258–4, "Man-made Radio Noise," which is included with this report as Appendix B, includes a discussion of man-made noise based on work published in 1974 by Spaulding and Disney [2], but opinions differ on whether these levels are still valid.

Man-made noise is described using the same statistical quantities, such as F_{am}, as is atmospheric noise. Five "environmental categories" are defined in Report 258–4 corresponding to different values for F_{am}: galactic (as defined in Report 322–3), quiet rural, rural, residential, and business. Figure 1 of Report 258–4 shows that F_{am} for each category of noise varies linearly with the logarithm of the noise frequency.

To describe an environment that may better correspond to the increasing noise levels that have occurred over the last 15 years, this report defines a new environmental category called "intense," which is even noisier than the "business" category. "Intense" noise is equivalent to the noise level measured in the vicinity of power lines, which was reported in [2].

The next section of this report describes how the above statistical parameters of atmospheric or man-made noise, together with other transmission system parameters, are used to calculate E_{min}.

IV. MINIMUM USABLE FIELD STRENGTH

The minimum usable field strength, E_{min}, is defined as the field strength necessary to permit a desired reception quality, under specified receiving conditions, in the presence of natural and man-made noise.[4] If noise were constant, one could define reception quality simply as a certain signal-to-noise ratio, then add that value to the noise level to obtain E_{min} directly. But because the noise level is always changing, a technically accurate E_{min} must instead be evaluated statistically.

The report now describes how the concept of system performance is used to develop a method for calculating E_{min}. The statistical terms that define system performance are necessarily abstract. Readers without a theoretical background in probability and statistics should not expect to gain a thorough understanding of the concept of system performance from this report, but should become familiar with the basic terminology.

---

2 F_{am} is the median of the hourly values of F_a within a time block.

3 The graph shows V_{dm}, which is the median of V_d for the specified time-block.

4 A more complete definition can be found in [3].

A. The Components of System Performance

For the purposes of this report, E_{min} is the field strength necessary to achieve a desired system performance, where system performance is defined in Report 322–3 in terms of three independent component parts: grade of service, time availability, and service probability. The concept of system performance used here is consistent with that for other communications systems. Each component of system performance must be specified before E_{min} can be calculated.

1. Grade of service

"Grade of service" represents the short-term reception quality of the system. The purpose of defining grades of service, which are common in many communication systems, is to develop subjective descriptions of quality that correspond to particular objective technical specifications. For example, common grades of service for commercial telephony systems are "just usable," "marginally commercial," and "good commercial." Example II in Section 6.5 of Report 322–3 defines the "marginally commercial" grade of service for a double-sideband telephony system to be a median signal-to-noise ratio of 64 dB in a 1 Hz bandwidth.

"Marginally commercial" provides a better subjective description of reception quality than does the technical specification "a median signal-to-noise ratio of 64 dB in a 1 Hz bandwidth." Knowing, for example, that a 5 mV/m field strength is required to obtain a SNR of 64 dB in a 1 Hz bandwidth is of little practical benefit without also knowing the relationship between the technical specification and the subjective description.

The terms used to specify grade of service depend on the particular communication system, but all grades of service for statistical systems must include a measure of time in addition to one of signal quality. The above example did not explicitly include a reference to time, but use of the term "median signal-to-noise ratio" implies a time percentage of 50%. Example I in Section 6.4 of Report 322–3 describes a frequency shift keying system in which grade of service is specified by the probability of bit error which, for a given transmission rate, corresponds to a certain number of errors per unit time.

In a telephony system such as AM, the grade of service is specified by an instantaneous signal-to-noise ratio and the percentage of time that the SNR is achieved. Note that the specification refers to the instantaneous SNR. Even for noise with a constant rms level, the instantaneous noise envelope voltage is constantly changing. Grade of service refers to the percentage of time that the signal is above the instantaneous level of the constantly changing noise, for a certain rms noise level.

At this time there are no generally accepted definitions in the United States for AM broadcasting grades of service. An instantaneous signal-to-noise ratio and percentage of time must be specified before E_{min} can be calculated, but there has been no relationship developed in which a certain combination of SNR and time percentage corresponds to Grade A or best quality service, a lower SNR to a Grade B or lesser quality service, and so forth. With further research, a relationship could be developed analogous to the TASO grades for television pictures. In the absence of defined grades of service, values that appear reasonable must be chosen for instantaneous SNR and time percentage, but those values cannot now be related to known levels of listener satisfaction.

2. Time availability

In the above discussion concerning grade of service, the time specification refers to the percentage of time the signal is above the instantaneous noise envelope voltage, for noise of constant rms level. But the rms noise level itself also changes from hour to hour within each four-hour seasonal time period (e.g., summer, 2000-2400 local time) shown in Report 322–3. "Time availability" is the percentage of time throughout the specified time period that a given grade of service or better will be achieved.

3. Service probability

Each parameter that describes the statistical nature of the noise has an uncertainty, which is described by its standard deviation. "Service probability" is the statistical confidence factor, required for any statistical description, that combines these various uncertainties. It is the probability that a specified grade of service or better will be achieved for a specified time availability.

To aid in understanding the concept of service probability, consider an E_{min} calculation made using the data in Report 322–3 for a particular season and time period, grade of service, and time availability, and for a service probability of 50%. For a given path from transmitter to receiver, 50% service probability means that there is a 50% chance that this value of E_{min} will be sufficient to achieve the specified grade of service and time availability.

B. Calculation of E_{min} by Computer

To provide information that will be useful to anyone wishing to develop specific recommendations for E_{min}, a PC-compatible computer program was written that allows the user to specify any desired set of input conditions, which consist of atmospheric or man-made noise parameters, system performance requirements, frequency, bandwidth, and standard deviation of the expected received signal strength.[5] Appendix C contains further information about the algorithm and instructions for program operation.

Sample E_{min} calculations have been made and are shown in Figure 1. The figure is arranged in order of worsening noise. Each example is for an instantaneous signal-to-noise ratio of 26 dB. Although the time percentage for grade of service can be specified differently from the percentage of time availability, in the examples the two percentages are specified identically; the columns labeled 50%-time, 90%-time, and

[5] See Appendix C for a discussion of standard deviation of the expected received signal strength.

Figure 1

CALCULATED MINIMUM USABLE FIELD STRENGTH, E_{min}

Signal-to-noise ratio = 26 dB Frequency = 1 MHz Service probability = 50%

Noise Type	Location or Category	Season and Local Time	Calculated E_{min} (mV/m) 50%-time	90%-time	99%-time
Atmospheric	Pacific Northwest	Winter, 0800–1200	<0.005	<0.005	0.03
Man-made	Rural		0.04	0.35	2.02
Man-made	Residential		0.07	0.67	4.69
Man-made	Business		0.11	1.04	7.52
Atmospheric	Midwest	Summer, 2000–2400	0.18	2.12	24.9
Man-made	Intense		0.56	5.89	46.7

99%-time refer to both grade of service and time availability. Each example is for a service probability of 50%. The examples show the values of field strength that would be needed for the instantaneous signal-to-noise ratio to be at least 26 dB, for the indicated percentage of time and for the indicated percentage of hours within the CCIR seasonal time period, with a confidence factor of 50%.

The bandwidth was specified as 10,666 Hz for all calculations. 10,666 Hz is the effective RF bandwidth of a receiver meeting the NRSC deemphasis standard, assuming infinite attenuation outside the ±10,000 Hz receiver passband.[6] The standard deviation of the expected received signal strength was specified as 2 dB and the frequency was specified as 1 MHz for all calculations.

The specific program input parameters for the two atmospheric noise examples were determined from Report 322-3 as follows:

Pacific Northwest, Winter, 0800–1200

F_{am}:	30 dB	Standard deviation:	4.5 dB
V_{dm}:	4.1 dB	Standard deviation:	2.2 dB
D_u:	9.2 dB	Standard deviation:	5.2 dB

Midwest, Summer, 2000–2400

F_{am}:	90 dB	Standard deviation:	4.8 dB
V_{dm}:	5.7 dB	Standard deviation:	1.5 dB
D_u:	8.2 dB	Standard deviation:	2.8 dB.

For the four man-made noise environments, F_{am}, V_{dm}, and D_u were taken from [2], if available, and are built into the program. The user is not required to specify these parameters.

Two general observations can be drawn from the data in Figure 1. First, under some circumstances noise levels can be extremely low. During winter in the Pacific Northwest, the 50%-time and 90%-time values for E_{min} are less than 5 microvolts per meter. Even in a business noise environment, a field strength of 0.1 mV/m is sufficient to provide a 26 dB signal-to-noise ratio approximately 50% of the time. This indicates that reception of a quality some may consider acceptable can occur even in areas of relatively low signal strength, such as the fringe areas of the 0.1 mV/m protected contour of a Class I station. If such a signal is the only kind available, as it may be in rural areas with no local radio station, it may provide listeners with perfectly usable service.

On the other hand, Figure 1 shows that it takes a strong signal to yield high time availabilities, especially in urban areas. A field strength of 1 mV/m is needed in a business noise environment merely to get a 90%-time signal-to-noise ratio of 26 dB. For a better SNR, the field strength would have to be correspondingly higher. To obtain 99%-time reliability, even with a signal-to-noise ratio of only 26 dB, in most locations AM signals must have field strengths in the 2-25 mV/m range.

This section has demonstrated that the calculated values of minimum usable field strength can vary widely depending on atmospheric and man-made noise environment and on required system performance. Thus no single protected contour is appropriate for all circumstances. Differing requirements should be accommodated by the Commission's allocation scheme.

6 Effective bandwidth is the bandwidth of a hypothetical white noise signal (constant power density) that has the same total noise power as noise that has been weighted by the deemphasis characteristic. The effective audio bandwidth was obtained by numerically integrating the NRSC deemphasis curve from 0 Hz to 10,000 Hz, using Simpson's rule with a step size of 50 Hz. The effective RF bandwidth is twice the effective audio bandwidth.

V. ADJACENT-CHANNEL PROTECTION RATIOS

The development of more realistic co-channel and adjacent-channel protection ratios is probably the most important technical issue in the AM improvement proceeding. The protection ratios that underlie existing allocation standards are largely responsible for the interference situation on the AM band. This section describes the factors that affect the protection ratio and discusses how protection ratios can be calculated that will reflect present and future technical parameters.

A. Factors Affecting Protection Ratio

The RF protection ratio is defined[7] as the RF desired-to-undesired (D/U) ratio at the receiver input[8] that will provide the required audio signal-to-interference ratio at the receiver output. The RF protection ratio depends on diverse parameters such as channel spacing, modulation characteristics, transmitter and receiver characteristics, human hearing characteristics, and subjective listening preferences. In particular, it depends on a number of technical parameters that have changed since the present allocation system was implemented, or that the broadcast industry hopes will change in the future:

1. The bandwidths of the transmitter and receiver and the preemphasis and deemphasis characteristics of the system. The NRSC standards and wider-bandwidth receivers should form the basis for new protection ratios.
2. The spectral energy distribution of the modulation signal. The spectral content of modern programming differs greatly from that found decades ago.
3. The amount of compression and limiting. The effects of heavy processing should be taken into account.
4. The amplitude and frequency response of the human ear. As listeners have become accustomed to improved quality sound reproduction from other media, their subjective preferences may have changed, which would affect their perception of interference.

7 A more rigorous definition of both audio and RF protection ratios can be found in [3].

8 The term "at the receiver input" can mean different things depending on context. In FCC allocation standards the term refers to the ratio of field strengths at the receiving antenna, but in the context of measurement practice it refers to RF voltages at the receiver's antenna terminals. In allocation standards based on protection ratios determined by conventional measurement techniques, receiving antenna directivity is assumed to be negligible; this is a reasonable assumption given the random orientation of the antenna and the random spatial relationship between the desired and undesired stations.

B. Determination of Protection Ratios

Protection ratios can be determined in several ways [4]. The most accurate method, and the only method for co-channel ratios, is through subjective listening tests, wherein listeners evaluate reception quality under specified conditions of desired and undesired signals and receiver characteristics. The protection ratio is chosen based on an agreed-upon listener satisfaction level. The subjective method is extremely time-consuming because it involves many variables and many people.

It is possible to determine adjacent-channel protection ratios through subjective listening tests. However, if listening tests are first used to determine the co-channel protection ratio, then various objective methods can be used to derive the adjacent-channel protection ratio relative to that co-channel ratio [5]. This relative adjacent-channel protection ratio, A_{rel}, is defined in [4].

A_{rel} is a construct — it does not represent an actual D/U ratio at any frequency — but it is useful because it can be calculated objectively and then used to derive the actual adjacent-channel protection ratio, A. The following equivalent equations relate A_{rel} to A and to the co-channel protection ratio, A_O:

$$A_{rel} = A - A_O$$
$$A = A_O + A_{rel}.$$

For example, the existing AM allocation system is based on a co-channel protection ratio at the protected contour of 20:1, or 26 dB, which means that the desired signal must be 26 dB greater than the undesired signal. The adjacent-channel protection ratio at the protected contour is 1:1, or 0 dB. Therefore, for the first adjacent channel,

$$A_{rel} = A - A_O$$
$$= 0 - 26$$
$$= -26 \text{ dB}.$$

All of the objective methods for obtaining relative protection ratios involve defining the technical parameters that make up the transmitter and receiver response. "Transmitter response" refers to the overall transmitted energy spectrum. "Receiver response" refers to the overall receiving system, which includes human hearing characteristics. In principle, if all of these technical parameters that affect A_{rel} are properly defined, the objective methods should yield the same protection ratios as would be obtained subjectively.

NAB has retained B. Angell & Associates, Inc., of Chicago to conduct the subjective tests needed to determine the required co-channel protection ratio, A_O. This companion report is intended to provide the background and tools necessary for interested parties to calculate the relative adjacent-channel protection ratio, A_{rel}, for any desired transmission and reception parameters. From A_O and A_{rel}, recommended values for the actual adjacent-channel protection ratio, A, can be derived.

C. Objective Methods for Determining Protection Ratios

Of the several objective methods described in [5] for determining A_{rel}, the most accurate is the "objective measurement method," which uses RF generators as the desired and undesired signals, modulates them with noise that simulates program material of the desired level and character, detects them with a receiver of the proper characteristics, and measures the signal-to-noise ratio with a properly weighted noise meter. While the objective measurement method is accurate, and serves as a reference for the other methods that do not involve measurement, it is time-consuming and requires specialized test equipment. The test equipment must be modified if the transmission or reception parameters are changed, which makes it difficult to use the objective measurement method with hypothetical transmission systems.

Another of the objective methods in [5] for determining A_{rel} is called the "numerical method," which involves a computer calculation that takes into account each of the objective parameters that affect the adjacent-channel protection ratio. It permits immediate determination of A_{rel} for any transmitting and receiving system, existing or projected. The numerical method is especially useful in the development of allocation standards because it can take into account the characteristics of the NRSC system, including future NRSC receivers.

D. Calculation of Protection Ratios by Computer

The CCIR numerical method is based on work done in Germany by Gröschel. His paper, "A mathematical model for the calculation of the adjacent-channel interference in single-sideband and double-sideband AM sound broadcasting systems," which discusses the numerical method in detail, is included with this report as Appendix D. The paper describes a computer program that determines A_{rel} by means of numerical integration.[9] A copy of this program was obtained from the author. It was re-written to translate the German expressions, to make it PC-compatible, to permit specification of technical parameters such as the NRSC standards that are appropriate to domestic AM broadcasting, and to make it convenient for users to modify the program to specify different hypothetical parameters. Appendix E contains instructions for program operation.

The computer program permits interested users to evaluate relative adjacent-channel protection ratios under varying conditions and to make appropriate recommendations to the FCC. Sample calculations have been made and are shown in Figure 2. For ease of interpretation, the values of A_{rel} calculated by the computer have been converted to actual protection ratios using the existing FCC co-channel protection ratio, A_O, of 26 dB. Note that if A_O were some higher value such as 40 dB, the adjacent-channel protection ratios shown in Figure 2 would have to be increased by 14 dB. Thus the protection ratios shown in Figure 2 can be considered minimal. For comparison, Figure 2 also shows the protection ratios implicit in existing allocation standards.[10]

The following parameters were used for all sample protection ratio calculations:

Transmission mode:	DSB/ISB
Modulation spectrum:	USASI noise
Modulation factor:	1.00
Transmitter noise:	100.0 dB below carrier
Intermodulation attenuation:	40.0 dB
Psophometric curve:	CCIR–468
Out-of-band selectivity:	100.0 dB
Notch filter:	None.

The remaining parameters were varied according to the desired transmission and reception mode. The transmission mode "Pre-NRSC" refers to transmission conditions prior to the adoption by stations of the NRSC audio standard,[11] in which an audio processor is used that has a simple 50-microsecond preemphasis curve and does not have the NRSC low-pass filter. "NRSC" refers to transmission with the preemphasis curve and low-pass filter of the NRSC audio standard; the NRSC RF mask limits were used as the out-of-band radiation model only in Sections B and C of Figure 2. The "5400 Hz bandwidth" mode refers to transmission with a sharp-cutoff 5400 Hz audio low-pass filter and no preemphasis.

The reception mode "Current Radios" refers to typical AM radios that begin to roll off about 2000 Hz, are down 20 dB at 5 kHz, and are down 40 dB at 10 kHz. "Ideal NRSC" refers to a radio using NRSC deemphasis and the same "brick wall" filter characteristics as an NRSC transmitter. Since a filter this sharp is unlikely in commercial AM radio receivers, a "Realistic NRSC" receiver was defined having a less selective band-limiting filter with a 60 dB per octave slope beyond 10 kHz; even this filter characteristic may be overly optimistic.

The specific program setup conditions for the various transmission and reception modes were as follows:

Pre-NRSC

Band limiting:	Low-pass
Attenuation:	40 dB/kHz
Bandwidth:	14000 Hz
Preemphasis:	50 μs
Out-of-band radiation:	CCIR

9 Gröschel's original program was written in BASIC for Hewlett-Packard desktop computers.

10 FCC Rules do not specify a second-adjacent-channel protection ratio. A ratio of –29.5 dB is specified internationally in [6]. The contour overlap table in Section 73.37(a) of the FCC Rules, which prohibits overlap of the 2 mV/m and 25 mV/m field strength contours of stations with a frequency separation of 20 kHz, does not provide a 30 dB protection ratio at the 0.5 mV/m protected contour.

11 The term "NRSC audio standard" refers to NRSC Standard No. NRSC–1, EIA Interim Standard EIA/IS–40, "NRSC AM Preemphasis/Deemphasis and Broadcast Audio Transmission Bandwidth Specifications."

Figure 2

REQUIRED ADJACENT-CHANNEL PROTECTION RATIOS

for Co-channel Protection Ratio of 26 dB

Transmission Mode	Reception Mode	Adjacent-channel Protection Ratio (dB) First (10 kHz)	Second (20 kHz)
	A. Out-of-band radiation: CCIR model		
Pre-NRSC	Current radios	17	–8
NRSC	Current radios	14	–30
NRSC	"Ideal" NRSC	21	–28
NRSC	"Realistic" NRSC	24	–7
5400 Hz audio bandwidth	Current radios	0	–47
	B. Out-of-band radiation: NRSC RF mask test limits		
NRSC	Current radios	18	(+) 3
NRSC	"Ideal" NRSC	20	(+) 7
NRSC	"Realistic" NRSC	21	(+) 8
	C. Out-of-band radiation: NRSC RF mask maximum limits		
NRSC	Current radios	20	(+) 15
NRSC	"Ideal" NRSC	22	(+) 16
NRSC	"Realistic" NRSC	22	(+) 16
	EXISTING ALLOCATION STANDARDS	0	–30

NRSC

Band limiting:	NRSC
Preemphasis:	NRSC
Out-of-band radiation:	CCIR, NRSC TEST, or NRSC MAX as indicated

5400 Hz audio bandwidth

Band limiting:	Low-pass
Attenuation:	20 dB/kHz
Bandwidth:	5400 Hz
Preemphasis:	None
Out-of-band radiation:	CCIR

Current Radios

Band limiting:	Low-pass
Attenuation:	8 dB/kHz
Bandwidth:	2500 Hz
Deemphasis:	None

"Ideal" NRSC

Band limiting:	NRSC
Deemphasis:	NRSC

"Realistic" NRSC

Band limiting:	Low-pass
Attenuation:	6 dB/kHz
Bandwidth:	10000 Hz
Deemphasis:	NRSC.

To interpret Figure 2, note that a higher protection ratio requires a lower undesired signal to prevent interference. Said another way, a higher protection ratio implies that a given undesired signal level will cause more interference.

Consider first the data in Section A of Figure 2 for the CCIR out-of-band radiation model. For stations operating under pre-NRSC conditions, the data indicate that a 17 dB first-adjacent-channel protection ratio is required, even with existing narrowband radios. A 17 dB protection ratio means that, at a station's 0.5 mV/m protected contour, an undesired signal 10 kHz removed should be 17 dB below 0.5 mV/m.

However, under the existing 0 dB allocation standard, that undesired signal could be as strong as 0.5 mV/m — 17 dB greater than it should be to avoid interference.[12]

Implementation of the NRSC audio standard for transmission while using narrowband radios makes only a modest 3 dB improvement in the first-adjacent-channel protection ratio, from 17 dB to 14 dB. However, NRSC transmission makes a major 22 dB improvement at the second adjacent channel: from –8 dB to –30 dB. This is an indication of the benefits to second-adjacent-channel interference of the NRSC bandwidth specification.

As receivers begin to implement the NRSC audio standard, their wider bandwidths will require protection ratios to increase far above those in existence today if adjacent-channel interference is to be avoided. The combination of NRSC transmission and "realistic" NRSC reception requires a first-adjacent-channel protection ratio of 24 dB — only 2 dB less than the 26 dB co-channel ratio. One can conclude that even if the FCC were to immediately change its contour overlap rules for new facilities to reflect higher protection ratios, wider bandwidth receivers would continue to experience adjacent-channel interference at the 0.5 mV/m contour for many years unless vast numbers of stations ceased operation.

To highlight the protection limitations inherent in existing allocation standards, the program was used to determine the transmission bandwidth that would be required with current radios to yield a first-adjacent-channel protection ratio equal to the existing 0 dB. Even with narrowband receivers, AM stations would be required to transmit with 5400 Hz audio bandwidth to obtain 0 dB protection. This is a clear indication of the magnitude of AM's present difficulties.

Sections B and C of Figure 2 repeat the calculations of Section A for NRSC transmission, but reflect use of the NRSC RF mask test limits and maximum limits, respectively, instead of the CCIR model, as the out-of-band radiation subfunction. While the two NRSC RF mask curves result in modest changes in the required first-adjacent ratios, they result in dramatic increases of up to 45 dB in the second-adjacent ratios. A 15–16 dB protection ratio is required if the NRSC maximum limits are assumed, which is 45–46 dB greater than the –30 dB of existing allocation standards.

These gross protection ratio changes occur because the NRSC limits assume far greater energy in the 10–25 kHz frequency band than does the CCIR model. Gröschel's CCIR model, with an intermodulation attenuation of 40 dB, has energy in the 10–25 kHz frequency band ranging from -71.7 dB to –94.5 dB. The NRSC test limits in that band range from –25 dB to –43.4 dB, and the NRSC maximum limits range from –25 dB to –35 dB.

Both Gröschel's out-of-band radiation model and the NRSC RF mask are said to be based on measurements of actual high-power transmitters, yet they yield vastly different results. If the NRSC mask really does represent the spurious energy radiated from modern transmitters, these data raise serious second-adjacent-channel allocation concerns. However, it may be that the NRSC RF mask represents the worst-case envelope of measured or expected spurious components from any transmitter; each transmitter may not be expected to radiate spurious energy up to the RF mask limits at every frequency. If so, then use of the NRSC limits in the out-of-band radiation subfunction is overly pessimistic and the CCIR model may provide more realistic results. Further investigation is needed to determine which model is correct.

Regardless of which out-of-band radiation model is assumed, the protection ratios shown in Figure 2 demonstrate that, although the NRSC audio standard may make a dramatic improvement in AM frequency response, it will exacerbate adjacent-channel interference problems in weaker signal areas where the desired-to-undesired signal is low. In those areas, NRSC receivers will be required to contain selectable bandwidth or variable bandwidth circuitry to avoid interference. Figure 2 indicates that existing protection ratios are entirely inadequate to prevent adjacent-channel interference, even with today's narrowband receivers.

VI. RSS CALCULATIONS AND ADJACENT-CHANNEL SKYWAVE INTERFERENCE

The existing methods specified in the FCC Rules for the calculation of nighttime skywave interference ignore many signals that may contribute substantially to the interference environment. Over the years, the number of these signals has multiplied, making the true interference environment much worse than it is calculated to be. This section examines the two most significant problems with present interference calculation methods: the exclusion method used when calculating the RSS, and the omission of adjacent-channel skywave signals from interference consideration.

A. The RSS and the 50% Exclusion Method

The RSS, or root-sum-square, is intended to characterize the nighttime interference level of a station by combining the effects of all interfering signals into one net number. Because the various interfering signals arrive with random phase and modulation, the proper way to add them is on a power basis rather than on a voltage basis. The field strength voltage of each interfering signal is squared to obtain power, the squares are added, and the square root is taken to return to voltage. This root-sum-square voltage is multiplied by 20 to obtain the quantity conventionally known as the "RSS." Thus the RSS is the field strength that a desired signal must have to be 20 times, or 26 dB above, the interference level on the channel. Since 26 dB is the protection ratio, a station with a field strength at or above the RSS will provide interference-free service as it is now defined. Therefore, the value of the RSS is the limit of interference-free service; the RSS is also commonly known as the "limit."

It is impossible to add a new station to a channel without creating some additional interference to all the other stations

12 "To avoid interference" means only to prevent the weighted signal-to-interference ratio from becoming worse than 26 dB.

on that channel, although the amount of interference added to many of the stations may be extremely small. So if the FCC Rules specified that the RSS was to be calculated by taking into account every interfering signal, and if the Rules also prohibited, as they now do, any increase in the RSS,[13] then it would be impossible to add any new stations at all. To make it easier to add new stations, the FCC adopted the fiction that a new station will not increase the existing RSS unless the new station's interference contribution is at least 50% of the existing RSS or more than the smallest interference contribution already in the RSS. This is known as the "50% exclusion method."

B. Understatement of Interference and Overstatement of Coverage

The 50% exclusion method makes it possible to legally add a significant amount of new interference to an existing station, as long as it is done without raising this artificial measure of interference, the 50%-exclusion RSS. This has indeed occurred. Interference conditions are worse than they are calculated to be, and much worse than was expected some 50 years ago when the 50% exclusion method was adopted. Computer studies of several hundred AM stations have been made and were reported in [7] and [8]. Even though these studies did not take all interference contributions into account (only the ten greatest contributors were included), they showed that the 50% exclusion method understates the true interference level on a channel by more than 4 dB for some stations. The average understatement was approximately 2 dB.

In addition to allowing new interference to be created, the 50% exclusion method results in unrealistic predictions of nighttime service. As discussed above, the RSS is the limit of interference-free service. Nighttime service contours are defined as the field strength contour having the value of the calculated RSS. A station with a calculated RSS of, for example, 3.0 mV/m is considered to have interference-free service out to the 3.0 mV/m contour. If that station happens to be one for which the 50% exclusion method results in underestimation of interference by 4 dB, the station's true interference-free service would extend only to the smaller 4.8 mV/m contour. In a large metropolitan area, the population within those two contours could differ by many thousands of persons.

C. Alternative RSS Calculation Methods

Several ways have been suggested to produce a more realistic or otherwise "better" RSS. First, the exclusion concept could be retained but the calculation procedure changed. One alternative is the "n-highest contributor method," in which a certain number of stations, such as the four or eight greatest interference contributors, are included in the RSS and the rest excluded. Another alternative is to change the exclusion percentage to some smaller number such as 35%, 25%, or 15%. Both alternatives would tend to raise the calculated RSS closer to the actual interference level by including more stations. Both alternatives would reduce the amount of new interference that could be caused[14] but would retain some ability to add new stations or to improve existing ones.

Second, exclusion could be eliminated entirely, requiring all interference contributions to be included in the RSS calculation, but stations could be permitted to cause incremental increases in interference of 1 dB or perhaps some smaller amount. This option would retain some potential for new stations or facility improvements. The advantage of this option over an exclusion method is that it eliminates an inconsistency in the Rules. Under the 50% exclusion method, a new station can go on the air, or a station that is not now a contributor to another station's RSS can improve its facilities, and each is permitted to cause up to 1 dB of additional interference. However, a station that is already a contributor to another station's RSS is not permitted to raise that RSS at all, so it would be prevented from a facility improvement even if that improvement would also cause only a 1 dB interference increase. The second option would eliminate this inconsistency.

Third, exclusion could be eliminated while retaining the prohibition against increases in the RSS. As discussed above, this would prevent all further increases in interference, but would also prevent most new stations and most improvements in facilities.

D. Comparison of Alternatives

The ramifications of the first option, which is to modify the exclusion method, have been investigated in detail by Lahm and reported in [8]. He found that the n-highest contributor method was undesirable, even though it would more accurately represent the true interference levels on a channel, because of its inconsistent effects on the threshold of entry into the RSS from station to station and from channel to channel. The n-highest contributor method would yield substantial differences in the amount of new interference that a new or modified facility could cause, depending on the particular distribution of existing interference contributions on its channel.

Lahm found that a reduction in exclusion percentage provides better results. For 35% exclusion, the calculated RSS is increased by an average of 0.9 dB over that now calculated with 50% exclusion. For 25% exclusion and 15% exclusion the average increase is 1.5 dB and 1.8 dB, respectively; note that the magnitude of the increase decreases with decreasing exclusion levels. These increases in calculated RSS were found to be relatively consistent from station to

[13] FCC Rules generally prohibit a new facility from increasing the RSS of another station if that RSS is above the normally protected value.

[14] A new RSS contribution of 50% will increase the actual interference level by up to 1 dB. Contributions of 35%, 25%, and 15% correspond to increased interference values of up to approximately 0.5 dB, 0.25 dB, and 0.1 dB, respectively.

station and channel to channel. Furthermore, the threshold of entry into the RSS was also consistent. A decrease in exclusion percentage from 50% to 25% has a substantial effect on the calculated RSS and on the amount of new interference that can be caused, while a further decrease to 15% has only a small marginal effect. Lahm concluded that an exclusion percentage of 25% was reasonable and in keeping with the desire to better define the interference-free coverage and to protect stations from interference.

The second option, which is to eliminate exclusion while permitting any station to increase interference by a specified amount, appears to offer no significant advantages over a 25% exclusion method; indeed, it appears to offer no significant benefits at all. The proposal to permit 1 dB or even 0.5 dB of additional interference to be caused is little different from the present undesirable situation that has permitted the creation of substantial increased interference. It would actually be worse, because in eliminating the FCC rule inconsistency mentioned above, all stations would be permitted to increase interference, not just new stations or stations that do not now contribute to the calculated RSS.

Even if the amount of permissible interference for the second option were to be defined as 0.25 dB, the problem of potential abuse through multiple applications for 0.25 dB interference increases would still need to be solved. Further, when comparing the first option using an exclusion percentage of 25%, with the second option using a corresponding increased interference amount of 0.25 dB, the FCC rule inconsistency becomes immaterial. It would be very unlikely for an existing station to be prevented from making a desired change only because it cannot cause a 0.25 dB RSS increase; the protection requirements could easily be met through the choice of power or antenna pattern.

In support of the third option, which is to completely eliminate exclusion, it has been suggested that the AM band is mature and that interference protection is more important than new stations or improved facilities. While this may be an accurate assessment, the third option does present severe practical problems without offsetting benefits. It would be very burdensome to include *all* stations in the calculated RSS. There may be 50 or more stations on one channel in the U.S. alone. Those stations, foreign stations, and possibly adjacent-channel stations[15] would all have to be included. The task of data gathering and computation, even with modern computer data bases, would become monumental. Yet even the long-term incremental interference-protection benefits of the third option over those of a reduced exclusion percentage are on the order of only 1 dB. The third option is not attractive.

The above comparison supports Lahm's conclusion that the existing RSS exclusion principle be retained but the exclusion percentage reduced to 25%. Such a change in the RSS calculation method would make the RSS a more accurate indicator of true interference levels on a channel. Predictions of coverage would be more accurate, causing the calculated interference-free contour level for some stations to change as much as several dB.

E. Future Interference Levels

One should not be overly optimistic about the effect that a change in RSS calculation method would have on interference levels in the AM band. Changing the exclusion method would not change the actual level of nighttime interference, it would change only the calculated level. No stations would be required to cause less interference if the exclusion method were changed. At best, an improved exclusion method can only prevent or reduce future increases in interference. Therefore, in evaluating the impact on interference of a new exclusion method, the important question is: how much does the actual interference level that could eventually exist differ from what now exists?

Consider a hypothetical Station A on a channel with 15 other nighttime signals. Station A's actual nighttime interference level, represented by its total RSS of 5.00 mV/m, is made up of contributions from all 15 of those signals. However, the present 50%-exclusion RSS of 3.50 mV/m understates that interference by about 3 dB. With 50% exclusion, a new interference contribution of 1.74 mV/m could be added, which would increase the total RSS to 5.29 mV/m, an increase of 0.49 dB. With 25% exclusion, a new interference contribution of 0.87 mV/m could be added, which would increase the total RSS to 5.08 mV/m, an increase of 0.14 dB. If exclusion were eliminated entirely, no increase would be possible, of course.

In this example, changing from 50% to 25% exclusion would make only a 0.35 dB difference in the amount of actual new interference that could be created by a new station. Eliminating exclusion entirely would make less than 0.5 dB difference. The small differences are a result of the maturity of the AM band, which has many stations per channel and significantly understated interference levels.

Although Station A was a hypothetical example, it is not unrepresentative. A computer study of many stations could be performed to better characterize the actual differences in effect between the various exclusion method alternatives. Even without such a study it is clear that, due to the maturity of the AM band, a change in RSS calculation method is unlikely to have a major impact on future interference. The effect on interference-free contour accuracy is much more significant.

F. The Effect of Multiple 10% Interferers

The existing RSS calculation method combines the 10%-time field strengths of all interfering signals to determine the total interference level. It might appear that the calculation procedure assumes "worst case" conditions; each interferer is assumed to be continuously present even though the 10%-time interference level is used in the calculation. Perhaps the present calculation method yields artificially high estimates of interference under multiple-interferer conditions. This section of the report demonstrates that the existing RSS calculation

15 See the discussion of adjacent-channel skywave interference in Section VI–G of this report.

method is indeed a proper procedure for combining multiple 10% interferers.

Section 73.182(l) of the FCC Rules defines interference to exist when the skywave field strength of an undesired station, or the RSS interference level of two or more stations, exceeds specified levels for 10% or more of the time. In other words, the total interference, as defined in theory, is considered to be the 10%-time value of the RSS combination of the individual interferers.

The definition differs from the following procedure which is used, in practice, to calculate the total interference:

1. The 10%-time field strength of each interfering signal is determined using the curves and formulas in Figures 1a, 1b, or 2, as appropriate, of Section 73.190
2. The individual 10%-time field strengths are combined in the RSS formula.

In other words, the total interference, as calculated in practice, is considered to be the RSS combination of the 10%-time values of the individual interferers.

Thus for the results of interference calculations to be correct, the 10%-time value of the RSS combination of the interferers must be equal to the RSS combination of the 10%-time values of the interferers. This equivalence is not intuitively obvious. However, its validity is demonstrated in the paper by Anderson, "Signal-to-Interference Ratio Statistics for AM Broadcast Groundwave and Skywave Signals in the Presence of Multiple Skywave Interferers," which is attached as Appendix F. Anderson's paper, prepared for inclusion in this report, directly addresses the issue of interference from multiple interferers. He has also provided a computer program, SKYIN, described in Appendix G, which permits interested users to perform their own calculations.

Anderson analyzes multiple interferers statistically, explicitly taking into account the continuous voltage variation of each one. In Section 7.0 of his paper he demonstrates that, regardless of the number or amplitude of the multiple interferers, the effect of the sum of the interferers on the signal-to-interference ratio is the same as the effect of a single interferer with equivalent power. Therefore, the existing RSS calculation method produces correct estimates of total 10%-time interference even though the 10%-time values of the interferers are individually specified prior to calculating the RSS.

G. Adjacent-channel Skywave Interference

It is apparent from Section V of this report that first-adjacent-channel signals can produce significant amounts of interference. Yet the FCC Rules provide no interference protection from nighttime adjacent-channel skywave interference. It is likely that much of the increased nighttime interference on the AM band over the last 40 years is due to adjacent-channel skywave signals.

Two approaches have been suggested for treating adjacent-channel skywave signals. In the Notice, the Commission suggests that one alternative would be to amend Section 73.182(n) of the Rules to require inclusion of skywave signals in the calculation of the adjacent-channel RSS.[16] While this alternative would result in accounting for adjacent-channel skywave interference in allocation studies, it would be a cumbersome method of achieving that desirable end. It would require additional time-consuming calculations, calculations that are not now normally required because, as described below, Section 73.182(n) is not pertinent to most nighttime allocation situations.

A station's protected daytime contour, which is generally the 0.5 mV/m contour, is usually more extensive than its protected nighttime contour. Therefore, the prohibition against daytime 0.5 mV/m contour overlap of adjacent-channel stations results in the two stations being so far apart that there is seldom any calculated adjacent-channel groundwave interference at night. If skywave signals were required to be included in the RSS calculations of nighttime adjacent-channel interference specified by Section 73.182(n), new RSS calculations would be required at numerous points along the protected contour.

The Commission's other suggested alternative, which is to include adjacent-channel skywave signals in conventional RSS calculations, would be a far better way to take account of adjacent-channel interference in allocation studies. A typical nighttime allocation study consists of RSS limit calculations for the pertinent stations on the proposed channel, with a showing that the proposed operation would not enter any RSS that is above the normally protected value. This showing is included in the application for construction permit.

Most RSS calculations are now done by computer. The co-channel stations to be included in the study are selected, the computer calculates the skywave field strengths of each station at each chosen site, and the RSS at each site is computed using the 50% exclusion rule. It would be a relatively simple task to include adjacent-channel stations in the study and to redefine the RSS formula to include adjacent-channel skywave signals weighted by the appropriate protection ratio. The application showings now required could be retained, but with the inclusion of adjacent-channel data. Substantial additional engineering time would not be required.

Inclusion of adjacent-channel skywave signals in the RSS would be in accordance with the CCIR methods in [9] and with procedures specified in the 1982 Region 2 Agreement [10]. Each specifies a formula for usable field strength which includes weighted adjacent-channel signals in an RSS calculation.

ACKNOWLEDGEMENTS

In addition to the funding provided by the National Association of Broadcasters, Hammett & Edison provided

16 Section 73.182(n) now specifies the inclusion of only groundwave signals in the calculation of the RSS value of undesired adjacent-channel field strengths.

significant resources of its own toward the completion of this report. The author is grateful for the firm's generous support.

Several individuals made substantial contributions to this report. Robert P. Smith, Jr., of Hammett & Edison developed the user-friendly ADJACENT programs from Gröschel's original work. Robert Orban of Orban Associates, Inc., San Francisco, supplied the design of the NRSC filter used in the computer programs. Bronwen L. Jones, consultant, helped in the evaluation of alternative psophometric curves. Richard A. Kennedy and James T. Gotshall of Delco Electronics Corporation helped to interpret adjacent-channel protection ratio data and supplied information about future NRSC receiver parameters. Karl D. Lahm, P.E., of Karl D. Lahm & Associates, Inc., Fairfax, Virginia, provided helpful insight on RSS issues.

Special thanks go to Harry R. Anderson, P.E., of H. R. Anderson & Associates, Inc., Eugene, Oregon. Mr. Anderson wrote computer programs EMIN and SKYIN and the paper of Appendix F. He was also instrumental in the preparation of the text sections on atmospheric and man-made noise, minimum usable field strength, and the effects of multiple 10% interferers. His knowledge of communications engineering principles, and his patient answers to innumerable questions, were greatly appreciated.

REFERENCES

[1] Spaulding, A.D. and Washburn, J.S.: "Atmospheric Radio Noise: Worldwide Levels and Other Characteristics." U.S. Department of Commerce, National Telecommunications and Information Administration Report 85–173, April 1985.

[2] Spaulding, A.D. and Disney, R.T.: "Man-made Radio Noise. Part I — Estimates for Business, Residential and Rural Areas." U.S. Department of Commerce, Office of Telecommunications Report 74–38, June 1974.

[3] "Terms and Definitions Used in Frequency Planning for Sound Broadcasting." CCIR Recommendation 638, XVIth Plenary Assembly, Dubrovnik 1986.

[4] "Radio-frequency Protection Ratios in LF, MF and HF Broadcasting." CCIR Recommendation 560–2, XVIth Plenary Assembly, Dubrovnik 1986.

[5] "Objective Measurement of Radio-frequency Protection Ratios in LF, MF and HF Broadcasting." CCIR Recommendation 559–1, XVIth Plenary Assembly, Dubrovnik 1986.

[6] "Final Acts of The Regional Administrative Broadcasting Conference (Region 2)." Rio de Janeiro 1981, Annex 2, Section 4.9.2.

[7] Dahlberg, E. and Everist, D.G.: "Investigate Alternate Method(s) of Determining Nighttime Groundwave Limits in the Presence of More Than One Interfering Groundwave Signal." Memorandum to Technical Subgroup of Radio Advisory Committee, October 14, 1987.

[8] Comments of Karl D. Lahm, P.E., in MM Docket No. 87–267, February 1, 1988.

[9] "Methods for the Assessment of Multiple Interference." CCIR Report 945–1, XVIth Plenary Assembly, Dubrovnik 1986.

[10] "Final Acts ... ," *op.cit.*, Annex 2, Section 4.7.1.

Appendix A

"Characteristics and Applications of Atmospheric Radio Noise Data." CCIR Report 322–3, XVIth Plenary Assembly, Dubrovnik 1986.

RAPPORT 322-3 | REPORT 322-3 | INFORME 322-3

CCIR

COMITÉ CONSULTATIF INTERNATIONAL DES RADIOCOMMUNICATIO
INTERNATIONAL RADIO CONSULTATIVE COMMITTEE
COMITÉ CONSULTIVO INTERNACIONAL DE RADIOCOMUNICACIO

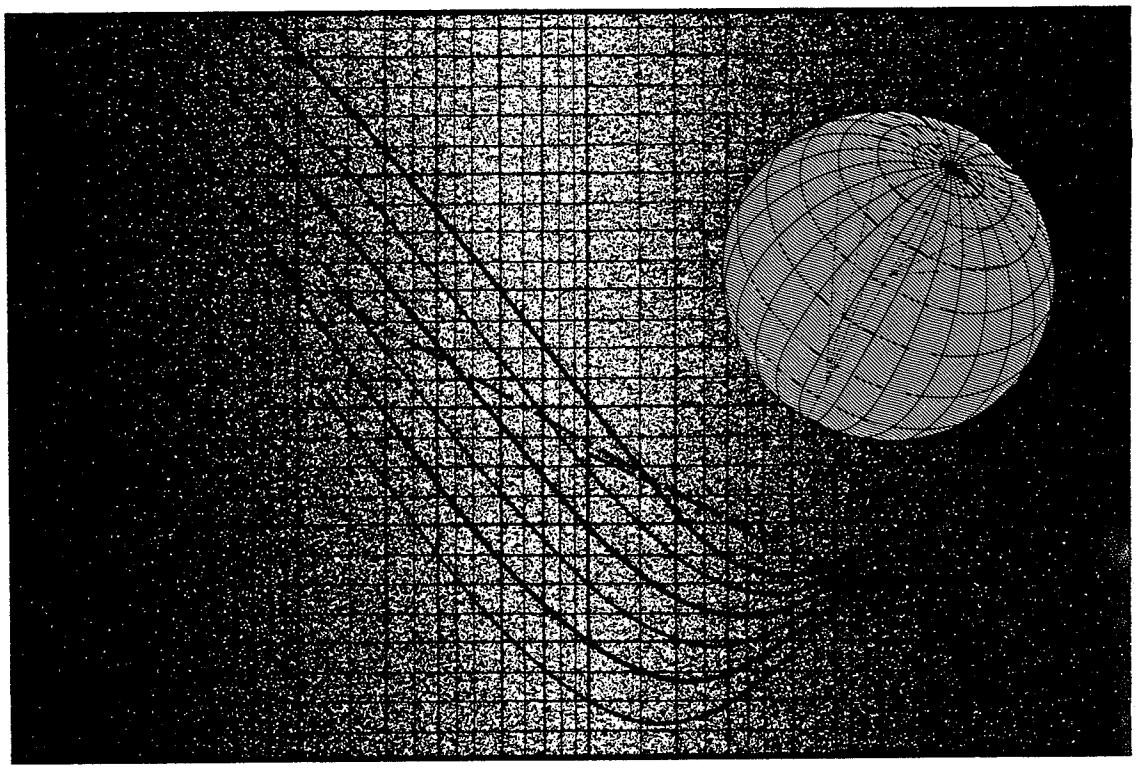

CARACTÉRISTIQUES DU BRUIT ATMOSPHÉRIQU RADIOÉLECTRIQUE ET APPLICATIONS

CHARACTERISTICS AND APPLICATIONS OF ATMOSPHERIC RADIO NOISE DATA

CARACTERÍSTICAS DEL RUIDO ATMOSFÉRICO RADIOELÉCTRICO Y APLICACIONES

Genève, 1988

TABLE DES MATIÈRES

CONTENTS

ÍNDICE

REPORT 322-3 *

CHARACTERISTICS AND APPLICATIONS OF ATMOSPHERIC RADIO NOISE DATA

(Study Programme 29B/6)

(1963-1974-1982-1986)

LIST OF SYMBOLS

Where a symbol is shown in both lower case and capital letters, the capital letter is used to represent the equivalent, in decibels, of the quantity denoted by the lower case letter.

A	Instantaneous amplitude of the noise envelope (dB)
A_{rms}	Root-mean-square value of the noise envelope voltage (dB)
APD	Amplitude-probability distribution of received noise envelope (exceedance probability)
b, B	Effective receiver noise bandwidth (Hz) ($B = 10 \log b$)
D	Deviation of a random variable from its median value (dB)
D_l	Lower decile, value of the average noise power exceeded 90% of the hours within a time block (dB below the median value for the time block)
D_R	Upper decile of signal-to-noise ratio (dB value exceeded 10% of the time)
D_S	Upper decile of the received signal power (dB value exceeded 10% of the time)
D_u	Upper decile, value of the average noise power exceeded 10% of the hours within a time block (dB above the median value for the time block)
E_e	Expected value of the signal field strength required for a given grade of service (dB(μV/m))
E_n	Root-mean-square noise field strength for a bandwidth b (dB(μV/m))
f	Operating noise factor of a receiving system
F	Operating noise figure of a receiving system ($F = 10 \log f$)
f_a	Effective antenna noise factor that results from the external noise power available from a loss-free antenna
F_a	Effective antenna noise figure ($F_a = 10 \log f_a$)
F_{am}	Median of the hourly values of F_a within a time block
f_c	Noise factor of the antenna circuit (its loss in available power)
f_{MHz}	Frequency (MHz)
f_r	Receiver noise factor
f_t	Noise factor of the transmission line (its loss in available power)
k	Boltzmann's constant = 1.38×10^{-23} J/K
K	Temperature (Kelvin)
P	Received signal power available from an equivalent loss-free antenna (dBW)
P_e	Expected median value of P (dBW)
p_n, P_n	Noise power available from an equivalent loss-free antenna ($P_n = 10 \log p_n$)
p_s, P_s	Received signal power required for a given signal-to-noise ratio, from a loss-free antenna ($P_s = 10 \log p_s$)
pdf	Probability density function
r, R	Signal-to-noise power ratio required ($R = 10 \log r$)
R_m	Median value of R
t	Standard normal deviate
T_a	Effective antenna temperature in the presence of external noise (K)
T_0	Reference temperature = 288 K

* This new version of Report 322 was adopted by the XVIth Plenary Assembly (Dubrovnik, 1986) for the purpose of facilitating further studies to be carried out by Study Group 6 (see Recommendation 372-4).

V_d Voltage deviation; the ratio (dB) of the root-mean-square envelope voltage to the average noise envelope voltage

V_{dm} Time-block median value of V_d

σ_D Standard deviation of D

σ_{Dl} Standard deviation of D_l

σ_{Du} Standard deviation of D_u

σ_{DR} Standard deviation of D_R

σ_{Fam} Standard deviation of F_{am}

σ_P Standard deviation of the expected received signal power

σ_R Standard deviation of R

σ_T Total standard deviation; total uncertainty of P_e

σ_{Vd} Standard deviation of V_d

1. Introduction

The determination of radio communication system performance and the resulting minimum signal level required for satisfactory reception is a matter of the proper statistical treatment of both the desired signal and the real-world noise (and interference) processes. System performance is highly dependent on the detailed statistical characteristics of both the signal and the noise. It has long been recognized that the ultimate limitation to a properly designed communication link will usually be the radio noise.

There are a number of types of radio noise that must be considered in any design; though, in general, one type will be the predominant noise and will be the deciding design factor. In broad categories, the noise can be divided into two types – noise internal to the receiving system and noise external to the receiving antenna. The internal noise is due to antenna and transmission line losses, or is generated in the receiver itself and has the characteristics of thermal noise (i.e., white Gaussian noise). Noise power is generally the most significant parameter (but seldom sufficient) in relating the interference potential of the noise to system performance. Since the noise level often results from a combination of external and internal noise, it is convenient to express the resultant noise by means of an overall operating noise factor that characterizes the performance of the entire receiving system. In so doing, it is then possible to make decisions concerning required receiving system sensitivity; that is, a receiver need have no more sensitivity than that dictated by the external noise. Indeed, world-wide minimum noise levels have been estimated for this purpose (Report 670). Also, the noise levels can then be compared to the desired signal level to determine the pre-detection signal-to-noise ratio. The pre-detection signal-to-noise ratio is an important system design parameter and is always required knowledge (required but seldom sufficient) when determining the effects of the external noise on system performance.

External noise can be divided into several types, each having its own characteristics. The most usual types are of atmospheric, galactic, and man-made origin. All these types are considered here, but since atmospheric noise usually predominates at frequencies below about 30 MHz, this Report deals primarily with this type and with its influence on the reception of signals. Unlike the internal noise, the external noise is generally highly non-Gaussian in character, usually being impulsive in nature.

The purpose of this Report is to present values of noise power and of other noise parameters, and to show, by example, the method of using these noise parameters and their statistical variations in the evaluation of the performance of a radio circuit. Additional examples of the use of the noise data in this Report and a summary of the effects of atmospheric radio noise (and similar forms of impulsive noise) on telecommunication systems performance are given in Spaulding [1982]. Also, recent results concerning atmospheric noise from lightning and means of developing appropriate communication systems to perform in this noise are summarized by URSI [1981], in Report 254 and in the references therein. Finally, Reports 258 and 670 give additional information concerning man-made and atmospheric noise, and Recommendation 339 gives required signal energy to noise power spectral density ratios for various systems operating in the presence of atmospheric noise.

The estimates for atmospheric noise levels given in this Report are for the average background noise level due to lightning in the absence of other signals, whether intentionally or unintentionally radiated. In addition, the noise due to local thunderstorms can be important for a significant percentage of the time. This local noise can also be significant at frequencies well above 30 MHz. Some information pertaining to local thunderstorm noise is available in Hagn and Shepherd [1984], Kotaki and Katoh [1983] and Kotaki [1984].

2. Radio noise estimates

This Report gives:

- estimates that take account of major reliable programmes of noise measurements,
- statistical information on the accuracy of the estimates,
- a statistical description of the fine structure of the noise,
- examples of using the estimates in the determination of system performance.

The data used were obtained from the 16 stations that used standardized recording equipment, the ARN-2 radio noise recorder, which was operated by a number of organizations in an international cooperative programme [URSI, 1962], a measurement station in Thailand that used equipment equivalent to the ARN-2, and 10 measurement stations within the USSR. The measurement station locations are shown in Fig. 1. Data from the stations during the period 1957 to 1966 inclusive were used in the analysis. Not all the stations produced data for the entire period. Data from the Southern Hemisphere are sparse. Details on the specifics of this data base of long-term atmospheric radio noise measurements and the analysis of these data are given in Spaulding and Washburn [1985].

For these predictions, the data were grouped into four seasons of the year and six four-hour periods of the day in each season. The aggregate of corresponding four-hour periods of the day throughout a season was defined as a time block. Thus, there are in the year twenty-four time blocks, each consisting of about 360 hours (four hours in each day for about ninety days).

The division of the year into four seasons of three months each was made in the following way, although it was realized that the seasonal pattern of noise variations existing in temperate regions was not necessarily followed at lower latitudes.

Month	Season	
	Northern Hemisphere	*Southern Hemisphere*
December, January, February	Winter	Summer
March, April, May	Spring	Autumn
June, July, August	Summer	Winter
September, October, November	Autumn	Spring

The main parameter presented is the median hourly value of the average noise power for each time block, and the variations in this parameter show systematic diurnal and seasonal variations of the noise. The variations of the hourly values within a time block have been treated statistically.

To facilitate the use of the noise data in this Report, computer programs are available from the CCIR Secretariat that give "exact" numerical representations of all the noise characteristics contained in this Report.

3. Description of the parameters used

As noted above, the single most important and basic noise parameter is noise power, although this single parameter (or any other single parameter) is almost never sufficient to determine the effects of the noise on system performance. Also, it is convenient to express the external noise in a form that allows for its combination with the internal noise, thereby given an overall operating noise threshold for a receiving system. Report 670 details how this noise threshold is obtained.

The noise power received from sources external to the antenna is expressed in terms of an effective antenna noise factor, f_a, which is defined by:

$$f_a = p_n / kT_0 b = T_a / T_0 \quad (1)$$

where:

p_n: noise power available from an equivalent loss free antenna (W),

k: Boltzmann's constant = 1.38×10^{-23} J/K,

T_0: reference temperature, taken as 288 K,

b: effective receiver noise bandwidth (Hz),

T_a: effective antenna temperature in the presence of external noise.

Equation (1) gives two equivalent methods of specifying the noise power, by the effective noise factor or by the effective noise temperature of the antenna. The value of T_0 has been taken as 288 K so that 10 log kT_0 is 204 dB below one Joule.

Since atmospheric noise is a spectrally broadband process, both f_a and T_a are independent of bandwidth (for normal communications bandwidths). Note that f_a is a dimensionless quantity, being the ratio of two powers (or, equivalently, two temperatures). The quantity f_a, however, gives, numerically, the available power spectral density in terms of kT_0 or the available power in terms of $kT_0 b$. The noise factor f_a is commonly given by the corresponding noise figure F_a, i.e., $F_a = 10 \log f_a$.

The antenna noise figure, F_a, in decibels, in this Report is for a lossless short vertical antenna over a perfectly conducting ground plane. Means of obtaining the appropriate antenna noise figure, F_a, for other types of antennas from the data in this Report are given in Report 670, the references therein, Hagn and Shepherd [1934] and Lauber and Bertrand [1977]. F_a is simply related to the vertical r.m.s. field strength (for the short vertical antenna) by:

$$E_n = F_a - 95.5 + 20 \log f_{\mathrm{MHz}} + 10 \log b \quad (2)$$

where:

E_n: r.m.s. noise field strength (dB(μV/m)) in bandwidth b (Hz),

F_a: noise figure for the centre frequency f_{MHz} (MHz).

Atmospheric radio noise is characterized by large, rapid fluctuations, but if the noise power is averaged over a period of several minutes, the average values are found to be nearly constant during a given hour, variations rarely exceeding ± 2 dB except near sunrise or sunset, or when there are local thunderstorms. The ARN-2 radio noise recorder yielded values of average power at each of eight frequencies for fifteen minutes each hour, and it is assumed that the resulting values of F_a used in the analysis were representative of the hourly values. Similar assumptions are made to obtain hourly F_a values for the other measurements (non-ARN-2) used in the analysis.

In predicting the expected noise level, the systematic trends, that is, the trends with time of day, season, frequency, and geographical location, are taken into account explicitly. There are other variations that must be taken into account statistically. The value of F_a for a given hour of the day varies from day to day, because of random changes in thunderstorm activity and propagation conditions. The median of the hourly values within a time block (the time-block median), is designated as F_{am}. Variations of the hourly values during the time block can be represented by the values exceeded for 10% and 90% of the hours, expressed as deviations D_u and D_l from the time block median. When plotted on a normal probability graph (level in dB), the amplitude distribution of the deviations, D, above the median can be represented with reasonable accuracy by a straight line through the median and upper decile values, and a corresponding line through the median and lower decile values can be used to represent values below the median.

It is natural to expect some correlation of atmospheric radio noise with sunspot activity, since both propagation conditions and thunderstorm activity seem to be affected by solar activity. Some measurements at very low frequencies, made many years ago, did seem to show such a correlation [Austin, 1932]. A thorough examination of the data for Boulder, Colorado (1957-1966) did not reveal any systematic variation of the noise with sunspot activity.

So far, we have dealt with the average power as represented by F_a (or T_a) as the most useful and common way of specifying the external noise level. When one is concerned with determining the effects of the external noise on system performance, more information about the received noise process than just its energy content (level) is almost always required. An exception would be if the external noise were a white Gaussian noise process, but this is almost never the case. Atmospheric noise (and man-made noise) is a random process. The fact that we are dealing with a random process means that the noise can be described only in probabilistic or statistical terms and cannot be represented by a deterministic waveform or any collection of deterministic waveforms.

The basic description of any random process is its probability density function (pdf) or distribution function. The first-order pdf of the received interference process is almost always required in order to determine system performance (although sometimes it is not sufficient). The received atmospheric noise process under consideration here is a bandpass process in that it is describable by an envelope process and a phase process. Since the phase process is known (phase uniformly distributed), the required pdf of the instantaneous amplitude can be obtained from the envelope amplitude pdf. Usually, also, the envelope pdf can be used directly in system performance analyses. The atmospheric noise envelope statistic is usually given as (and measured as) a cumulative exceedance distribution, termed the "amplitude probability distribution" or APD. For some envelope level, A_i, the APD is the fraction of the total measurement time, T, for which the envelope was above level A_i.

A large number of APDs have been measured in several countries, and reasonably consistent results have been obtained [URSI, 1962; Clarke, 1962; Science Council of Japan, 1960; see also URSI, 1975, 1978, 1981, 1984, and references therein]. For presenting the data in an operationally useful form, it is convenient to construct a family of idealized curves, one of which can be chosen to represent a practical APD to a sufficient accuracy. This has been done by using a system of coordinates in which a Rayleigh distribution (representing the envelope of thermal-type noise), is a straight line with a slope of -0.5. The low amplitude parts of an atmospheric noise curve have this slope, the high amplitude parts are represented by a second straight line, with a greater slope, and the two lines are joined by an arc of a circle. The construction of these curves involved the use of quantities related to the r.m.s. average, and mean logarithmic values of the distribution, parameters that have been recorded in routine noise measurements [Crichlow *et al.*, 1960a, 1960b]. In practice, because the average voltage and mean logarithmic voltage are found to be closely correlated, the ratio of r.m.s. to average voltage, V_d(dB), is sufficient to specify the curve that can be used to represent the distribution [Spaulding *et al.*, 1962]. A set of the APD curves is reproduced in Fig. 27, which gives the probability ($\times$ 100) that an envelope level A_0 (given relative to the envelope r.m.s. level, A_{rms}) will be exceeded. Figure 27 represents one "model" for the APD parametric in the parameter V_d. Many other models for atmospheric noise statistics have been developed, and a historical summary of the various main models and their interrelationships has been given by Spaulding [1977, 1982] and by Shaver *et al.* [1972]. Numerical representation (coefficients and computer programs) of the APD model in this Report is available in Spaulding and Washburn [1985]. It should be noted that the actual noise power is one-half the envelope power (as given by A_{rms}).

The APD curves (Fig. 27) can be used for a wide range of bandwidths. The estimates of V_d given in this Report, however, are for a bandwidth of 200 Hz, so a means to convert the 200 Hz V_d to other bandwidths is needed. Herman and De Angelis [1987] conducted an extensive study in order to develop a V_d bandwidth relationship. Figure 26 gives the results of this study and gives a means to convert the 200 Hz V_d to the corresponding V_d in other bandwidths. The results of Fig. 26 are strictly valid only at MF, although recent results indicate they are valid also at HF. Care should be exercised, therefore, when applying these results to lower frequencies (i.e., LF, VLF, ELF).

4. Methods used to obtain the estimates

Values of F_a, collected from the measurement stations previously mentioned, were edited to remove, as far as possible, the effects of man-made noise and unwanted signals. The remaining values were considered to represent actual atmospheric radio noise. The time block median 1 MHz values were compared with the Report 322-2 values and corrections derived. The means for obtaining the 1 MHz values from the totality of measurements at all the measurement frequencies and the numerical interpolation and mapping procedures used to obtain the world-wide 1 MHz F_{am} values for each time block are detailed in Spaulding and Washburn [1985].

Only data from measurement stations that employed ARN-2 equipment were used to obtain the variation of F_{am} with frequency (i.e., for frequencies other than 1 MHz). An analysis of these data indicated no significant difference from the frequency variations given in Report 322-2. The same is true for the deviations, D_u, D_l, of the decile value of F_a from the median value F_{am}, for each time block, and also for the median value, V_{dm}, of the voltage deviation V_d.

To obtain a measure of the variability of the noise with respect to the predicted values in each time block, standard deviations of F_{am}, D_u, D_l, and V_d, as functions of frequency, were found.

5. The noise data or estimates

World charts, showing the expected median values of background atmospheric radio noise, F_{am} in dB above kT_0b, at 1 MHz for each season, 4-hour-time block, in local time, are shown in Figs. 2a to 25a. The only geographical variation given is for the 1 MHz F_{am}. The variation of F_{am} with frequency for each season-time block is given in Figs. 2b to 25b and the variation with frequency of the other noise parameters is given in Figs. 2c to 25c.

Galactic noise levels, from Cottony and Johler [1952] and verified using a vertical antenna, are shown on the frequency curves (Figs. 2b to 25b). Within a $\pm$ 2 dB temporal variation (neglecting ionospheric shielding), the values shown will be the upper limit of galactic noise but in any given situation the received noise should be determined considering critical frequencies and the directional properties of the antenna.

In many locations and at some frequencies, man-made noise is a limiting factor in radiocommunication for at least part of the time. Although this type of noise depends on local conditions, a curve of expected values at a quiet receiving location has been added. The values shown are the "average" of the man-made values recorded at sites chosen to ensure a minimum amount of man-made noise (the ARN-2 sites). Man-made noise levels, in terms of F_a, and their variations for various environmental categories (business, residential, rural and quiet rural, etc.) are given in Report 258. The noise levels for "quiet rural" locations given in Report 258 are taken from this Report. Additional information concerning man-made noise is summarized in Hagn [1982], Skomal [1978] and URSI [1975, 1978, 1981, 1984].

It will be observed that values of atmospheric noise are indicated that are below the expected levels of man-made noise and galactic noise. These values should be used with caution, as they represent only estimates of what atmospheric noise levels would be recorded if the other types of noise were not present. An examination of the data, however, shows that such low levels were, on rare occasions, actually measured.

On Figs. 2c to 25c are the estimated values of D_u, D_l, V_{dm}, σ_{Du}, σ_{Dl}, σ_{Vd}, and σ_{Fam}. D_u will normally be used for assessing minimum required signal strengths, but D_l may be needed to determine whether the internal noise of a receiving system is negligible under the quieter external noise conditions.

The variation of F_{am} with frequency (Figs. 2b to 25b) is given by a least squares numerical mapping of the totality of ARN-2 data for all the measurement frequencies [Spaulding and Washburn, 1985]. The parameter σ_{Fam} represents, as a function of frequency, the variation of the F_{am} data about the "mapped" (or estimated) values. The curves for σ_{Fam} will be seen to extend only up to 10 MHz, since at higher frequencies the predominant noise at many measurement locations was often of galactic origin.

Originally, separate curves for D_u, D_l, σ_{Du}, and σ_{Dl} were derived using data from measurement locations in temperate and tropical zones. No statistically significant difference between the two zones was obtained and, therefore, this Report gives a single curve for the entire Earth's surface. These curves should be used with some caution, especially at the higher frequencies.

APD curves corresponding to various values of V_d, are given in Fig. 27, in which the r.m.s. envelope voltage, A_{rms}, is taken as the reference. The measured values of V_d vary about the predicted median value, V_{dm}, and their variation is given by σ_{Vd}. The V_{dm} estimates given are for a 200 Hz bandwidth. The corresponding V_{dm} for other bandwidth can be obtained from Fig. 26. As noted earlier, this bandwidth conversion should be used with caution at the lower frequencies (VLF and LF).

The figures are used in the following way. The value of F_{am} for 1 MHz is found from the noise charts (Figs. 2a to 25a) for the season under consideration. Using this value as the noise grade, the value of F_{am} for the required frequency is determined from the frequency curves (Figs. 2b to 25b). The variability parameters σ_{Fam}, D_u, σ_{Du}, etc., are obtained for the required frequency from Figs. 2c to 25c. If the value of $D(= F_a - F_{am})$ or the

value of σ_D is required for any percentage (less than 50%) of time other than 10%, the values can be found by plotting D_u and σ_{D_u} on a normal probability graph (with ordinate values in decibels) and drawing straight lines through 0 dB at 50% and the 10% values, as shown in Fig. 28. That is, the noise power is log-normally distributed (above 50%). Values at percentages greater than 50% can be obtained in the same manner using D_l and σ_{D_l}.

6. Application of noise data to system evaluation

The treatment here is not intended to be comprehensive; however, it is considered desirable to give some indication of how the data may be used in the study of telecommunication system performance. Additional examples and information are given in Spaulding [1982], URSI [1975, 1978, 1981, 1984], and the references therein.

As noted earlier, it is desirable to express the external noise as an antenna noise factor, so that it can be combined with the noise generated within the receiving system to give an overall operating noise factor, f (Report 670) [Barsis *et al.*, 1961]. If the receiver is free from spurious responses and all elements prior to the receiver are at the reference temperature T_0, then f is given by:

$$f = f_a - 1 + f_c f_l f_r \tag{3}$$

where:

f_c: noise factor of the antenna (its loss in available power),

f_l: noise factor of the transmission line (its loss in available power), and

f_r: noise factor of the receiver (10 log f_r is the familiar receiver noise figure).

The operating noise factor, f, is useful in determining the relation between the signal power, p_s, available from a loss-free antenna and the corresponding signal-to-noise ratio, r, at the intermediate frequency output of the receiver, since:

$$p_s = frkT_0b \tag{4}$$

or:

$$P_s = R + F + B - 204 \tag{5}$$

where:

$F = 10 \log f$

$B = 10 \log b$, etc.

In evaluating the operating noise figure, F, for use in equation (5), it is necessary to consider all of the parameters in equation (3). However, in many cases, one source of noise will predominate, and only one of the component noise factors will be important. At low frequencies, a receiving system with poor internal noise characteristics may be used, since the values of f_a are large, and will determine the value of f. In general, F_a will decrease with increasing frequency, and, at the higher frequencies, the antenna tends to become more efficient and f_c approaches unity. Under these conditions, f_l and/or f_r may become important in the determination of f (Report 670).

The relation (5) is used to obtain the required average signal power from the required signal-to-noise ratio, R (dB). The required R always depends on the detailed statistical characteristics of both the noise and signal processes. For the noise, the APD (or statistics derivable from it) is almost always required (but sometimes not sufficient) information. Also, since the determination of system performance involves predicting the future (statistically) and such predictions are subject to error, it is common to define system performance in terms of three independent component parts: grade of service, time availability, and service probability [Barsis *et al.*, 1961; Spaulding, 1982].

6.1 *Grade of service* represents the average performance for stationary noise and signal processes. Typical examples are probability of symbol error versus signal-to-noise ratio for digital systems, articulation index versus signal-to-noise ratio for voice systems, etc.

6.2 *Time availability* is the percentage of time a given grade of service or better will be achieved.

6.3 *Service probability* is the probability that a specified grade of service or better will be achieved for a specified time availability. It is the "standard" statistical confidence factor required for any statistical description.

When the desired performance of a system has been defined, it is necessary to evaluate the various factors affecting this performance. For the sake of clarity and simplicity, the performance will, in the following two examples, be evaluated in terms of the characteristics of the available signal and noise powers at the terminals of the equivalent loss-free receiving antenna. In both examples it will be assumed that a short vertical rod antenna is used and that the predominant noise is atmospheric noise external to the system. In the first example, ground-wave propagation is assumed, so that the signal level is constant and only the noise level is variable. The second example involves sky-wave propagation and thus both the signal and noise levels vary with time. In both examples, the variation of the noise power is log-normal (i.e., dB values normally distributed) and the signal power is also log-normal (but constant, zero variance, in the first example). This results, then, in the signal-to-noise ratio, r, also being log-normal. This means that the standard procedures (based on the normal distribution) to determine statistical confidence factors (service probability) can be followed. The determination of the service probability involves not only uncertainties associated with the noise parameters but also the uncertainties of all values involved in the prediction process.

6.4 *Example I*

Determine the performance of a binary symmetric non-coherent frequency shift keying (NCFSK) system with reception at Geneva, Switzerland, under the following conditions.

Frequency: 50 kHz

Time of day: 2000-2400 local time

Season: summer

Bandwidth: 100 Hz

Propagation: ground wave (resulting in a constant signal)

Grade of service: probability of bit error of 5×10^{-4}. This corresponds approximately to 1% teletype errors in a five unit start-stop system.

The problem is to assess the probability that a given received signal power will provide the specified grade of service for any given percentage of time.

The expected value (mean value) of received power, P_e, required for a particular grade of service for a given external noise figure, F_a, is from relation (5):

$$P_e = F_a + R + B - 204 \qquad \text{dBW} \tag{6}$$

where R is the required pre-detection signal-to-noise ratio (dB) for the given bandwidth.

When the receiving antenna is a short vertical rod over a ground plane, the corresponding field strength, E_e, is given by:

$$E_e = P_e + 20 \log f_{\text{MHz}} + 108.5 \qquad \text{dB}(\mu\text{V/m}) \tag{7}$$

The first step is to determine the required R (and its variation). Following Montgomery [1954], we have the following results for any arbitrary additive noise that is independent from one integration period (bit length) to the next and that has uniformly distributed phase. For the symmetric binary NCFSK system, the probability of a bit being in error is given by one half the probability that the noise envelope exceeds the signal envelope. Therefore, the required signal-to-noise ratio can be obtained directly from the APD (Fig. 27) for the appropriate V_d. From Fig. 19c, the 200 Hz V_{dm} at 50 kHz is 8.5 dB and σ_{Vd} is 1.2 dB. Using Fig. 26, this translates to the 100 Hz V_d ranging between 6.6 and 8.9 dB (from the 200 Hz V_d range of 7.3 to 9.7 dB) with the 100 Hz V_{dm} being 7.7 dB. The APDs can be used directly to determine the median required signal-to-noise ratio (R) and its variation. However, this is also available in Akima *et al.* [1969] where probability of bit error versus signal-to-noise characteristics for various V_d's is given (using the APDs of Fig. 27 of this Report). The required R for a V_d of 7.7 is 20.3 dB with a variation of approximately 0.8 dB based on the above expected V_d range; that is, $\sigma_R = 0.8$ dB. It should be noted [Akima *et al.*, 1969] that if the signal was Rayleigh fading the required R will be 28 dB and σ_R would be 0 dB, since for small probability of errors, probability of error is independent of V_d. This is not true for other forms of fading (e.g., log-normal) or if diversity reception is employed. In these cases, probability of error is quite dependent on the APD (i.e., V_d).

F_a must now be derived from the median value F_{am} plus a deviation D consistent with the percentage of time during which satisfactory service must be obtained (time availability). From Fig. 19a, the 1 MHz value is 74 dB and the value of F_{am} at 50 kHz is 133 dB with a standard deviation, $\sigma_{F_{am}}$, of 3.4 dB (Fig. 19b, 19c). To obtain values of F_a for percentages of time other than 50% (given by F_{am}), D_u (6.4 dB from Fig. 19c) is used to obtain $D = F_a - F_{am}$ as shown on Fig. 28. Likewise, σ_D is obtained using σ_{D_u} (1.9 dB from Fig. 19c) as also shown on Fig. 28.

Equation (6) is next evaluated (with $F_a = F_{am} + D$) using the appropriate D for the required time availability. From equation (6), then, with $R = 20.3$ dB, $F_{am} = 133$ dB, and $B = 20$ dB, we obtain:

$$P_e = D - 30.7 \qquad \text{dBW} \tag{8}$$

This is the usual prediction of the signal power required (or required field strength from equation (7)) to produce the specified grade of service for various time availabilities. The required signal power for various time availabilities is shown on Fig. 29. Since, however, the prediction uncertainties have not been taken into account yet, only one-half of such circuits will meet the design criteria.

The uncertainties to consider are given by the following standard deviations:

σ_P: the standard error of achieving the expected "constant" received signal power. This must be derived from propagation and other data and, for the purposes of this example, is assumed to be 2 dB;

σ_R: uncertainty in the required signal-to-noise ratio, 0.8 dB as derived above;

$\sigma_{F_{am}} = 3.4$ dB (from Fig. 19c);

σ_D: standard deviation of D (from Fig. 28).

The resulting standard deviation, σ_T, is obtained, since the errors are uncorrelated from:

$$\sigma_T^2 = \sigma_P^2 + \sigma_R^2 + \sigma_{F_{am}}^2 + \sigma_D^2 \tag{9}$$

σ_T is also shown on Fig. 29 and enables us to determine the service probability (confidence) that the indicated time availability will be achieved, as follows.

Since, as noted earlier, only log-normal distributions are involved, for any given value of received power, P, the time availability can be determined as a function of the service probability from:

$$t = (P - P_e) / \sigma_T \tag{10}$$

where t is the standard normal deviate. Figure 30 gives the values of t as a function of service probability.

If a probability of only 0.5 (50% confidence) is required that a specified time availability will be achieved, $t = 0$, $P = P_e$, and the required powers are given by Fig. 29. Suppose, however, we specify that we want to be 90% confident (service probability of 0.9) that our grade of service (probability of bit error of 5×10^{-4}) or better will be achieved 90% of the time (or better), then $t = 1.3$ (Fig. 30), $\sigma_T = 4.45$ dB (Fig. 29), $P_e = 24.3$ dBW (Fig. 29) so that, from equation (10), the required signal strength is -18.5 dBW. In general, using equation (8) and equation (10):

$$P = D - 30.7 + t\sigma_T \tag{11}$$

Results for service probabilities of 0.5, 0.8, 0.9 and 0.99 are shown on Fig. 31.

6.5 *Example II*

Determine the performance of an A3E telephony double-sideband system with reception at Geneva, Switzerland, under the following conditions:

Frequency:	5 MHz
Time of day:	2000-2400 local time
Season:	summer
Bandwidth:	6 kHz
Propagation:	ionospheric (resulting in a fading signal)
Grade of service:	marginally commercial.

Again the problem is to assess the probability that a given received signal power will provide the specified grade of service or better for any given percentage of time. Here, both the signal and atmospheric noise have statistical variation. For ionospheric propagation, it is usually noted that the short-term (within an hour, say) distribution of the signal is Rayleigh and the long-term fading of the hourly (say) median values is log-normal (Report 266). The resulting normal distribution of signal median dB values, for this example, has a standard deviation of 8 dB (Report 266), which results in an upper decile value for the signal, D_s, of $1.27 \times 8 = 10$ dB. Based on the variation noted in Report 266 for the standard deviation of the long-term signal fading distribution, a value of $\sigma_{DS} = 2$ dB is used.

Recommendation 339 gives a median required carrier power to noise power in a 1 Hz bandwidth of 64 dB for marginally commercial A3E emissions. This gives a median required signal-to-noise ratio R of 26 dB. For analogue systems these performance requirements are based on white Gaussian noise. In general, a given voice understandability can be achieved with a smaller R in impulsive (e.g., atmospheric) noise than in white Gaussian noise [Spaulding, 1982]. Figure 19c gives a V_{dm} of 4.5 dB at 5 MHz and a 200 Hz bandwidth. This translates to a 6 kHz bandwidth V_{dm} of 7.5 dB (Fig. 26). Spaulding [1982] gives results for AM voice systems in atmospheric noise ($V_d = 12$ dB). These results indicate that we can probably safely reduce the required R_m by about 6 dB (at least, assuming no noise limiting). We, therefore, will specify a required R_m of 20 dB, with a σ_R of 3 dB.

As in Example I, the 1 MHz F_{am} value for Geneva for June, July, August and 2000-2400 h is 74 dB. From Figs. 19b and 19c, the 5 MHz F_{am} value is 56 dB with a standard deviation σ_{Fam} of 4.1 dB. Also from Fig. 19c, $D_u = 4.8$ dB and $\sigma_{Du} = 1.3$ dB. Since the signal-to-noise ratio is log-normally distributed (as it was in Example I), we proceed as before. The upper decile for R is given by:

$$D_R^2 = D_S^2 + D_u^2 \tag{12}$$

since the signal and noise processes are independent. The deviation $D = R - R_m$ ($D_R = 11.1$ dB) and σ_D (using a decile value given by $\sigma_{DR} = \sqrt{\sigma_{D_u}^2 + \sigma_{D_S}^2} = 2.4$ dB) are shown on Fig. 32.

The deviation, D, now accounts for the long-term statistical variation of both the signal power and the noise power.

In order to obtain the service probability, the prediction uncertainties are given by the following standard deviations:

σ_P: standard deviation in the expected received signal power. We have specified the short-term and long-term fading distributions of P, but there still is a prediction error for the expected value, due to, for example, errors in the ionospheric propagation prediction method used. We will use 5 dB for σ_P;

σ_R: uncertainty in the required R, 3 dB as discussed earlier;

$\sigma_{Fam} = 4.1$ dB (Fig. 19c);

σ_D: standard deviation of D (Fig. 32), which is a function of the required time availability.

The standard deviation σ_T is shown on Fig. 33. Also shown on Fig. 33 is the expected median value of the received signal power, P_e, for the different time availabilities, from equation (6), given by:

$$P_e = F_{am} + R_m + D + B - 204$$

or:

$$P_e = D - 90.2 \qquad \text{dBW} \tag{13}$$

Finally, Fig. 34 shows the required received signal power versus time availability for service probabilities of 0.5, 0.8, 0.9 and 0.99 using, as in Example I:

$$P = P_e + t\,\sigma_T \tag{14}$$

7. The influence of the directivity and polarization of antennas

All the noise information presented in this Report, including the examples given in the last section, relates to a short vertical receiving antenna. Although such an antenna may be used in practice at low frequencies, long-distance communication at high frequencies is normally achieved by the use of a highly-directional antenna. Some allowance must therefore be made for the effects of directivity and polarization on the signal-to-noise ratio.

It is assumed that the signal gain is reasonably well known, although it is dependent on the relative importance of the various propagation modes, which vary with time. The effective noise factor of the antenna, insofar as it is determined by atmospheric noise, may be influenced in several ways. If the noise sources were distributed isotropically, the noise factor would be independent of the directional properties. In practice, however, the azimuthal direction of the beam may coincide with the direction of an area where thunderstorms are prevalent, and the noise factor will be increased correspondingly, compared with the omnidirectional antenna. On the other hand, the converse may be true. The directivity in the vertical plane may be such as to differentiate in favour of, or against, the reception of noise from a strong source. The movement of storms in and out of the antenna beam may be expected to increase the variability of the noise, even if the average intensity is unchanged.

Experimental information on the effects of directivity is scarce, and in some respects conflicting. In an equatorial region (Singapore), the median value of F_a for certain directional antennas was found to be somewhat higher (about 4 dB on the average), than that for a vertical rod antenna over the same period [Bradley and Clarke, 1964]. This figure is considerably lower than the maximum possible antenna gain, as would be expected from the widespread nature of the storms, but the fact that there was, on the average, some gain in noise in a wide range of storm conditions suggests that there was a tendency for the noise to be received more from the lower angles of elevation. In the Federal Republic of Germany also, directional antennas had, on the average, higher noise factors [Kronjäger and Vogt, 1959]. In order to determine the effects of antenna directivity on the signal-to-noise ratio, it is necessary to take into account the storm locations and the critical frequency of the ionosphere in addition to the antenna polar diagram. Rather detailed information on thunderstorm locations is now available [e.g., Kotaki and Katoh, 1983; Kotaki, 1984; Crichlow *et al.*, 1971].

Even less information is available on the effects of antenna polarization but for a first approximation, it may be assumed that the received noise would be comparable with either polarization, provided the antenna height is large compared with the wavelength. Some limited data on polarization (and directivity) for antennas "close" to the ground is available in Hagn *et al.* [1968] and Hagn and Shepherd [1984]. Additional information is also available (primarily in the references) from URSI [1975, 1978, 1981, 1984].

REFERENCES

AKIMA, H., AX, G. G. and BEERY, W. M. [1969] Required signal-to-noise ratios for HF communication systems. ESSA Tech. Rep. ERL 131-ITS 92 (NTIS Order No. AD-697579).

AUSTIN, L. W. [1932] Solar activity and radio telegraphy. *Proc. IRE*, Vol. 20, 280.

BARSIS, A. P., NORTON, K. A., RICE, P. L. and ELDER, P. H. [1961] Performance predictions for single tropospheric communication links and for several links in tandem. NBS Tech. Note 102.

BRADLEY, P. A. and CLARKE, C. [1964] Atmospheric radio noise and signals received on directional aerials at high frequencies. *Proc. IEE*, Vol. III, 1534-1540.

CLARKE, C. [1962] Atmospheric radio noise studies based on amplitude probability measurements at Slough, England, during the International Geophysical Year. *Proc. IEE*, Vol. 109B, 393.

COTTONY, H. V. and JOHLER, J. R. [1952] Cosmic radio noise intensities in the VHF band. *Proc. IRE*, Vol. 40, 1053.

CRICHLOW, W. Q., DAVIS, R. C., DISNEY, R. T. and CLARK, M. W. [1971] Hourly probability of world-wide thunderstorm occurrence. Office of Telecommunications Research Report OT/ITS RR 12 (NTIS Order No. COM75-11202).

CRICHLOW, W. Q., ROUBIQUE, C. J., SPAULDING, A. D. and BEERY, W. M. [1960a] Determination of the amplitude-probability distribution of atmospheric radio noise from statistical moments. *NBS J. Res.*, Vol. 64D, 49.

CRICHLOW, W. Q., SPAULDING, A. D., ROUBIQUE, C. J. and DISNEY, R. T. [1960b] Amplitude-probability distributions for atmospheric radio noise. NBS Monograph 23.

HAGN, G. H. [1982] Man-made electromagnetic noise. *Handbook of Atmospherics*, Chapter 7. Ed. H. Volland, CRC Press, Boca Raton, FL, USA.

HAGN, G. H., CHINDAHPORN, R. and YARBORROUGH, J. M. [1968] HF atmospheric radio noise on horizontal dipole antennas in Thailand. Special Technical Report 47, Stanford Research Institute, Menlo Park, CA 94025, USA (NTIS Order No. AD68-1879).

HAGN, G. H. and SHEPHERD, R. A. [1984] Selected radio noise topics. Final Report, Contract NT83 RAC-36001, SRI-5002-FR/84, SRI International, Arlington, VA, USA (NTIA Order No. PB86 173218).

HERMAN, J. R. and DE ANGELIS, X. A. [January-February, 1987] Bandwidth expansion effects on the voltage deviation parameter (V_d) of MF and HF atmospheric radio noise. *Radio Sci.*, Vol. 22, **1**, 26-36.

KOTAKI, M. [1984] Global distribution of atmospheric radio noise derived from thunderstorm activity. *J. Atmos. Terr. Phys.*, Vol. 46, **10**, 867-877.

KOTAKI, M. and KATOH, C. [1983] The global distribution of thunderstorm activity observed by the Ionospheric Sounding Satellite (ISS-b). *J. Atmos. Terr. Phys.*, Vol. 45, **12**, 833-847.

KRONJÄGER, W. and VOGT, K. [1959] Über das Aussengeräusch kommerzieller Antennenanlagen (On the external noise of commercial antenna installations). *NTZ*, **12**, 371.

LAUBER, W. R. and BERTRAND, J. M. [28-30 June, 1977] Preliminary urban VHF/UHF radio noise intensity measurements in Ottawa, Canada. Proc. 2nd Symposium on Electromagnetic Compatibility, Montreux, Switzerland, 357-362 (IEEE Catalog No. 77CH1224-5EMC).

MONTGOMERY, G. F. [1954] A comparison of amplitude and angle modulation for narrow-band communication of binary-coded messages in fluctuation noise. *Proc. IRE*, Vol. 42, 447.

SCIENCE COUNCIL OF JAPAN [1960] Compilation of data in Japan for atmospheric radio noise during the IGY, 1957/58. Japanese National Committee for IGY.

SHAVER, H. N., HATFIELD, V. E. and HAGN, G. H. [1972] Man-made radio noise parameter identification task. Final Report, Contract N00039-71-A-0223, Standard Research Institute, Menlo Park, CA, USA (NTIS Order No. AD904405).

SKOMAL, E. N. [1978] *Man-Made Radio Noise*. Van Nostrand Reinhold, New York, NY, USA.

SPAULDING, A. D. [12-15 June, 1977] Stochastic modelling of the electromagnetic interference environment. Conf. Record, 42.2-114-42.2-123. IEEE International Conference on Communications (ICC '77), Chicago, ILL, USA (IEEE Catalog No. 77CH1209-6C SCB).

SPAULDING, A. D. [1982] Atmospheric radio noise and its effects on telecommunication systems. *Handbook of Atmospherics*, Chapter 6. Ed. H. Volland, CRC Press, Boca Raton, FL, USA.

SPAULDING, A. D., ROUBIQUE, C. J. and CRICHLOW, W. Q. [1962] Conversion of the amplitude-probability distribution function for atmospheric radio noise from one bandwidth to another. *NBS J. Res.*, Vol. 66D, 713.

SPAULDING, A. D. and WASHBURN, J. S. [1985] Atmospheric radio noise: Worldwide levels and other characteristics. National Telecommunications and Information Administration Report 85-173 (NTIS Order No. PB85-212942).

URSI [1962] The measurement of characteristics of terrestrial radio noise. Special Report No. 7. Elsevier, London, UK.

URSI [1975] *Review of Radio Science 1972-1974*, Radio noise of terrestrial origin, 127-133. International Union of Radio Science, Brussels, Belgium.

URSI [1978] *Review of Radio Science 1975-1977*, Interference environment, 57-66. International Union of Radio Science, Brussels, Belgium.

URSI [1981] *Review of Radio Science 1978-1980*, EM noise and interference, E1-E13. International Union of Radio Science, Brussels, Belgium.

URSI [1984] *Review of Radio Science 1981-1983*, Electromagnetic noise and interference, E1-E15. International Union of Radio Science, Brussels, Belgium.

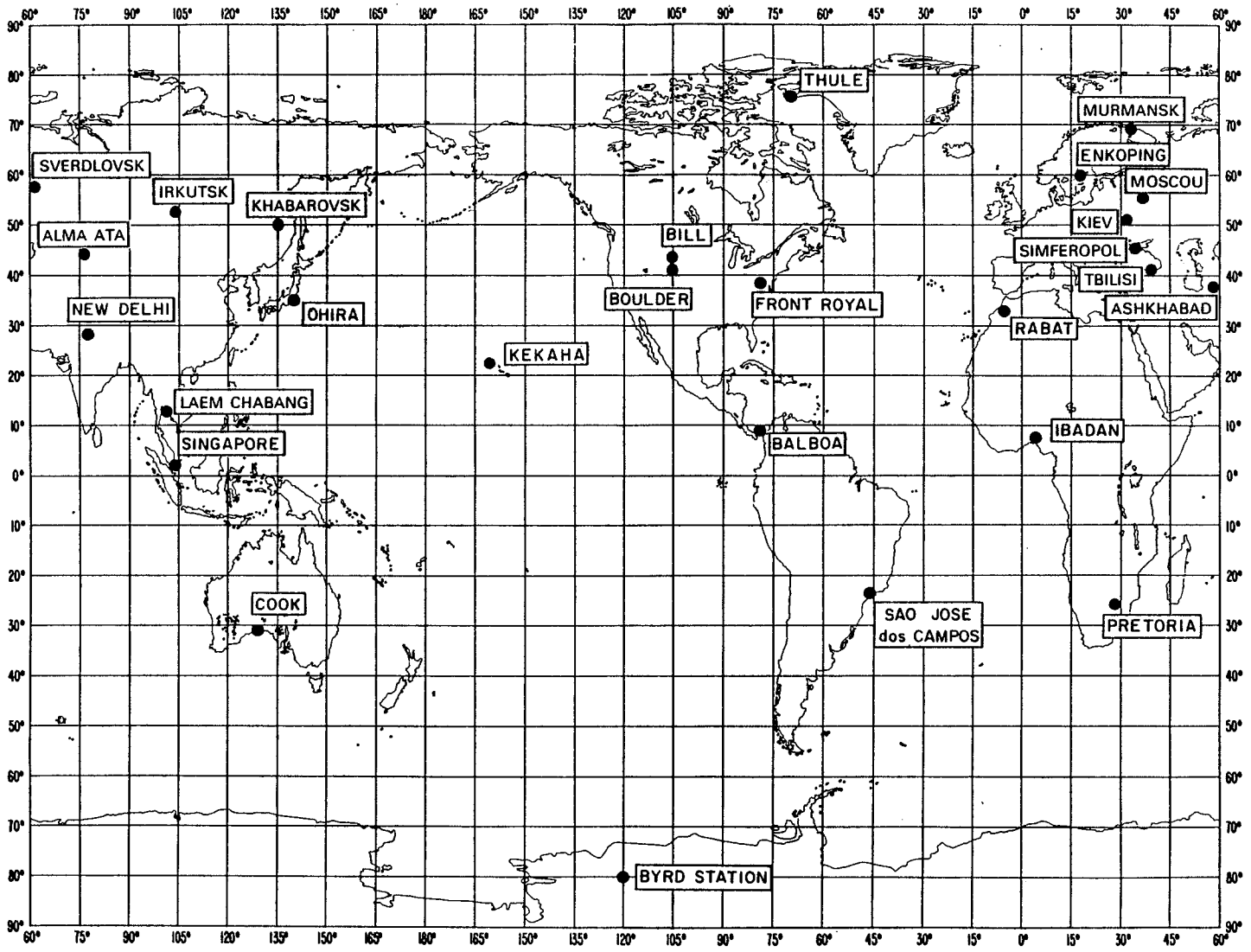

FIGURE 1 – *Stations qui ont fourni des données de bruit radioélectrique*
FIGURE 1 – *Stations which provided radio noise data*
FIGURA 1 – *Estaciones de medida que han suministrado datos del ruido radioeléctrico*

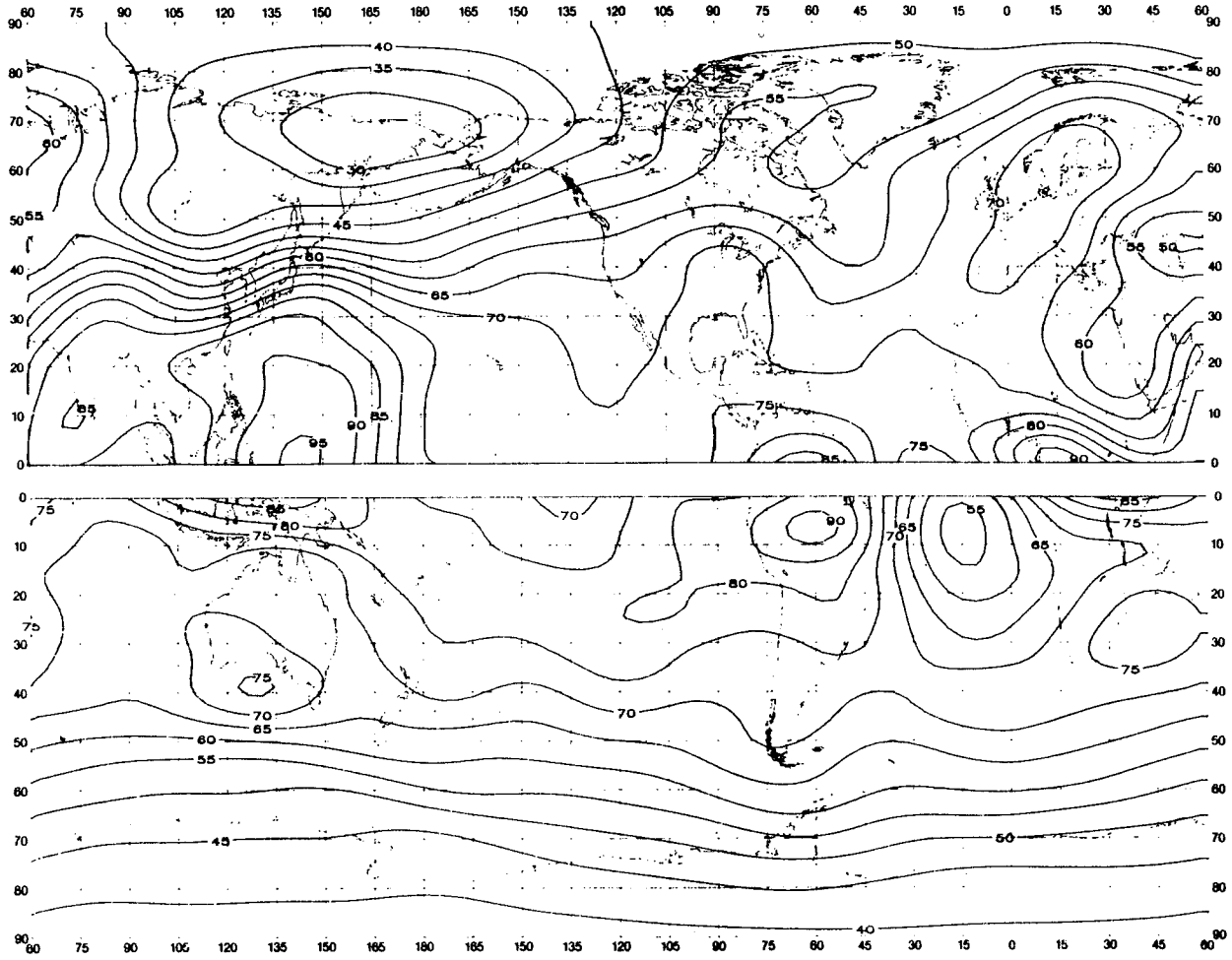

FIGURE 2a – *Valeurs attendues du bruit atmospherique radioelectrique, F_{am}, en dB au-dessus de kT_0b à 1 MHz (Hiver; 0000-0400 heure locale)*
FIGURE 2a – *Expected values of atmospheric radio noise, F_{am} (dB above kT_0b at 1 MHz) (Winter; 0000-0400 LT)*
FIGURA 2a – *Valores probables del ruido atmosférico, F_{am}, en dB por encima de kT_0b en 1 MHz (Invierno; 0000-0400 hora local)*

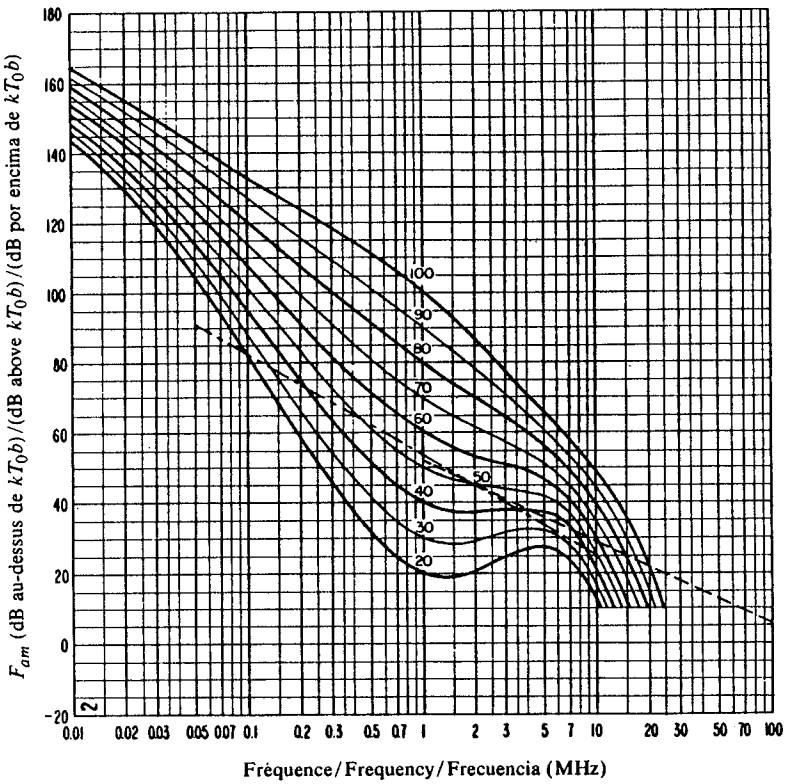

FIGURE 2b – *Variation du bruit radioélectrique en fonction de la fréquence (Hiver; 0000-0400 heure locale)*

FIGURE 2b – *Variation of radio noise with frequency (Winter; 0000-0400 LT)*

FIGURA 2b – *Variaciones del ruido radioeléctrico con la frecuencia (Invierno; 0000-0400 hora local)*

——— Valeurs attendues du bruit atmosphérique/Expected values of atmospheric noise/Valores probables del ruido atmosférico

—·—·— Valeurs attendues du bruit artificiel en un emplacement de réception calme/Expected values of man-made noise at a quiet receiving location/Valores probables del ruido artificial en un punto de recepción tranquilo

– – – – – Valeurs attendues du bruit galactique/Expected values of galactic noise/Valores probables del ruido galáctico

Note – Pour des raisons d'ordre pratique, le point anglais a été utilisé dans cette version trilingue au lieu de la virgule décimale.

Nota – Por razones prácticas se ha utilizado un punto en lugar de una coma para indicar las cifras

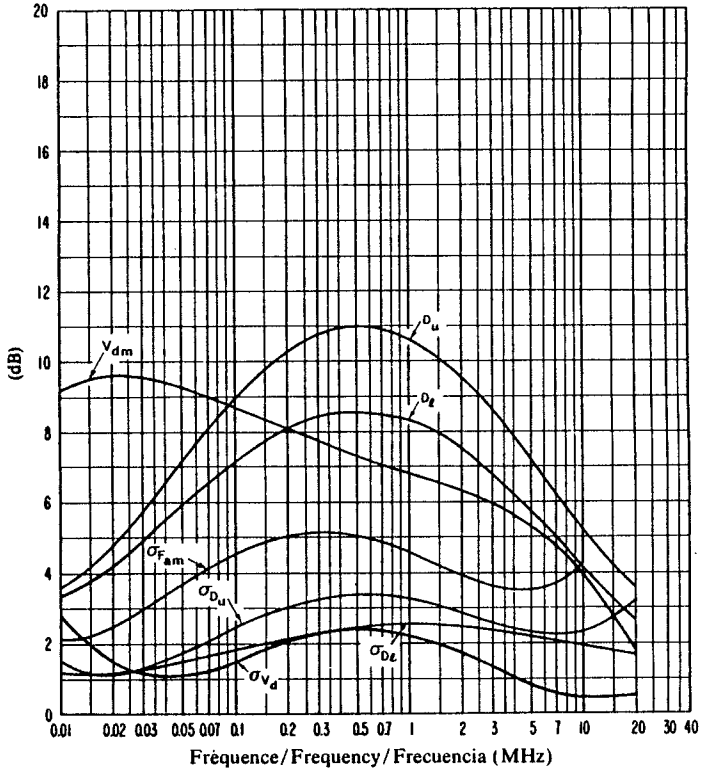

FIGURE 2c – *Données sur la variabilité et le caractère du bruit (Hiver; 0000-0400 heure locale)*

FIGURE 2c – *Data on noise variability and character (Winter; 0000-0400 LT)*

FIGURA 2c – *Datos sobre la variabilidad y el carácter del ruido (Invierno; 0000-0400 hora local)*

$\sigma_{F_{am}}$ – Ecart type des valeurs de F_{am}/Standard deviation of values of F_{am}/Desviación típica de los valores de F_{am}

D_u – Rapport du décile supérieur à la valeur médiane de F_{am}/Ratio of upper decile to median value, F_{am}/Relación del decilo superior al valor mediano, F_{am}

σ_{D_u} – Ecart type des valeurs de D_u/Standard deviation of values of D_u/Desviación típica de los valores de D_u

D_l – Rapport de la valeur médiane de F_{am} au décile inférieur/Ratio of median value, F_{am}, to lower decile/Relación del valor mediano F_{am} al decilo inferior

σ_{D_l} – Ecart type des valeurs de D_l/Standard deviation of value of D_l/Desviación típica de los valores de D_l

V_{dm} – Valeur attendue de l'écart médian de la tension moyenne (valeurs pour une largeur de bande de 200 Hz)/Expected value of median deviation of average voltage. The values shown are for a bandwidth of 200 Hz/Valor probable de la desviación mediana de la tensión media (valores para una anchura de banda de 200 Hz)

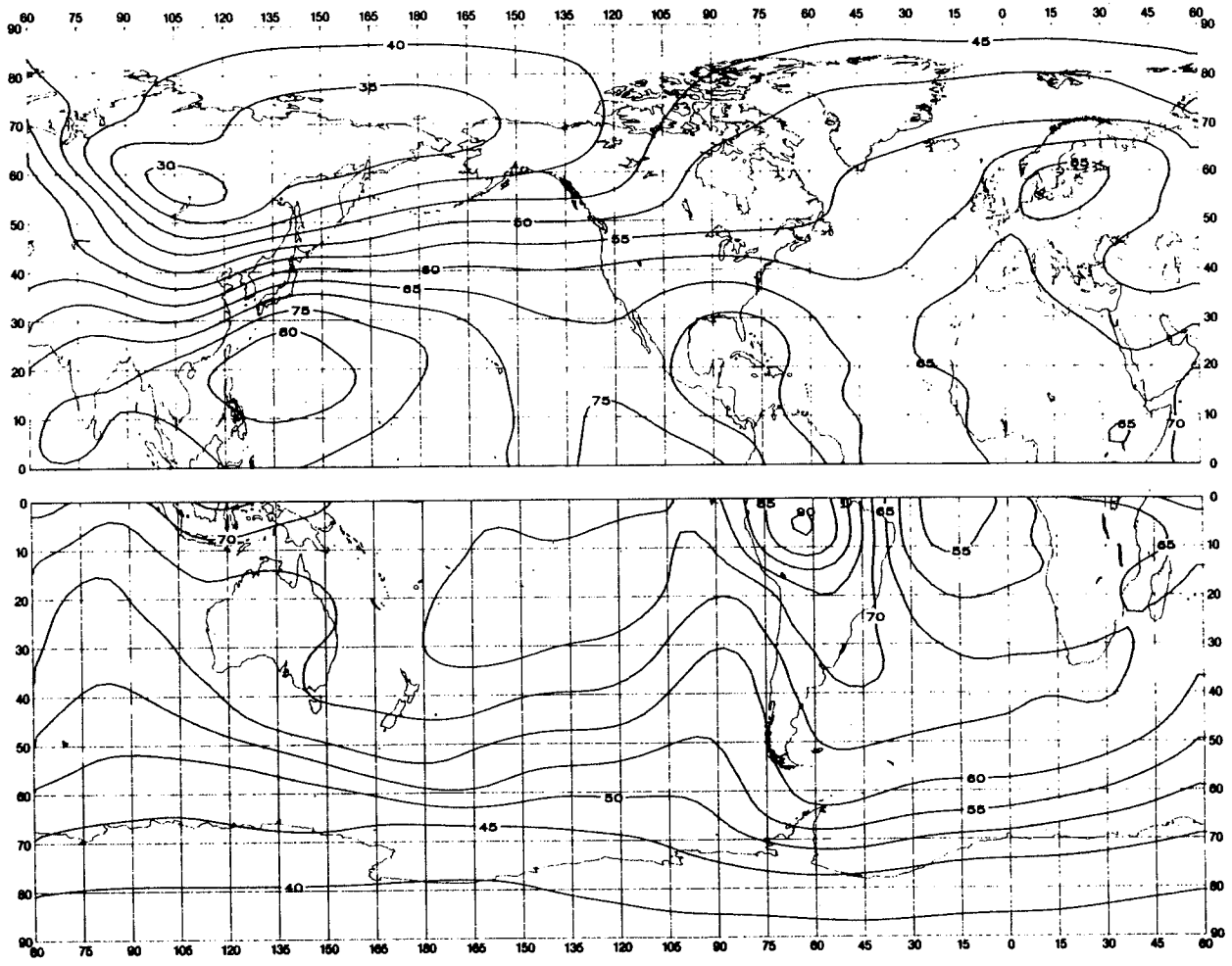

FIGURE 3a – *Valeurs attendues du bruit atmosphérique radioélectrique, F_{am}, en dB au-dessus de kT_0b à 1 MHz (Hiver; 0400-0800 heure locale)*
FIGURE 3a – *Expected values of atmospheric radio noise, F_{am} (dB above kT_0b at 1 MHz) (Winter; 0400-0800 LT)*
FIGURA 3a – *Valores probables del ruido atmosférico, F_{am}, en dB por encima de kT_0b en 1 MHz (Invierno; 0400-0800 hora local)*

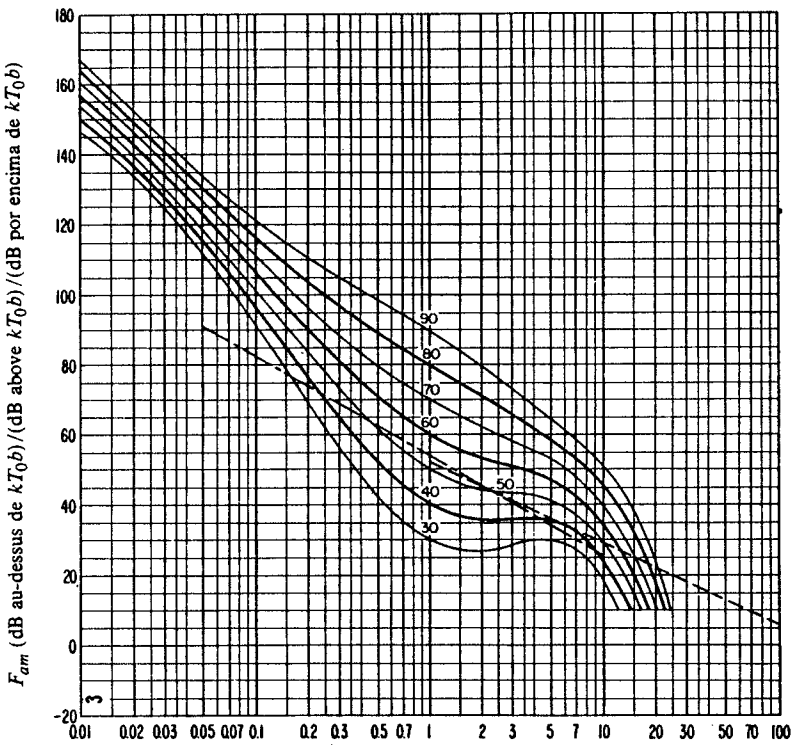

FIGURE 3b – *Variation du bruit radioélectrique en fonction de la fréquence (Hiver; 0400-0800 heure locale)*

FIGURE 3b – *Variation of radio noise with frequency (Winter; 0400-0800 LT)*

FIGURA 3b – *Variaciones del ruido radioeléctrico con la frecuencia (Invierno; 0400-0800 hora local)*

Voir la légende de la Fig. 2b/See legend of Fig. 2b/Véase la leyenda de la fig. 2b

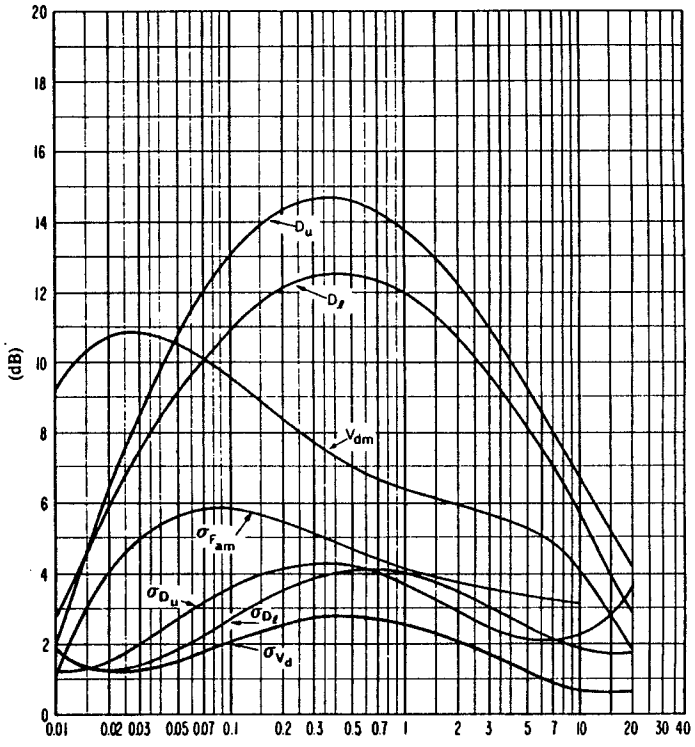

FIGURE 3c – *Données sur la variabilité et le caractère du bruit (Hiver; 0400-0800 heure locale)*

FIGURE 3c – *Data on noise variability and character (Winter; 0400-0800 LT)*

FIGURA 3c – *Datos sobre la variabilidad y el carácter del ruido (Invierno; 0400-0800 hora local)*

Voir la légende de la Fig. 2c/See legend of Fig. 2c/Véase la leyenda de la fig. 2c

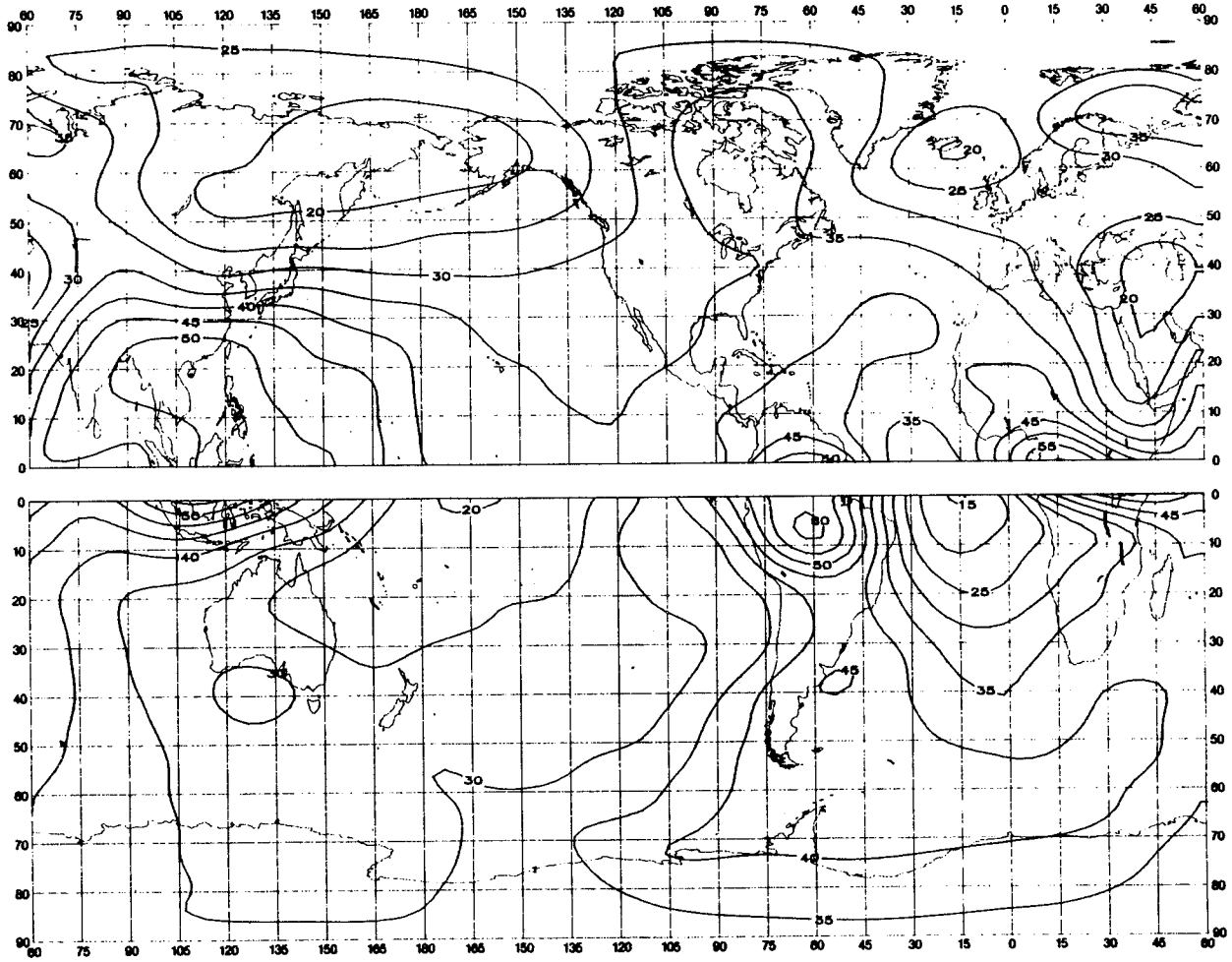

FIGURE 4a – *Valeurs attendues du bruit atmospherique radioélectrique, F_{am}, en dB au-dessus de kT_0b à 1 MHz (Hiver; 0800-1200 heure locale)*
FIGURE 4a – *Expected values of atmospheric radio noise, F_{am} (dB above kT_0b at 1 MHz) (Winter; 0800-1200 LT)*
FIGURA 4a – *Valores probables del ruido atmosférico, F_{am}, en dB por encima de kT_0b en 1 MHz (Invierno; 0800-1200 hora local)*

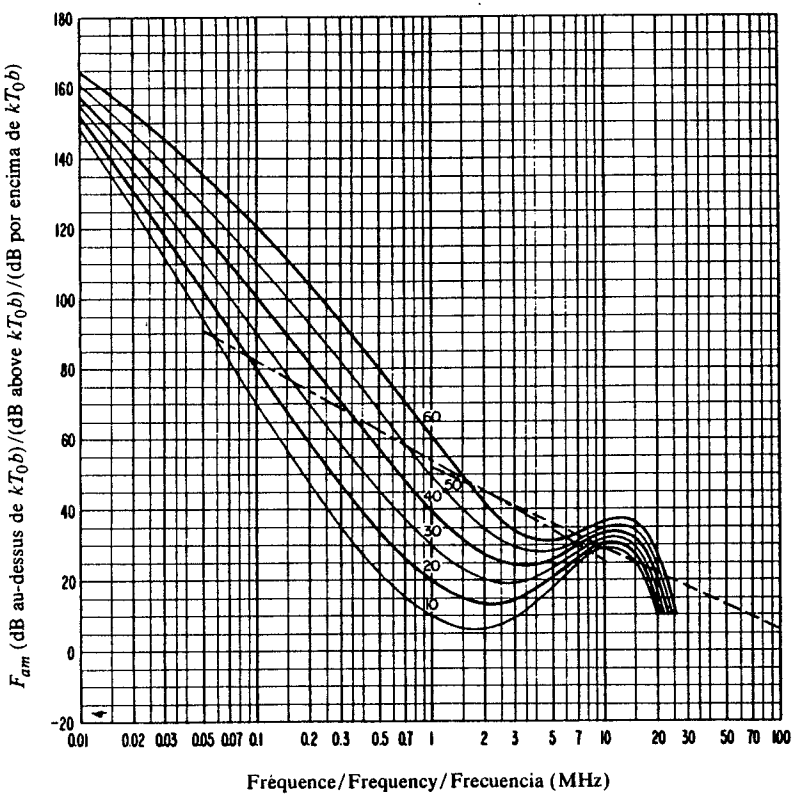

FIGURE 4b – *Variation du bruit radioélectrique en fonction de la fréquence (Hiver; 0800-1200 heure locale)*

FIGURE 4b – *Variation of radio noise with frequency (Winter; 0800-1200 LT)*

FIGURA 4b – *Variaciones del ruido radioeléctrico con la frecuencia (Invierno; 0800-1200 hora local)*

Voir la légende de la Fig. 2b/See legend of Fig. 2b/Véase la leyenda de la fig. 2b

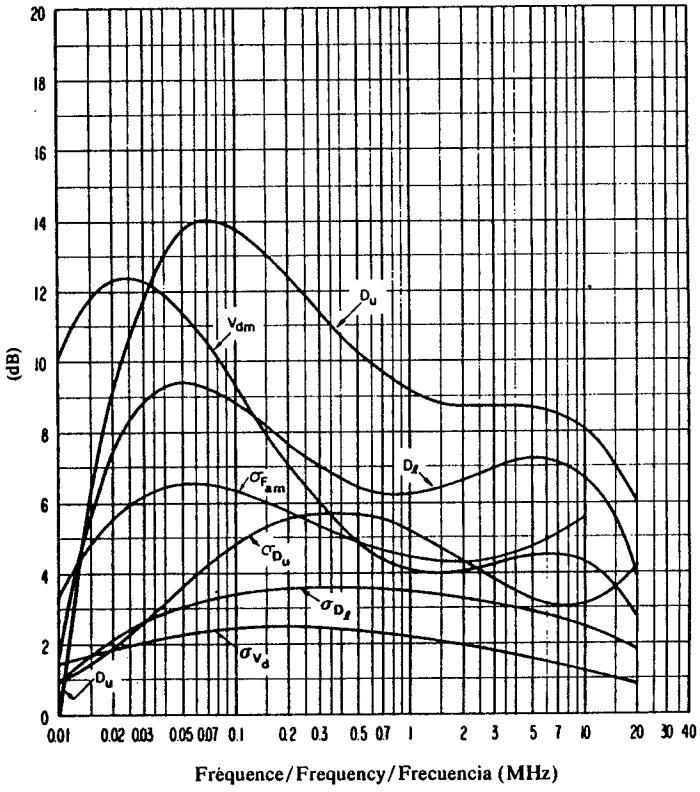

FIGURE 4c – *Données sur la variabilité et le caractère du bruit (Hiver; 0800-1200 heure locale)*

FIGURE 4c – *Data on noise variability and character (Winter; 0800-1200 LT)*

FIGURA 4c – *Datos sobre la variabilidad y el carácter del ruido (Invierno; 0800-1200 hora local)*

Voir la légende de la Fig. 2c/See legend of Fig. 2c/Véase la leyenda de la fig. 2c

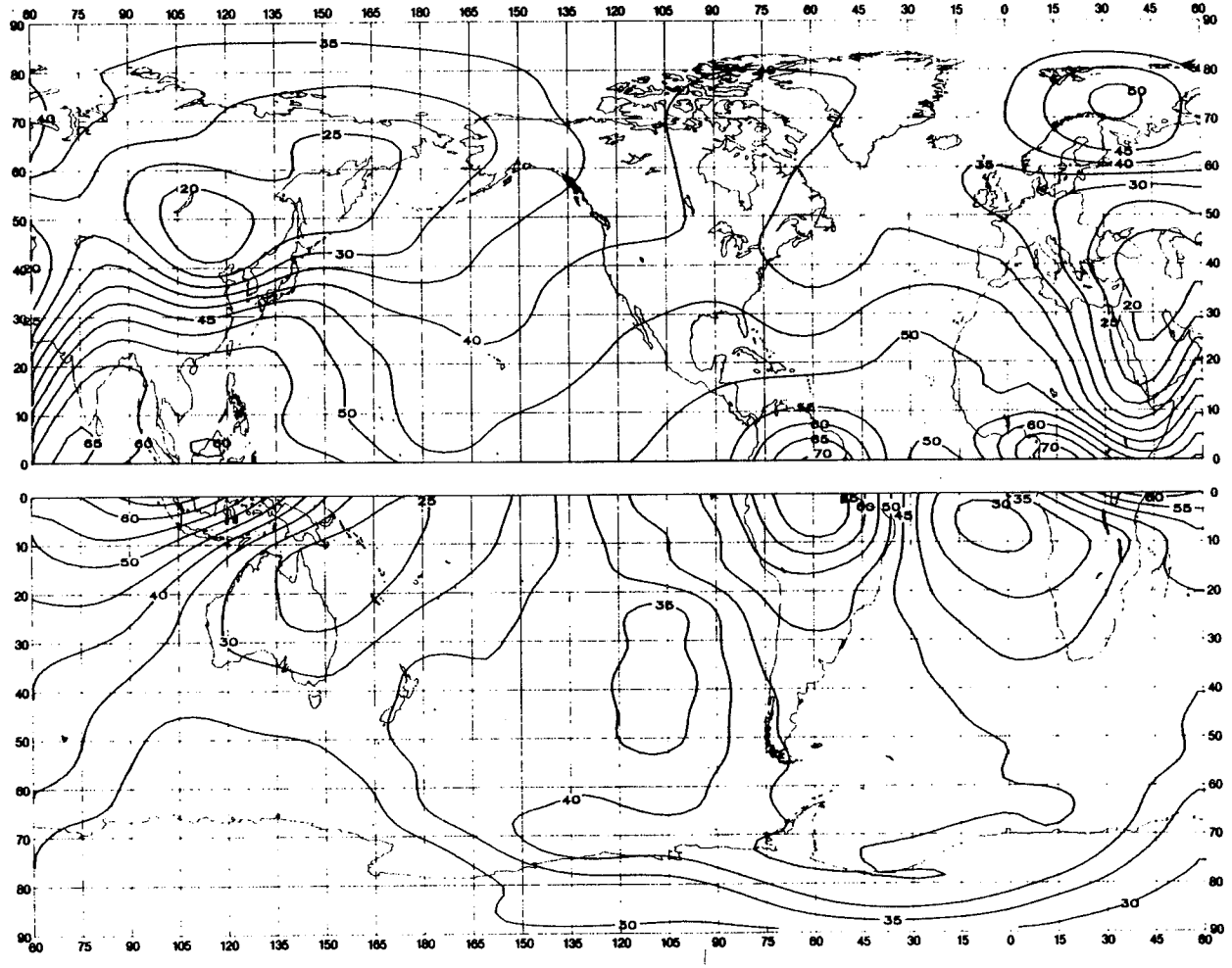

FIGURE 5a – *Valeurs attendues du bruit atmosphérique radioélectrique, F_{am}, en dB au-dessus de kT_0b à 1 MHz (Hiver; 1200-1600 heure locale)*
FIGURE 5a – *Expected values of atmospheric radio noise, F_{am} (dB above kT_0b at 1 MHz) (Winter; 1200-1600 LT)*
FIGURA 5a – *Valores probables del ruido atmosférico, F_{am}, en dB por encima de kT_0b en 1 MHz (Invierno; 1200-1600 hora local)*

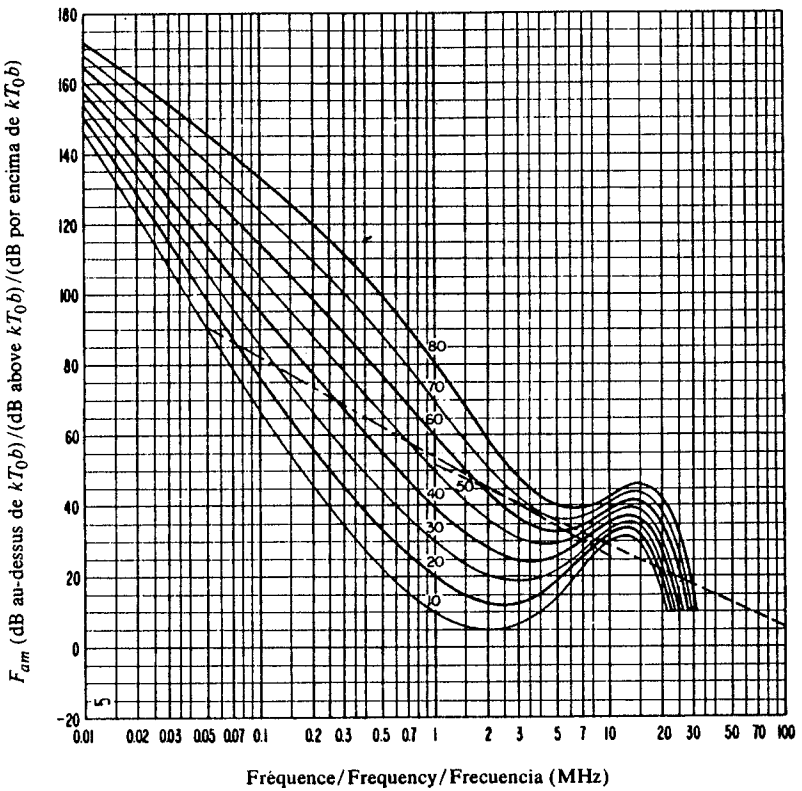

FIGURE 5b – *Variation du bruit radioélectrique en fonction de la fréquence (Hiver; 1200-1600 heure locale)*

FIGURE 5b – *Variation of radio noise with frequency (Winter; 1200-1600 LT)*

FIGURA 5b – *Variaciones del ruido radioeléctrico con la frecuencia (Invierno; 1200-1600 hora local)*

Voir la légende de la Fig. 2b/See legend of Fig. 2b/Véase la leyenda de la fig. 2b

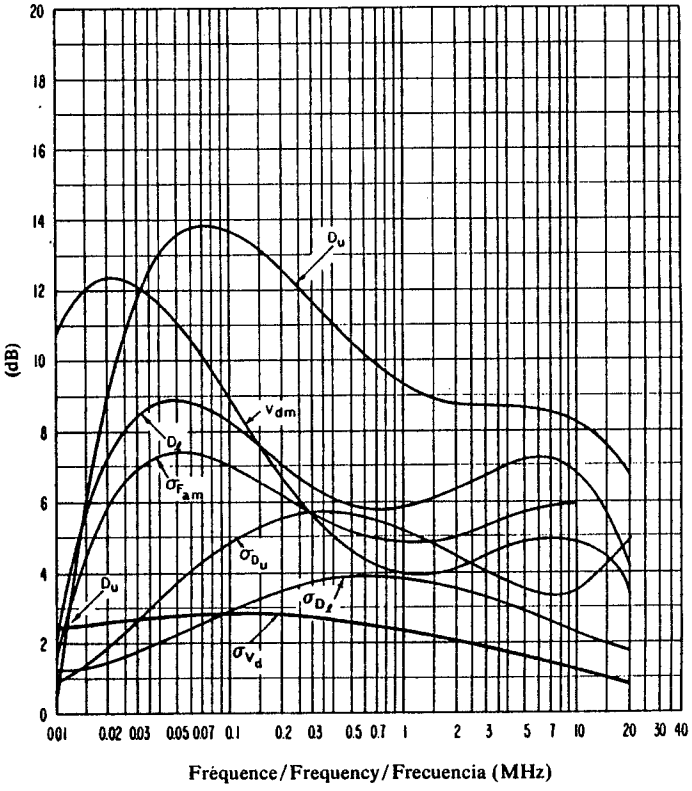

FIGURE 5c – *Données sur la variabilité et le caractère du bruit (Hiver; 1200-1600 heure locale)*

FIGURE 5c – *Data on noise variability and character (Winter; 1200-1600 LT)*

FIGURA 5c – *Datos sobre la variabilidad y el carácter del ruido (Invierno; 1200-1600 hora local)*

Voir la légende de la Fig. 2c/See legend of Fig. 2c/Véase la leyenda de la fig. 2c

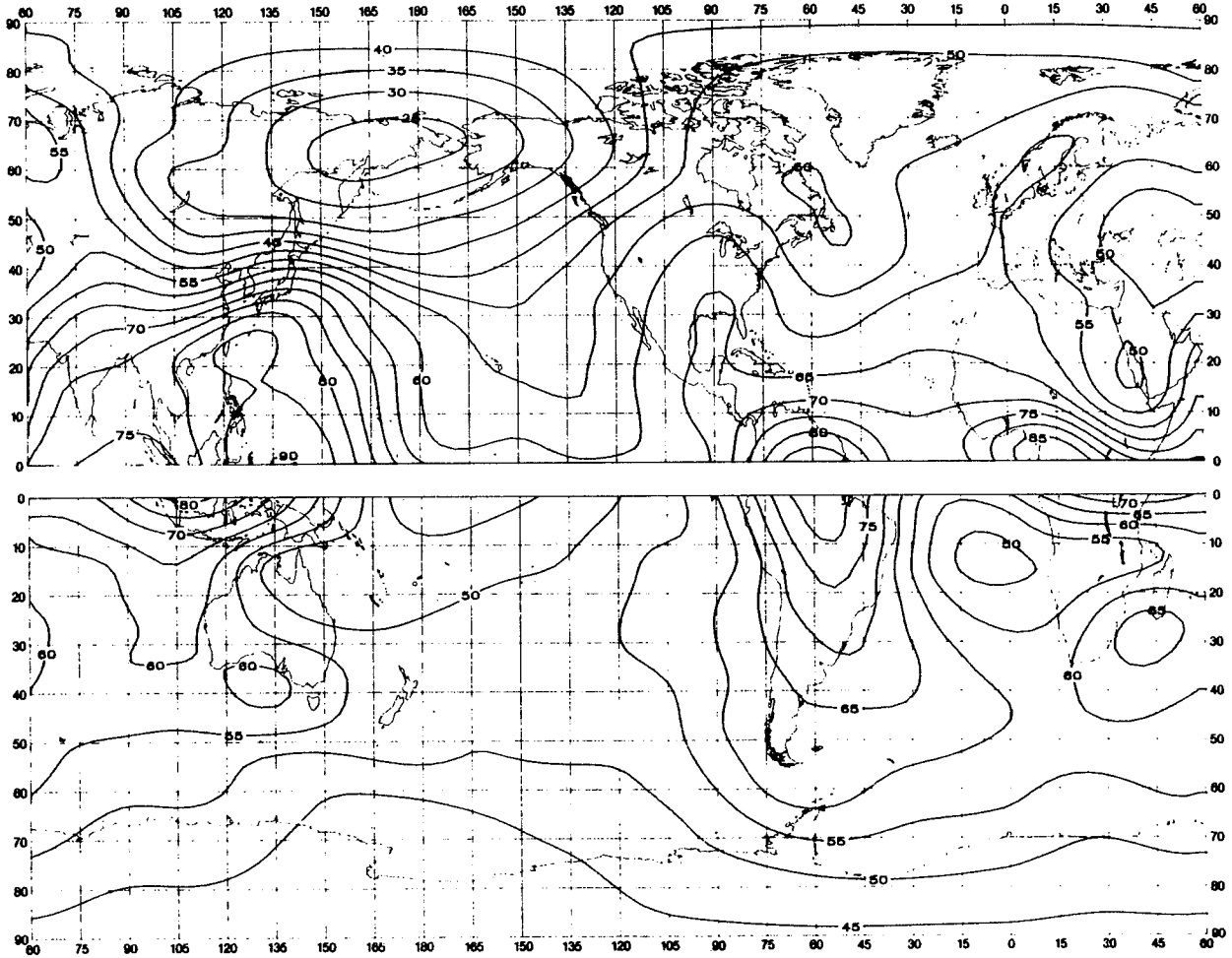

FIGURE 6a – *Valeurs attendues du bruit atmosphérique radioélectrique, F_{am}, en dB au-dessus de kT_0b à 1 MHz (Hiver; 1600-2000 heure locale)*
FIGURE 6a – *Expected values of atmospheric radio noise, F_{am} (dB above kT_0b at 1 MHz) (Winter; 1600-2000 LT)*
FIGURA 6a – *Valores probables del ruido atmosférico, F_{am}, en dB por encima de kT_0b en 1 MHz (Invierno; 1600-2000 hora local)*

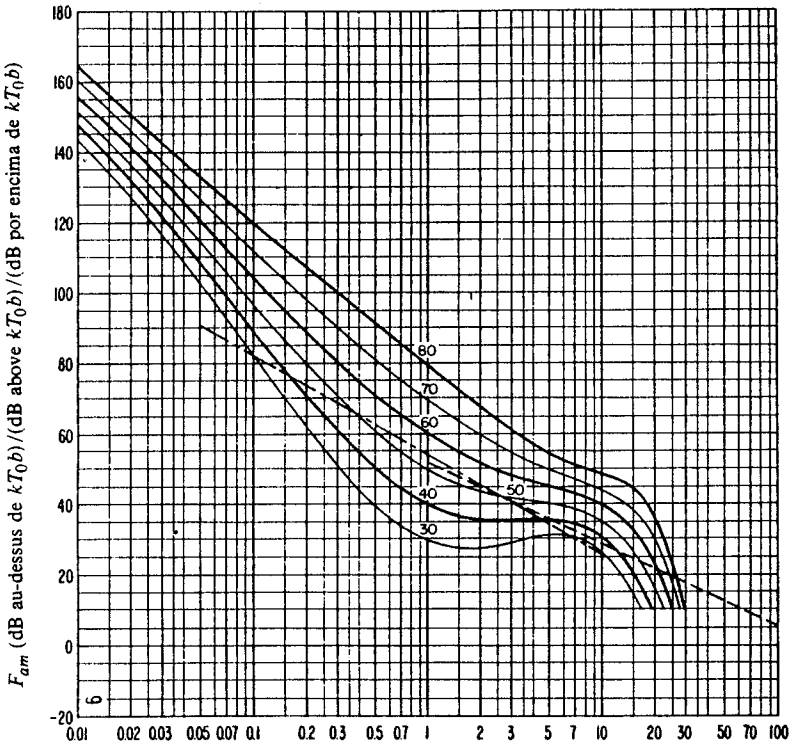

FIGURE 6b – *Variation du bruit radioélectrique en fonction de la fréquence (Hiver; 1600-2000 heure locale)*

FIGURE 6b – *Variation of radio noise with frequency (Winter; 1600-2000 LT)*

FIGURA 6b – *Variaciones del ruido radioeléctrico con la frecuencia (Invierno; 1600-2000 hora local)*

Voir la lègende de la Fig. 2b/See legend of Fig. 2b/Véase la leyenda de la fig. 2b

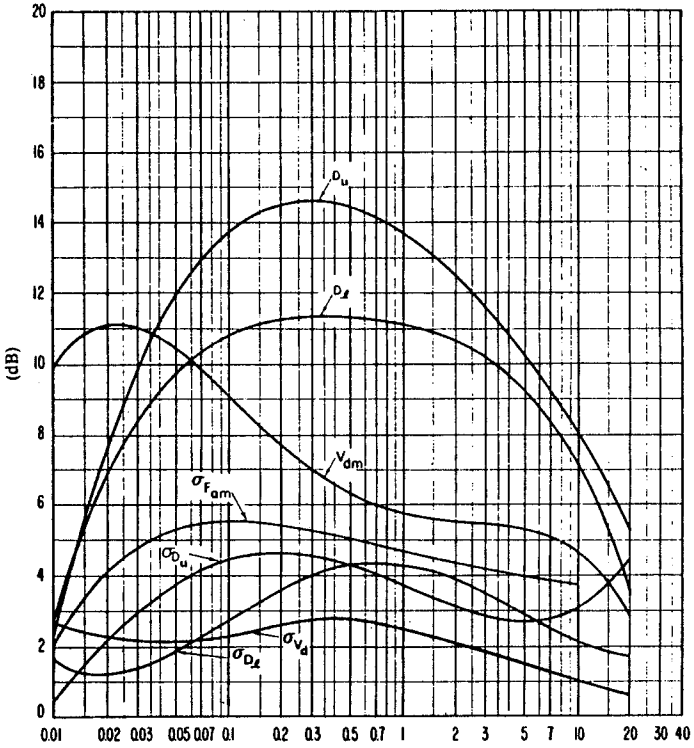

FIGURE 6c – *Données sur la variabilité et le caractère du bruit (Hiver; 1600-2000 heure locale)*

FIGURE 6c – *Data on noise variability and character (Winter; 1600-2000 LT)*

FIGURA 6c – *Datos sobre la variabilidad y el carácter del ruido (Invierno; 1600-2000 hora local)*

Voir la lègende de la Fig. 2c/See legend of Fig. 2c/Véase la leyenda de la fig. 2c

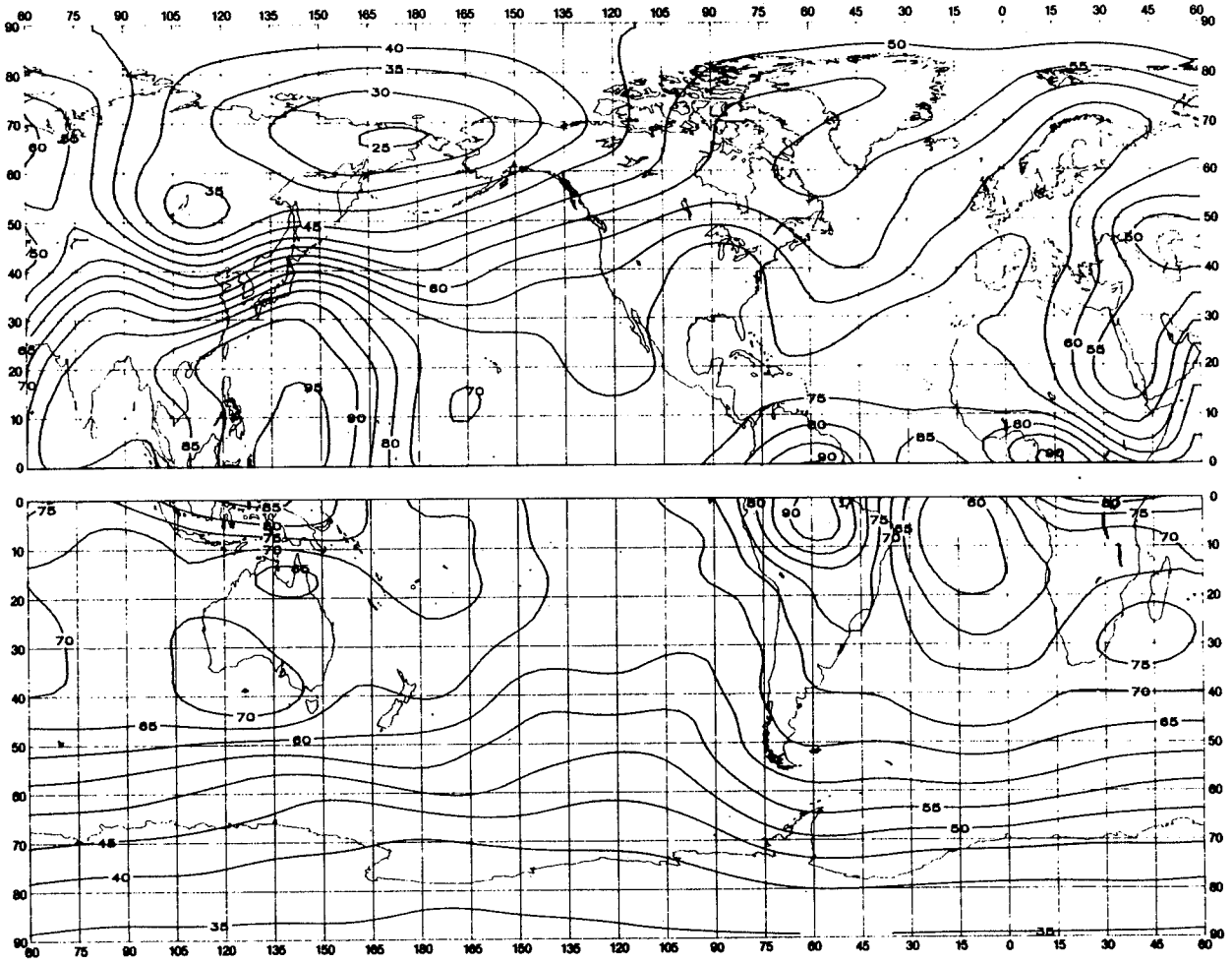

FIGURE 7a – *Valeurs attendues du bruit atmosphérique radioélectrique, F_{am}, en dB au-dessus de kT_0b à 1 MHz (Hiver; 2000-2400 heure locale)*
FIGURE 7a – *Expected values of atmospheric radio noise, F_{am} (dB above kT_0b at 1 MHz) (Winter; 2000-2400 LT)*
FIGURA 7a – *Valores probables del ruido atmosférico, F_{am}, en dB por encima de kT_0b en 1 MHz (Invierno; 2000-2400 hora local)*

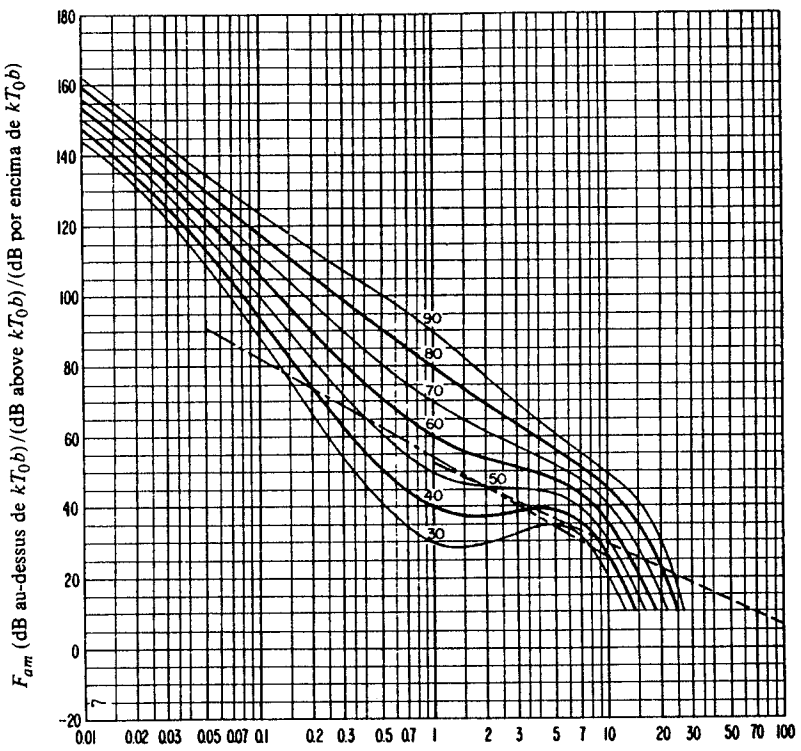

FIGURE 7b – *Variation du bruit radioélectrique en fonction de la fréquence (Hiver; 2000-2400 heure locale)*

FIGURE 7b – *Variation of radio noise with frequency (Winter; 2000-2400 LT)*

FIGURA 7b – *Variaciones del ruido radioeléctrico con la frecuencia (Invierno; 2000-2400 hora local)*

Voir la légende de la Fig. 2b/See legend of Fig. 2b/Véase la leyenda de la fig. 2b

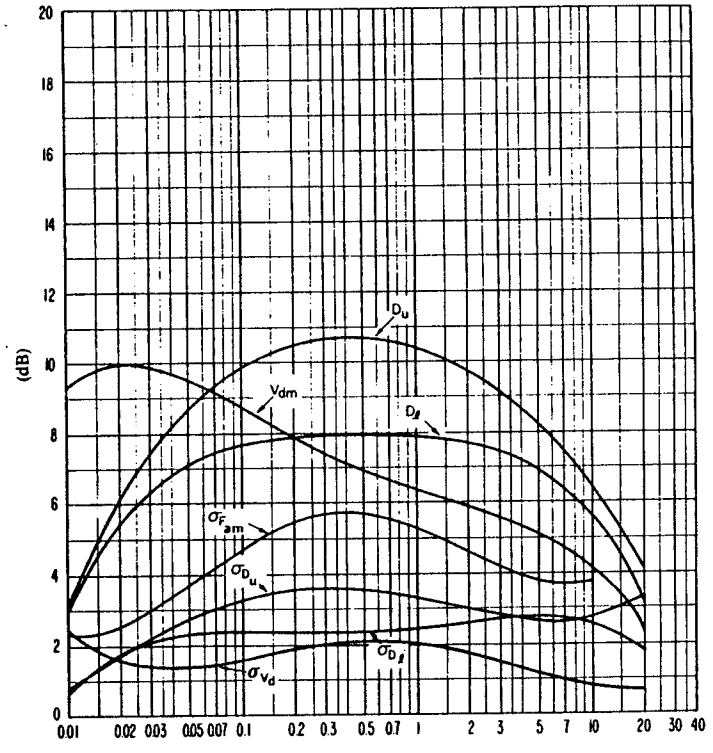

FIGURE 7c – *Données sur la variabilité et le caractère du bruit (Hiver; 2000-2400 heure locale)*

FIGURE 7c – *Data on noise variability and character (Winter; 2000-2400 LT)*

FIGURA 7c – *Datos sobre la variabilidad y el carácter del ruido (Invierno; 2000-2400 hora local)*

Voir la légende de la Fig. 2c/See legend of Fig. 2c/Véase la leyenda de la fig. 2c

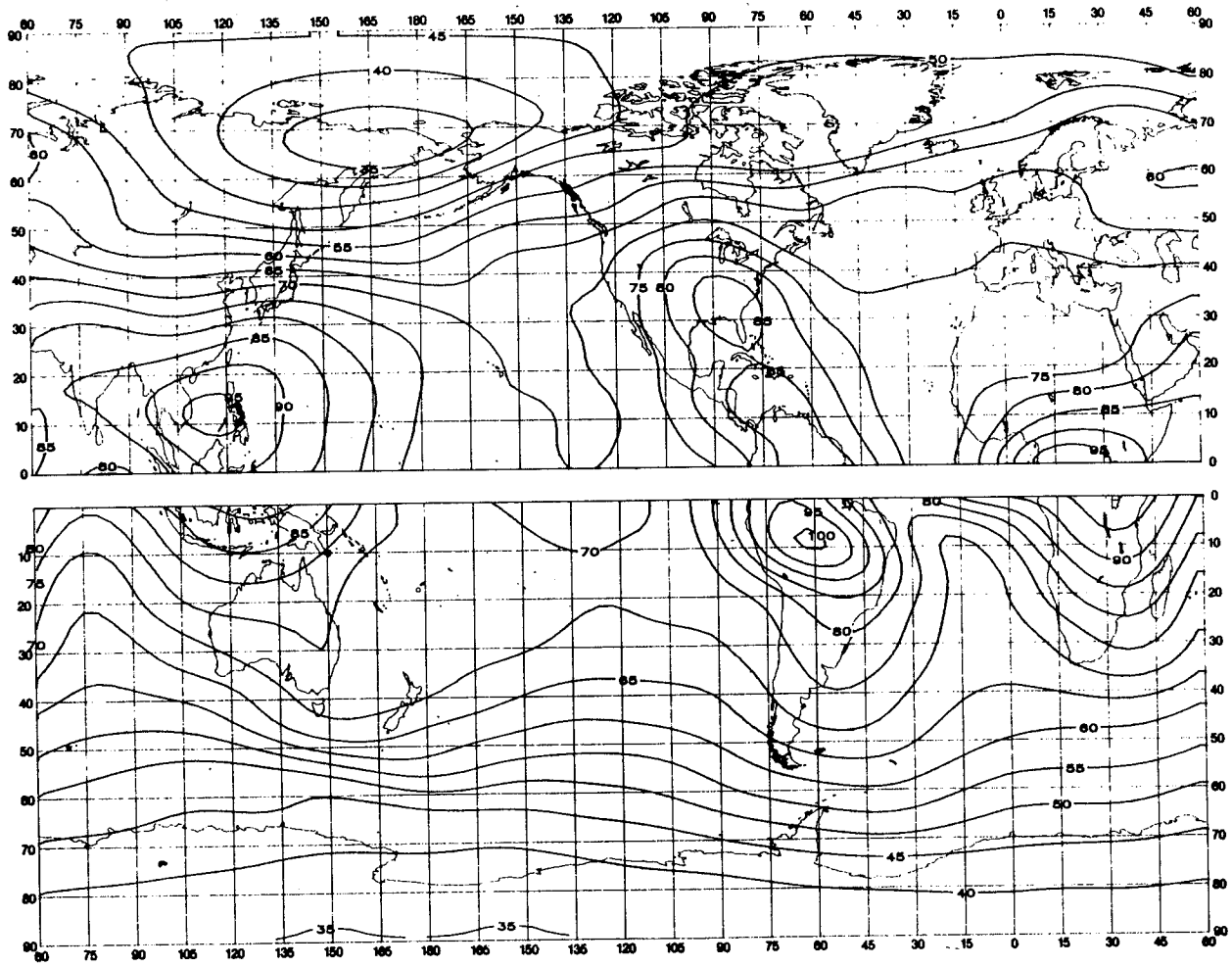

FIGURE 8a – *Valeurs attendues du bruit atmosphèrique radioélectrique, F_{am}, en dB au-dessus de kT_0b à 1 MHz (Printemps; 0000-0400 heure locale)*
FIGURE 8a – *Expected values of atmospheric radio noise, F_{am} (dB above kT_0b at 1 MHz) (Spring; 0000-0400 LT)*
FIGURA 8a – *Valores probables del ruido atmosférico, F_{am}, en dB por encima de kT_0b en 1 MHz (Primavera; 0000-0400 hora local)*

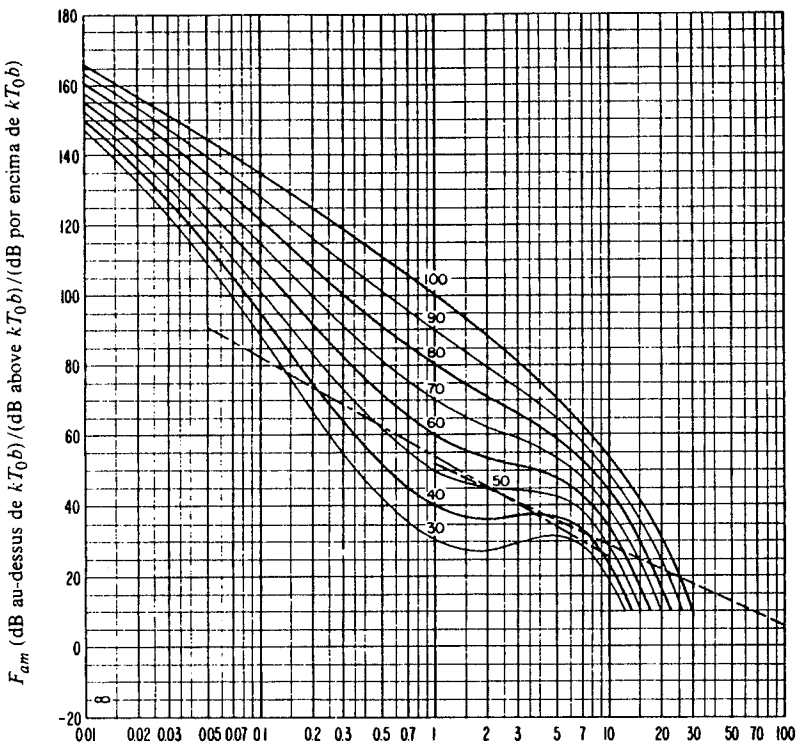

FIGURE 8b – *Variation du bruit radioélectrique en fonction de la fréquence (Printemps; 0000-0400 heure locale)*

FIGURE 8b – *Variation of radio noise with frequency (Spring; 0000-0400 LT)*

FIGURA 8b – *Variaciones del ruido radioeléctrico con la frecuencia (Primavera; 0000-0400 hora local)*

Voir la légende de la Fig. 2b/See legend of Fig. 2b/Véase la leyenda de la fig. 2b

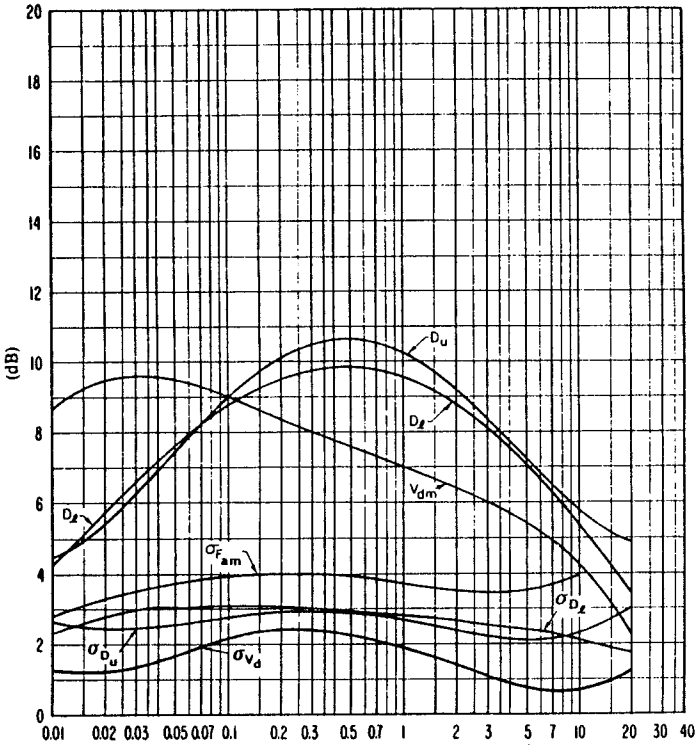

FIGURE 8c – *Données sur la variabilité et le caractère du bruit (Printemps; 0000-0400 heure locale)*

FIGURE 8c – *Data on noise variability and character (Spring; 0000-0400 LT)*

FIGURA 8c – *Datos sobre la variabilidad y el carácter del ruido (Primavera; 0000-0400 hora local)*

Voir la légende de la Fig. 2c/See legend of Fig. 2c/Véase la leyenda de la fig. 2c

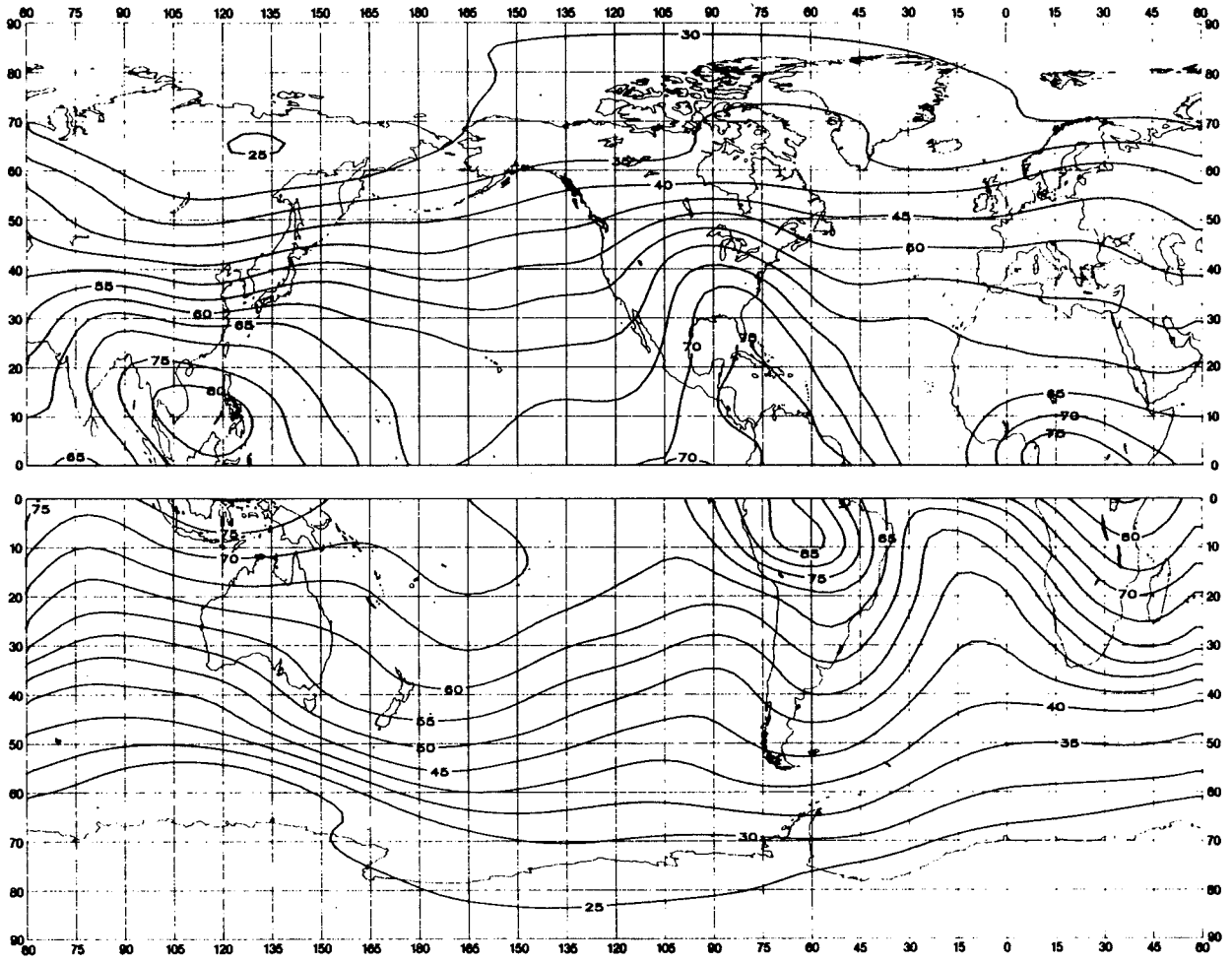

FIGURE 9a – *Valeurs attendues du bruit atmosphérique radioélectrique, F_{am}, en dB au-dessus de kT_0b à 1 MHz (Printemps; 0400-0800 heure locale)*
FIGURE 9a – *Expected values of atmospheric radio noise, F_{am} (dB above kT_0b at 1 MHz) (Spring; 0400-0800 LT)*
FIGURA 9a – *Valores probables del ruido atmosférico, F_{am}, en dB por encima de kT_0b en 1 MHz (Primavera; 0400-0800 hora local)*

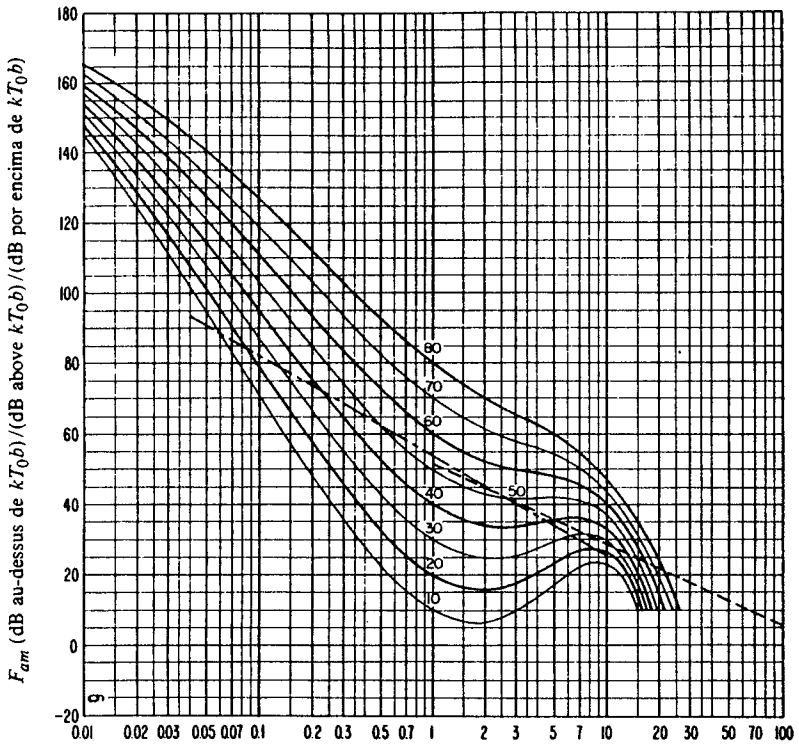

FIGURE 9b – *Variation du bruit radioélectrique en fonction de la fréquence (Printemps; 0400-0800 heure locale)*

FIGURE 9b – *Variation of radio noise with frequency (Spring; 0400-0800 LT)*

FIGURA 9b – *Variaciones del ruido radioeléctrico con la frecuencia (Primavera; 0400-0800 hora local)*

Voir la légende de la Fig. 2b/See legend of Fig. 2b/Véase la leyenda de la fig. 2b

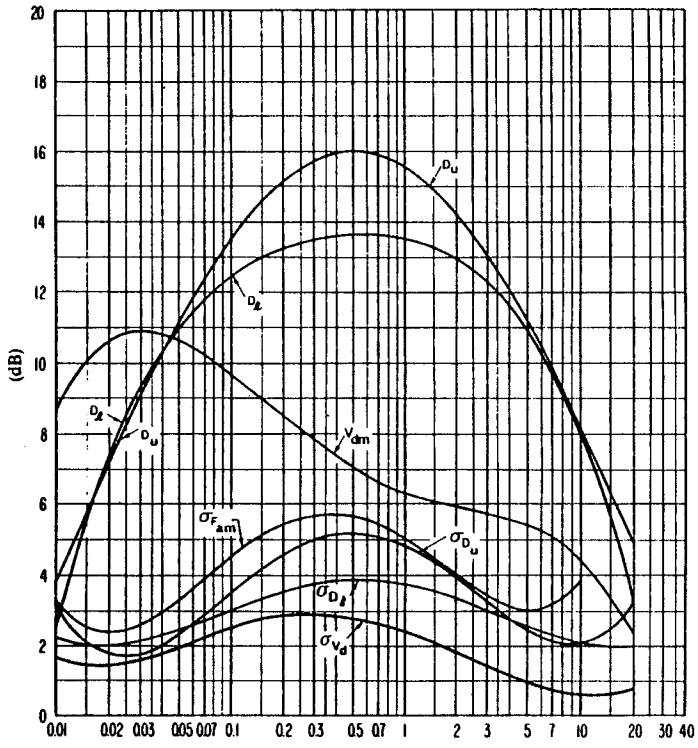

FIGURE 9c – *Données sur la variabilité et le caractère du bruit (Printemps; 0400-0800 heure locale)*

FIGURE 9c – *Data on noise variability and character (Spring; 0400-0800 LT)*

FIGURA 9c – *Datos sobre la variabilidad y el carácter del ruido (Primavera; 0400-0800 hora local)*

Voir la légende de la Fig. 2c/See legend of Fig. 2c/Véase la leyenda de la fig. 2c

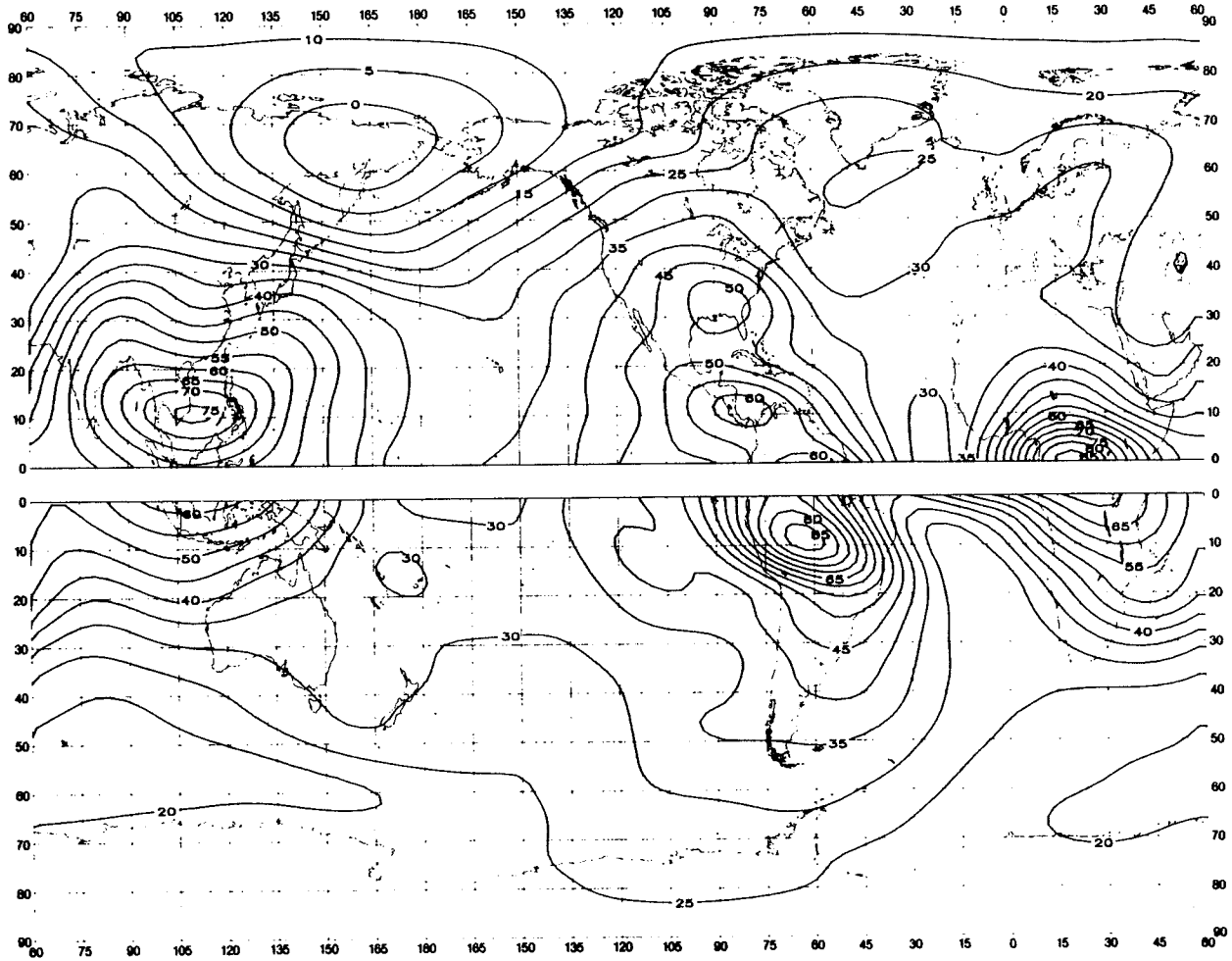

FIGURE 10a – *Valeurs attendues du bruit atmospherique radioélectrique, F_{am}, en dB au-dessus de kT_0b à 1 MHz (Printemps; 0800-1200 heure locale)*
FIGURE 10a – *Expected values of atmospheric radio noise, F_{am} (dB above kT_0b at 1 MHz) (Spring; 0800-1200 LT)*
FIGURA 10a – *Valores probables del ruido atmosférico, F_{am}, en dB por encima de kT_0b en 1 MHz (Primavera; 0800-1200 hora local)*

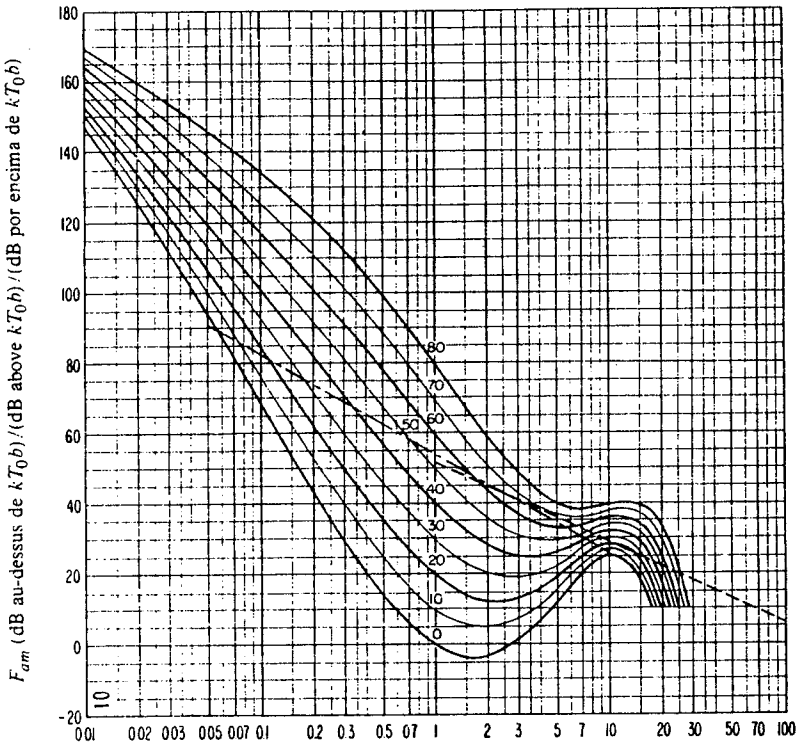

FIGURE 10b – *Variation du bruit radioélectrique en fonction de la fréquence (Printemps; 0800-1200 heure locale)*

FIGURE 10b – *Variation of radio noise with frequency (Spring; 0800-1200 LT)*

FIGURA 10b – *Variaciones del ruido radioeléctrico con la frecuencia (Primavera; 0800-1200 hora local)*

Voir la légende de la Fig. 2b/See legend of Fig. 2b/Vease la leyenda de la fig. 2b

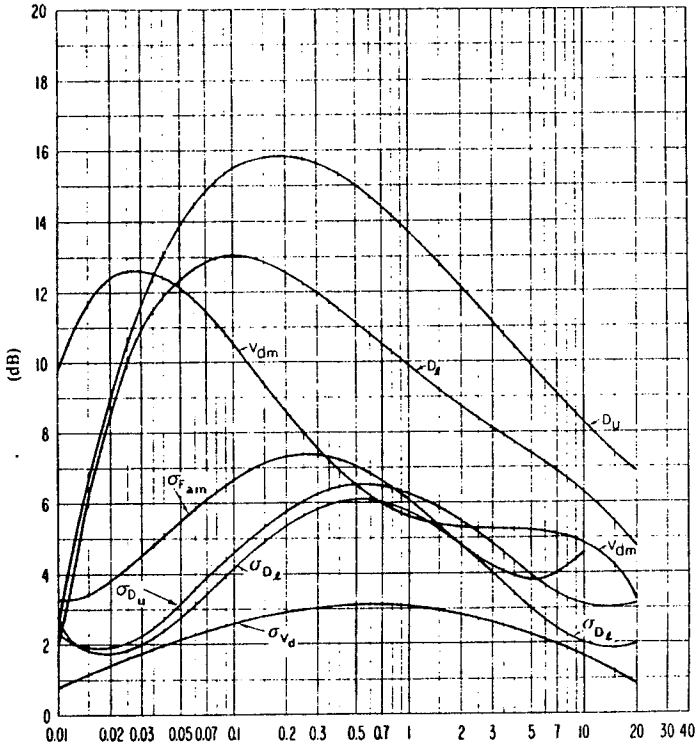

FIGURE 10c – *Données sur la variabilité et le caractère du bruit (Printemps; 0800-1200 heure locale)*

FIGURE 10c – *Data on noise variability and character (Spring; 0800-1200 LT)*

FIGURA 10c – *Datos sobre la variabilidad y el carácter del ruido (Primavera; 0800-1200 hora local)*

Voir la légende de la Fig. 2c/See legend of Fig. 2c/Véase la leyenda de la fig. 2c

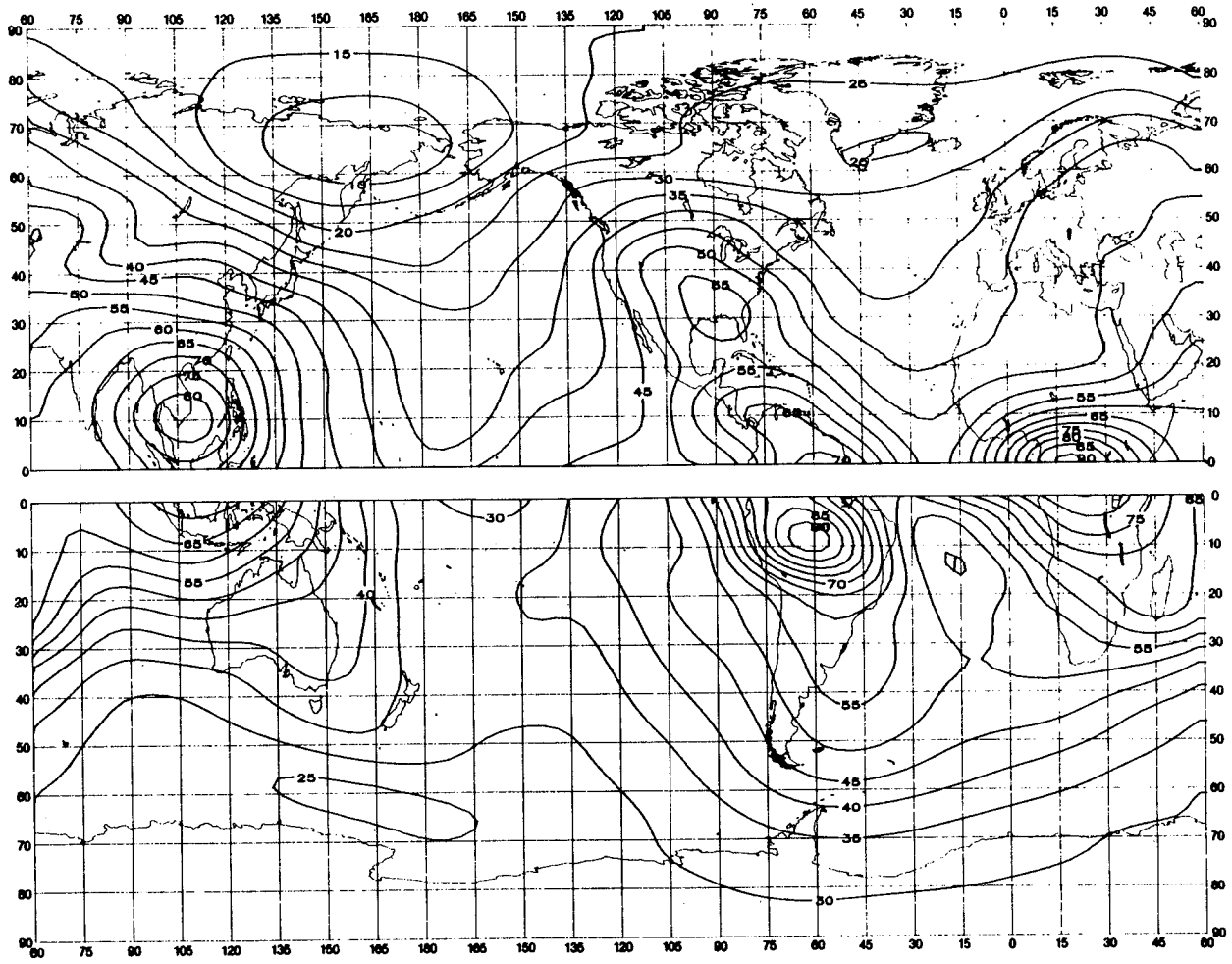

FIGURE 11a – *Valeurs attendues du bruit atmosphérique radioélectrique, F_{am}, en dB au-dessus de kT_0b à 1 MHz (Printemps; 1200-1600 heure locale)*
FIGURE 11a – *Expected values of atmospheric radio noise, F_{am} (dB above kT_0b at 1 MHz) (Spring; 1200-1600 LT)*
FIGURA 11a – *Valores probables del ruido atmosférico, F_{am}, en dB por encima de kT_0b en 1 MHz (Primavera; 1200-1600 hora local)*

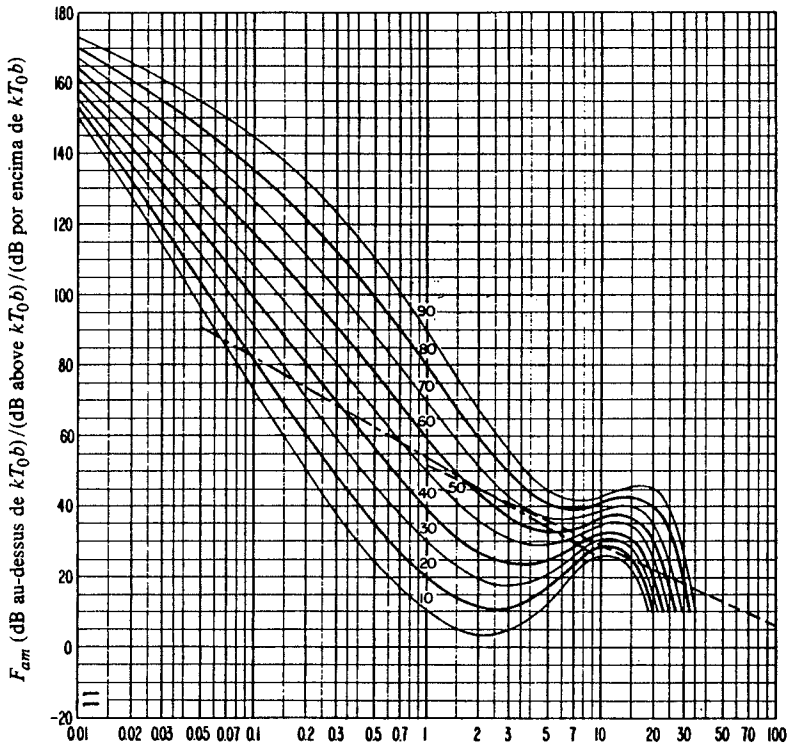

FIGURE 11b – *Variation du bruit radioélectrique en fonction de la fréquence (Printemps; 1200-1600 heure locale)*

FIGURE 11b – *Variation of radio noise with frequency (Spring; 1200-1600 LT)*

FIGURA 11b – *Variaciones del ruido radioeléctrico con la frecuencia (Primavera; 1200-1600 hora local)*

Voir la légende de la Fig. 2b/See legend of Fig. 2b/Véase la leyenda de la fig. 2b

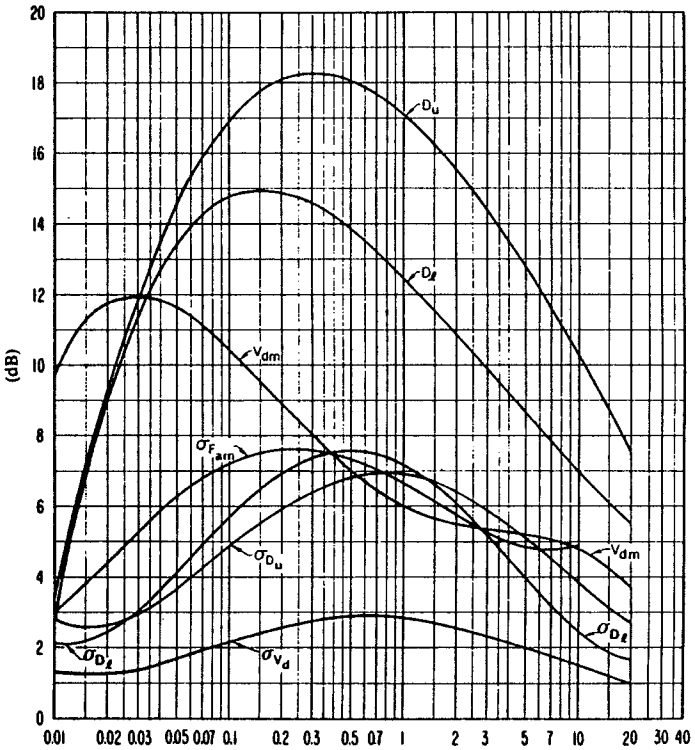

FIGURE 11c – *Données sur la variabilité et le caractère du bruit (Printemps; 1200-1600 heure locale)*

FIGURE 11c – *Data on noise variability and character (Spring; 1200-1600 LT)*

FIGURA 11c – *Datos sobre la variabilidad y el carácter del ruido (Primavera; 1200-1600 hora local)*

Voir la légende de la Fig. 2c/See legend of Fig. 2c/Véase la leyenda de la fig. 2c

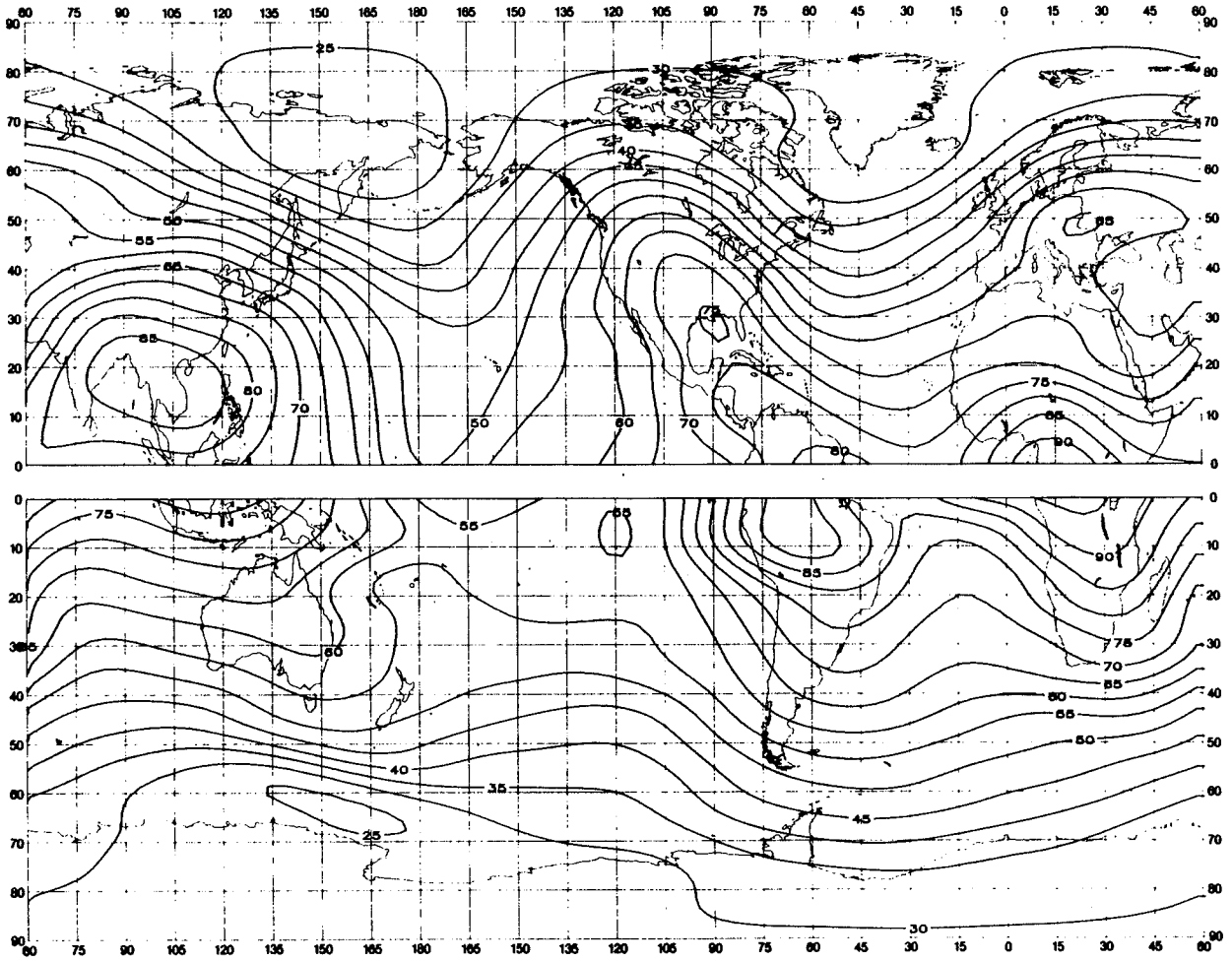

FIGURE 12a – *Valeurs attendues du bruit atmosphérique radioélectrique, F_{am}, en dB au-dessus de kT_0b à 1 MHz (Printemps; 1600-2000 heure locale)*
FIGURE 12a – *Expected values of atmospheric radio noise, F_{am} (dB above kT_0b at 1 MHz) (Spring; 1600-2000 LT)*
FIGURA 12a – *Valores probables del ruido atmosférico, F_{am}, en dB por encima de kT_0b en 1 MHz (Primavera; 1600-2000 hora local)*

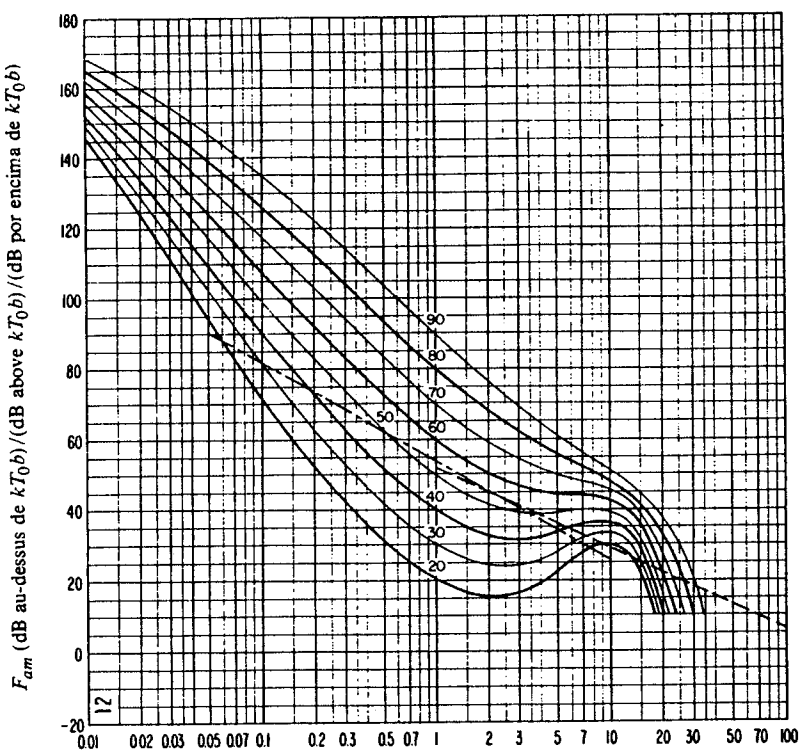

FIGURE 12b – *Variation du bruit radioélectrique en fonction de la fréquence (Printemps; 1600-2000 heure locale)*

FIGURE 12b – *Variation of radio noise with frequency (Spring; 1600-2000 LT)*

FIGURA 12b – *Variaciones del ruido radioeléctrico con la frecuencia (Primavera; 1600-2000 hora local)*

Voir la lègende de la Fig. 2b/See legend of Fig. 2b/Véase la leyenda de la fig. 2b

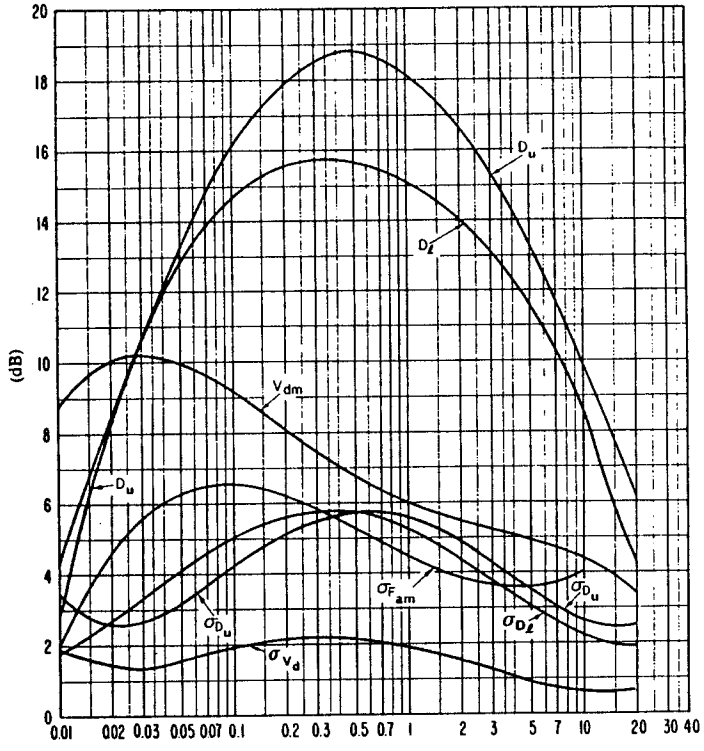

FIGURE 12c – *Données sur la variabilité et le caractère du bruit (Printemps; 1600-2000 heure locale)*

FIGURE 12c – *Data on noise variability and character (Spring; 1600-2000 LT)*

FIGURA 12c – *Datos sobre la variabilidad y el carácter del ruido (Primavera; 1600-2000 hora local)*

Voir la lègende de la Fig. 2c/See legend of Fig. 2c/Véase la leyenda de la fig. 2c

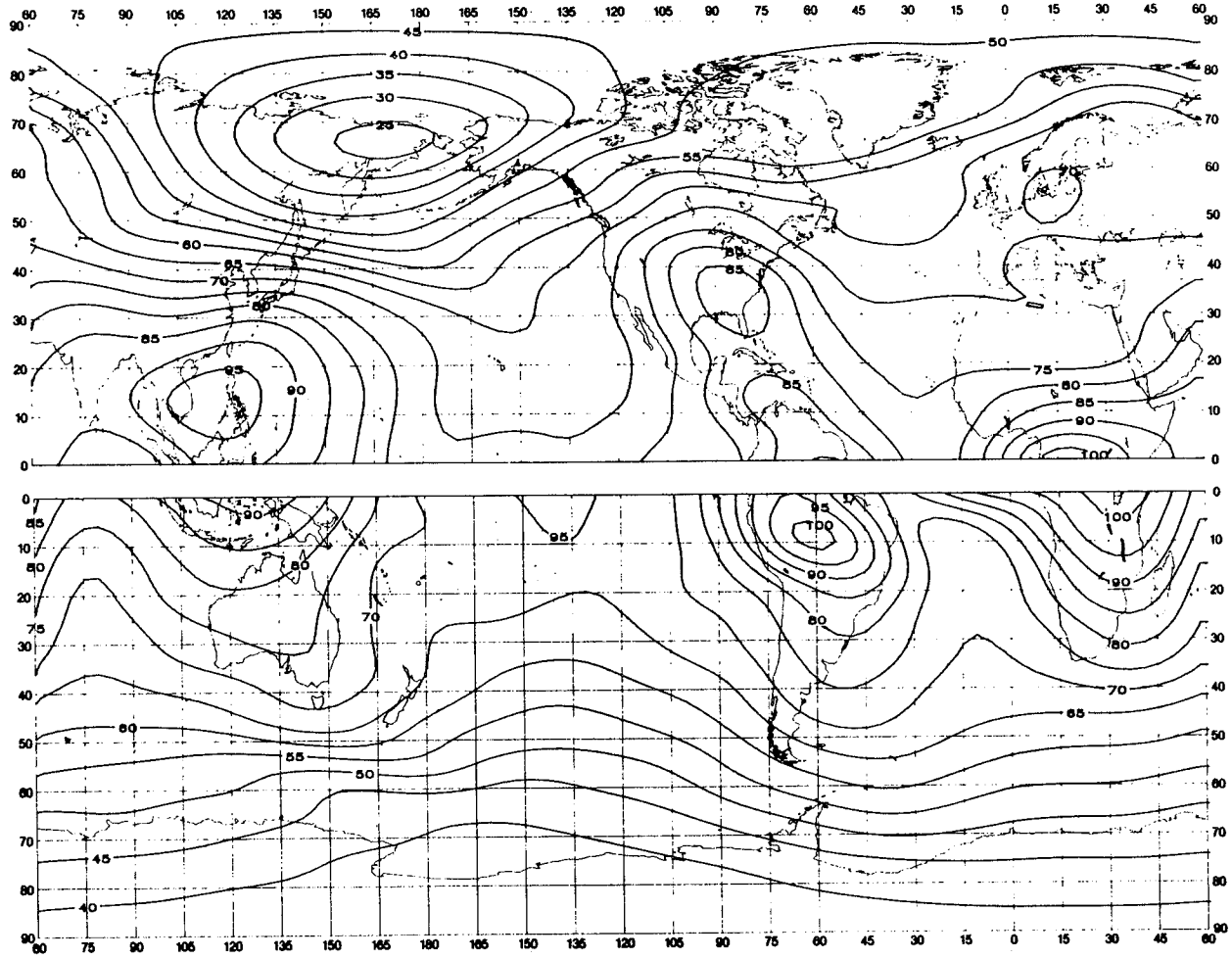

FIGURE 13a – *Valeurs attendues du bruit atmosphérique radioélectrique, F_{am}, en dB au-dessus de kT_0b à 1 MHz (Printemps; 2000-2400 heure locale)*
FIGURE 13a – *Expected values of atmospheric radio noise, F_{am} (dB above kT_0b at 1 MHz) (Spring; 2000-2400 LT)*
FIGURA 13a – *Valores probables del ruido atmosférico, F_{am}, en dB por encima de kT_0b en 1 MHz (Primavera; 2000-2400 hora local)*

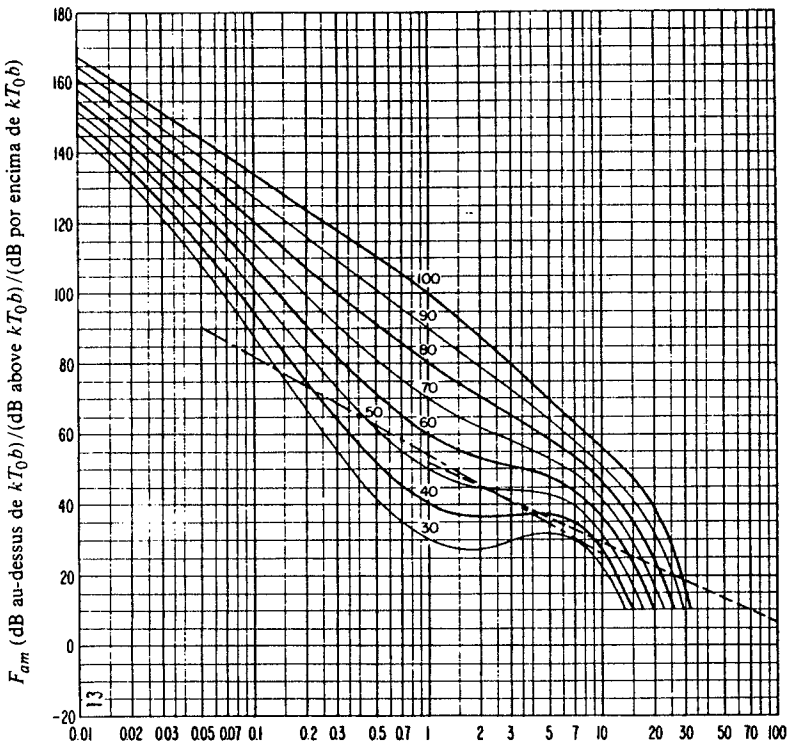

FIGURE 13b – *Variation du bruit radioélectrique en fonction de la fréquence (Printemps; 2000-2400 heure locale)*

FIGURE 13b – *Variation of radio noise with frequency (Spring; 2000-2400 LT)*

FIGURA 13b – *Variaciones del ruido radioeléctrico con la frecuencia (Primavera; 2000-2400 hora local)*

Voir la légende de la Fig. 2b/See legend of Fig. 2b/Véase la leyenda de la fig. 2b

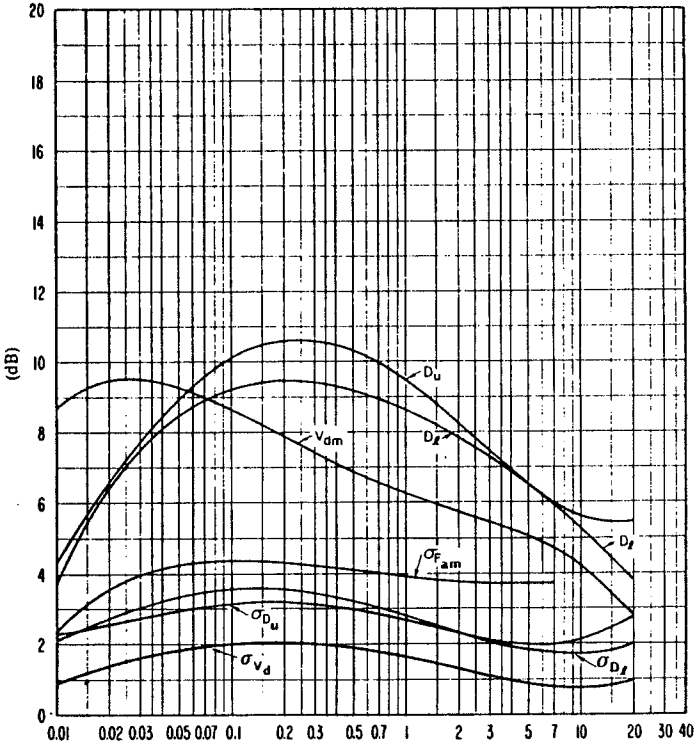

FIGURE 13c – *Données sur la variabilité et le caractère du bruit (Printemps; 2000-2400 heure locale)*

FIGURE 13c – *Data on noise variability and character (Spring; 2000-2400 LT)*

FIGURA 13c – *Datos sobre la variabilidad y el carácter del ruido (Primavera; 2000-2400 hora local)*

Voir la légende de la Fig. 2c/See legend of Fig. 2c/Véase la leyenda de la fig. 2c

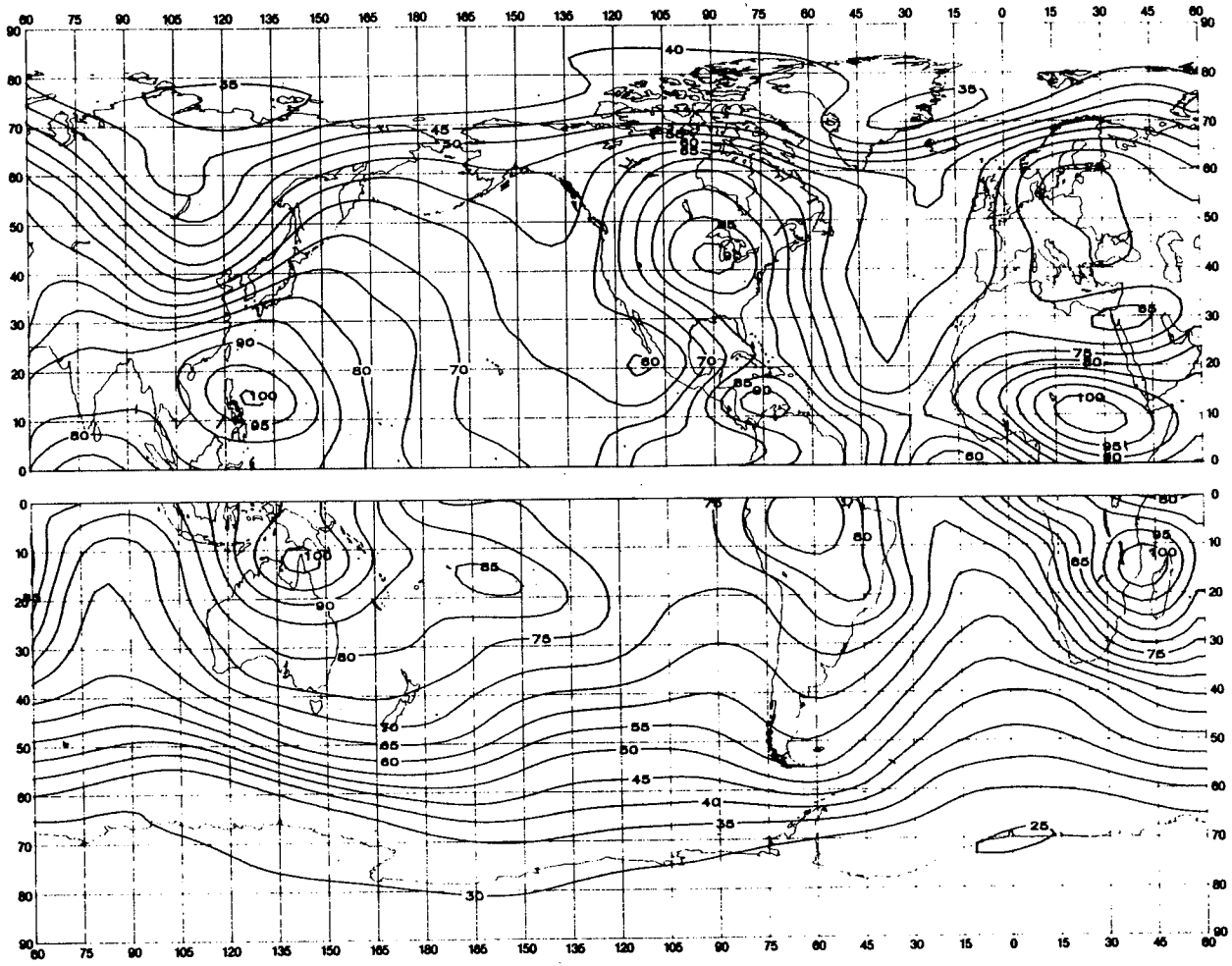

FIGURE 14a – *Valeurs attendues du bruit atmosphérique radioélectrique, F_{am}, en dB au-dessus de kT_0b à 1 MHz (Eté; 0000-0400 heure locale)*
FIGURE 14a – *Expected values of atmospheric radio noise, F_{am} (dB above kT_0b at 1 MHz) (Summer; 0000-0400 LT)*
FIGURA 14a – *Valores probables del ruido atmosférico, F_{am}, en dB por encima de kT_0b en 1 MHz (Verano; 0000-0400 hora local)*

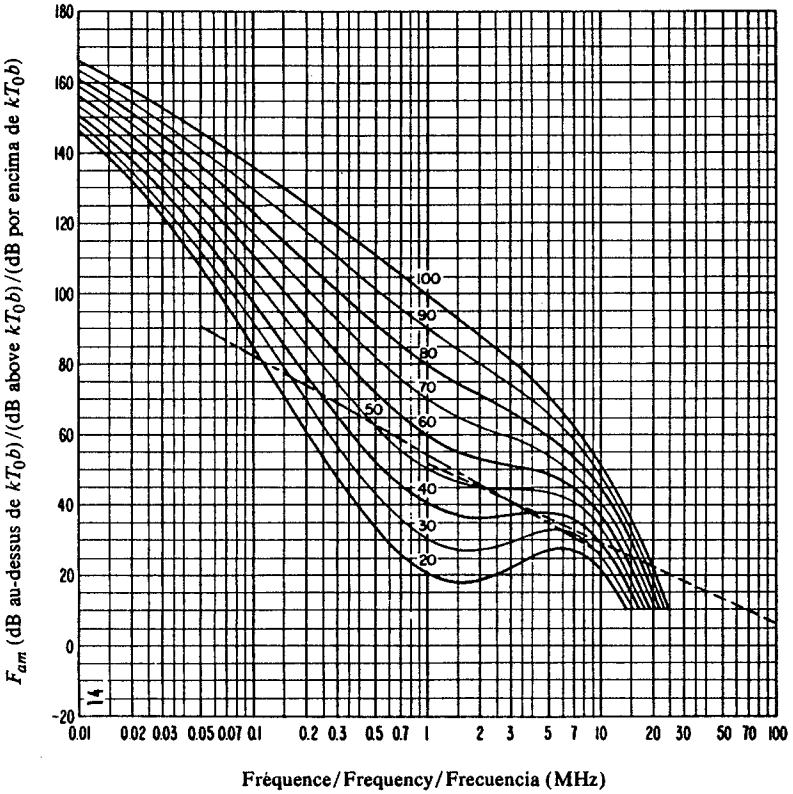

FIGURE 14b – *Variation du bruit radioélectrique en fonction de la fréquence (Eté; 0000-0400 heure locale)*

FIGURE 14b – *Variation of radio noise with frequency (Summer; 0000-0400 LT)*

FIGURA 14b – *Variaciones del ruido radioeléctrico con la frecuencia (Verano; 0000-0400 hora local)*

Voir la légende de la Fig. 2b/See legend of Fig. 2b/Véase la leyenda de la fig. 2b

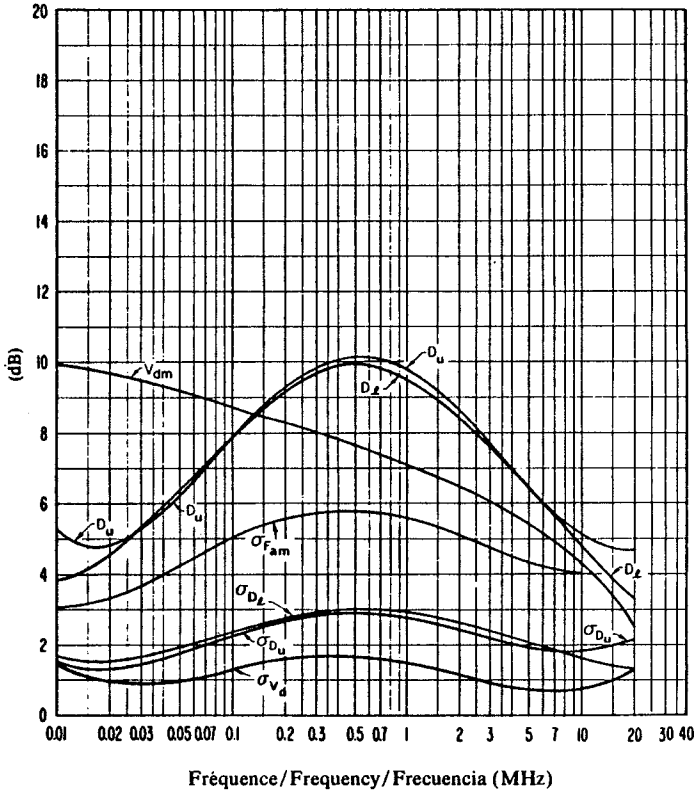

FIGURE 14c – *Données sur la variabilité et le caractère du bruit (Eté; 0000-0400 heure locale)*

FIGURE 14c – *Data on noise variability and character (Summer; 0000-0400 LT)*

FIGURA 14c – *Datos sobre la variabilidad y el carácter del ruido (Verano; 0000-0400 hora local)*

Voir la légende de la Fig. 2c/See legend of Fig. 2c/Véase la leyenda de la fig. 2c

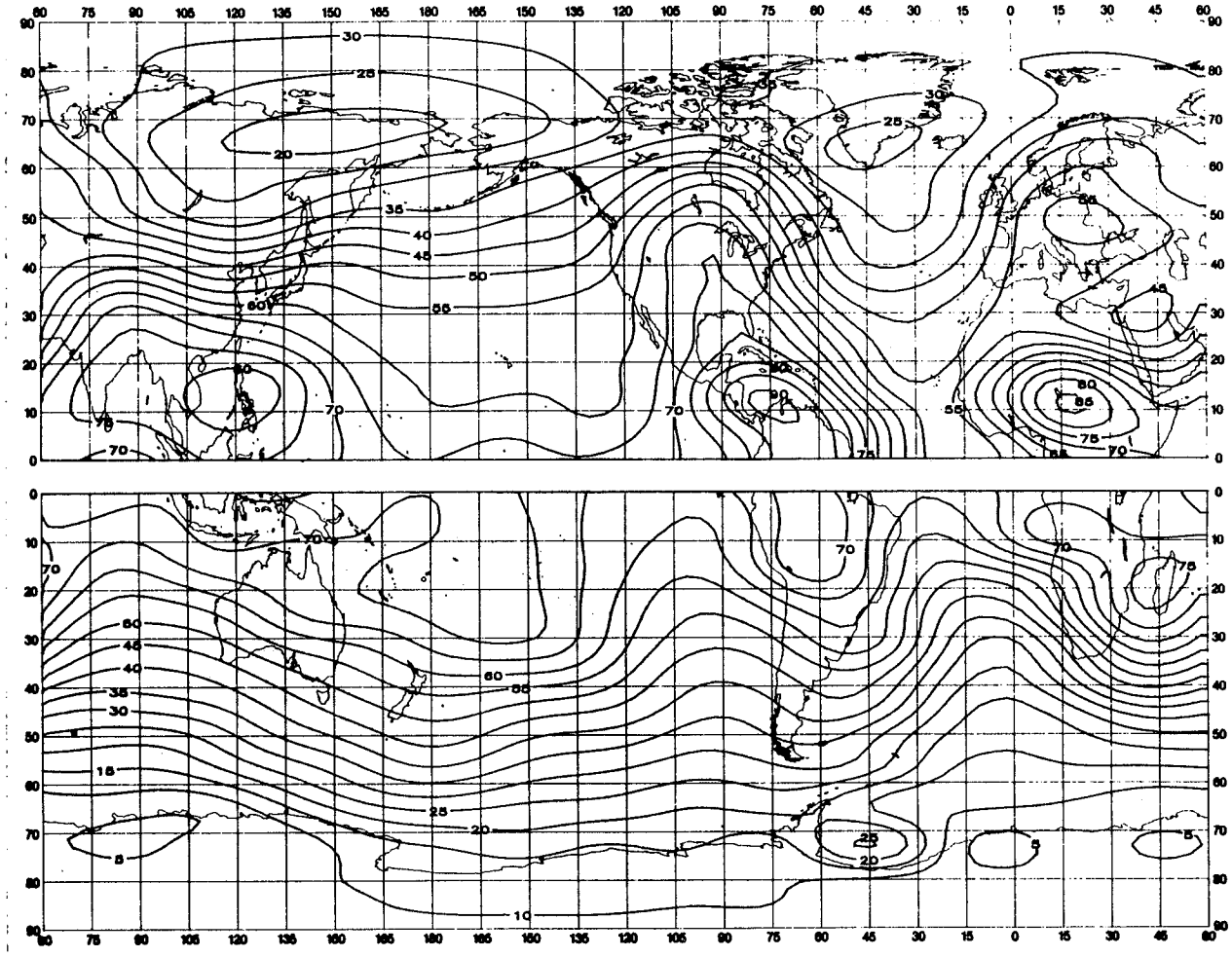

FIGURE 15a – *Valeurs attendues du bruit atmosphérique radioélectrique, F_{am}, en dB au-dessus de kT_0b à 1 MHz (Eté; 0400-0800 heure locale)*
FIGURE 15a – *Expected values of atmospheric radio noise, F_{am} (dB above kT_0b at 1 MHz) (Summer; 0400-0800 LT)*
FIGURA 15a – *Valores probables del ruido atmosférico, F_{am}, en dB por encima de kT_0b en 1 MHz (Verano; 0400-0800 hora local)*

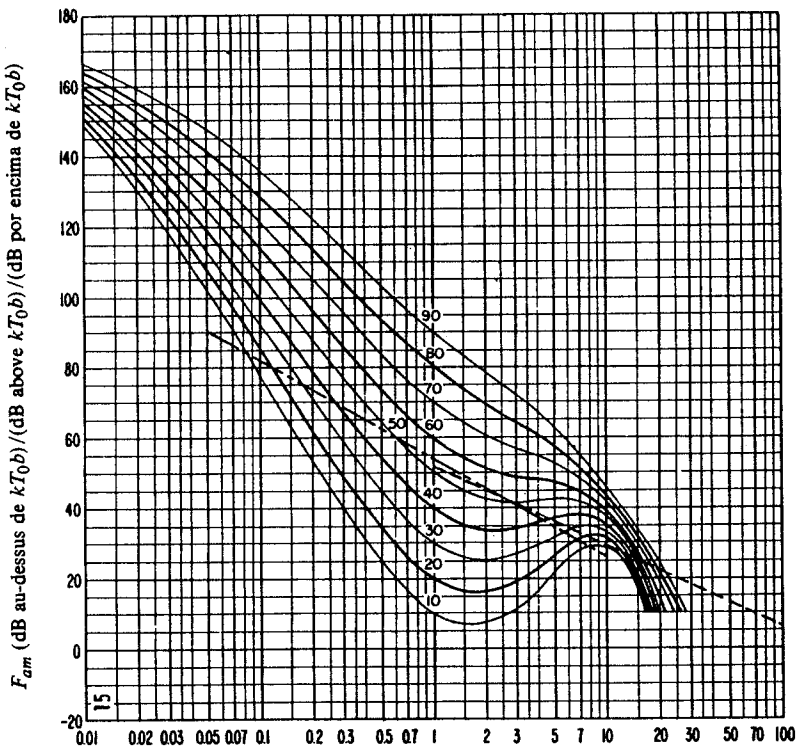

FIGURE 15b – *Variation du bruit radioélectrique en fonction de la fréquence (Eté; 0400-0800 heure locale)*
FIGURE 15b – *Variation of radio noise with frequency (Summer; 0400-0800 LT)*
FIGURA 15b – *Variaciones del ruido radioeléctrico con la frecuencia (Verano; 0400-0800 hora local)*

Voir la légende de la Fig. 2b/See legend of Fig. 2b/Véase la leyenda de la fig. 2b

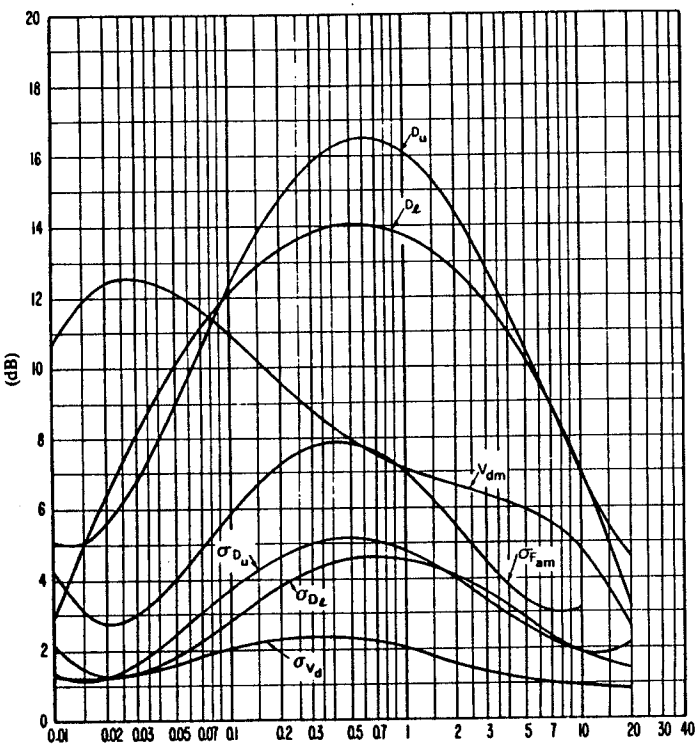

FIGURE 15c – *Données sur la variabilité et le caractère du bruit (Eté; 0400-0800 heure locale)*
FIGURE 15c – *Data on noise variability and character (Summer; 0400-0800 LT)*
FIGURA 15c – *Datos sobre la variabilidad y el carácter del ruido (Verano; 0400-0800 hora local)*

Voir la légende de la Fig. 2c/See legend of Fig. 2c/Véase la leyenda de la fig. 2c

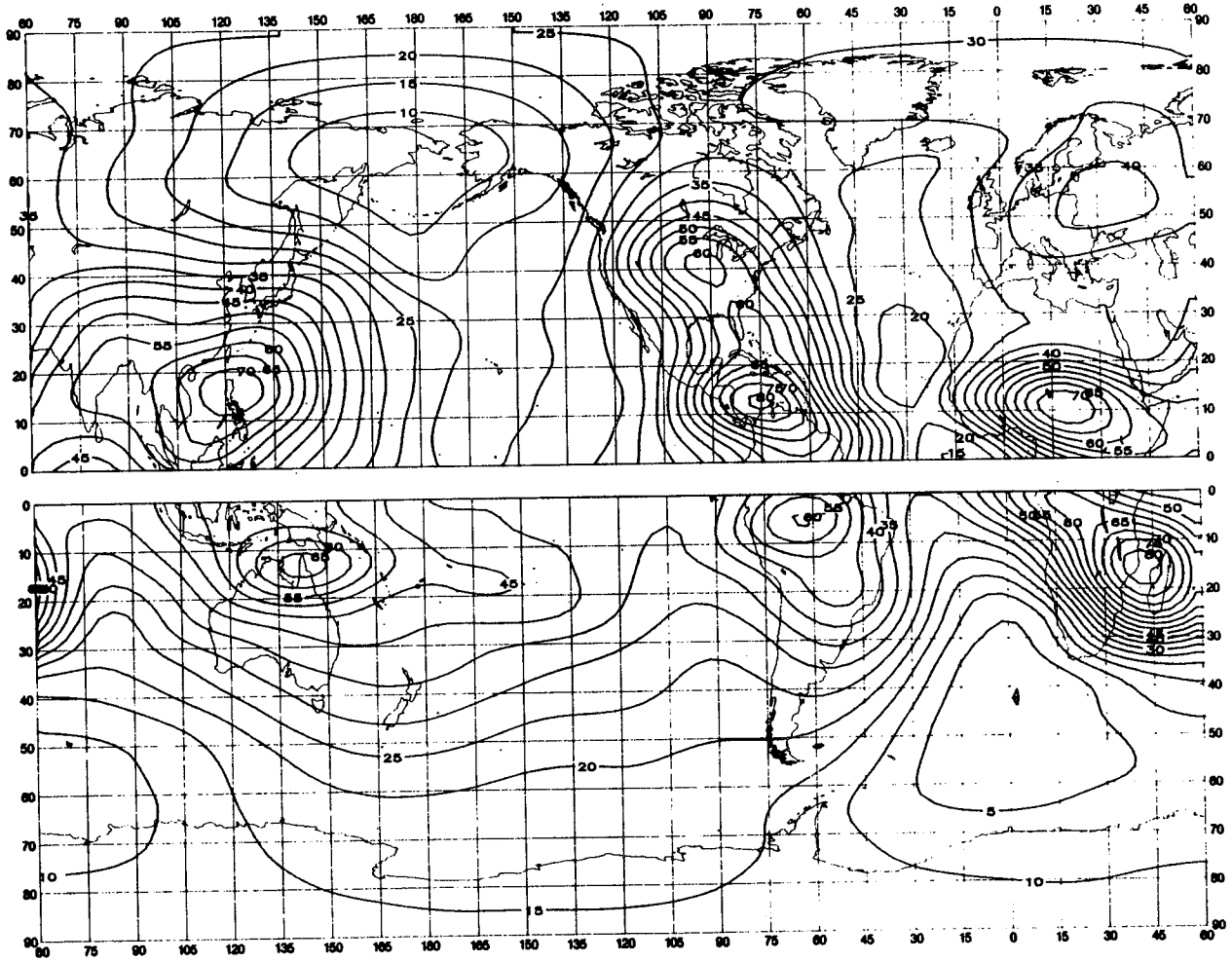

FIGURE 16a – *Valeurs attendues du bruit atmosphérique radioélectrique, F_{am}, en dB au-dessus de kT_0b à 1 MHz (Eté; 0800-1200 heure locale)*
FIGURE 16a – *Expected values of atmospheric radio noise, F_{am} (dB above kT_0b at 1 MHz) (Summer; 0800-1200 LT)*
FIGURA 16a – *Valores probables del ruido atmosférico, F_{am}, en dB por encima de kT_0b en 1 MHz (Verano; 0800-1200 hora local)*

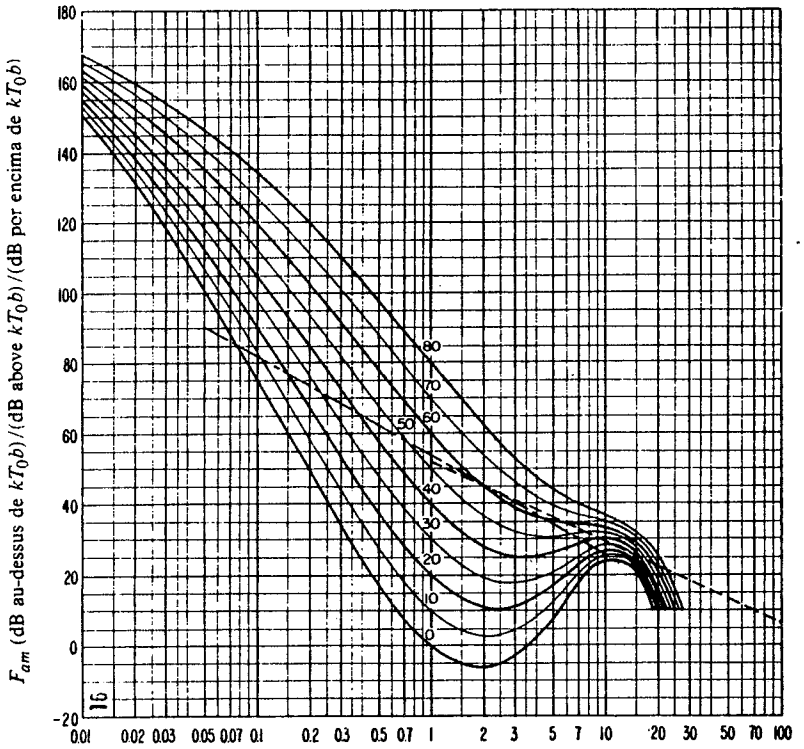

FIGURE 16b – *Variation du bruit radioélectrique en fonction de la fréquence (Eté; 0800-1200 heure locale)*

FIGURE 16b – *Variation of radio noise with frequency (Summer; 0800-1200 LT)*

FIGURA 16b – *Variaciones del ruido radioeléctrico con la frecuencia (Verano; 0800-1200 hora local)*

Voir la légende de la Fig. 2b/See legend of Fig. 2b/Véase la leyenda de la fig. 2b

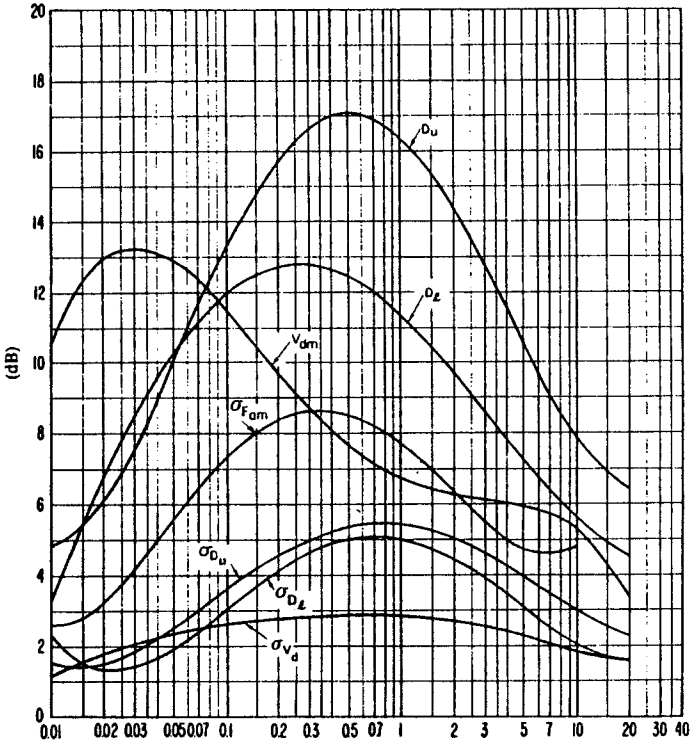

FIGURE 16c – *Données sur la variabilité et le caractère du bruit (Eté; 0800-1200 heure locale)*

FIGURE 16c – *Data on noise variability and character (Summer; 0800-1200 LT)*

FIGURA 16c – *Datos sobre la variabilidad y el carácter del ruido (Verano; 0800-1200 hora local)*

Voir la légende de la Fig. 2c/See legend of Fig. 2c/Véase la leyenda de la fig. 2c

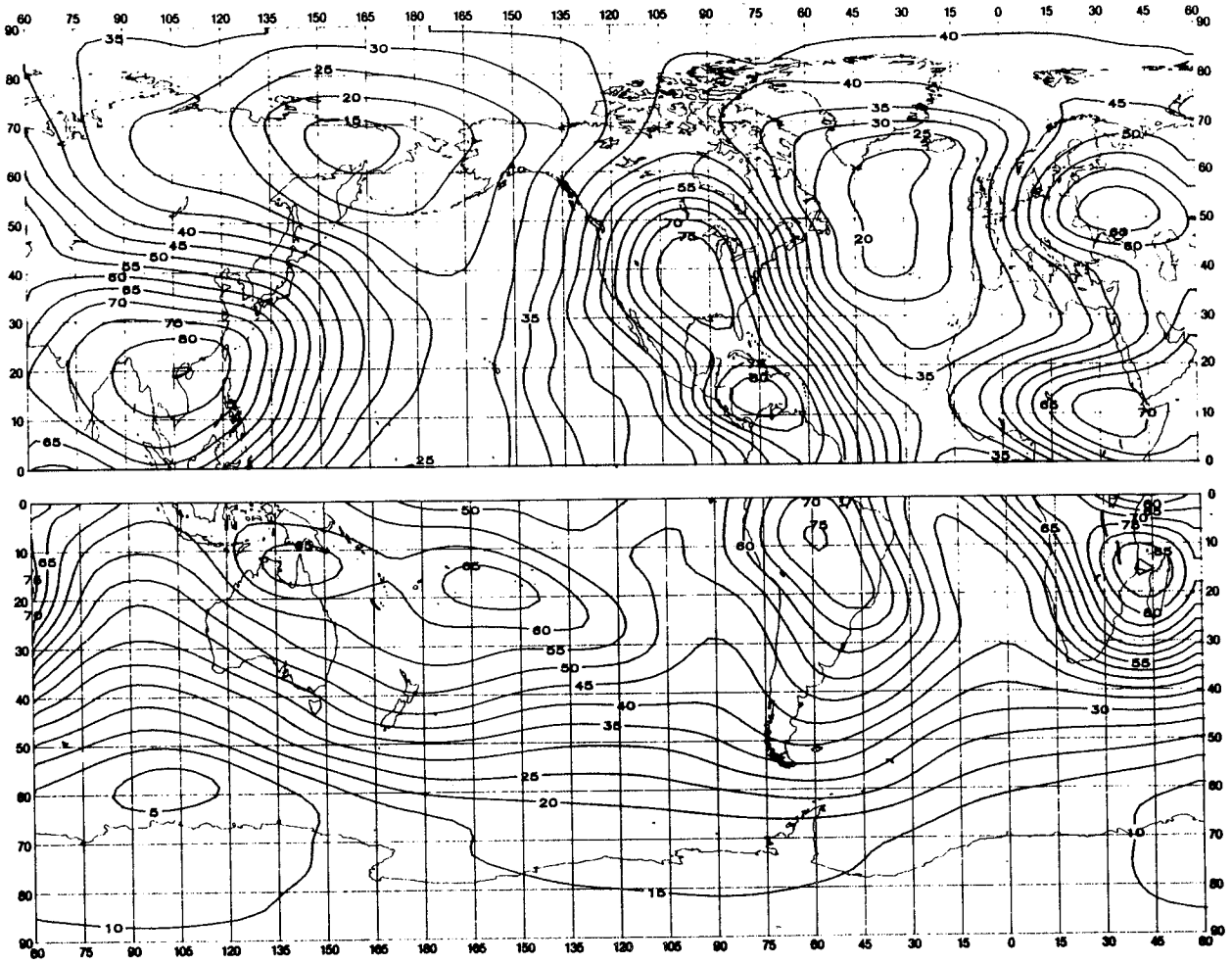

FIGURE 17a – *Valeurs attendues du bruit atmosphérique radioélectrique, F_{am}, en dB au-dessus de kT_0b à 1 MHz (Eté; 1200-1600 heure locale)*
FIGURE 17a – *Expected values of atmospheric radio noise, F_{am} (dB above kT_0b at 1 MHz) (Summer; 1200-1600 LT)*
FIGURA 17a – *Valores probables del ruido atmosférico, F_{am}, en dB por encima de kT_0b en 1 MHz (Verano; 1200-1600 hora local)*

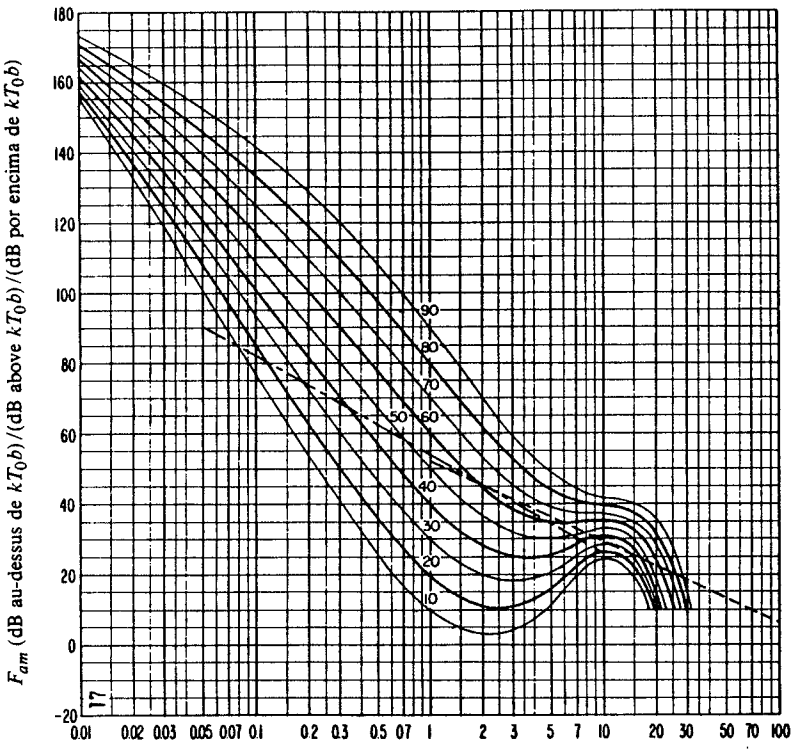

FIGURE 17b – *Variation du bruit radioélectrique en fonction de la fréquence (Eté; 1200-1600 heure locale)*

FIGURE 17b – *Variation of radio noise with frequency (Summer; 1200-1600 LT)*

FIGURA 17b – *Variaciones del ruido radioeléctrico con la frecuencia (Verano; 1200-1600 hora local)*

Voir la légende de la Fig. 2b/See legend of Fig. 2b/Véase la leyenda de la fig. 2b

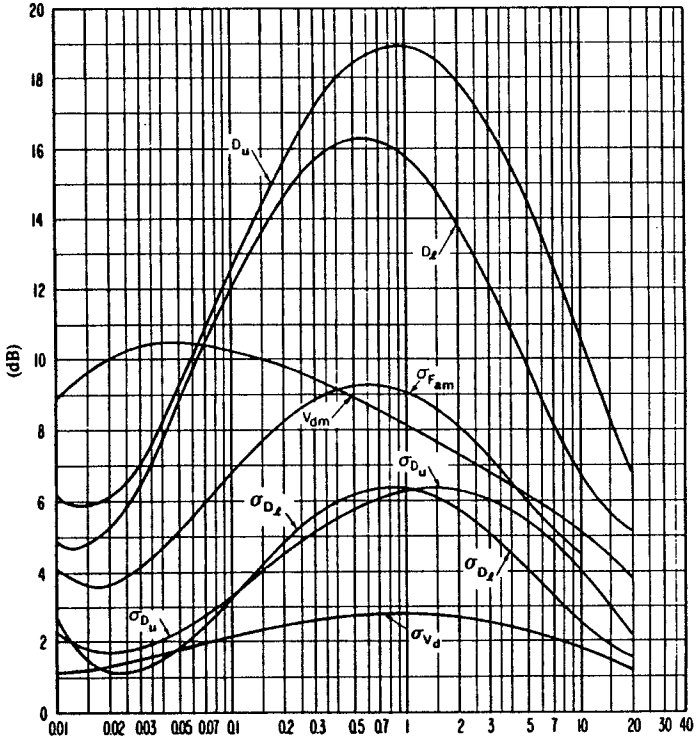

FIGURE 17c – *Données sur la variabilité et le caractère du bruit (Eté; 1200-1600 heure locale)*

FIGURE 17c – *Data on noise variability and character (Summer; 1200-1600 LT)*

FIGURA 17c – *Datos sobre la variabilidad y el carácter del ruido (Verano; 1200-1600 hora local)*

Voir la légende de la Fig. 2c/See legend of Fig. 2c/Véase la leyenda de la fig. 2c

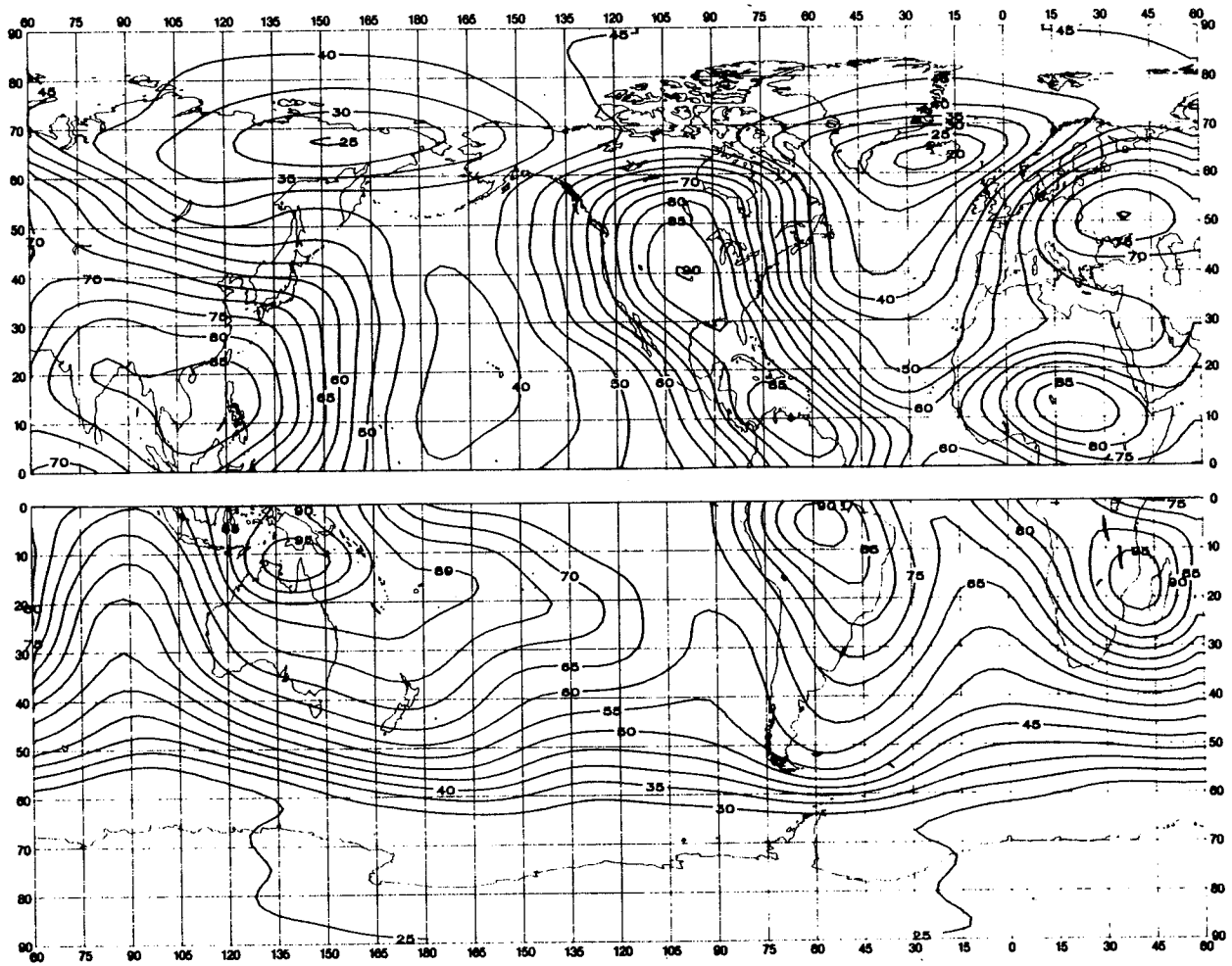

FIGURE 18a – *Valeurs attendues du bruit atmosphérique radioélectrique, F_{am}, en dB au-dessus de kT_0b à 1 MHz (Eté; 1600-2000 heure locale)*
FIGURE 18a – *Expected values of atmospheric radio noise, F_{am} (dB above kT_0b at 1 MHz) (Summer; 1600-2000 LT)*
FIGURA 18a – *Valores probables del ruido atmosférico, F_{am}, en dB por encima de kT_0b en 1 MHz (Verano; 1600-2000 hora local)*

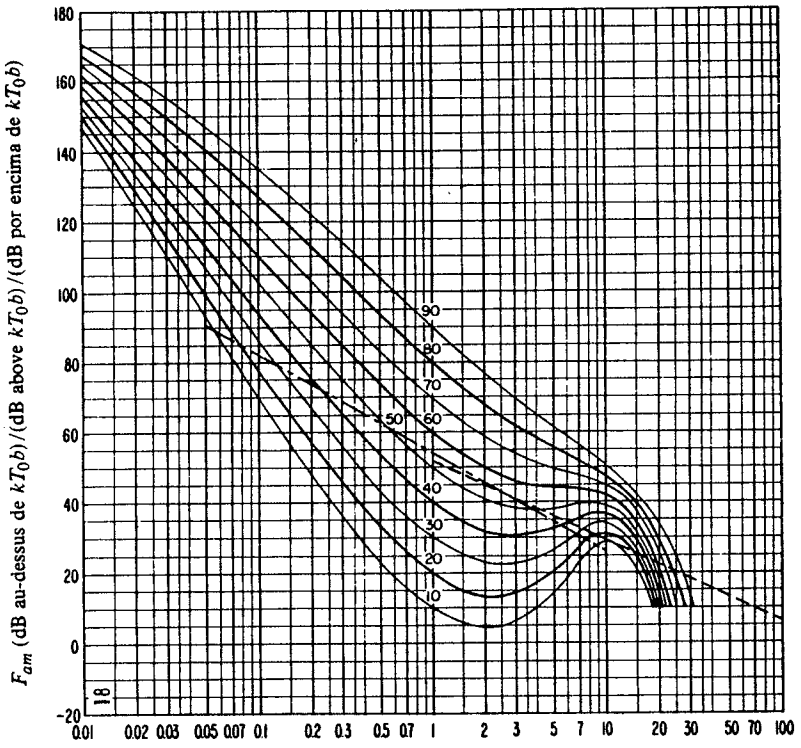

FIGURE 18b – *Variation du bruit radioélectrique en fonction de la fréquence (Eté; 1600-2000 heure locale)*

FIGURE 18b – *Variation of radio noise with frequency (Summer; 1600-2000 LT)*

FIGURA 18b – *Variaciones del ruido radioeléctrico con la frecuencia (Verano; 1600-2000 hora local)*

Voir la légende de la Fig. 2b/See legend of Fig. 2b/Véase la leyenda de la fig. 2b

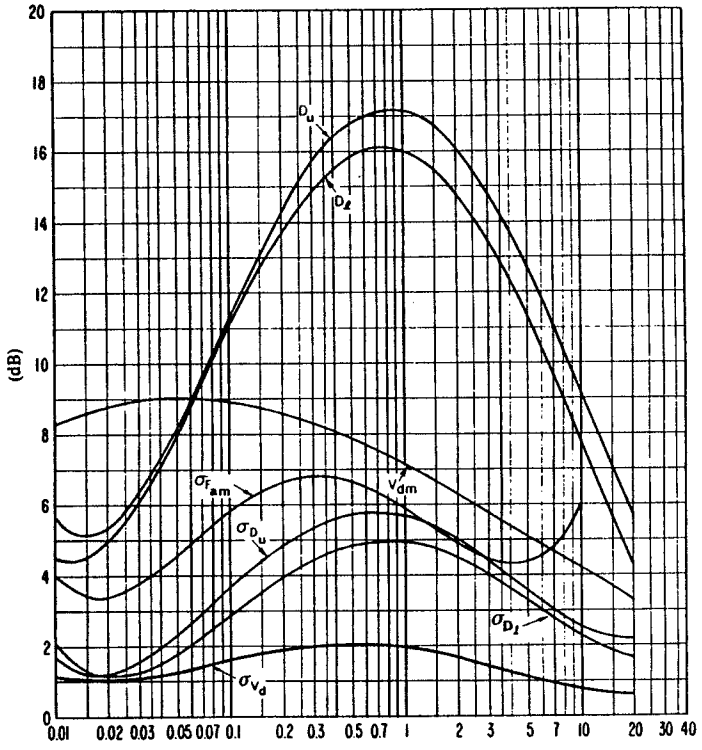

FIGURE 18c – *Données sur la variabilité et le caractère du bruit (Eté; 1600-2000 heure locale)*

FIGURE 18c – *Data on noise variability and character (Summer; 1600-2000 LT)*

FIGURA 18c – *Datos sobre la variabilidad y el carácter del ruido (Verano; 1600-2000 hora local)*

Voir la légende de la Fig. 2c/See legend of Fig. 2c/Véase la leyenda de la fig. 2c

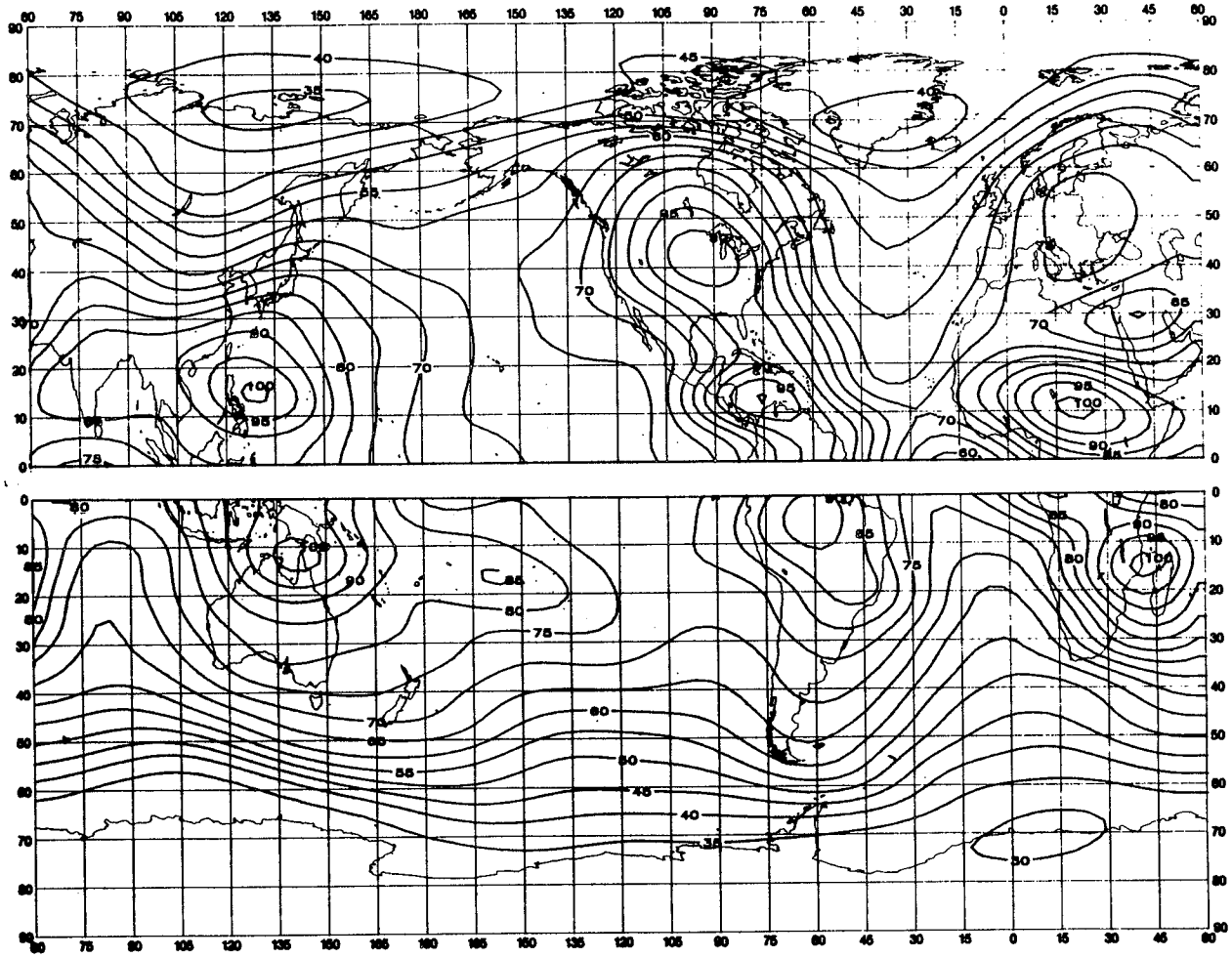

FIGURE 19a – *Valeurs attendues du bruit atmosphérique radioélectrique, F_{am}, en dB au-dessus de kT_0b à 1 MHz (Eté; 2000-2400 heure locale)*
FIGURE 19a – *Expected values of atmospheric radio noise, F_{am} (dB above kT_0b at 1 MHz) (Summer; 2000-2400 LT)*
FIGURA 19a – *Valores probables del ruido atmosférico, F_{am}, en dB por encima de kT_0b en 1 MHz (Verano; 2000-2400 hora local)*

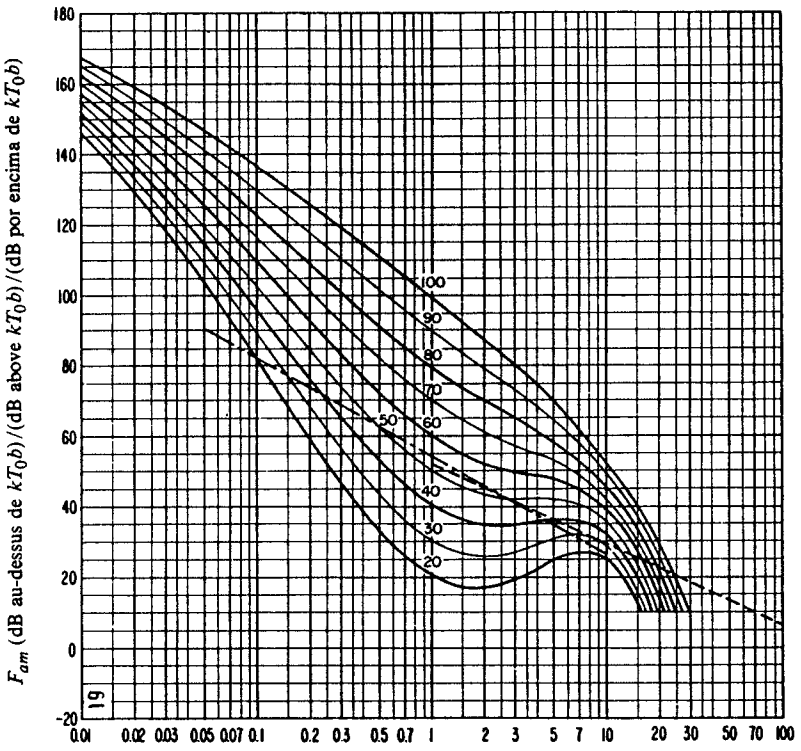

FIGURE 19b – *Variation du bruit radioélectrique en fonction de la fréquence (Eté; 2000-2400 heure locale)*

FIGURE 19b – *Variation of radio noise with frequency (Summer; 2000-2400 LT)*

FIGURA 19b – *Variaciones del ruido radioeléctrico con la frecuencia (Verano; 2000-2400 hora local)*

Voir la légende de la Fig. 2b/See legend of Fig. 2b/Véase la leyenda de la fig. 2b

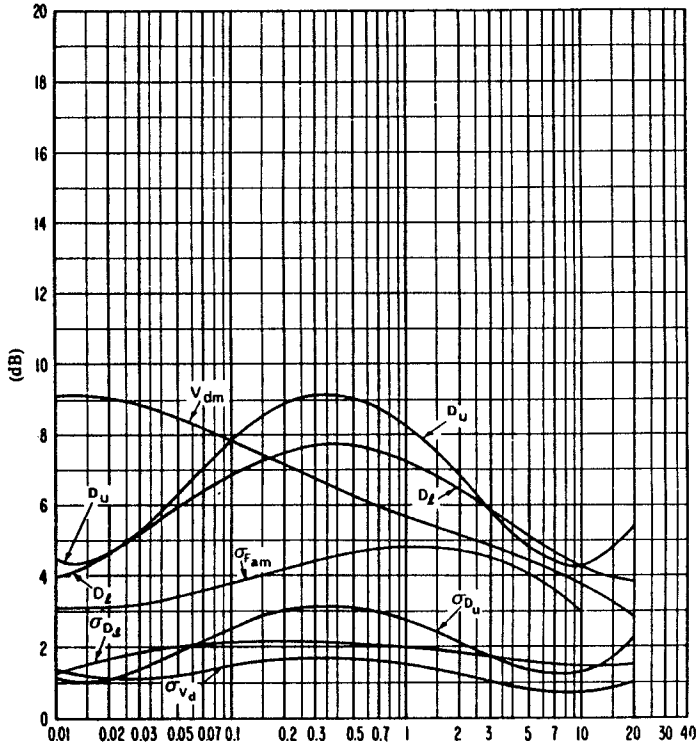

FIGURE 19c – *Données sur la variabilité et le caractère du bruit (Eté; 2000-2400 heure locale)*

FIGURE 19c – *Data on noise variability and character (Summer; 2000-2400 LT)*

FIGURA 19c – *Datos sobre la variabilidad y el carácter del ruido (Verano; 2000-2400 hora local)*

Voir la légende de la Fig. 2c/See legend of Fig. 2c/Véase la leyenda de la fig. 2c

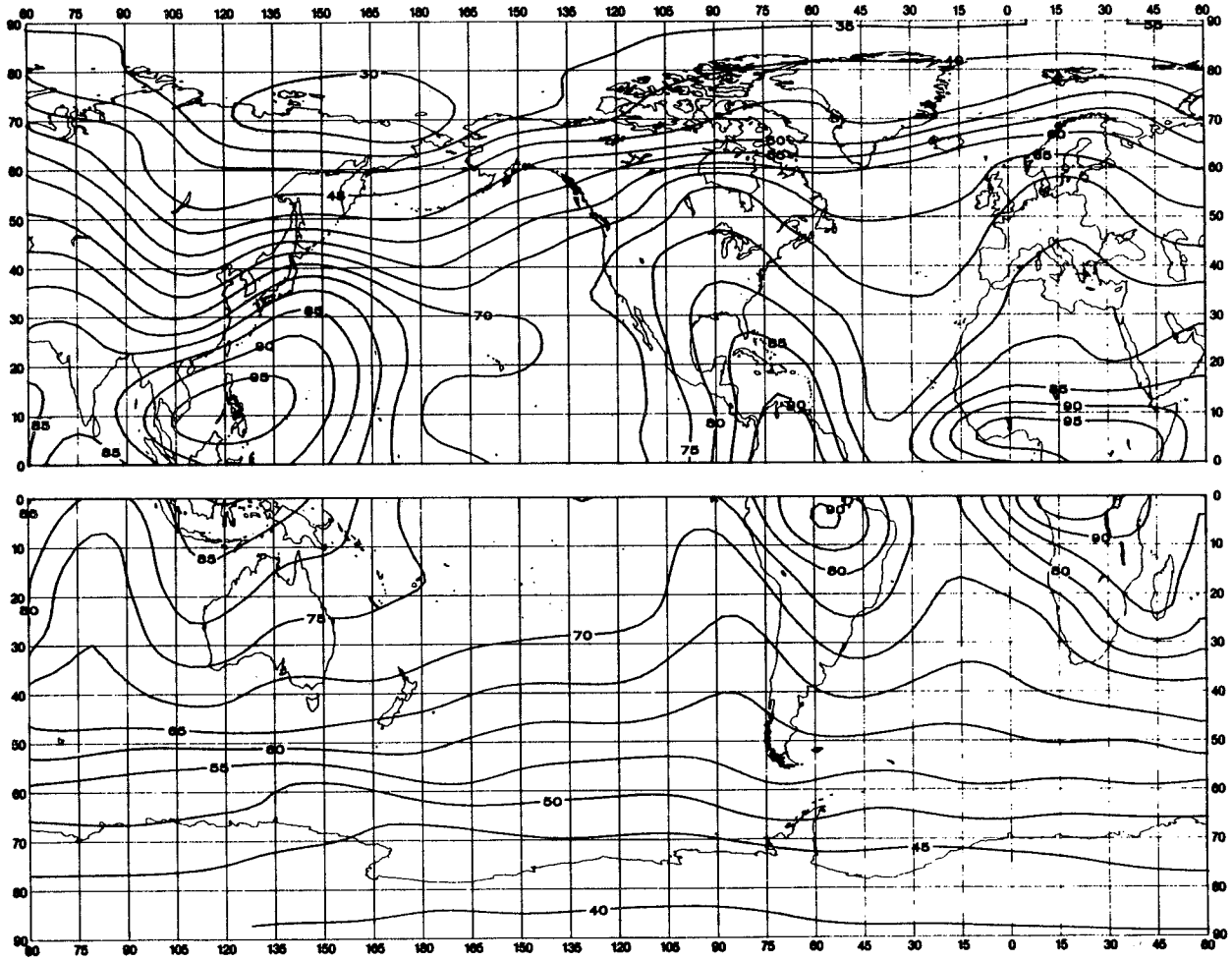

FIGURE 20a – *Valeurs attendues du bruit atmosphérique radioélectrique, F_{am}, en dB au-dessus de kT_0b à 1 MHz (Automne; 0000-0400 heure locale)*
FIGURE 20a – *Expected values of atmospheric radio noise, F_{am} (dB above kT_0b at 1 MHz) (Autumn; 0000-0400 LT)*
FIGURA 20a – *Valores probables del ruido atmosférico, F_{am}, en dB por encima de kT_0b en 1 MHz (Otoño; 0000-0400 hora local)*

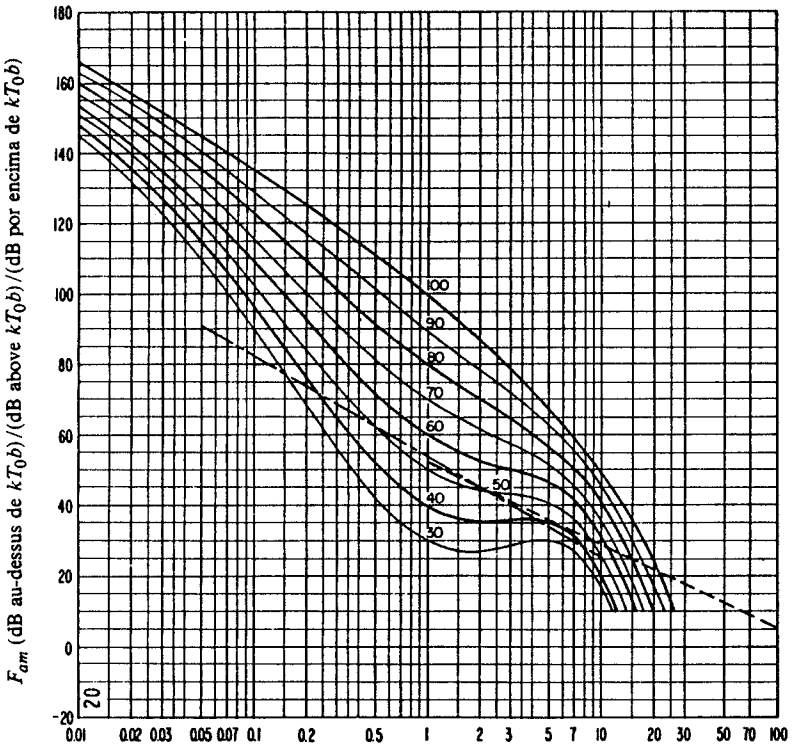

FIGURE 20b – *Variation du bruit radioélectrique en fonction de la fréquence (Automne; 0000-0400 heure locale)*

FIGURE 20b – *Variation of radio noise with frequency (Autumn; 0000-0400 LT)*

FIGURA 20b – *Variaciones del ruido radioeléctrico con la frecuencia (Otoño; 0000-0400 hora local)*

Voir la légende de la Fig. 2b/See legend of Fig. 2b/Véase la leyenda de la fig. 2b

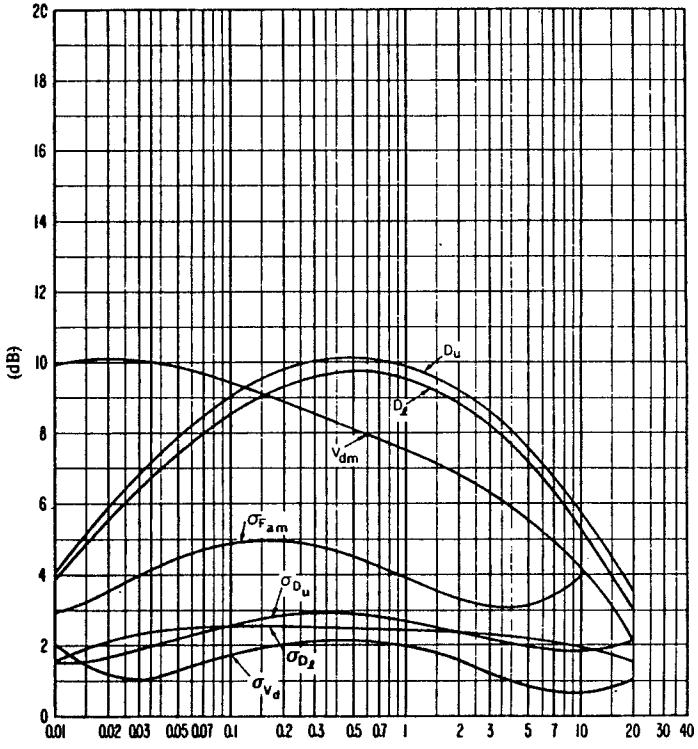

FIGURE 20c – *Données sur la variabilité et le caractère du bruit (Automne; 0000-0400 heure locale)*

FIGURE 20c – *Data on noise variability and character (Autumn; 0000-0400 LT)*

FIGURA 20c – *Datos sobre la variabilidad y el carácter del ruido (Otoño; 0000-0400 hora local)*

Voir la légende de la Fig. 2c/See legend of Fig. 2c/Véase la leyenda de la fig. 2c

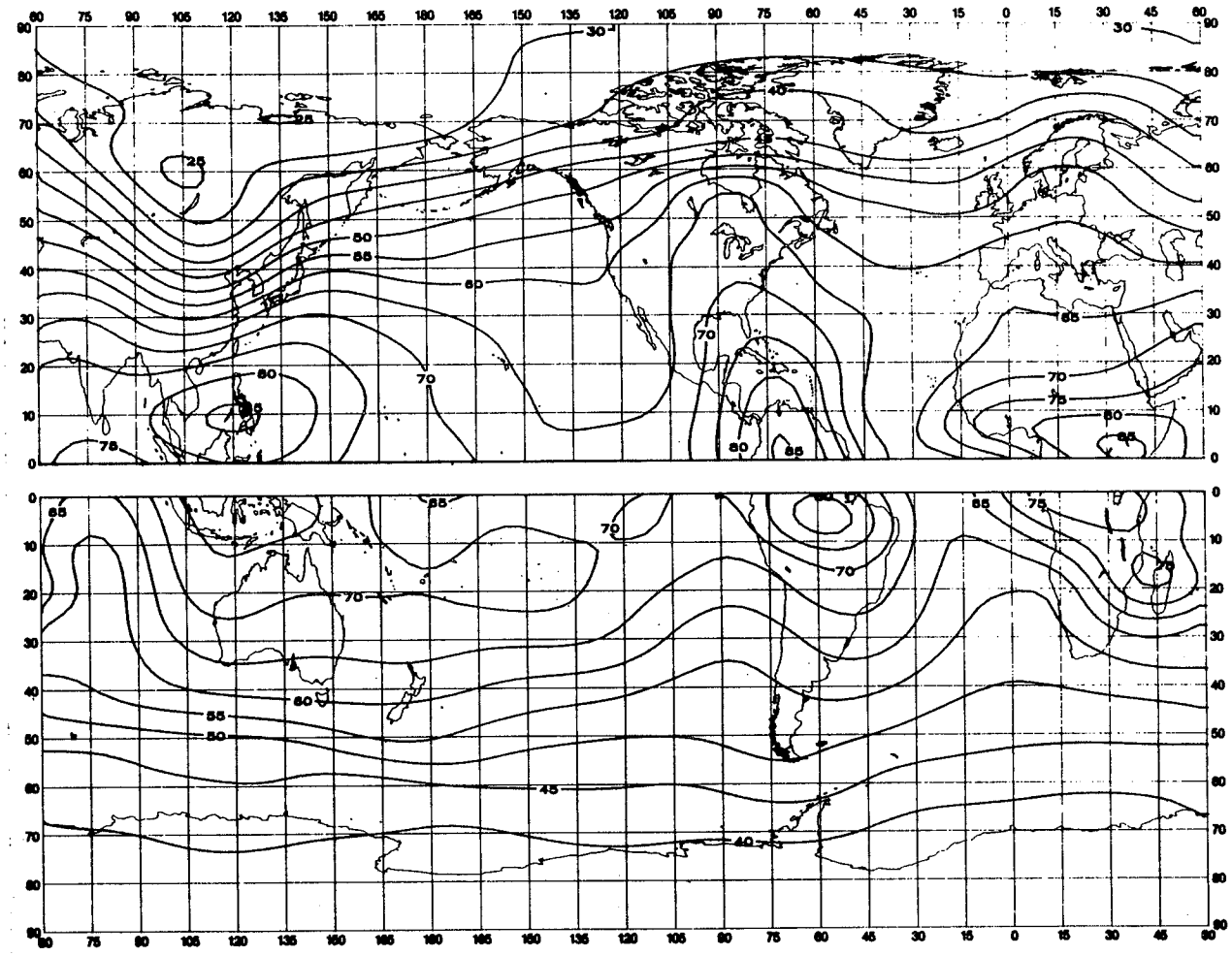

FIGURE 21a – *Valeurs attendues du bruit atmosphérique radioélectrique, F_{am}, en dB au-dessus de kT_0b à 1 MHz (Automne; 0400-0800 heure locale)*
FIGURE 21a – *Expected values of atmospheric radio noise, F_{am} (dB above kT_0b at 1 MHz) (Autumn; 0400-0800 LT)*
FIGURA 21a – *Valores probables del ruido atmosférico, F_{am}, en dB por encima de kT_0b en 1 MHz (Otoño; 0400-0800 hora local)*

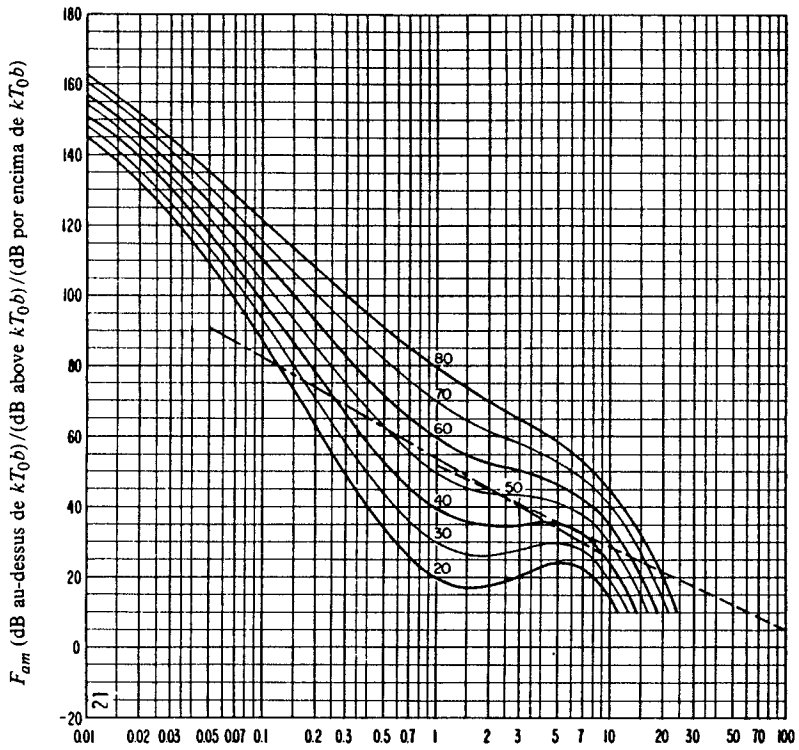

FIGURE 21b – *Variation du bruit radioélectrique en fonction de la fréquence (Automne; 0400-0800 heure locale)*

FIGURE 21b – *Variation of radio noise with frequency (Autumn; 0400-0800 LT)*

FIGURA 21b – *Variaciones del ruido radioeléctrico con la frecuencia (Otoño; 0400-0800 hora local)*

Voir la légende de la Fig. 2b/See legend of Fig. 2b/Véase la leyenda de la fig. 2b

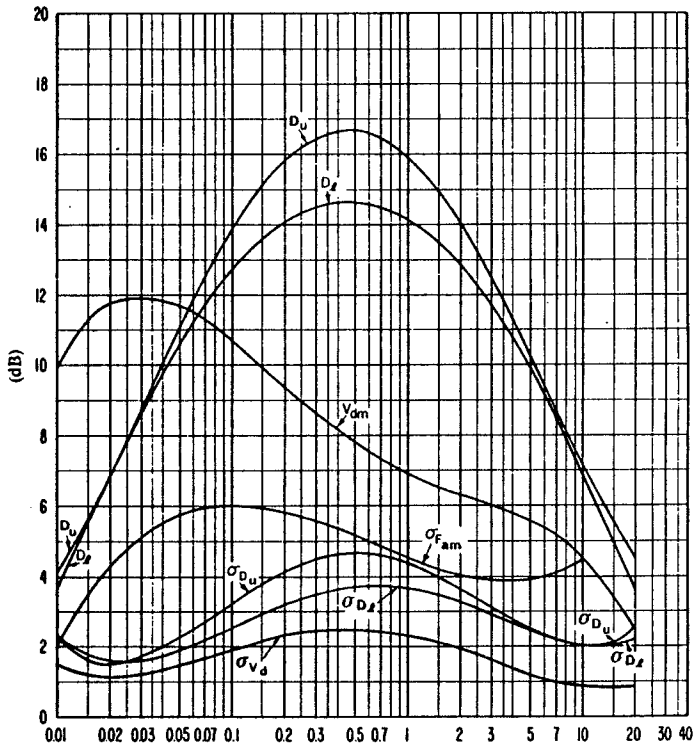

FIGURE 21c – *Données sur la variabilité et le caractère du bruit (Automne; 0400-0800 heure locale)*

FIGURE 21c – *Data on noise variability and character (Autumn; 0400-0800 LT)*

FIGURA 21c – *Datos sobre la variabilidad y el carácter del ruido (Otoño; 0400-0800 hora local)*

Voir la légende de la Fig. 2c/See legend of Fig. 2c/Véase la leyenda de la fig. 2c

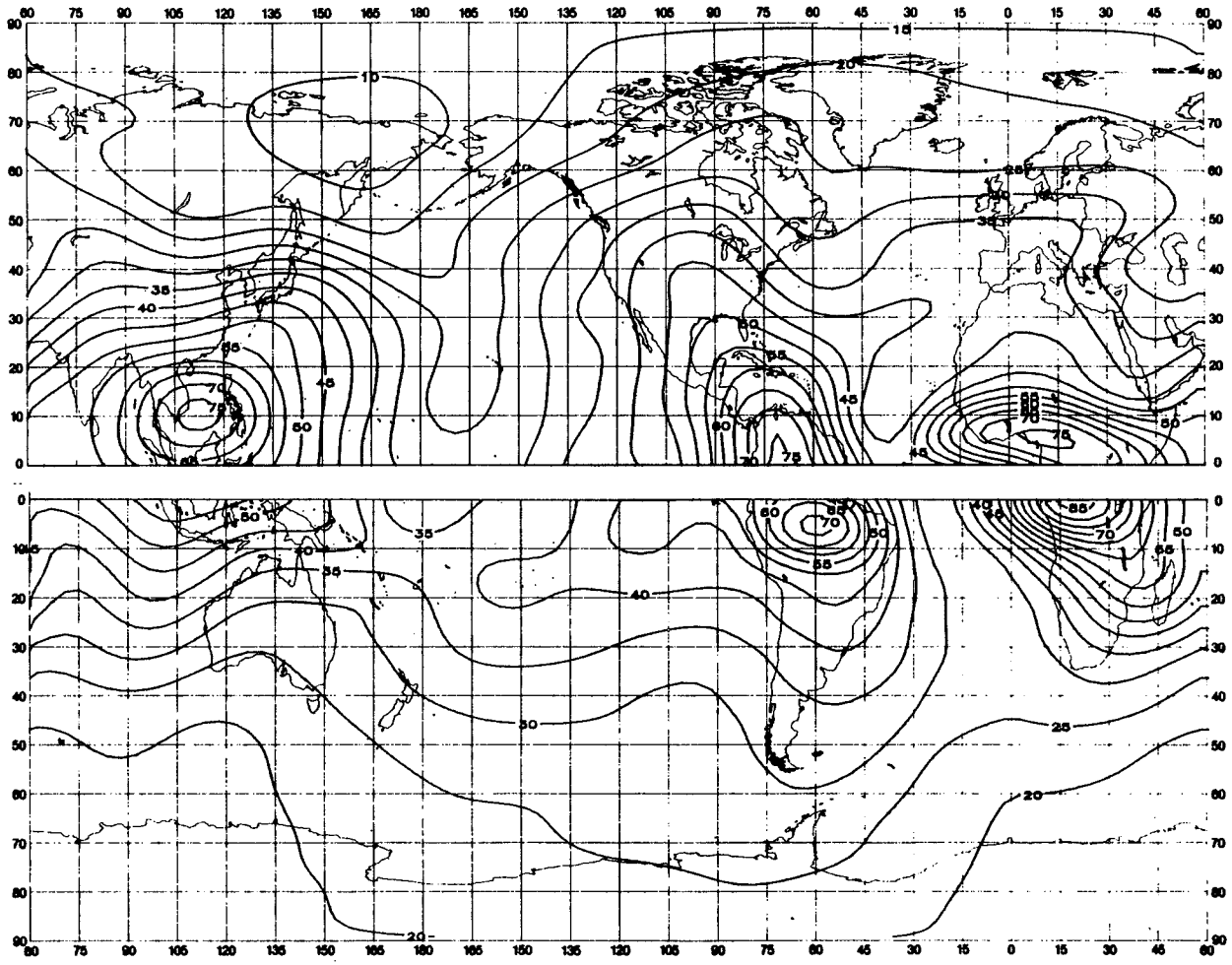

FIGURE 22a – *Valeurs attendues du bruit atmosphérique radioélectrique, F_{am}, en dB au-dessus de kT_0b à 1 MHz (Automne; 0800-1200 heure locale)*
FIGURE 22a – *Expected values of atmospheric radio noise, F_{am} (dB above kT_0b at 1 MHz) (Autumn; 0800-1200 LT)*
FIGURA 22a – *Valores probables del ruido atmosférico, F_{am}, en dB por encima de kT_0b en 1 MHz (Otoño; 0800-1200 hora local)*

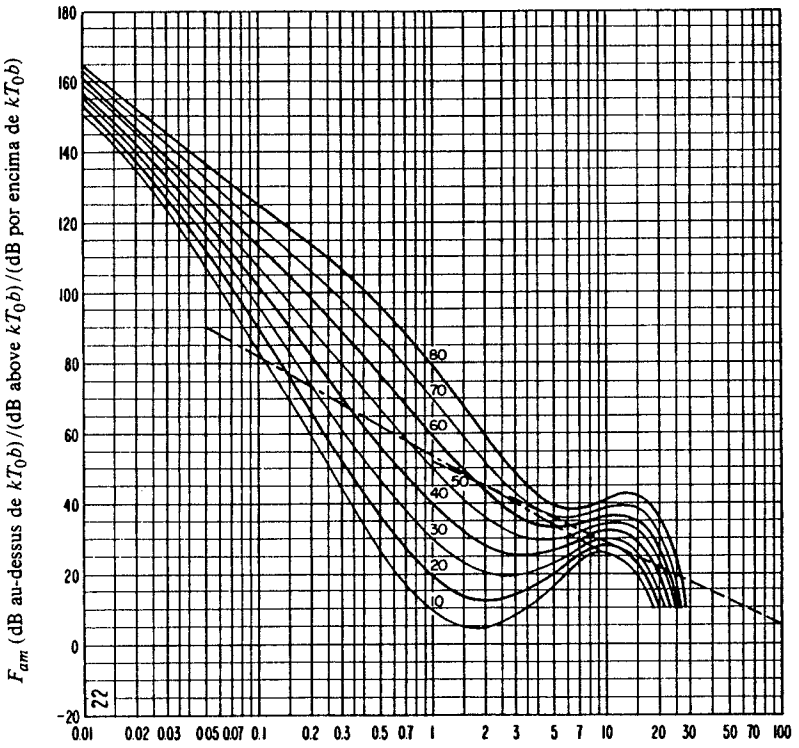

FIGURE 22b – *Variation du bruit radioélectrique en fonction de la fréquence (Automne; 0800-1200 heure locale)*

FIGURE 22b – *Variation of radio noise with frequency (Autumn; 0800-1200 LT)*

FIGURA 22b – *Variaciones del ruido radioeléctrico con la frecuencia (Otoño; 0800-1200 hora local)*

Voir la légende de la Fig. 2b/See legend of Fig. 2b/Véase la leyenda de la fig. 2b

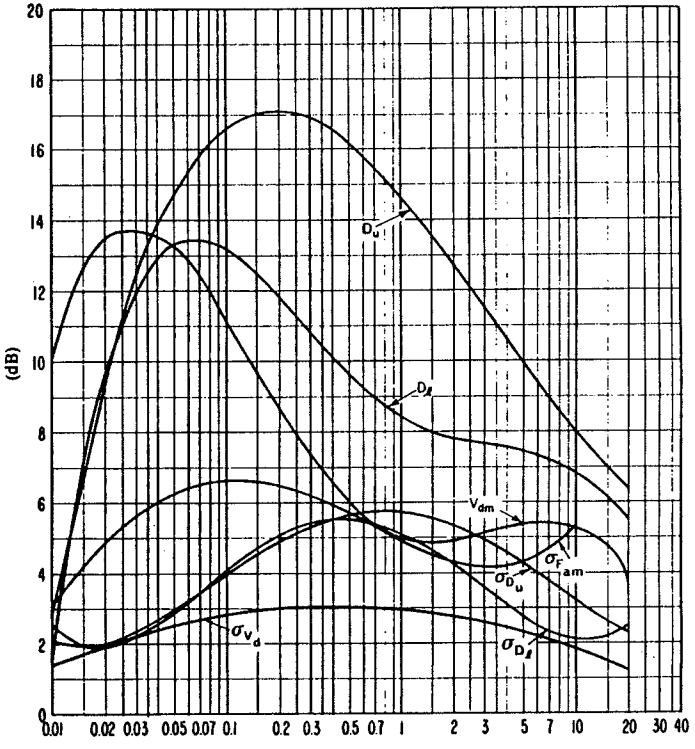

FIGURE 22c – *Données sur la variabilité et le caractère du bruit (Automne; 0800-1200 heure locale)*

FIGURE 22c – *Data on noise variability and character (Autumn; 0800-1200 LT)*

FIGURA 22c – *Datos sobre la variabilidad y el carácter del ruido (Otoño; 0800-1200 hora local)*

Voir la légende de la Fig. 2c/See legend of Fig. 2c/Véase la leyenda de la fig. 2c

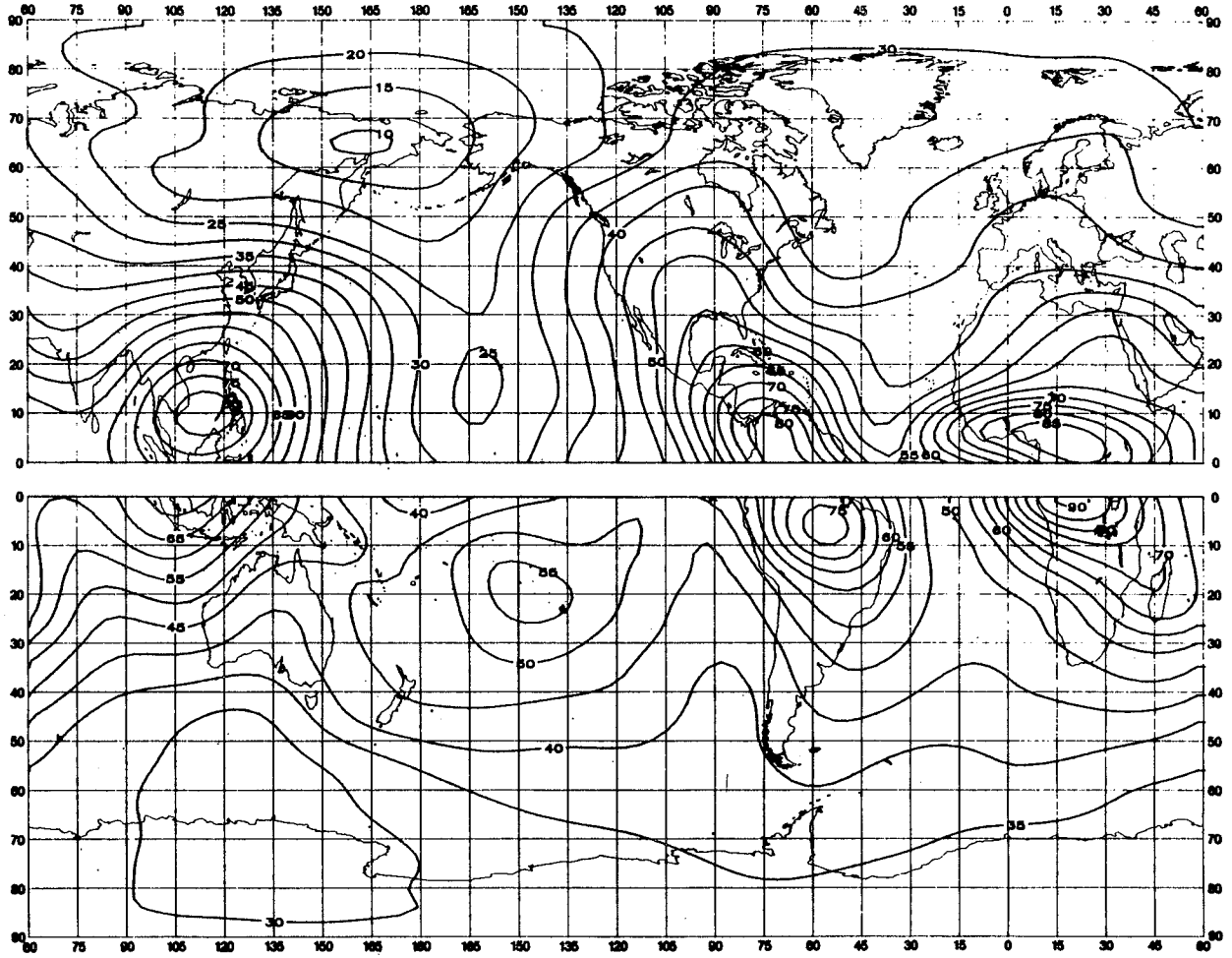

FIGURE 23a – *Valeurs attendues du bruit atmosphérique radioélectrique, F_{am}, en dB au-dessus de kT_0b à 1 MHz (Automne; 1200-1600 heure locale)*
FIGURE 23a – *Expected values of atmospheric radio noise, F_{am} (dB above kT_0b at 1 MHz) (Autumn; 1200-1600 LT)*
FIGURA 23a – *Valores probables del ruido atmosférico, F_{am}, en dB por encima de kT_0b en 1 MHz (Otoño; 1200-1600 hora local)*

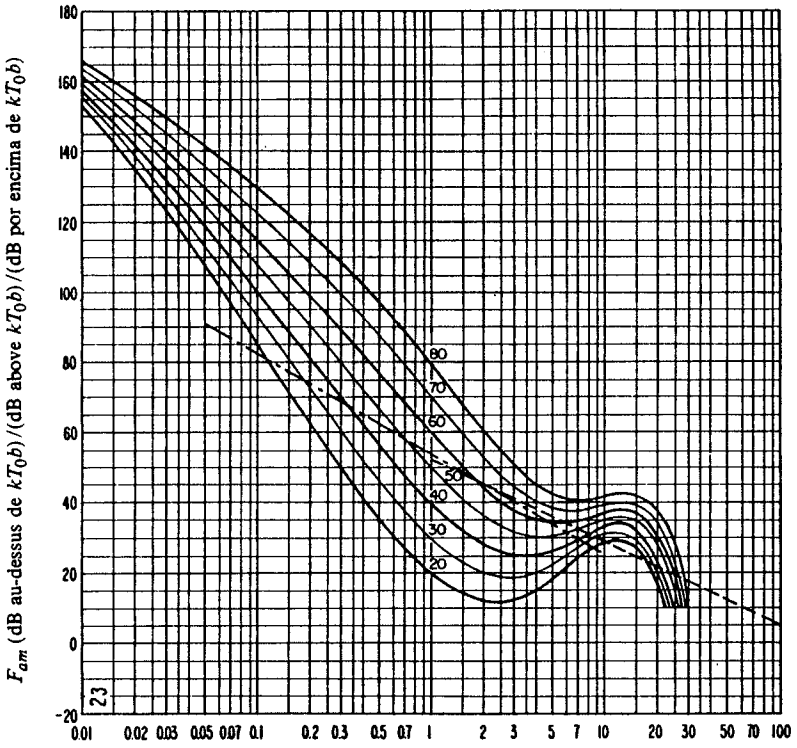

FIGURE 23b – *Variation du bruit radioélectrique en fonction de la fréquence (Automne; 1200-1600 heure locale)*

FIGURE 23b – *Variation of radio noise with frequency (Autumn; 1200-1600 LT)*

FIGURA 23b – *Variaciones del ruido radioeléctrico con la frecuencia (Otoño; 1200-1600 hora local)*

Voir la légende de la Fig. 2b/See legend of Fig. 2b/Véase la leyenda de la fig. 2b

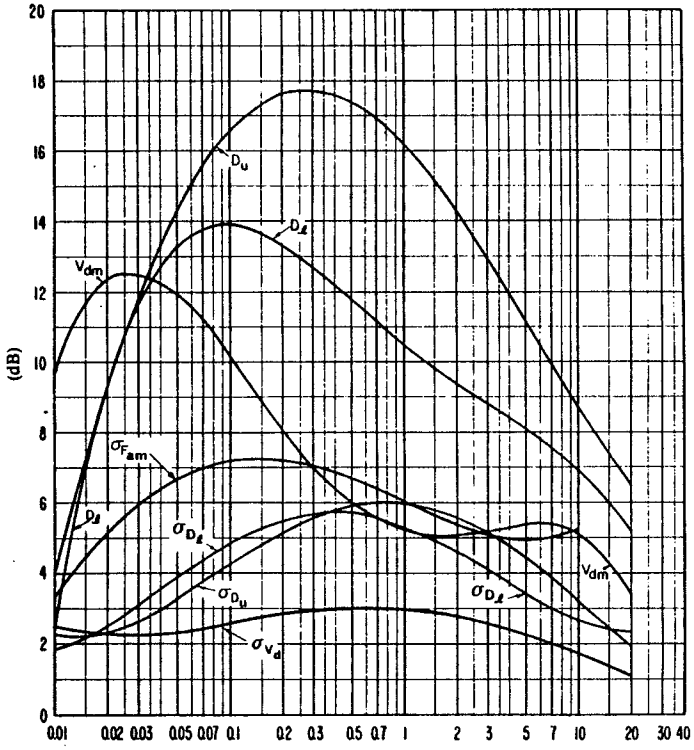

FIGURE 23c – *Données sur la variabilité et le caractère du bruit (Automne; 1200-1600 heure locale)*

FIGURE 23c – *Data on noise variability and character (Autumn; 1200-1600 LT)*

FIGURA 23c – *Datos sobre la variabilidad y el carácter del ruido (Otoño; 1200-1600 hora local)*

Voir la légende de la Fig. 2c/See legend of Fig. 2c/Véase la leyenda de la fig. 2c

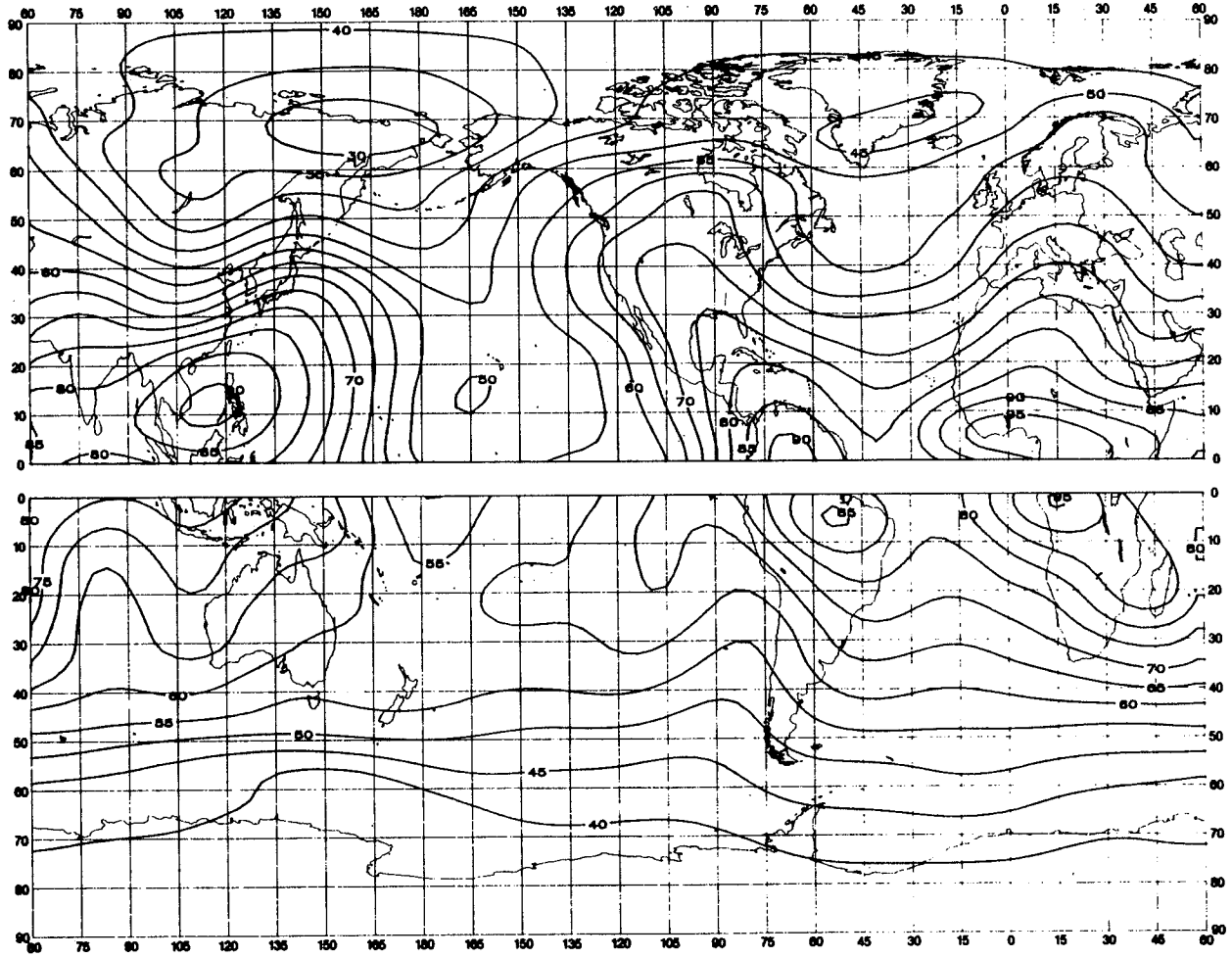

FIGURE 24a – *Valeurs attendues du bruit atmosphérique radioélectrique, F_{am}, en dB au-dessus de kT_0b à 1 MHz (Automne; 1600-2000 heure locale)*
FIGURE 24a – *Expected values of atmospheric radio noise, F_{am} (dB above kT_0b at 1 MHz) (Autumn; 1600-2000 LT)*
FIGURA 24a – *Valores probables del ruido atmosférico, F_{am}, en dB por encima de kT_0b en 1 MHz (Otoño; 1600-2000 hora local)*

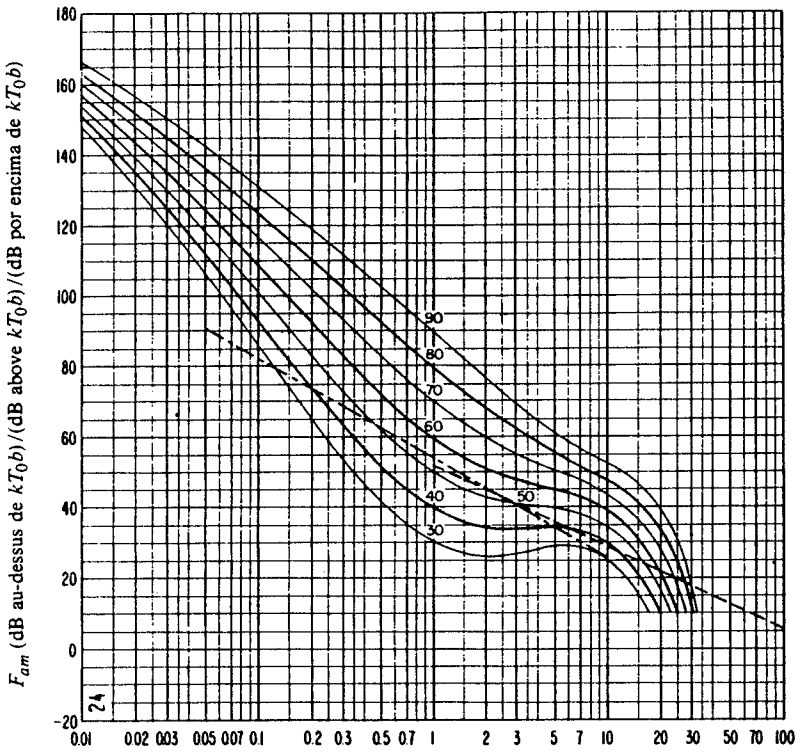

FIGURE 24b – *Variation du bruit radioélectrique en fonction de la fréquence (Automne; 1600-2000 heure locale)*

FIGURE 24b – *Variation of radio noise with frequency (Autumn; 1600-2000 LT)*

FIGURA 24b – *Variaciones del ruido radioeléctrico con la frecuencia (Otoño; 1600-2000 hora local)*

Voir la légende de la Fig. 2b/See legend of Fig. 2b/Véase la leyenda de la fig. 2b

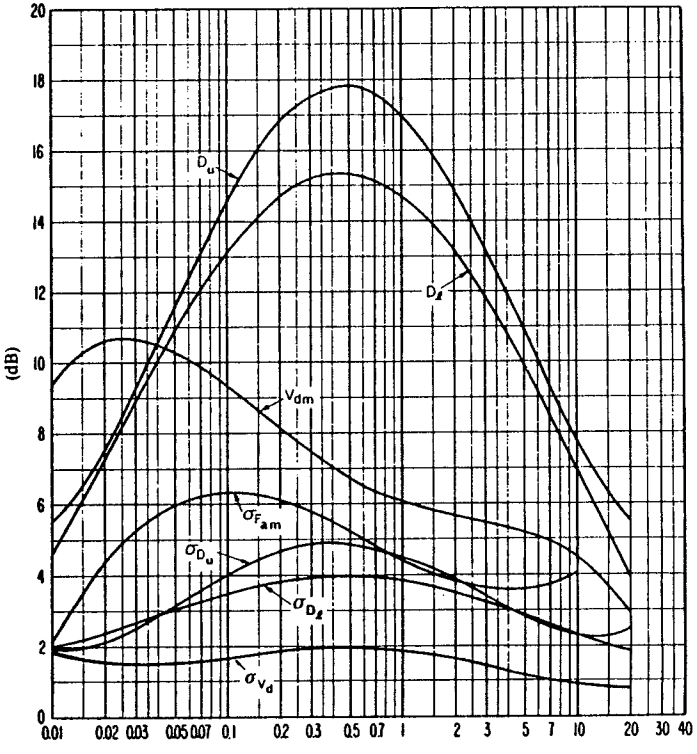

FIGURE 24c – *Données sur la variabilité et le caractère du bruit (Automne; 1600-2000 heure locale)*

FIGURE 24c – *Data on noise variability and character (Autumn; 1600-2000 LT)*

FIGURA 24c – *Datos sobre la variabilidad y el carácter del ruido (Otoño; 1600-2000 hora local)*

Voir la légende de la Fig. 2c/See legend of Fig. 2c/Véase la leyenda de la fig. 2c

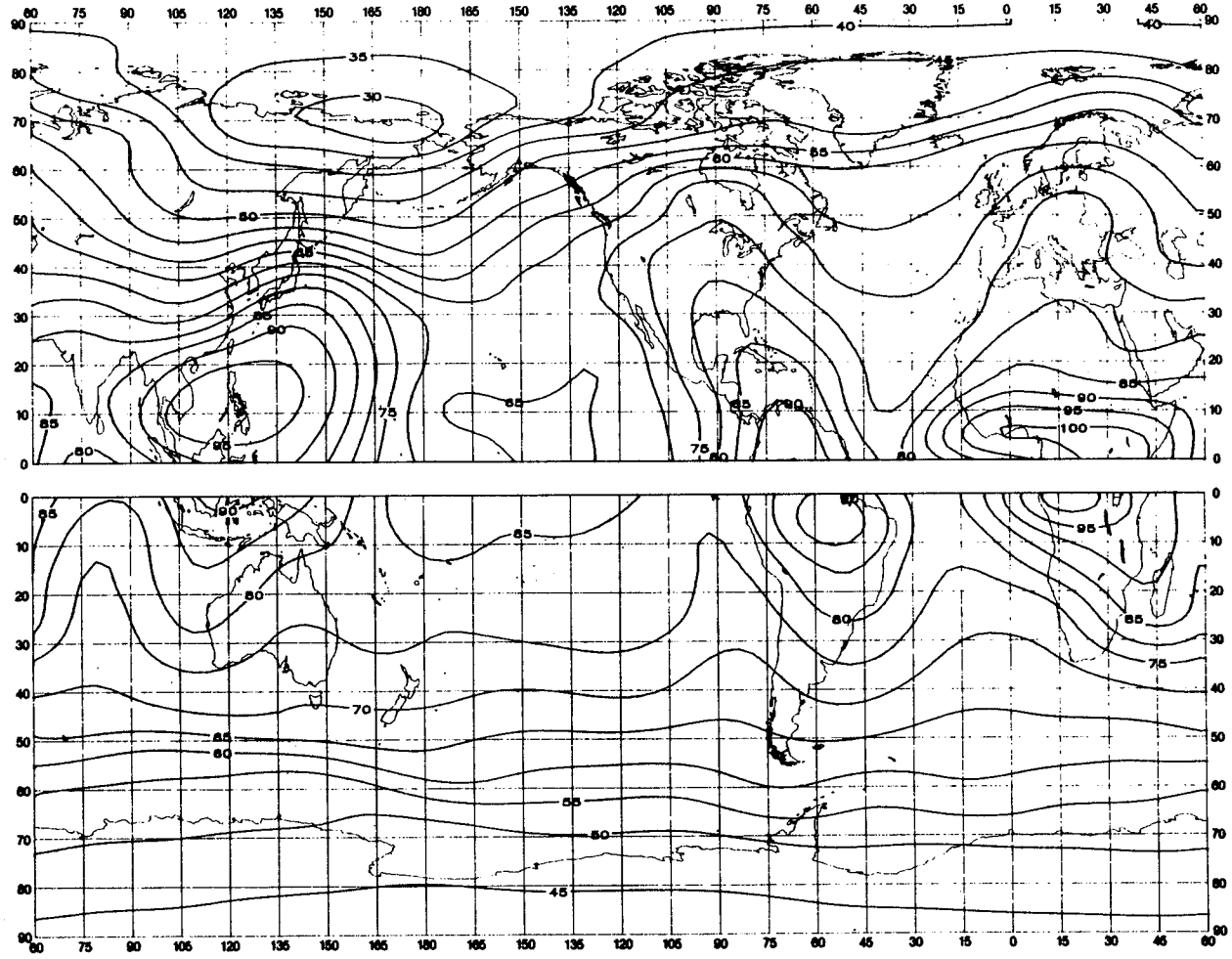

FIGURE 25a – *Valeurs attendues du bruit atmosphérique radioélectrique, F_{am}, en dB au-dessus de kT_0b à 1 MHz (Automne; 2000-2400 heure locale)*
FIGURE 25a – *Expected values of atmospheric radio noise, F_{am} (dB above kT_0b at 1 MHz) (Autumn; 2000-2400 LT)*
FIGURA 25a – *Valores probables del ruido atmosférico, F_{am}, en dB por encima de kT_0b en 1 MHz (Otoño; 2000-2400 hora local)*

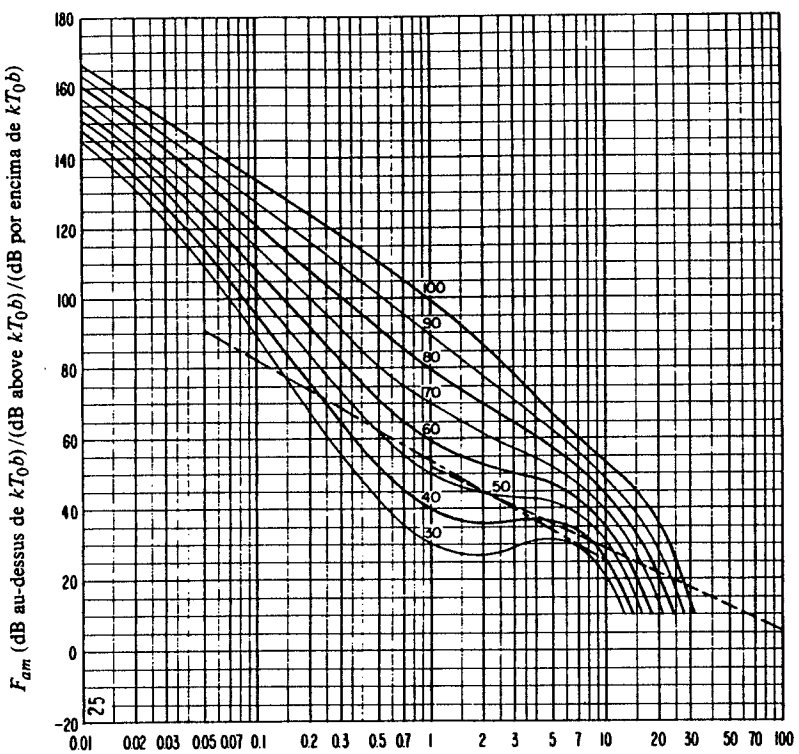

FIGURE 25b – *Variation du bruit radioélectrique en fonction de la fréquence (Automne; 2000-2400 heure locale)*

FIGURE 25b – *Variation of radio noise with frequency (Autumn; 2000-2400 LT)*

FIGURA 25b – *Variaciones del ruido radioeléctrico con la frecuencia (Otoño; 2000-2400 hora local)*

Voir la légende de la Fig. 2b/See legend of Fig. 2b/Véase la leyenda de la fig. 2b

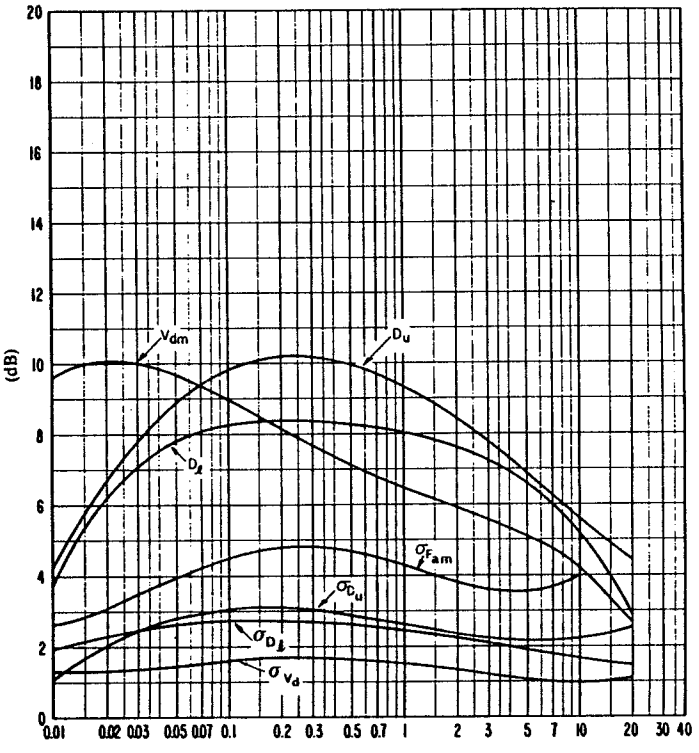

FIGURE 25c – *Données sur la variabilité et le caractère du bruit (Automne; 2000-2400 heure locale)*

FIGURE 25c – *Data on noise variability and character (Autumn; 2000-2400 LT)*

FIGURA 25c – *Datos sobre la variabilidad y el carácter del ruido (Otoño; 2000-2400 hora local)*

Voir la légende de la Fig. 2c/See legend of Fig. 2c/Véase la leyenda de la fig. 2c

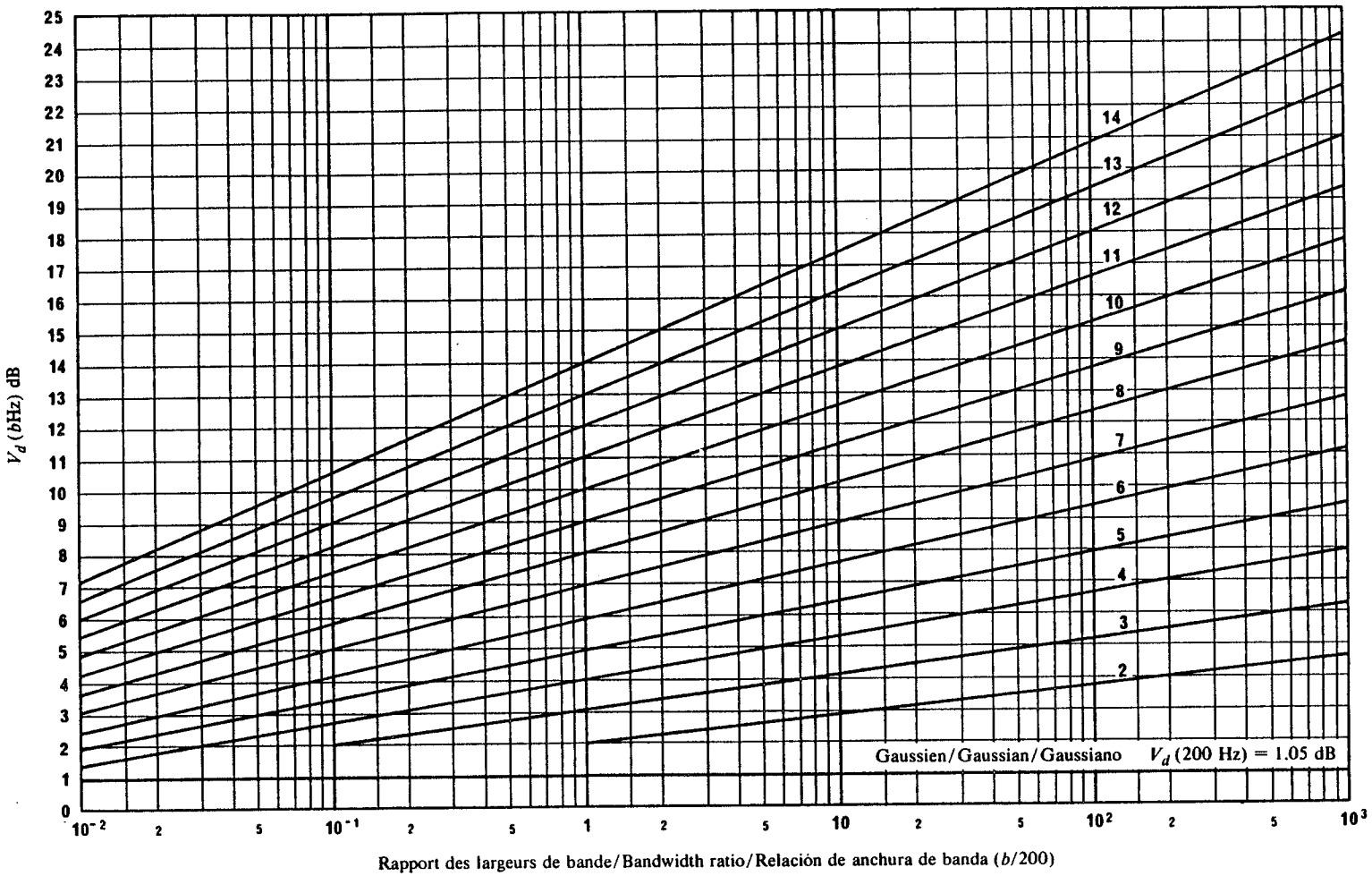

FIGURE 26 – *Conversion des valeurs de V_d valables pour une largeur de bande de 200 Hz, V_{dm}, en valeurs de V_d valables pour d'autres largeurs de bande, b*

FIGURE 26 – *Translation of a 200 Hz bandwidth V_d, V_{dm}, to other bandwidths, b*

FIGURA 26 – *Conversión de V_d para una anchura de banda de 200 Hz, V_{dm}, en valores para otras anchuras de banda, b*

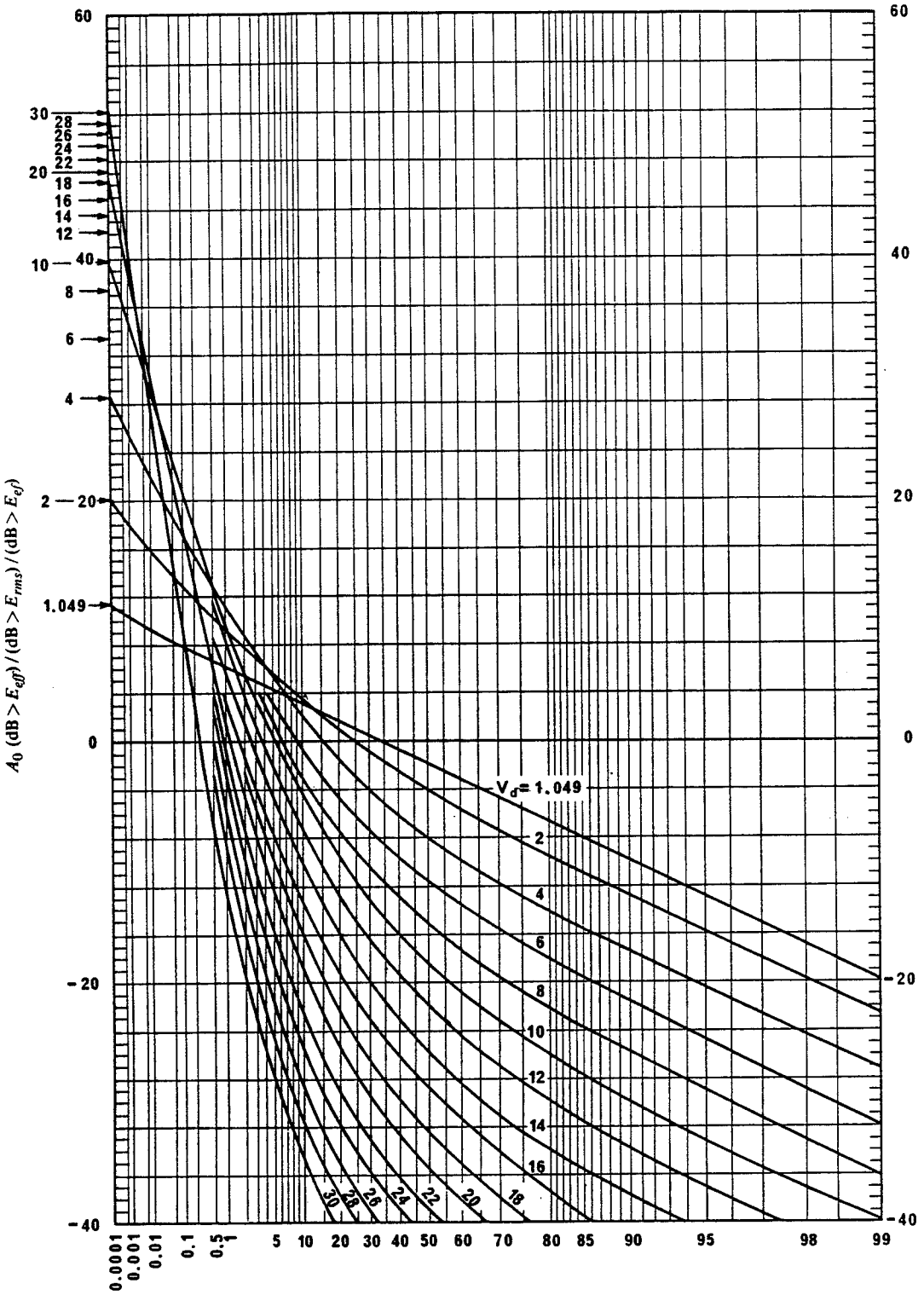

Pourcentage du temps pendant lequel la valeur de l'ordonnée est dépassée/Percentage of time ordinate exceeded/
Porcentaje de tiempo durante el cual se rebasa el valor de ordenadas

FIGURE 27 – *Distributions de probabilité d'amplitude du bruit atmosphérique radioélectrique pour différentes valeurs de V_d*

FIGURE 27 – *Amplitude probability distributions for atmospheric radio noise for various values of V_d*

FIGURA 27 – *Distribuciones de la probabilidad de amplitud (DPA) del ruido radioeléctrico atmosférico para diversos valores de V_d*

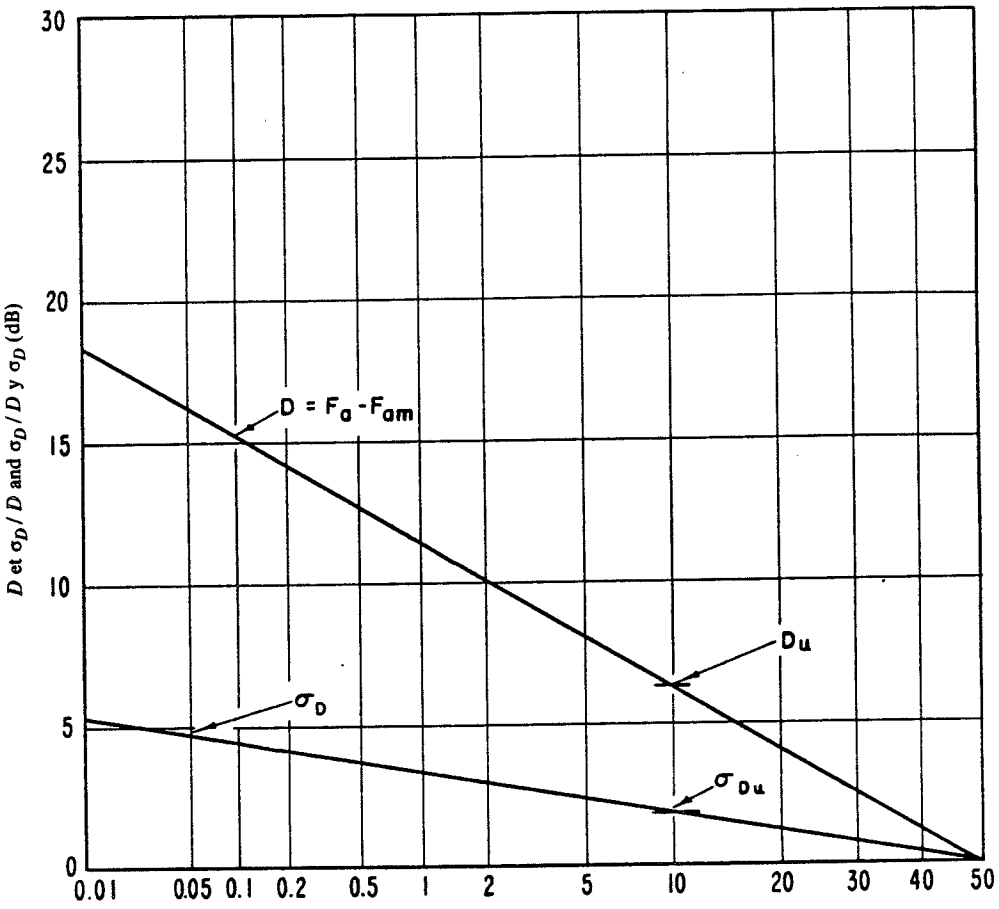

FIGURE 28 – *Valeurs attendues de D et de leurs écarts types* σ_D
FIGURE 28 – *Expected values of D and their standard deviations* σ_D
FIGURA 28 – *Valores probables de D y de sus desviaciones típicas,* σ_D

Eté; 2000-2400 heure locale
Fréquence: 50 kHz

Summer; 2000-2400 LT
Frequency: 50 kHz

Verano; 2000-2400 hora local
Frecuencia: 50 kHz

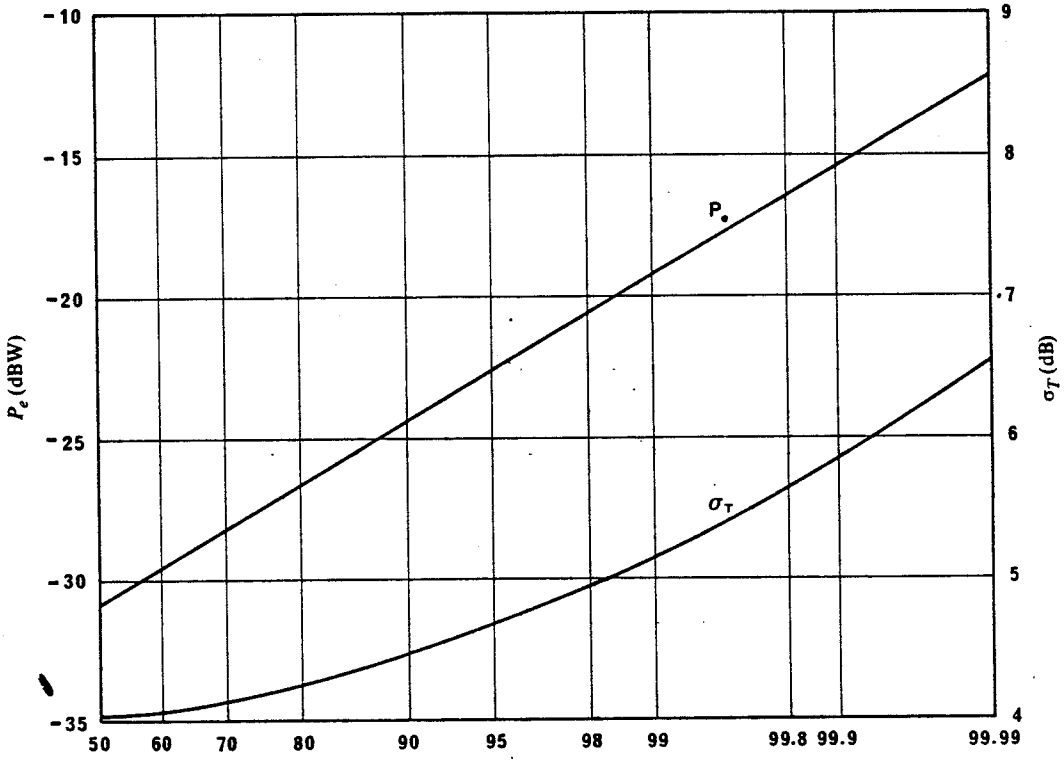

FIGURE 29 – *Valeurs de P_e et de leurs écarts types σ_T*
FIGURE 29 – *Values of P_e and their standard deviations σ_T*
FIGURA 29 – *Valores de P_e y de sus desviaciones típicas, σ_T*

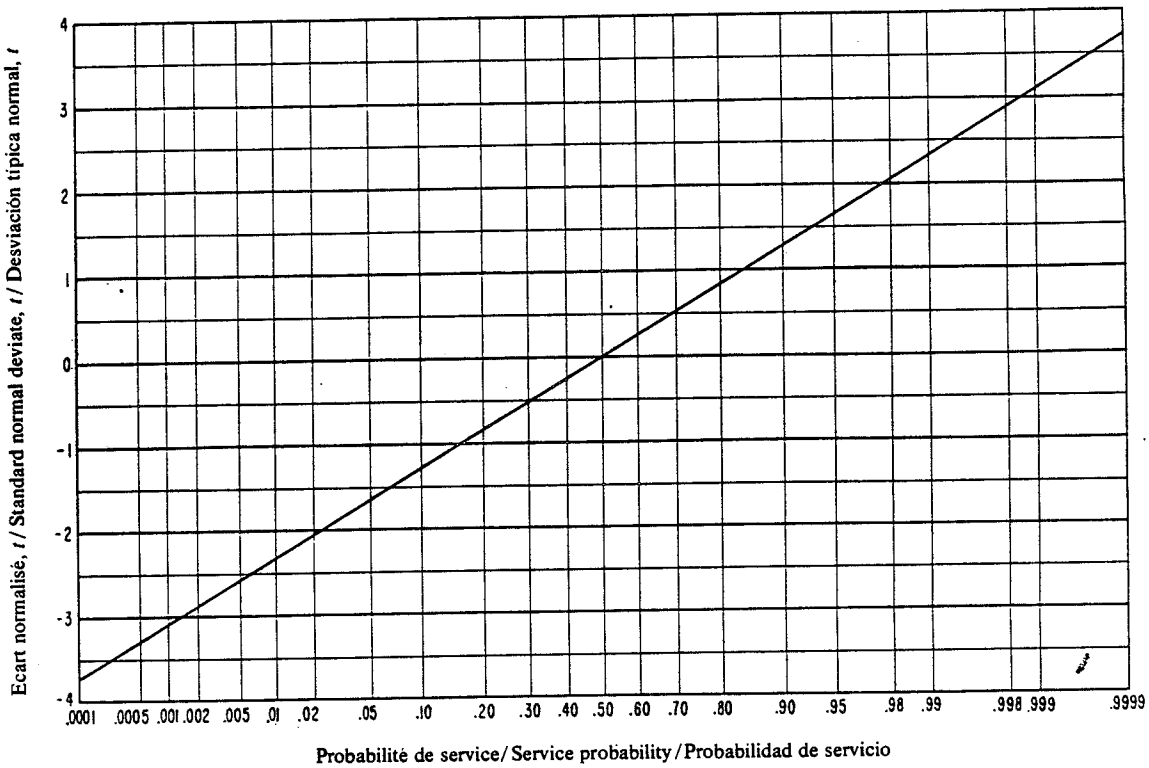

FIGURE 30 – *Probabilité de service en fonction de l'écart normalisé t*
FIGURE 30 – *Service probability as a function of the standard normal deviate, t*
FIGURA 30 – *Probabilidad de servicio en función de la desviación típica normal, t*

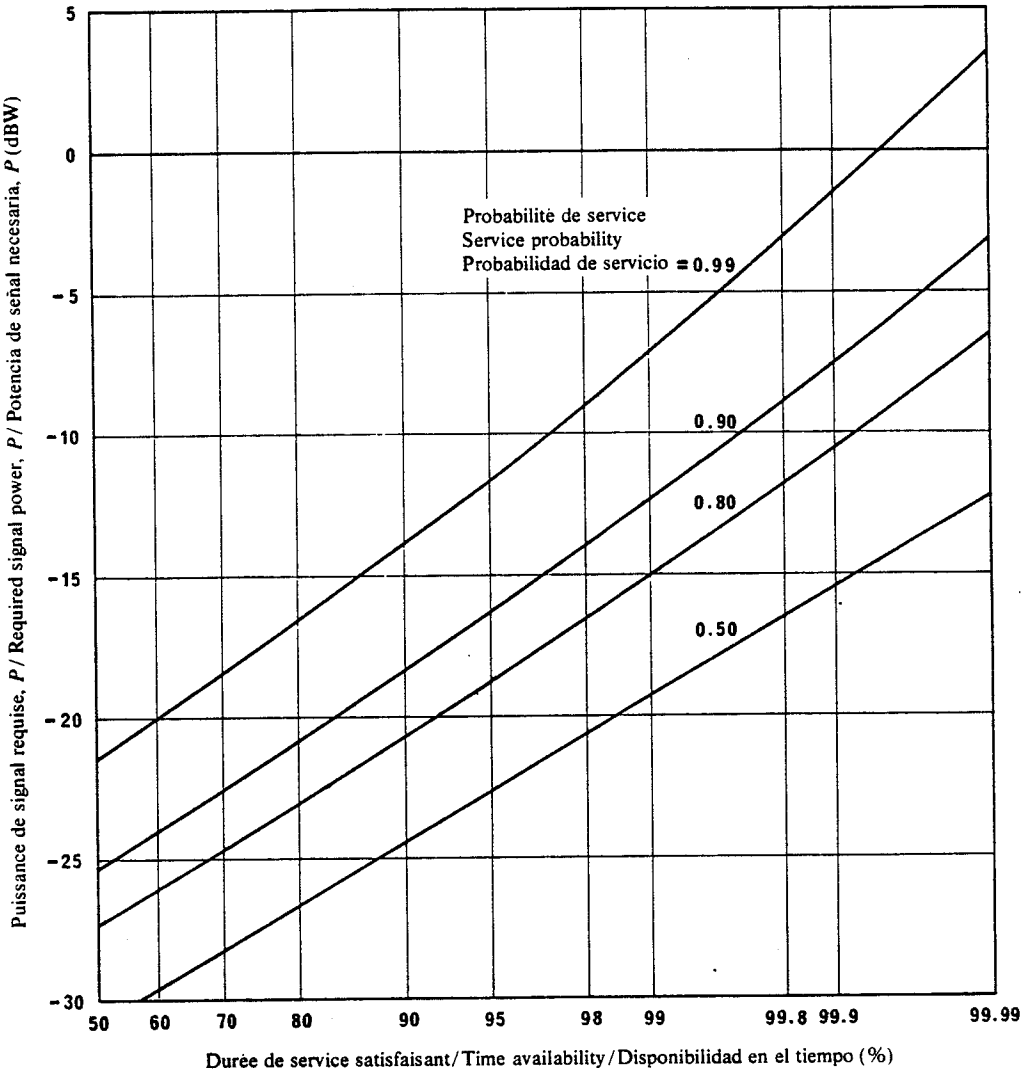

FIGURE 31 – *Puissance de signal requise en fonction de la durée de service satisfaisant, pour différentes probabilités de service (niveaux de confiance)*

FIGURE 31 – *Required signal power versus time availability for various service probabilities (confidence levels)*

FIGURA 31 – *Potencia de señal necesaria.P, en función de la disponibilidad en el tiempo para diversos valores de la probabilidad de servicio (niveles de confianza)*

Genève, Suisse
Eté: 2000-2400 heure locale
Fréquence: 50 kHz
Largeur de bande: 100 Hz
Erreur binaire: 5×10^{-4}
Type de service: non cohérent à MDF

Geneva, Switzerland
Summer: 2000-2400 LT
Frequency: 50 kHz
Bandwidth: 100 Hz
Binary errors: 5×10^{-4}
Type of service: NCFSK

Ginebra, Suiza
Verano: 2000-2400 hora local
Frecuencia: 50 kHz
Anchura de banda: 100 Hz
Errores binarios: 0,05%
Tipo de servicio: MDF no coherente

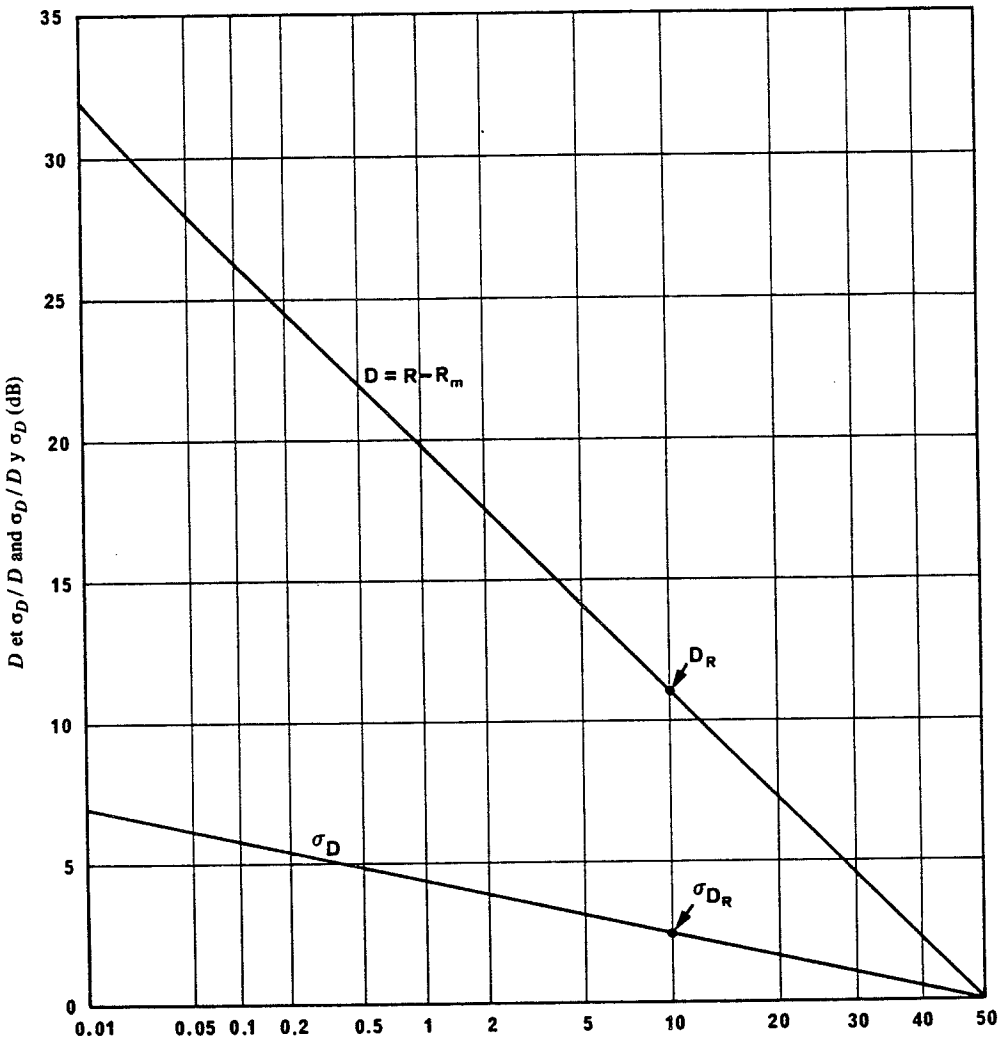

FIGURE 32 – *Valeurs de D et de leurs écarts types* σ_D
FIGURE 32 – *Values of D and their standard deviations* σ_D
FIGURA 32 – *Valores de D y de sus desviaciones típicas,* σ_D

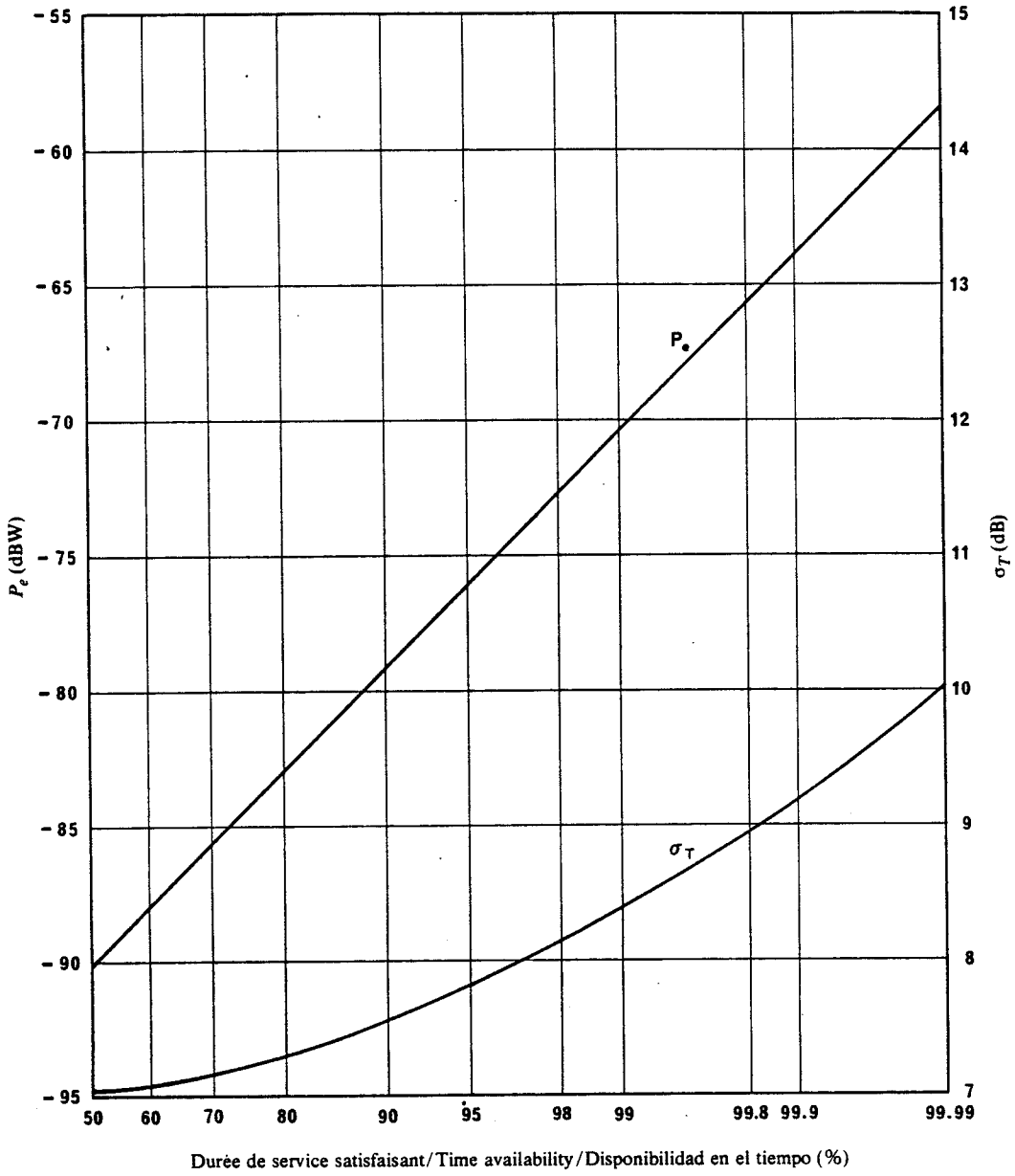

FIGURE 33 – *Valeurs de P_e et de leurs écarts types σ_T*
FIGURE 33 – *Values of P_e and their standard deviations σ_T*
FIGURA 33 – *Valores de P_e y de sus desviaciones típicas, σ_T*

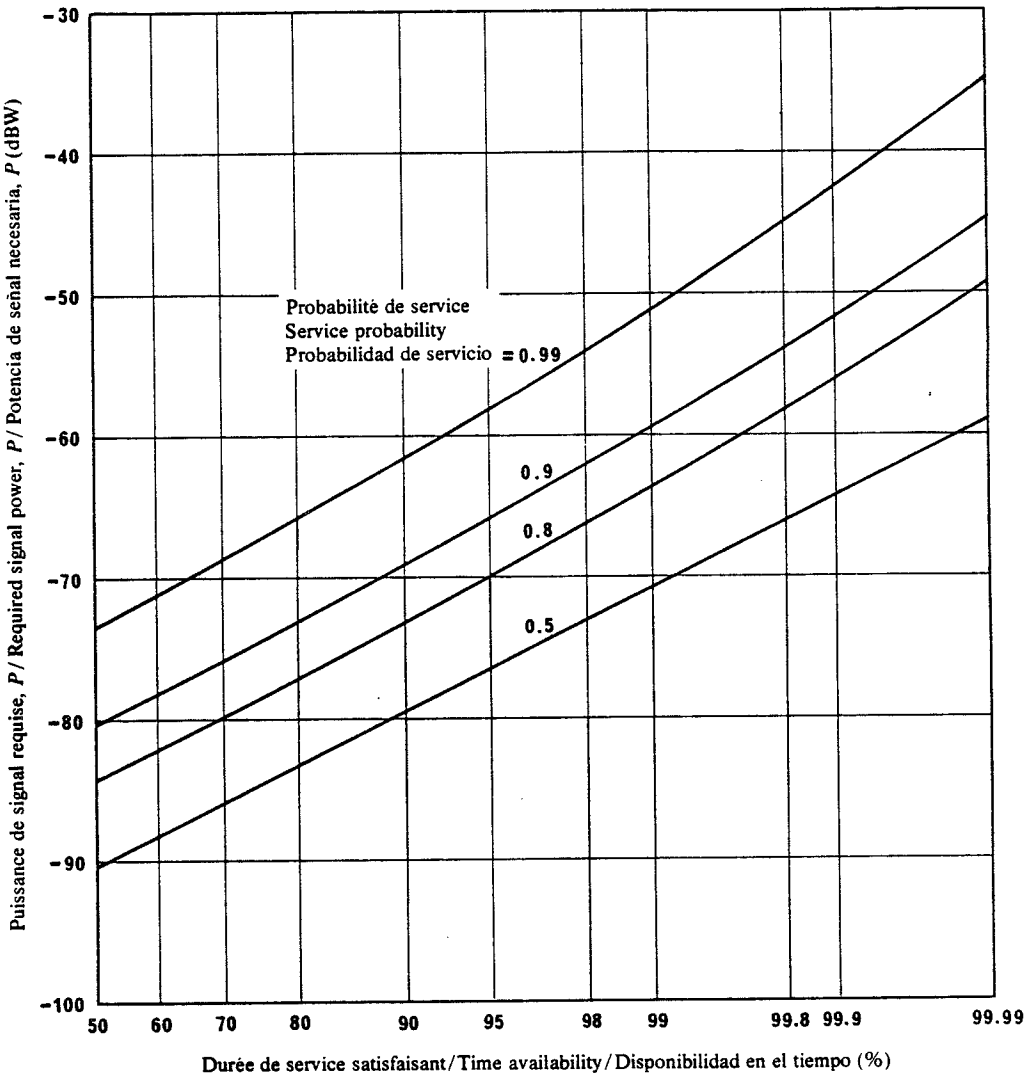

FIGURE 34 – *Puissance de signal requise en fonction de la durée de service satisfaisant, pour différentes probabilités de service (niveaux de confiance)*

FIGURE 34 – *Required signal power versus time availability for various service probabilities (confidence levels)*

FIGURA 34 – *Potencia de señal necesaria, P, en función de la disponibilidad en el tiempo para diversos valores de la probabilidad de servicio (niveles de confianza)*

Genève, Suisse
Eté: 2000-2400 heure locale
Fréquence: 5 MHz
Largeur de bande: 6 kHz
Téléphonie A3E, qualité tout juste commerciale

Geneva, Switzerland
Summer: 2000-2400 LT
Frequency: 5 MHz
Bandwidth: 6 kHz
A3E telephony, marginally commercial service

Ginebra, Suiza
Verano: 2000-2400 hora local
Frecuencia: 5 MHz
Anchura de banda: 6 kHz
Telefonía A3E, servicio marginalmente comercial

Appendix B

"Man-made Radio Noise." CCIR Report 258–4, XVIth Plenary Assembly, Dubrovnik 1986, Vol. VI, pp. 207–214.

REPORT 258-4*

MAN-MADE RADIO NOISE

(Study Programme 29C/6)

(1963-1970-1974-1978-1982)

1. In the solution of telecommunication problems, it is highly desirable to be able to estimate the radio noise at any location as caused by different types of noise sources. At certain locations, unintended man-made noise may be dominant. Since such noise can arise from a number of sources, such as power lines, industrial machinery, ignition systems, etc., it varies markedly with location and time [Hagn, 1973, 1981; Herman, 1971, 1979; Horner, 1971; Skomal, 1978; URSI, 1975, 1978 and 1981].

2. Current information is not available for estimating man-made noise intensities under all conditions but from limited observations [JTAC, 1968; Spaulding and Disney, 1974; and Spaulding *et al.*, 1975] it is possible to derive typical values.

3. Median values of man-made noise power expressed in terms of F_a (dB above thermal noise at T_0 = 288 K, see Reports 322 and 670) attributed to man-made sources are shown in Fig. 1 as curves A to D, for business, residential, rural, and quiet rural areas, respectively, in the United States of America [Spaulding and Disney, 1974]. Measurements from 103 areas during 1966-1971 inclusive were used in the determination of the upper three curves. Business areas are defined as any area where the predominant usage thoughout the area is for any type of business (e.g. stores and offices, industrial parks, large shopping centres, main streets or highways lined with various business enterprises, etc.). Residential areas are defined as any area used predominantly for single or multiple family dwellings with a density of at least five single family units per hectare and no large or busy highways. Rural areas are defined as areas where dwellings are no more than one every two hectares. Attached to the use of these area classifications is the qualification that localized, intense noise sources are excluded. Curve D (for quiet rural areas) corresponds to the values of man-made noise at carefully selected quiet receiving sites as reported in Report 322. The dashed curve E, for galactic-noise obtained from Report 322, is included for reference. Further limited measurements in the USA reported by Spaulding and Disney [1974] relate to parks and university campuses (which generally have less vehicular traffic, electrical equipment and other types of noise source than business or residential areas) and relate to interstate highways (where the main source is ignition noise).

* This Report is brought to the attention of Study Group 1.

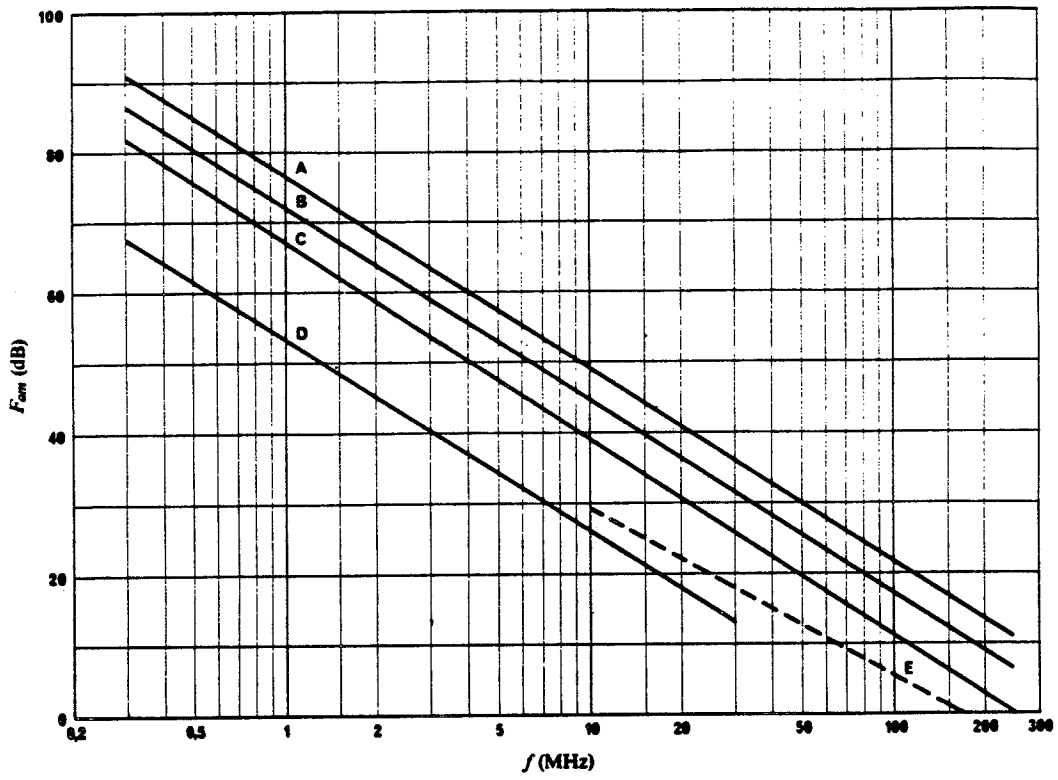

FIGURE 1 – *Median values of man-made noise power for a short vertical lossless grounded monopole antenna*

Environmental category:
A: business
B: residential
C: rural
D: quiet rural
E: galactic

In all cases, as with the data of Fig. 1, results are consistent with a linear variation of the median value, F_{am}, with frequency f of the form:

$$F_{am} = c - d \log f \qquad (1)$$

With f expressed in MHz, c and d take the values given in Table I. Note that equation (1) is valid in the range 0.3 to 250 MHz for all the environmental categories except those of curves D and E as indicated on the figure.

TABLE I — *Values of the constants c and d*

Environmental category	*c*	*d*
Business (curve A)	76.8	27.7
Inter-state highways	73.0	27.7
Residential (curve B)	72.5	27.7
Parks and university campuses	69.3	27.7
Rural (curve C)	67.2	27.7
Quiet rural (curve D)	53.6	28.6
Galactic noise (curve E)	52.0	23.0

Table II gives the variations measured within an hour about the hourly median value of noise power at a specified location. Upper and lower decile values D_u and D_l respectively are quoted for a selection of frequencies and for three types of environmental category.

An indication of the variation encountered from location to location within each environmental category is given by Spaulding and Disney [1974]. For all frequencies combined these authors quote the standard deviation of the median value as 7.5 and 6.5 dB, respectively, for business, residential and rural areas. A better estimate of the location variability of F_{am} for these environmental categories for a specific frequency may be obtained from the standard deviations σ_{NL} given in Table II for the measurement frequencies used.

Hagn and Sailors [1979] have presented four statistical-distribution models of increasing complexity (simple Gaussian, composite Gaussian, χ-square, Gaussian from χ-square) which utilize the time and location variability of F_a to predict the exceedence probabilities of man-made radio noise available power levels for short, vertically-polarized antennas located near the ground. The models are useful in predicting the probability that the short-term signal-to-noise ratio for a given communication system equals or exceeds a value required for successful communications [Hagn, 1980]. The parameters for these models at each of the measurement frequencies are summarized in Table III. For the simple Gaussian model, the mean is approximated by F_{am} and the standard deviation is σ_N where:

$$\sigma_N = \sqrt{\sigma_{NL}^2 + \sigma_{NT}^2} \tag{2}$$

assuming that the temporal and spatial variabilities are uncorrelated. The parameter α_{NT} is the standard deviation of the temporal variability and values are obtained from D_u and D_l of Table II using:

$$\sigma_{NT} = \frac{1}{1.28}\left[\frac{D_u^2 + D_l^2}{2}\right]^{\frac{1}{2}} \tag{3}$$

For the composite Gaussian model, the standard deviations for the upper and lower halves of the distribution are given by σ_{Nu} and σ_{Nl}, respectively, and the mean is given by F_{am}. The corresponding upper and lower deciles are given by D_{Nu} and D_{Nl}. The composite Gaussian model is the simplest model which takes into account skewness ($D_{Nu} \neq D_{Nl}$) in the distribution. The χ-square model also takes into account skewness. In the χ-square model, the parameter ν is the number of degress of freedom. The χ-square model satisfies the relationship $F_a = a + b_{\chi 2}$. The mean noise $\bar{F}_a = a + b\nu$, and the standard deviation $\sigma_{N_{\chi 2}} = b\,(2\nu)^{1/2}$, where a, b, and ν are given in Table III for ten discrete frequencies between 0.25 MHz and 250 MHz. For details of fitting data with a χ-square distribution and the use of the parameters ν, a, and b of Table III, see Zacharisen and Crow [1970]. A second Gaussian model is given in Table III using parameters estimated from the χ-square approximations. For this model, the mean is given by $F_{a_{\chi 2}}$ and the standard deviation by $\sigma_{N_{\chi 2}}$. When the skew is not too great, all four models predict similar values between the deciles; however, the χ-square model gives the best fit to the entire distribution. The simple Gaussian model should be used when the skew is not too high ($\nu \geq 10$) and when a simple model is required as in interference analysis [Sailors, *et al.*, 1977] (Report 657). The composite Gaussian model (which accounts for skewness) is the choice when a means is available to determine the appropriate half of the distribution. To date it has not been possible to choose one of these four models as consistently being the best. The above description may be used as a guideline for picking the appropriate model for a specific case.

TABLE II — *Representative values of selected measured noise parameters for business, residential and rural environmental categories*

Frequency (MHz)	Environmental category											
	Business				Residential				Rural			
	F_{am} (dB (kT_0))	D_u (dB)	D_l (dB)	σ_{NL} (dB)	F_{am} (dB (kT_0))	D_u (dB)	D_l (dB)	σ_{NL} (dB)	F_{am} (dB (kT_0))	D_u (dB)	D_l (dB)	σ_{NL} (dB)
0.25	93.5	8.1	6.1	6.1	89.2	9.3	5.0	3.5	83.9	10.6	2.8	3.9
0.50	85.1	12.6	8.0	8.2	80.8	12.3	4.9	4.3	75.5	12.5	4.0	4.4
1.00	76.8	9.8	4.0	2.3	72.5	10.0	4.4	2.5	67.2	9.2	6.6	7.1
2.50	65.8	11.9	9.5	9.1	61.5	10.1	6.2	8.1	56.2	10.1	5.1	8.0
5.00	57.4	11.0	6.2	6.1	53.1	10.0	5.7	5.5	47.8	5.9	7.5	7.7
10.00	49.1	10.9	4.2	4.2	44.8	8.4	5.0	2.9	39.5	9.0	4.0	4.0
20.00	40.8	10.5	7.6	4.9	36.5	10.6	6.5	4.7	31.2	7.8	5.5	4.5
48.00	30.2	13.1	8.1	7.1	25.9	12.3	7.1	4.0	20.6	5.3	1.8	3.2
102.00	21.2	11.9	5.7	8.8	16.9	12.5	4.8	2.7	11.6	10.5	3.1	3.8
250.00	10.4	6.7	3.2	3.8	6.1	6.9	1.8	2.9	0.8	3.5	0.8	2.3

F_{am}: median value

D_u, D_l: upper, lower decile deviations from the median value within an hour at a given location

σ_{NL}: standard deviation of location variability

TABLE III — *Summary of noise model parameters*

Environmental category	Freq. (MHz)	Simple Gaussian		Composite Gaussian				χ-square			Gaussian from χ-square	
		F_{am} (dB (kT_0))	σ_N (dB)	σ_{Nu} (dB)	σ_{Nl} (dB)	D_{Nu} (dB)	D_{Nl} (dB)	v	*a*	*b*	$F_{a\chi^2}$ (dB (kT_0))	$\sigma_{N\chi^2}$ (dB)
Business	0.25	93.5	8.3	8.8	7.8	11.3	9.9	92.16	37.51	0.61	93.9	8.3
	0.50	85.1	11.6	12.8	10.3	16.4	13.2	32.12	39.26	1.46	86.1	11.7
	1.00	76.8	6.3	8.0	3.9	10.2	5.0	3.51	69.77	2.46	78.4	6.5
	2.50	65.8	12.4	13.0	11.8	16.7	15.1	142.29	− 38.56	0.74	66.3	12.4
	5.00	57.4	9.2	10.5	7.8	13.5	10.0	16.58	31.70	1.62	58.5	9.3
	10.00	49.1	7.7	9.5	5.3	12.1	6.8	4.95	38.38	2.49	50.7	7.8
	20.00	40.8	8.7	9.6	7.7	12.3	9.9	32.66	6.18	1.08	41.5	8.7
	48.00	30.2	11.1	12.5	9.5	16.0	12.2	20.91	− 4.69	1.73	31.4	11.2
	102.00	21.2	11.4	12.8	9.8	16.4	12.6	21.95	− 15.62	1.73	22.3	11.5
	250.00	10.4	5.6	6.4	4.5	8.3	5.8	12.28	− 2.80	1.13	11.1	5.6
Residential	0.25	89.2	6.8	8.1	5.3	10.3	6.8	8.67	75.88	1.66	90.3	6.9
	0.50	80.8	8.5	10.5	5.7	13.5	7.4	4.67	69.42	2.84	82.7	8.7
	1.00	72.5	6.5	8.2	4.3	10.5	5.5	4.02	64.49	2.37	74.0	6.7
	2.50	61.5	10.4	11.3	9.4	14.4	12.0	45.36	12.58	1.09	62.2	10.4
	5.00	53.1	8.4	9.6	7.1	12.3	9.1	17.11	29.28	1.45	54.1	8.5
	10.00	44.8	6.1	7.2	4.9	9.2	6.2	10.38	31.57	1.36	45.7	6.2
	20.00	36.5	8.3	9.5	6.9	12.2	8.8	14.80	14.75	1.54	37.5	8.4
	48.00	25.9	8.8	10.4	6.8	13.3	8.7	8.90	8.53	2.11	27.3	8.9
	102.00	16.9	7.9	10.1	4.6	13.0	5.9	3.09	8.98	3.35	19.0	8.2
	250.00	6.1	4.9	6.1	3.2	7.8	4.1	4.13	0.00	1.74	7.2	5.0
Rural	0.25	83.9	7.2	9.1	4.5	11.7	5.7	3.52	75.82	2.80	85.7	7.4
	0.50	75.5	8.5	10.7	5.4	13.7	6.9	3.78	65.57	3.17	77.6	8.7
	1.00	67.2	9.5	10.1	8.8	13.0	11.3	75.34	9.41	0.77	67.7	9.5
	2.50	56.2	10.2	11.2	9.0	14.4	11.5	28.78	18.36	1.35	57.1	10.2
	5.00	47.8	9.4	9.0	9.7	11.5	12.4	260.87	154.61	0.41	47.6	9.4
	10.00	39.5	6.8	8.1	5.1	10.4	6.5	7.49	27.37	1.78	40.7	6.9
	20.00	31.2	6.9	7.6	6.2	9.7	8.0	39.08	0.87	0.79	31.7	7.0
	48.00	20.6	4.5	5.2	3.5	6.7	4.5	9.84	11.27	1.02	21.3	4.5
	102.00	11.6	7.1	9.0	4.5	11.6	5.8	3.72	3.25	2.71	13.3	7.4
	250.00	0.8	3.0	3.5	2.3	4.5	3.0	9.20	− 5.29	0.71	1.2	3.0

4. Measurements made at HF in the United Kingdom indicate that curve D is appropriate for rural areas and that the man-made noise powers in business and residential areas are below those given by curves A and B. Measurements made at VHF in business and residential areas indicate man-made noise powers some 10 dB below those of curves A and B.

These results seem to suggest that differences in patterns of utilization of electrical and mechanical appliances or in the national statutory regulation of interference can lead to differing values of man-made noise power and that, until further evidence is available, the curves in Fig. 1 should be treated with caution.

5. Skomal [1973, 1978] has reviewed man-made noise data collected in a range of countries at various distances from metropolitan areas. Results over the frequency range 500 kHz to 1 GHz are summarized. In the frequency range of about 300 to 800 MHz there is evidence that the rate of decrease of noise power with frequency is significantly less than that at lower frequencies as given in Table I. This is consistent with the presence of a localized maximum in the UHF-band emission spectrum of vehicular ignition interference.

6. At four sites in downtown Ottawa, Canada, measurements of the UHF-VHF radio environment were carried out over a 17-day period in November, 1976 by Lauber and Bertrand [1977]. A linear regression equation of the median values of F_a data for all four sites for the frequencies 200 to 500 MHz is given as $F_{am} = -15.8 \log f + 48.4$ (f in MHz). In the frequency range from 200 to 300 MHz, the results using this equation compare favourably with those using the business area equation of Spaulding and Disney [1974]. The standard deviation σ_N and upper and lower deciles, D_u and D_l, for these data are given in Table IV for the measurement frequencies 200, 300, 400 and 500 MHz.

TABLE IV — *F_{am} distribution parameters for business areas*

Frequency (MHz)	Standard deviation σ_N (dB)	D_u (dB)	D_l (dB)
200	4.7	5.0	6.0
300	4.6	7.0	4.5
400	4.2	5.5	4.5
500	4.1	6.5	2.5

7. Beyond 1 GHz for business areas and 250 MHz for residential and rural areas, the measurement of man-made noise has been difficult because the available receivers have been internal noise-limited. In such a receiver system, the external noise does not affect its operating noise-threshold appreciably (Reports 413, (Oslo, 1966) and 670). Man-made noise measurements in an urban environment at frequencies between 1.7 and 35 GHz have been reported by Pratt *et al.* [1978] using radiometer techniques; however, the results were always below the reference temperature of 288 K.

8. Measurements made in the MF and HF range to determine the propagation attenuation coefficient of man-made noise α, as a function of residential density ρ, have in Poland led to the empirical relationship

$$\log \alpha = -3.47 + 0.690 \log \rho$$

where α is in dB/m and ρ is residential density in inhabitants/hectare. The influence of frequency on the value of attenuation coefficient was found to be insignificant [Rymarowicz, 1974 and 1975].

An unexpected result of measurements made in the MF range was lower man-made noise intensity in the residential areas of cities in the highly industrialized parts of the country. This is contrary to the generally held opinion about increase in the man-made noise power with increase of industrialization. This may probably be due to greater attenuation over paths through dense settlement patterns in highly industrialized regions, while the density of noise sources remained sensibly unchanged [Morón and Rymarowicz, 1975]. Further investigations are necessary to confirm these results.

9. Measurements of the amplitude probability distributions (APD's) of man-made noise both from the overall environment and from specific sources have been made at many locations [Spaulding *et al.*, 1971, Lauber and Bertrand, 1979; Hagn, 1981].

The results of mathematical modelling of amplitude statistics using empirical and theoretical models have been reported by Lauber and Bertrand [1979]. A summary of a wide selection of mathematical models, mostly designed for atmospheric noise, has been given by Spaulding [1981]. A new series of statistical-physical models which use the characteristics of the physical processes to derive expressions for the amplitude statistics have been developed by Middleton [1979a, b]. To date, these models have been applied to a number of measured APD's with excellent agreement.

REFERENCES

HAGN, G. H. [1973] Radio noise of terrestrial origin. *Radio Sci.*, Vol. 8, 6, 613-621.

HAGN, G. H. [1980] VHF radio system performance model for predicting communications operational ranges in irregular terrain. *IEEE Trans. Comm.*, Vol. COM-2B, 1637-1644.

HAGN, G. H. [1981] Man-made electromagnetic noise. *Handbook of Atmospherics.* Ch. 7, Ed. H. Volland, CRC Press, Boca Raton, Fla., USA.

HAGN, G. H. and SAILORS, D. B. [1979] Empirical models for probability distributions of short-term mean environmental man-made radio noise levels. 3rd Symposium and Technical Exhibition on Electromagnetic Compatibility, Rotterdam, 355-360 (available from EMC Symposium 1979, Postbus 5810, NL-2280 Rijswijk (ZH)), Netherlands.

HERMAN, J. R. [1971] Survey of man-made radio noise. *Progress in Radio Science*, Vol. I, 315-348, URSI, Brussels, Belgium.

HERMAN, J. R. [1979] *Electromagnetic Ambients and Man-Made Noise*, Vol. III, Multi-Volume EMC Encyclopedia Series. Don White Consultants, Inc., Gainsville, Va. 22065, USA.

HORNER, F. [1971] Techniques used for the measurement of atmospheric and man-made noise. *Progress in Radio Science*, Vol. II, 177-182, URSI, Brussels, Belgium.

JTAC [1968] Unintended radiation. *Suppl. 9 to Spectrum Engineering – The Key to Progress.* IEEE, New York, NY, USA.

LAUBER, W. R. and BERTRAND, J. M. [1977] Preliminary urban VHF/UHF radio noise intensity measurements in Ottawa, Canada. 2nd Symposium and Technical Exhibition on Electromagnetic Compatibility, Montreux, Switzerland, 357-362. (IEEE No. 77CH1224-5 EMC).

LAUBER, W. R. and BERTRAND, J. M. [1979] Statistical measurements and modelling of HVDC powerline noise. IEEE International Symposium on Electromagnetic Compatibility, 9-11 October, San Diego, Calif., USA, 224-231 (IEEE 79CH1383-9 EMC).

MIDDLETON, D. [1979a] Canonical non-Gaussian noise models: their implications for measurements and for prediction of receiver performance. *IEEE Trans. Electromag. Compt.*, Vol. EMC-21, 3, 209-220.

MIDDLETON, D. [1979b] Procedures for determining the parameters of the first-order canonical models for class *A* and class *B* electromagnetic interference. *IEEE Trans. Electromag. Compt.*, Vol. EMC-21, 3, 190-208.

MORÓN, W. and RYMAROWICZ, Z. [1975] Urban man-made noise in high industrialized and low industrialized regions in the medium wave range. 1st Symposium and Technical Exhibition on Electromagnetic Compatibility, Montreux, Switzerland, 284-287.

PRATT, T., BROWNING, D. J. and RAHHAL, Y. [1978] Radiometric investigations of the urban microwave noise environment at 1.7, 8.8 and 35 GHz. Proc. IEE International Conference on Antennas and Propagation, Part 2 – Propagation, London, UK, 28-30 November (IEE Conf. Publ. No. 169).

RYMAROWICZ, Z. [1974] Man-made noise in the medium frequency range in the cities of Lower Silesia and its dependence on population and industrialization of the city (in Polish). Institute of Telecommunications, Ph.D. thesis.

RYMAROWICZ, Z. [1975] Noise propagation in urban areas in medium and short wave range. 1st Symposium and Technical Exhibition on Electromagnetic Compatibility, Montreux, Switzerland, 281-283.

SAILORS, D. B., KUGEL, C. P. and HAYDON, G. W. [1977] Predicting the compatibility of high frequency skywave communication systems. *IEEE Trans. Electromag. Compt.*, Vol. EMC-19, 331-342.

SKOMAL, E. N. [1973] An analysis of metropolitan incidental radio noise data. *IEEE Trans. Electromag. Compt.*, Vol. EMC-15, 45-57.

SKOMAL, E. N. [1978] *Man-made Radio Noise.* Van Nosrand Reinhold, Co., New York, NY, USA.

SPAULDING, A. D. [1981] *Handbook of Atmospherics*, Ch. 6. Ed. H. Holland. CRC Press, Boca Raton, Florida, USA.

SPAULDING, A. D., AHLBECK, W. H. and ESPELAND, L. R. [1971] Urban residential man-made radio analysis and predictions. OT Telecommunications Research and Engineering Rep. 14, US Govt. Printing Office, Washington, DC 20402.

SPAULDING, A. D. and DISNEY, R. T. [1974] Man-made noise: Part I, OT Rep. 74-38. US Govt. Printing Office, Washington, DC 20402.

SPAULDING, A. D., DISNEY, R. T. and HUBBARD, A. G. [1975] Man-made noise: Part II, OT Rep. 75-63. US Govt. Printing Office, Washington, DC 20402.

URSI [1975] *Rev. of Radio Sci.* 1972-1974, 128-132. International Union of Radio Science, Brussels, Belgium.

URSI [1978] *Rev. of Radio Sci.* 1975-1977, 57-64. International Union of Radio Science, Brussels, Belgium.

URSI [1981] *Rev. of Radio Sci.* 1978-1980, E1-E13, International Union of Radio Science, Brussels, Belgium.

ZACHARISEN, D. H. and CROW, E. L. [1970] Fitting distributions of telecommunication variables with Chi-square distributions. *Radio Sci.*, Vol. 5, 1307-1315.

Appendix C
Instructions for Operation of Program "EMIN"

Introduction

These instructions describe the operation of a computer program for the calculation of minimum usable field strength, E_{min}.

Diskette description

The diskette is a double-density 5-1/4" 360 kb floppy. The master diskette contains the executable file EMIN.EXE. The source code file EMIN.FOR is available on a separate diskette from NAB upon request. The program may be copied, such as to a hard disk, but no additional disk space is necessary for program execution. The program was compiled with Microsoft FORTRAN v4.01 and is designed to run on almost any PC-compatible computer.

Hardware requirements

A typically equipped PC with 256 kb or more is required. The program was designed to use the capabilities of the math coprocessor. The program contains emulation routines that will permit it to run without the coprocessor, but it will run more slowly. A coprocessor-equipped machine is recommended.

All output data appears on the screen. Neither a printer nor graphics capability is required.

Program description

The noise environment for AM broadcast reception is dominated by two noise types: atmospheric and man-made noise. Both are typically characterized as non-gaussian, white noise processes that are non-stationary; that is, their statistical properties change with time and bandwidth. To estimate E_{min} in the presence of this type of noise, the statistical properties of the noise must be evaluated in a specified bandwidth.

The program allows the user to specify any desired set of parameters to define the grade of service, average noise power, statistical variation of the noise, bandwidth, frequency, and the parameters needed to assess the time availability and service probability. Operation of the program is self-explanatory using the information displayed during the run.

Grade of service

The program first performs a grade of service analysis, finding the level of signal necessary to be above the noise level by the specified number of dB for the specified percentage of time. This is found by evaluating the amplitude probability distribution (APD) function for the noise. The APD function gives the instantaneous noise level exceeded a certain percentage of time relative to the rms noise level. The APD function used in the program is a computer model presented in [1], which approximates the empirical descriptions presented in CCIR Report 322-3. Based on the studies in [2], both atmospheric and man-made noise have similar statistical properties, so the same APD computer model can be used for both types.

The three parameters used to construct the APD are F_{am}, V_{dm}, and bandwidth. F_{am}, which represents the average noise power, moves the amplitude of the APD up or down but does not affect its shape. The shape of the APD is determined by V_{dm} and bandwidth. The value of V_{dm} given in the noise measurement data is for an effective noise bandwidth of 200 Hz. Its value is automatically adjusted by the program to the actual noise bandwidth, using the equations found in [3]. For atmospheric noise, the program user obtains the value for V_{dm} from the graphs in Report 322-3. For man-made noise, the values for V_{dm} were derived from [2] and are built into the program.

Time availability

The result of the grade of service analysis is a signal level, R (dB), which is the level of the required received signal above the average noise level. This indicates that the specified grade of service will be available for 50 percent of the time since the calculation of R was based on the median value, F_{am}. If a higher time availability is required, the value of F_{am} is adjusted based on its statistical variation, as indicated by the upper decile, D_u. For example, for a time availability of 90 percent, the value of F_{am} is adjusted upward by adding the value of D_u, since the 90-percent point is exactly the upper decile value.

The value of F_{am}, as adjusted, is F_a. The program automatically adjusts F_{am} for a specified time availability. For atmospheric noise, this is done using the D_u supplied by the user. For man-made noise, the values for D_u were taken from [2], if available, and are built into the program.

With the value of F_a and R known, the program calculates the value of E_{min} using the equation

$$E_{min}\ (\text{dBmV/m}) = F_a + R + 10\log_{10}(BW) + 20\log_{10}f_{MHz} + 48.5$$

where E_{min} is the minimum usable field strength, in dB relative to 1 mV/m

BW is the effective noise bandwidth in Hz, and

f_{MHz} is the frequency in MHz.

Service probability

The value for E_{min} calculated using the above equation is only an estimate. Since median values for all parameters were used to determine this value for E_{min}, this estimate provides the specified grade of service for the specified time availability for only 50 percent of the paths or circuits. This is equivalent to a service probability of 50 percent.

To increase the service probability, or confidence level, above 50 percent, E_{min} must be increased to take into account the uncertainties in the estimates of the parameters used to determine E_{min}. The uncertainty or variability in any estimate is indicated by its standard deviation, or σ value. Each of the parameters that was used to formulate the variables in the equation for E_{min} (F_{am}, V_{dm}, D_u) has an associated standard deviation which is provided in Report 322–3. For man-made noise, these parameters are generally not available and will therefore appear in the output as zeros.

A fourth element of uncertainty is the accuracy with which a given value of field strength can be predicted. When calculating the signal required to produce a desired signal-to-noise ratio, the signal is assumed to be known and constant. In reality it, too, varies from its expected value. This uncertainty is represented by the standard deviation of the expected received signal strength. For AM broadcast groundwave signals, considerable differences may exist between the actual and the predicted field strength due to uncertainties in the ground conductivity, reflections from nearby metallic objects (wires, buildings, towers), or physical elements (hills and abrupt conductivity boundaries) along the propagation path. These uncertainties are not accounted for in the current FCC field strength prediction method. Based on a relatively small amount of data, one study [4] found that the standard deviation of actual field strengths compared to predicted field strengths was about 1.4 dB. For skywave or other types of propagation paths, another value may be more appropriate.

With all four standard deviations or uncertainty factors identified, the total uncertainty can be found as the root-sum-square of the four individual standard deviations. That is, the variance of the final estimate for E_{min} is equal to the sum of variances of each constituent part of E_{min}. This summing operation is performed by the computer program.

With the total standard deviation, σ_T, found for the estimated E_{min}, E_{min} can be adjusted for service probabilities other than 50 percent. Assuming the variation is normally distributed, E_{min} is increased by $\sigma_T t$, where t is the standard normal deviate. For a service probability of 50 percent, t equals 0. For a service probability of 90 percent, t equals about 1.28. The program automatically evaluates t to determine the final adjusted value of E_{min} that achieves the required service probability.

Program execution

The program is run by typing "EMIN<ret>". A title screen will appear, followed by an instruction screen. The user is then asked sequentially for the required input data as discussed above. When all data has been entered, the program will display "Working . . ." while E_{min} is being calculated.

When the calculation is complete, a results screen will be displayed which tabulates all of the input data and the calculated value of E_{min}. Results can be printed using the "PrtSc" keyboard command. The user can then select another run or exit from the program.

References

[1] Akima, H.: "A Method of Numerical Representation for the Amplitude Probability Distribution of Atmospheric Radio Noise." U.S. Department of Commerce, Office of Telecommunications Report OT/TRER 27, March 1972.

[2] Spaulding, A.D. and Disney, R.T.: "Man-made Radio Noise. Part I — Estimates for Business, Residential and Rural Areas." U.S. Department of Commerce, Office of Telecommunications Report 74–38, June 1974.

[3] Herman, J.R. and De Angelis, X.A.: "Bandwidth Expansion Effects of the Voltage Deviation Parameter (V_d) of MF and HF Atmospheric Radio Noise." Radio Science, Vol. 22 No. 1, January-February 1987, pp. 26-36.

[4] Anderson, H.R.: "Location Statistics of AM Broadcast Groundwave Signal Amplitudes." IEEE Transactions on Broadcasting, Vol. BC-32 No. 2, June 1986, pp. 23–26.

Appendix D

Gröschel, G: "A mathematical model for the calculation of the adjacent-channel interference in single-sideband and double-sideband AM sound broadcasting systems." EBU Review – Technical, No. 169, June 1978, pp. 122–136.

A mathematical model for the calculation of the adjacent-channel interference in single-sideband and double-sideband AM sound-broadcasting systems

G. Gröschel

Reprinted from E.B.U. Review – Technical, No. 169 (June, 1978)

Published by the Technical Centre of the European Broadcasting Union

Avenue Albert Lancaster 32, B-1180 Brussels (Belgium)

This article describes a mathematical model applicable to AM sound broadcasting systems, by means of which it is possible to calculate, as a function of the transmission-system characteristics, the relative RF protection ratio that represents the effect of adjacent-channel interference. The calculation simulates the C.C.I.R. objective measurement method and has the advantage that the influence of various parameters in the transmission system can easily be investigated without having real equipment available for testing. After a description of the mathematical elements required for that numerical method, various examples are evaluated and the parameters chosen are discussed with regard to their effect on a possible future SSB transmission system for AM sound broadcasting.

A mathematical model for the calculation of the adjacent-channel interference in single-sideband and double-sideband AM sound-broadcasting systems*

G. Gröschel**

1. Introduction

In preparation for the 1974/75 LF/MF Broadcasting Conference, a method for the calculation of adjacent-channel interference in AM sound-broadcasting systems using double-sideband modulation (DSB) was developed as a function of the system parameters [1] and converted into a mathematical model which, subject to slight modifications, makes possible also corresponding examinations of systems with bandwidth-saving modulation methods, such as transmissions using a single sideband (SSB) or two sidebands independent of one another (ISB). The C.C.I.R. has been requested to investigate such systems with a view to their subsequent application [2, 3].

The model described below has in the meantime been incorporated in the C.C.I.R. documentation [6], in addition to a graphical method [4] and a numerical method employing polygon-type approximations [5].

The mutual interference (adjacent-channel interference) that must be expected between two adjacent channels in an AM sound-broadcasting network in Bands 5 (LF), 6 (MF) and 7 (HF) is, among other parameters, determinant for the configuration of the transmitter network and for the quality of the received signals.

The effect of adjacent-channel interference in AM sound broadcasting is characterised by the relative RF protection ratio A_{rel} [7, 8] which depends not only on the spectral energy distribution of the modulation signal and the physiological sensitivity characteristic of the human ear, but also, in a complicated manner, on the technical characteristics of the transmitter and receiver. The most important characteristics of the transmitter and receiver, whose influences are to be considered here, are as follows :

- the channel spacing ΔF ;
- the bandwidth of the transmitter B_N and of the receiver B_R ;
- the attenuation slopes α_S and α_R of the band-limiting filters at the transmitter and at the receiver respectively ;
- the carrier reduction T ;
- the depth of modulation m_{eff} ;
- the spectral energy distribution of the modulation signal ;
- the out-of-band radiation of the transmitter (characterised by the relative amplitude D_3 of the intermodulation products in the transmitter when modulated with two tones of equal amplitude) ;
- the pre-emphasis and de-emphasis at high frequencies, to which the signal to be transmitted is subjected at the transmitter and at the receiver respectively ;
- the compression of the dynamic range ;
- the suppression of adjacent-channel carriers at the receiver by means of a notch filter.

So far, if one disregards the costly subjective measuring methods that produced very scattered results, only the objective measuring method described in [6] has been available for the measurement of the RF protection ratio. That method only enables measurements to be made on systems that have already been developed and constructed, and it is therefore not suitable for the initial optimisation of the system parameters, for example, as regards the best utilisation of the frequency bands available, with the best possible transmission quality. On the other hand, the numerical methods mentioned above, which use electronic computers, enable rapid calculations of the relative RF protection ratio to be made for any parameters for the transmitters and receivers, and in that manner, the future transmission systems may be optimised.

---

* Dieser Aufsatz erscheint gleichzeitig in Deutsch under dem Titel " Ein mathematisches Modell zur Berechnung der Nachbarkanalstörung in Einseitenband- und Zweiseitenbandsystemen des AM-Tonrundfunks " in Rundfunktechnische Mitteilungen, Heft 3, 1978.

** Mr. Gröschel is with the Fernmeldetechnisches Zentralamt of the Deutsche Bundespost at Darmstadt.

2. The objective measuring method

In order to reduce the outlay and the considerable scatter (inevitable with that type of evaluation) of the results of subjective listening tests for the determination of the relative RF protection ratio, an objective measuring method has been developed [6], wherein the interfering transmission and the wanted transmission are simulated by a test transmitter modulated with band-limited weighted noise ($m = 50$ %), tuned to the frequency f_1, the wanted reception channel being simulated by a standardised receiver tuned to the neighbouring frequency f_2. As a function of the detuning $\Delta F = f_2 - f_1$ of the receiver, the interference power weighted by means of a psophometer is measured at the receiver output and expressed as a proportion of the wanted power that is obtained there with $\Delta F = 0$. That ratio is known as the relative RF protection ratio A_{rel}. It is expressed in decibels and indicates the minimum value of the ratio of the field strengths of the wanted and interfering transmitters with carrier frequencies differing by ΔF, such that the signal-to-noise ratio at the output of the receiver (co-channel protection ratio) does not fall below a particular value.

It is assumed in this connection that, in the case of reception in the adjacent channel, the subjective impression of the interference is proportional to the ratio of the weighted wanted power to the weighted interference power. That assumption is valid in the case of amplitude modulation.

3. Principle of the numerical method

For the purpose of the calculation of the relative RF protection ratio, the physical process (that is to say, the determination of the wanted power, the weighted interference power in the adjacent channel and of their ratio) underlying the objective measuring method is simulated by a mathematical model. Two adjacent channels having the carrier frequencies f_S and f_R are assumed, their frequency difference ΔF being equal to the channel spacing in question. The radiated spectrum related to an increment of bandwidth B_{eff} is simulated by a function F_S which depends on the relative frequency $|f|$. That function is composed of multiplicative partial functions (such as the rate-of-cut of the band-limiting filter, spectral energy distribution in the sideband, pre-emphasis etc.) and of additive partial functions (for example, out-of-band radiation, carrier level, noise spectrum). Similarly, the overall attenuation of the receiver, including the weighting of the interference power by the psophometric filter, is represented by a function F_R dependent on the relative frequency $f^* = |(\Delta F - f)|$. That function, too, is composed of multiplicative partial functions (such as band limitation, de-emphasis, psophometric weighting) and additive partial functions (for example, out-of-band selectivity).

With DSB modulation, F_S and F_R are symmetrical with the associated carrier frequencies. With SSB modulation, on the other hand, one sideband in the radiated spectrum must be suppressed by the mathematical simulation of the attenuation of a filter with steep attenuation slopes, and the out-of-band radiation must be simulated by an additive term asymmetrical to the carrier. At the same time, the bandwidth of the receiver filter must be halved, and its centre frequency must be displaced by half that bandwidth in the direction of the radiated sideband relative to the reception carrier.

With ISB modulation, the radiated spectrum, apart from the reduced level of the carrier, corresponds to the spectrum for DSB modulation. The reception filter is, however, composed of two partial filters symmetrically displaced by half the passband with reference to the reception carrier.

The slight asymmetry of the attenuation curves of the transmitter and receiver filters (band-pass filters) which generally exists in practice, has been disregarded here. However, it could be taken into account at any time through the adoption of a more refined attenuation function.

So that the subjective impression of the interference due to the unwanted power in the adjacent channel can be correctly appreciated, the function F_R must contain the weighting of the psophometric filter. The basic characteristics of the functions F_S and F_R, and the most important partial functions, as well as the significance of the notation used, are shown in *Fig. 1*.

The radiated spectrum $F_S(f)$, being centered on the carrier frequency f_S, gives rise in the receiver, which is tuned to the frequency f_R of the adjacent channel, to an interference power ΔP_S, which can be calculated by the integration of the product $F_S^2 \cdot F_R^2$ with a given channel spacing ΔF. One thus obtains :

$$\Delta P_S = \int_{f_1}^{f_2} F_S^2(|f|) \cdot F_R^2(|\Delta F - f|)\, df \qquad (1)$$

If the integration according to (1) is carried out for $\Delta F = 0$ (receiver tuned to wanted carrier), then the wanted reception power ΔP_N is obtained. The corresponding RF protection ratio A_{rel} is the ratio of the interference power to the wanted power in the reception channel, that is, in dB :

$$A_{rel} = 10 \log \frac{\Delta P_S}{\Delta P_N} \qquad (2)$$

By varying ΔF, it is thus possible to calculate the adjacent-channel RF protection ratio A_{rel} as a function of the channel spacing. Moreover, the method of calculation makes it possible to calculate separately the interference components in the adjacent channel that are due respectively to the carrier (beat tone) and to the sidebands. The integration according to (1) is appropriately carried out by means of electronic computers*, using numerical integration methods. For most problems, a solution based on bandwidth increments of $B_{eff} = 100$ Hz is sufficient.

In the following, we shall indicate the functions F_S and F_R and their partial functions for amplitude-modulated DSB transmissions (class of emission A3), for ISB transmissions (class of emission A3B) and for SSB transmissions (class of emission A3A). In the case of single-sideband transmissions, an attenuated carrier is taken.

* In this particular case, a desk model HP 9830 with 16 K-Byte storage capacity is utilised. The computer program is written in BASIC.

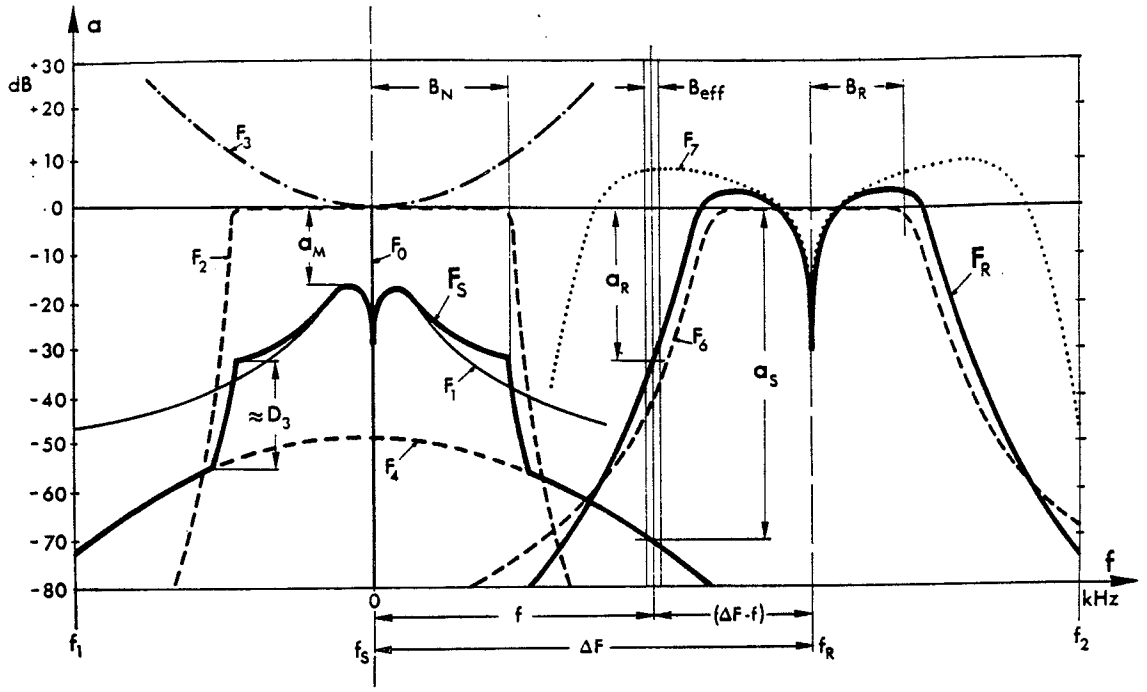

Fig. 1. — Partial functions and notation for a DSB system.

Abscissa : f = relative frequency (referred to the transmitted carrier).
Ordinate : a = relative level (or attenuation) referred to the carrier level or the peak envelope power.

B_N = 3-dB bandwidth of the transmitter (overall)
B_R = 3-dB bandwidth of the receiver (overall)
B_{eff} = incremental bandwidth to which the power-density spectrum refers and within which the power density and the receiver attenuation are in all cases taken as being constant, for the calculation
f_S = carrier frequency of the transmitter
f_R = carrier frequency of the adjacent channel
ΔF = channel spacing
f_1, f_2 = lower and upper limits of integration
F_0 = carrier
F_1 = spectral energy distribution in the sideband
F_2 = attenuation of the filter for the band limitation at the transmitter
F_3 = pre-emphasis at the transmitter
F_4 = out-of-band radiation of the transmitter
F_S = function representing the spectrum of the transmitter
D_3 = attenuation of the 3rd-order intermodulation products of the transmitter when measured with two tones
a_M = relative level of the maximum power density in the sideband, referred to the carrier level
F_6 = attenuation of the filter for the band limitation at the receiver
F_7 = attenuation of the psophometer filter
F_R = function representing the overall attenuation of the receiver, including the weighting by the psophometer filter (weighted receiver attenuation)
a_S = level of the transmitter spectrum at the frequency f
a_R = weighted receiver attenuation at the frequency f

4. The radiated spectrum

The function F_S, which approximates to the radiated spectrum, is composed of individual partial functions which are linked with one another additively or multiplicatively, depending upon the physical cause of their formation or their effect. The essential properties of the radiated spectrum can be sufficiently accurately simulated by means of six partial functions, as follows :

$$F_S(f) = F_0(f) + a_M [F_1(f) F_2(f) F_3(f)] + \sqrt{[F_4(f)^2 + F_5(f)^2]} \quad (3)$$

wherein

F_0 = carrier function,
a_M = relative level of the maximum of the power density spectrum in the sideband, referred to the carrier level,
F_1 = spectral energy distribution of the modulation signal,
F_2 = attenuation of the band-limiting filter,
F_3 = pre-emphasis at the transmitter,
F_4 = out-of-band radiation,
F_5 = noise spectrum of the transmitter.

All the levels in the spectrum, in the case of DSB modulation, are referred to the carrier level (0 dB), and with ISB or SSB modulation to the peak envelope power (0 dB). The carrier and peak envelope powers are taken as unity.

4.1. Carrier

The carrier is a single-frequency oscillation in the continuous power-density spectrum, whose level when measured is independent of the bandwidth of a tuned level meter. A solution, that can be used for the type of integration applied here, can be obtained by replacing the carrier by an additive term $F_0(f)$, which produces the desired carrier level in the centre of the corresponding bandwidth B_{eff} and which, still within the limits of that bandwidth, falls off on both sides to negligibly small values. There applies :

$$F_0(f) = 10^{-\left(\frac{T}{20} + 50|f|\right)} \quad (4)$$

wherein T = carrier reduction (in dB), referred to the full carrier or to the peak envelope power.

For single-sideband transmissions, the peak envelope powers are always maintained constant in all of the observations that follow. The relations between the level of the carrier and the level of the sideband oscillations, therefore, depend on the degree of carrier suppression T. Those relations are dealt with in [9].

4.2. Power density in the sidebands

The power density in the sidebands depends on :

- the modulation signal $F_1(f)$,
- the depth of modulation m_{eff} or, with ISB or SSB modulation, the relative level of power components p_{eff},
- the compression factor K,
- the pre-emphasis at the transmitter $F_3(f)$,
- the attenuation of the band-limiting filter of the transmitter $F_2(f)$,
- the carrier suppression T, because the peak envelope power is maintained constant.

The dependence on frequency of the power density in the sidebands is represented by the product of $F_1(f)$, $F_2(f)$, $F_3(f)$ and a_M.

The relative level p_{eff} indicates the percentage of voltage in relation to the voltage available for the sideband components (permissible maximum voltage of the transmitter less the voltage of the residual carrier) that is effectively radiated in the sideband signal.

4.3. Spectral power density of the modulation signal

For the present investigations, standardised weighted noise according to [6] has been taken as the modulation signal, whose relative level, referred to the maximum value at 210 Hz [10], is represented by $F_1(f)$. There applies :

$$F_1(f) = \frac{A_0\ A_2\ f^2}{\sqrt{B_8 f^8 + B_6 f^6 + B_4 f^4 - B_2 f^2 + B_0}} \qquad (5)$$

wherein

$A_0 = 2{,}836$ $\quad$ $B_4 = 4{,}716.10^4$
$A_2 = 77{,}65$ $\quad$ $B_2 = 4{,}085.10^8$
$B_8 = 9{,}243.10^{-9}$ $\quad$ $B_0 = 1{,}274.10^{13}$
$B_6 = 8{,}674.10^{-2}$

The factor A_0 compensates the passband attenuation of the weighting network described in [6].

The factor a_M defines the position of the maximum of the power-density spectrum in the sideband, relative to the carrier or to the peak envelope power [10]. It takes into account the depth of modulation m_{eff}, the carrier suppression T, the compression factor K and the element of bandwidth B_{eff}, to which the power density of the radiated spectrum is referred. B_E, the equivalent bandwidth, is an auxiliary factor, which is explained in greater detail below.

For DSB modulation :

$$a_M = \frac{m_{eff}^2}{2} \cdot \frac{B_{eff}}{2\,B_E} \cdot 10^{(\sqrt{K}/25)} \qquad (6)$$

for ISB modulation :

$$a_M = p_{eff}^2 \cdot [1 - 10^{(-T/20)}]^2 \cdot \frac{B_{eff}}{2\,B_E} \cdot 10^{(\sqrt{K}/25)} \qquad (7)$$

and for SSB modulation :

$$a_M = p_{eff}^2 \cdot [1 - 10^{(-T/20)}]^2 \cdot \frac{B_{eff}}{B_E} \cdot 10^{(\sqrt{K}/25)} \qquad (8)$$

Fig. 2 indicates the empirical relationship assumed in the model between the compression factor K and the increase due thereto of the depth of modulation m_{eff} or p_{eff}.

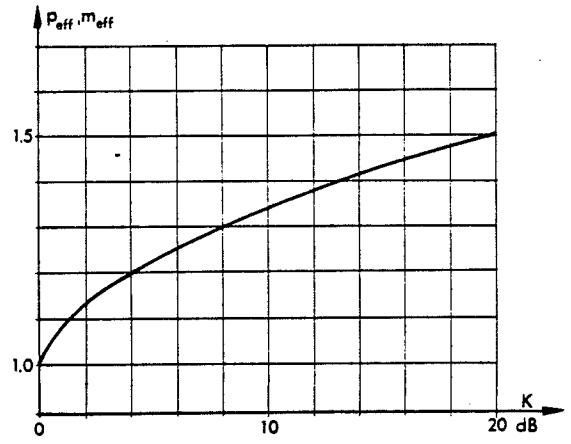

Fig. 2. — Increase of the depth of modulation with compression.

Abscissa : degree of compression (in dB).
Ordinate : increase of depth of modulation (factor).

Fig. 3 indicates how, with DSB modulation, the value a_M depends on the bandwidth B_N of the transmitter. The auxiliary value B_E (equivalent bandwidth) is appropriately introduced here. B_E is the bandwidth required for modulation with white noise (constant power density in the sideband), that produces the same sideband power as modulation with standard-

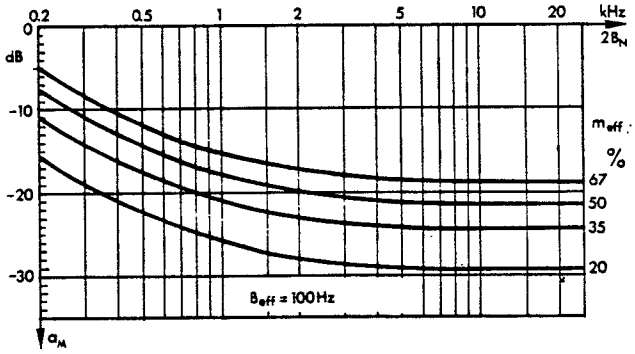

Fig. 3. — Position of the maximum of the power-density spectrum in the sideband, with DSB modulation.

Abscissa : necessary RF bandwidth 2 B_N (in kHz)
Ordinate : maximum level a_M of the sideband spectrum (in dB) relative to the carrier level
Parameter : effective depth of modulation m_{eff} ; effective noise bandwidth B_{eff} of the analysing device.

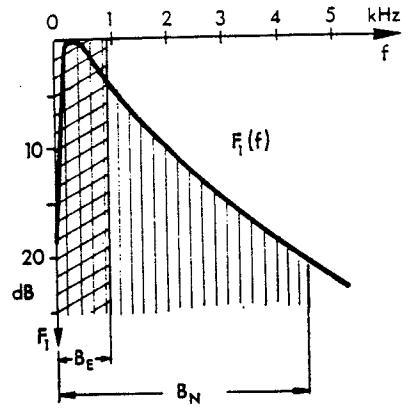

Fig. 4. — Relationship between the equivalent bandwidth B_E and the required bandwidth B_N.

Abscissa : relative frequency f (in kHz)
Ordinate : spectral power density of the modulation signal relative to the maximum at 210 Hz (in dB).

ised weighted noise and with the transmitter bandwidth B_N [10]. B_E is defined as follows :

$$B_E = \int_{-0}^{+\infty} F_1^2(f)\ F_2^2(f)\ F_3^2(f)\ df \qquad (9)$$

This ensures that the desired depth of modulation of the transmitter retains the value assumed for the calculation, even when pre-emphasis or different band-limitation is applied. The relationship in principle between B_E and B_N is depicted in *Fig. 4*. It applies to standardised weighted noise according to [6].

4.4. Band-limitation of the transmitter

The attenuation of a filter limiting the width of the passband of the transmitter is simulated by the function $F_2(f)$, a multiplicative term. Any attenuation functions can be applied here. For the investigations described in Section 8 on single-sideband emission systems, filters with a Butterworth characteristic have been assumed, whose attenuation can be represented [11] by the expression :

$$F_2(f) = \frac{1}{\sqrt{1 + \left(\frac{|f|}{B_N}\right)^{N_S}}} \qquad (10)$$

The variable f here is the frequency deviation from the carrier. The necessary audio-frequency bandwidth B_N of the transmitter determines the 3-dB point of the attenuation. By means of the exponent N_S, the rate-of-cut α_S of the attenuation characteristic of the transmitter filter is determined, measured at the point of inflection, the steepest point of the attenuation function. *Fig. 5* gives an example of such attenuation characteristics with the constant 3-dB bandwidth $B_N = 4500$ Hz, for various attenuation slopes α_S.

In the attenuation characteristic chosen, the steepest slope occurs at the frequency f_m (inflection point) referred to the carrier :

$$f_m = B_N \cdot (N-1)^{1/N} \qquad (11)$$

For a given bandwidth B_N, the maximum attenuation slope α (in dB/kHz) can be calculated from the exponent N and vice-versa, by applying the following relation (applicable also to the reception filter) :

$$|\alpha| = \frac{4343}{B_N} (N-1)^{[(N-1)/N]} \qquad (12)$$

The relationship $\alpha = f(N)$, with the bandwidth B_N as parameter, is depicted in *Fig. 6*.

In many cases of mutual interference between adjacent channels, the LF/MF Broadcasting Conference, Geneva 1975, agreed limitations of the radiated audio bandwidth to system-adapted values ($\approx$ 4500 Hz) and included these in the Plan. The attenuation characteristic of a filter which has been utilised in the transmitters in the Federal Republic of Germany for some time, and has a 3-dB bandwidth of 4500 Hz and an attenuation slope of about 60 dB per octave, corresponds approximately to the following attenuation function :

$$F_2(f) = \frac{\sqrt{1 + \left(\frac{|f|}{5150}\right)^{15}}}{\sqrt{1 + \left(\frac{|f|}{4280}\right)^{49}}} \qquad (13)$$

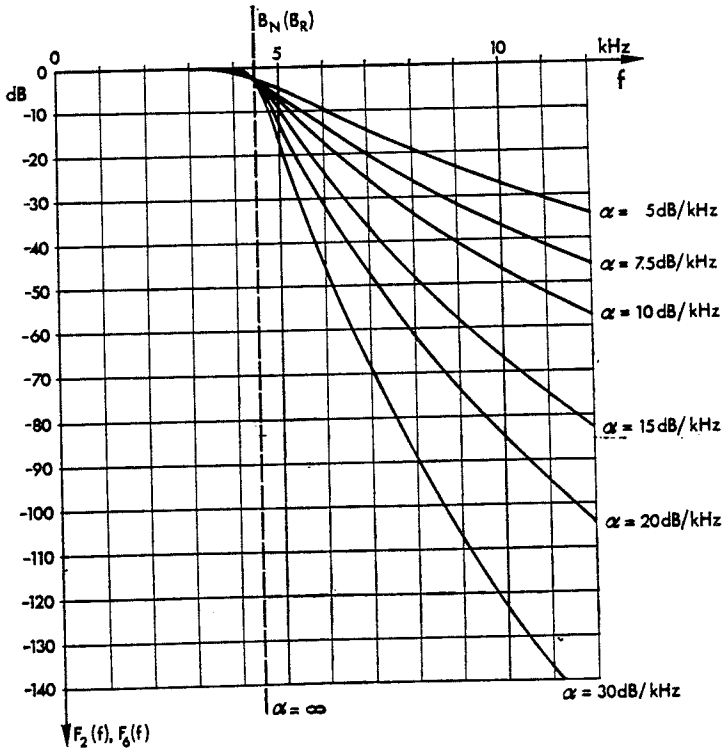

Fig. 5. — Attenuation of the band-limiting filters.

Abscissa : relative frequency f (in kHz)
Ordinate : attenuation (in dB)
Parameter : attenuation slope at the inflection point (in dB/kHz).

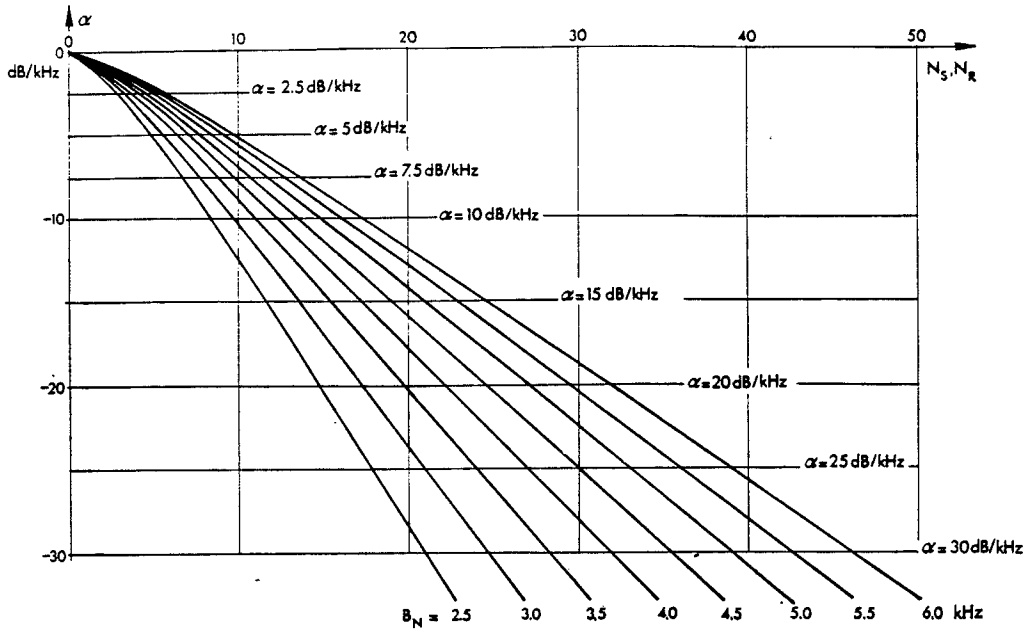

Fig. 6. — Dependence of the exponents of the attenuation functions on the bandwidth and on the attenuation slope.

Abscissa : exponent of the attenuation function
Ordinate : slope of the attenuation at the inflection point α (in dB/kHz)
Parameter : necessary bandwidth B_N (in kHz).

The precise attenuation characteristic is given in [12].

4.5. Pre-emphasis at the transmitter

For the purpose of investigating the influence of a deviation of the spectral energy density of the modulation signal from that of the standardised weighted noise [6], the function $F_3(f)$, another multiplicative term, was introduced, by means of which it is possible to simulate an emphasis of high audio frequencies resembling pre-emphasis with FM.

$$F_3(f) = \sqrt{1 + (2\pi\tau_S f)^2 \cdot 10^{-12}} \qquad (14)$$

wherein τ_S is the time-constant (in μs) of the equivalent RC circuit producing the same attenuation. The degree of AF emphasis can be modified by the time-constant. *Fig. 7* depicts the variation of $F_3(f)$ with τ_S as parameter.

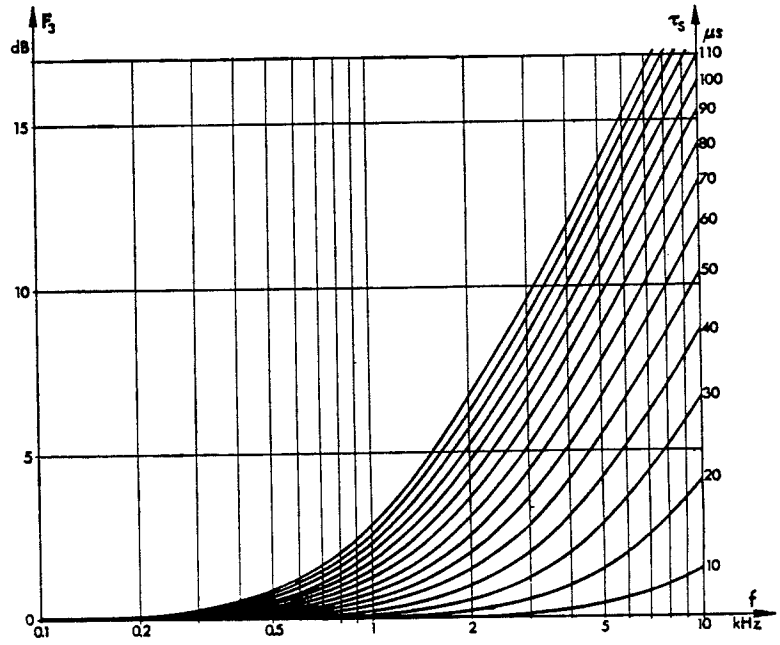

Fig. 7. — Pre-emphasis.

Abscissa : relative frequency f (in kHz)
Ordinate : pre-emphasis B_3 (in dB)
Parameter : time-constant τ_S (in μs).

4.6. The out-of-band radiation

The components of the power-density spectrum that occur immediately outside the required bandwidth $2 . B_N$ of the transmitter are termed out-of-band radiation [13]. They are produced by the non-linearity distortion of the modulating signal in the transmitter. The effect of that distortion on the out-of-band radiation is characterised by the intermodulation factors of third and fifth orders D_3 and D_5 [14], which are measured when the transmitter is modulated with two tones of equal amplitude (double tone).

The out-of-band radiation is very dependent on the intermodulation factors, on the depth of modulation of the transmitter and on the pre-emphasis of the modulation signal. Measurements with weighted noise [10] on high-power transmitters using DSB modulation have indicated that :

- the levels of the out-of-band radiation at the band limits $f_1 \pm B_N$ are lower by the amount of the third-order intermodulation factor D_3 than the wanted levels at the edge of the passband ;
- with DSB modulation, the out-of-band radiation beyond the required bandwidth $2 . B_N$ falls off, symmetrically to the carrier, on both sides by about 15 dB/octave. With SSB modulation, the out-of-band radiation is asymmetric to the carrier ;
- to a first approximation, the level difference Δa of the out-of-channel transmission remains unchanged, even when the depth of modulation and the bandwidth are modified.

For the mathematical simulation of the out-of-band radiation, the additive term $F_4^*(f)$ of the following expression is used :

$$F_4^*(f) = \frac{1}{\sqrt{1 + \left(\frac{|f|}{3000}\right)^{5.8}}} \qquad (15)$$

which, in its position relative to the levels in the wanted band, is deviated at the point $f_1 \pm B_N$, as a function of τ_S and m_{eff}, in such a manner that the condition

$$\Delta a \approx D_3 \qquad (16)$$

which was determined empirically, is maintained. The additive partial function $F_4(f)$ thus adopts the following form :

$$F_4(f) = F_4^*(f) . Q^* \qquad (17)$$

with

$$Q^* = \sqrt{1 + \left(\frac{B_N}{3000}\right)^{5.8}} . \sqrt{a_M} . F_1(B_N) . F_2(B_N) . \sqrt{\frac{100}{B_{eff}}} . 10^{-(0.95 D_3/20)} \qquad (18)$$

The relationships for the formation of Q^* are explained in more detail in *Fig. 8* (drawn in logarithmic scale).

4.7. Transmitter noise energy spectrum

An additional noise energy spectrum of the transmitter, due, for example, to a decade master-oscillator, can be simulated by a further additive term $F_5(f)$. In the case under study, a constant noise level $S_0 =$ −100 dB (relative to the carrier level) has been assumed, very much simplified. Therefore :

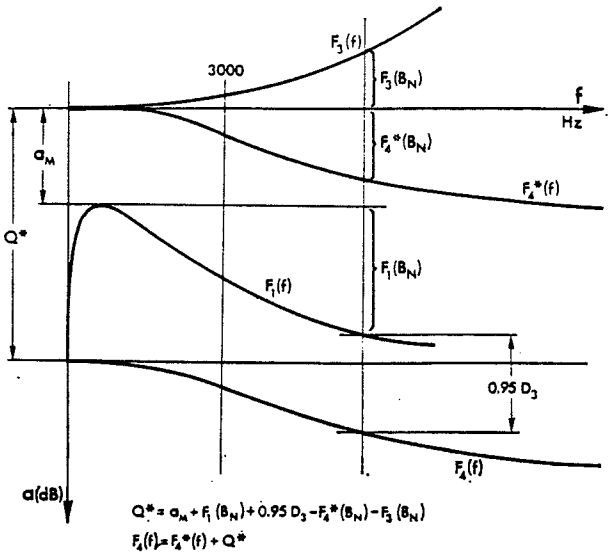

Fig. 8. — Level relations of the out-of-band radiation.

Abscissa : relative frequency (in Hz)
Ordinate : attenuation a (in dB).

$$F_5(f) = 10^{(S_0/20)} . \sqrt{\frac{100}{B_{eff}}} \qquad (19)$$

The out-of-band radiation and the noise energy spectrum are added quadratically.

5. Simulation of the receiver characteristics and of the weighting by the psophometer

The influences of the band-limiting filter of the de-emphasis and of the weighting of the interference power in the receiver are summarised in the function $F_R(f^*)$. It is composed of the following multiplicative and additive terms :

$$F_R(f^*) = F_6(f^*) \; F_7(f^*) \; F_8(f^*) \; F_9(f^*) + F_{10}(f^*) \qquad (20)$$

wherein the relative frequency f^* depends in the following manner on the channel spacing ΔF and on the relative frequency f (referred to the transmitter carrier) :

$$f^* = |\Delta F - f| \qquad (21)$$

5.1. Attenuation of the band-limiting filters of the receiver

The entire frequency-dependent attenuation of the receiver, which is distributed over the RF and AF stages, is summarised in the multiplicative term $F_6(f^*)$ which is derived similarly to the corresponding term $F_2(f)$ of the transmitter :

$$F_6(f^*) = \frac{1}{\sqrt{1 + \left(\frac{|f^*|}{B_R}\right)^{\alpha_R}}} \qquad (22)$$

Analogously, too, the 3-dB point of the attenuation is determined for the receiver with B_R (in Hz), and with α_R the slope (in dB/kHz) of the attenuation characteristic of the band-limiting filter. Equation (12) and *Figs. 5* and *6* apply here correspondingly.

For many investigations, it is advantageous to assume the average selectivity characteristics of a reference receiver. The E.B.U.'s MBF reference receiver can be regarded as being such a receiver. It has a 3-dB bandwidth of 2 kHz and a maximum attenuation slope of its filters of about 8 dB/kHz. The attenuation curve may be represented approximately by the expression :

$$F_6(f^*) = \frac{1}{\sqrt{[1 + (f^* 2300)^4] \cdot [1 + (f^* 3300)^4] \cdot [1 + (f^* 4100)^4]}} \qquad (23)$$

Fig. 9 shows the attenuation according to equation (23), as well as several attenuation curves measured on different receivers. It will be seen that the selectivity of the MBF receiver is already clearly better than that of the simple or even of the average-quality receivers.

5.2. Weighting with the psophometric filter

In order that the subjective impression of the interference in the disturbed adjacent channel, which is a function of the frequency-dependent sensitivity of the human ear, is correctly assessed, the interference power ΔP_S, which occurs within the receiver passband, must be weighted with the frequency-dependent attenuation of the psophometric filter. This requires a further multiplicative term $F_7(f^*)$. The attenuation of the psophometric filter at present used and standardised [15] may be represented by :

$$F_7(f^*) = \frac{4\,|f^*|}{\sqrt{A^2(f^*) + B^2(f^*)}} \qquad (24)$$

with

$$A(f^*) = -K_6(f^*)^6 + K_4(f^*)^4 - K_2(f^*)^2 + K_0 \qquad (25)$$

and

$$B(f^*) = K_5\,|f^*|^5 - K_3\,|f^*|^3 + K_1\,|f^*| \qquad (26)$$

as well as the constants :

$K_0 = 0{,}4010.10^4$ $\quad K_4 = 8{,}1023.10^{-12}$
$K_1 = 2{,}2124$ $\quad K_5 = 5{,}1866.10^{-16}$
$K_2 = 5{,}3848.10^{-4}$ $\quad K_6 = 1{,}9000.10^{-20}$
$K_3 = 8{,}3417.10^{-8}$

Up to the frequency $f^* = 20$ kHz, the approximation according to equations (24), (25) and (26) does not deviate by more than $\pm$ 0.2 dB from the nominal values indicated in [15]. By way of comparison, we also indicate an approximation for the psophometric attenuation used previously [16] :

$$F_{7a}(f^*) = \frac{7.08 \cdot 10^{-5} \cdot |f^*|^{1.425} \cdot \sqrt{1 + (f^*/11400)^{14}}}{[1 + (f^*/1200)^2] \cdot [1 + (f^*/6300)^4] \cdot [1 + (f^*/8600)^{22}]} \qquad (27)$$

5.3. De-emphasis in the receiver

Another multiplicative term $F_3(f^*)$ makes it possible to investigate the effect on the adjacent-channel interference of de-emphasis in the receiver.

$$F_3(f^*) = \frac{1}{\sqrt{1 + (2\pi\,\tau_R\,f^*)^2 \cdot 10^{-12}}} \qquad (28)$$

The desired de-emphasis is chosen by means of the time-constant τ_R of the equivalent RC circuit.

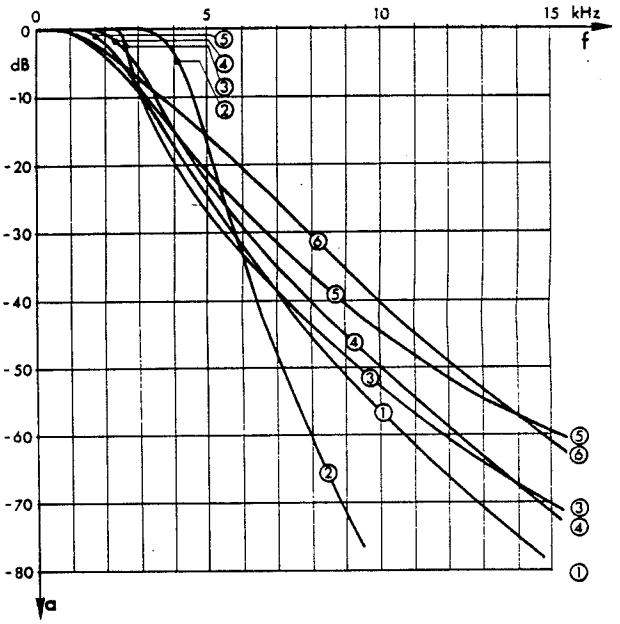

Fig. 9. — Receiver attenuation curves.

Abscissa : relative frequency f (in kHz)
Ordinate : attenuation a (in dB)

(1) E.B.U. reference receiver MBF ($\alpha_R \approx 7.5$ dB/kHz)
(2) I.R.T. receiver with mechanical IF filter ($\alpha_R \approx 16$ dB/kHz)
(3) Four-stage hybrid IF filter ($\alpha_R \approx 20$ dB/kHz)
(4) Hybrid IF filter ($\alpha_R \approx 12$ dB/kHz)
(5) Commercial equipment, superior medium quality ($\alpha_R \approx 6.5$ dB/kHz)
(6) Commercial equipment, superior medium quality ($\alpha_R \approx 5$ dB/kHz).

5.4. Suppression of the carrier interference by a notch filter

In HF broadcasting, in particular, the inclusion of a notch filter with a narrow attenuation range in the audio-frequency amplifier downstream of the demodulation stage in the receiver, has proved to be very satisfactory for the selective suppression of the interference component due to the carrier. The centre frequency of the notch filter corresponds to the channel spacing, so that the carrier whistle is suppressed in the case of optimum tuning to the wanted signal. In the calculation, this is effected most easily by not taking into account the interference component which is dealt with separately. In the computer program, this corresponds to the inclusion of an extremely narrow notch filter which infinitely attenuates only the carrier itself.

If it is necessary to take into account the fact that a real notch filter suppresses, in addition to the carrier, also part of the wanted spectrum, then, for example, the attenuation function $F_9\,(f^*)$ of a single series-tuned circuit of magnification factor Q and resonant frequency f_r may be applied, upstream of which a resistance R is inserted for the voltage division :

$$F_9\,(f^*) = \frac{\sqrt{R_r^2 + \left(\frac{L}{C}\right)\left(\frac{f^*}{f_r} - \frac{f_r}{f^*}\right)^2}}{\sqrt{(R_r + R)^2 + \left(\frac{L}{C}\right)\cdot\left(\frac{f^*}{f_r} - \frac{f_r}{f^*}\right)^2}} \qquad (29)$$

The attenuation resistance R_r is a function of the Q factor and the L/C ratio of the series-tuned circuit :

$$R_r = \frac{1}{Q}\cdot\sqrt{\frac{L}{C}} \qquad (30)$$

5.5. Out-of-band selectivity of the receiver

The additive term $F_{10}\,(f^*)$ makes it possible to simulate a value of the receiver out-of-band selectivity deviating from infinity. We have here assumed, as the most simple case, a constant value R_0 (in dB), which may be represented as follows :

$$F_{10}\,(f) = 10^{(R_0/20)} \qquad (31)$$

Fig. 10, finally, depicts an example of the typical characteristic of the overall attenuation of the receiver $F_R\,(f)$, with a notch filter for SSB modulation, and the associated power-density spectrum of the transmitter $F_S\,(f)$.

6. Limitations of the numerical method

In the numerical method described above, the adjacent-channel RF protection ratio is calculated from the power ratio of the wanted and interfering signals received. It must be taken into consideration here that the power of the wanted signal ($\Delta F = 0$) is demodulated by means of its own coherent carrier, whereas the interfering power is the result of the demodulation of the sideband components (or of the partial noise bands) of the interfering transmission by means of the carrier of the wanted signal. Randomly-distributed phase differences $\Delta\varphi$ occur in the latter case. In the case of co-channel interference ($\Delta F = 0$) therefore, the measured interfering power is smaller by 3 dB than the result of the calculation, because of its non-coherent demodulation with the wanted carrier [17]. That difference does not occur with single-sideband systems. These differences must be taken into account when comparing the calculated and measured results.

By means of the mathematical model described, it is possible to deal separately with the interference component attributable to the carrier in the adjacent

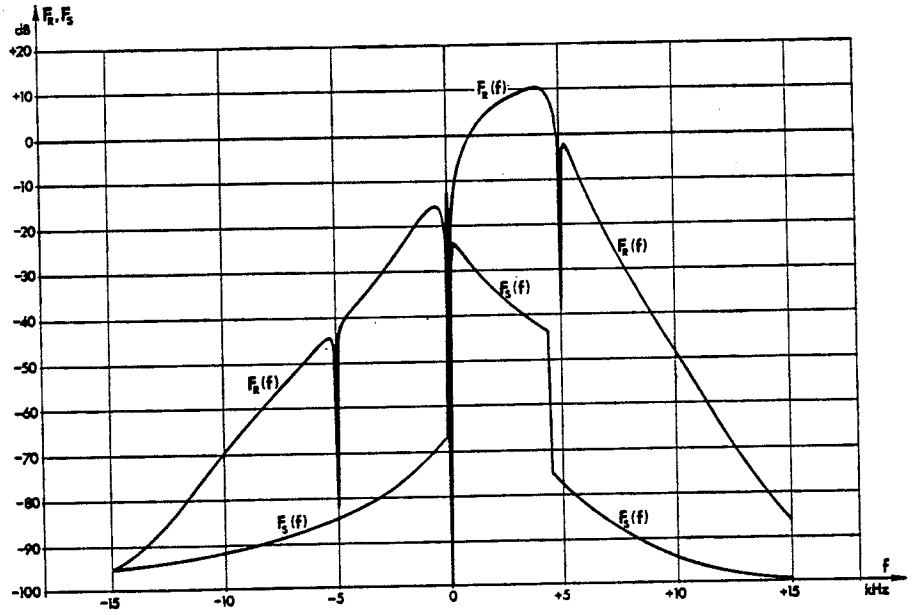

Fig. 10. — Example of functions $F_S(f)$ and $F_R(f)$ for an SSB system.

Abscissa : relative frequency f (in kHz)
Ordinate : level or attenuation (in dB).

channel (beat tone), on the one hand, and with the interference attributable to the sidebands, on the other hand. The carrier interference is given by :

$$\Delta P_T = K\ F_S^2(0)\ F_R^2\ (\Delta F) \qquad (32)$$

and the interference power attributable to the sidebands by :

$$\Delta P_{SB} = \Delta P_S - \Delta P_T \qquad (33)$$

$$= \int_{f_1}^{f} F_S^2(f)\ F_R^2(f^*)\ df - K\ F_S^2(0)\ F_R^2(\Delta F)$$

If another spectral energy distribution (for example, the conventional speech signal according to C.C.I.T.T. Recommendation G.227, Geneva 1976, Vol. III-1 pp. 145-147) and the associated psophometer curve are assumed, it is possible to apply the method described also to other AM systems (for example, telephony).

7. Comparison between calculation and measurement

The system parameters were measured on a low-power SSB system (SSB receiver and SSB transmitter-drive unit), and the relative RF protection ratio was calculated as a function of the channel spacing ΔF, by means of the mathematical model. The calculated values were compared with the values measured directly. The results are depicted in *Fig. 11.*

For relative RF protection ratios of about —40 dB, the measured values do not differ from the calculated values by more than ± 1 dB. It is only in the range below —40 dB that the measurement is increasingly influenced by the noise voltages of the equipment and by the intermodulation distortion in the receiver, which can no longer be neglected. Non-linearity effects in the receiver have not been taken into account in the calculation.

8. Application of the mathematical model

Below we shall examine, by means of the numerical method described above, for an SSB sound-broadcasting system having an ideal, infinitely steep, band-limitation at the transmitter radiating the upper sideband, how the adjacent-channel RF protection ratio depends on the following parameters :

- out-of-band radiation,
- slope of the attenuation at the edge of the band in the receiver,
- carrier reduction,
- receiver bandwidth,
- suppression of the interference component attributable to the carrier, by means of a notch filter.

In addition, the following are assumed :

- constant effective modulation depth $p_{eff} = 35\ \%$,
- frequency-independent carrier-noise level $S_0 = -100$ dB (referred to the peak envelope power),
- frequency-independent out-of-band selectivity of the receiver $R_0 = -100$ dB,
- carrier reduction $T = 12$ dB.

The parameters chosen for this application example are based on the values for a possible future SSB system in Band 7 (HF) : channel spacing 5 kHz, bandwidth 4.5 kHz, residual carrier —12 dB.

8.1. Influence of the out-of-band radiation

Fig. 12 depicts the relative RF protection ratio A_{rel} as a function ΔF for various values of the intermodulation attenuation D_3 in the case of ideal (rectangular) band-limitation of the transmitter and of the receiver, bandwidth $B_N = B_R = 4.5$ kHz and the other parameters as mentioned above.

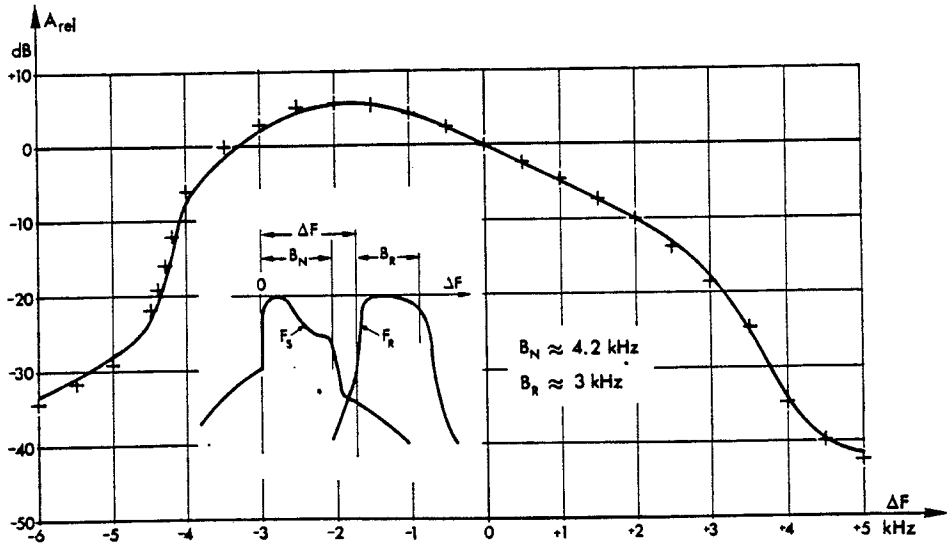

Fig. 11. — Comparison between calculated and measured results for an SSB system.

Abscissa : channel spacing ΔF (in kHz)
Ordinate : relative RF protection ratio A_{rel} (in dB)
+ + + + : measured values.

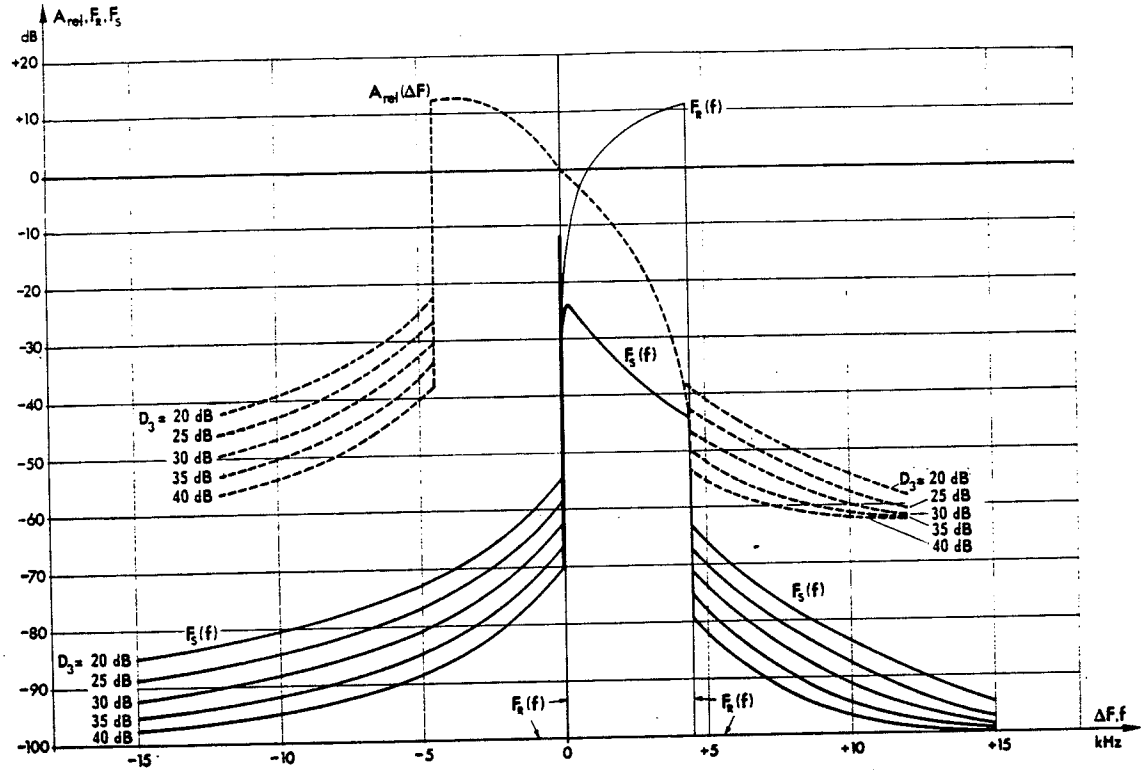

Fig. 12. — Influence of the out-of-band radiation.

Abscissa : relative frequency f or channel spacing ΔF (in kHz)
Ordinate : relative RF protection ratio A_{rel}; transmitter spectrum $F_S(f)$; weighted overall attenuation of the receiver $F_R(f)$ (in dB)
Parameter : intermodulation attenuation D_3 of the transmitter (in dB).

What is remarkable is the considerable asymmetry relative to the carrier of the curve of A_{rel} (ΔF), which is typical of SSB systems. For example, with a 5-kHz channel spacing, the protection ratio A_{rel} for the upper adjacent channel attains already —41 dB, whereas the value for the lower adjacent channel, with the same channel spacing, is, A_{rel} = —25 dB, or worse by 16 dB.

With a very moderate transmitter linearity (D_3 = 20 dB), the out-of-band radiation, even in the most unfavourable case of the lower adjacent channel, permits, with a 5-kHz channel spacing, protection ratios of better than —25 dB. Without too great an outlay, intermodulation attenuations of D_3 = 30 to 40 dB can be attained from high-power SSB sound-broadcasting transmitters, which result in RF protection ratios better than —30 dB. So far as the RF protection ratio is concerned therefore, the out-of-band radiation does not present too serious a problem.

The considerable asymmetry of the protection ratios for the upper and lower adjacent channels with SSB systems could have an effeect on the planning of optimum SSB transmitter networks. That matter is worthy of investigation.

8.2. Influence of the receiver bandwidth

If the ideal band limitation of the transmitter with a 4.5-kHz bandwidth is retained, but the bandwidth of the receiver is attenuated between 3 and 7.5 kHz with a 15-dB/kHz attenuation slope, one obtains the results depicted in *Fig. 13*.

The receiver bandwidth B_R, for a constant transmitter bandwidth B_N, has a stronger influence on the relative RF protection ratio against interference from the lower adjacent channel only. It has almost no influence on that against interference from the upper adjacent channel, because there the RF protection ratio is determined practically only by the power density in the sideband and by the attenuation of the psophometric filter.

If the receiver bandwidth (with a 15 dB/kHz attenuation slope) is modified in the same way as the transmitter bandwidth (with ideal rectangular band-limitation), then the relative RF protection ratio against interference from the lower adjacent channel changes only negligibly (max. 1 dB), whereas the ratio against that from the upper adjacent channel is raised by a maximum of 7.5 dB in the range ΔF = 3 to 7 kHz only. That result, which is depicted in *Fig. 14*, is to be compared with the results depicted in *Fig. 13* (constant transmitter bandwidth) ; it leads to the conclusion that the increase in sideband power occurring with greater transmitter bandwidth (hachured area in *Fig. 14*) affects only the upper adjacent channel.

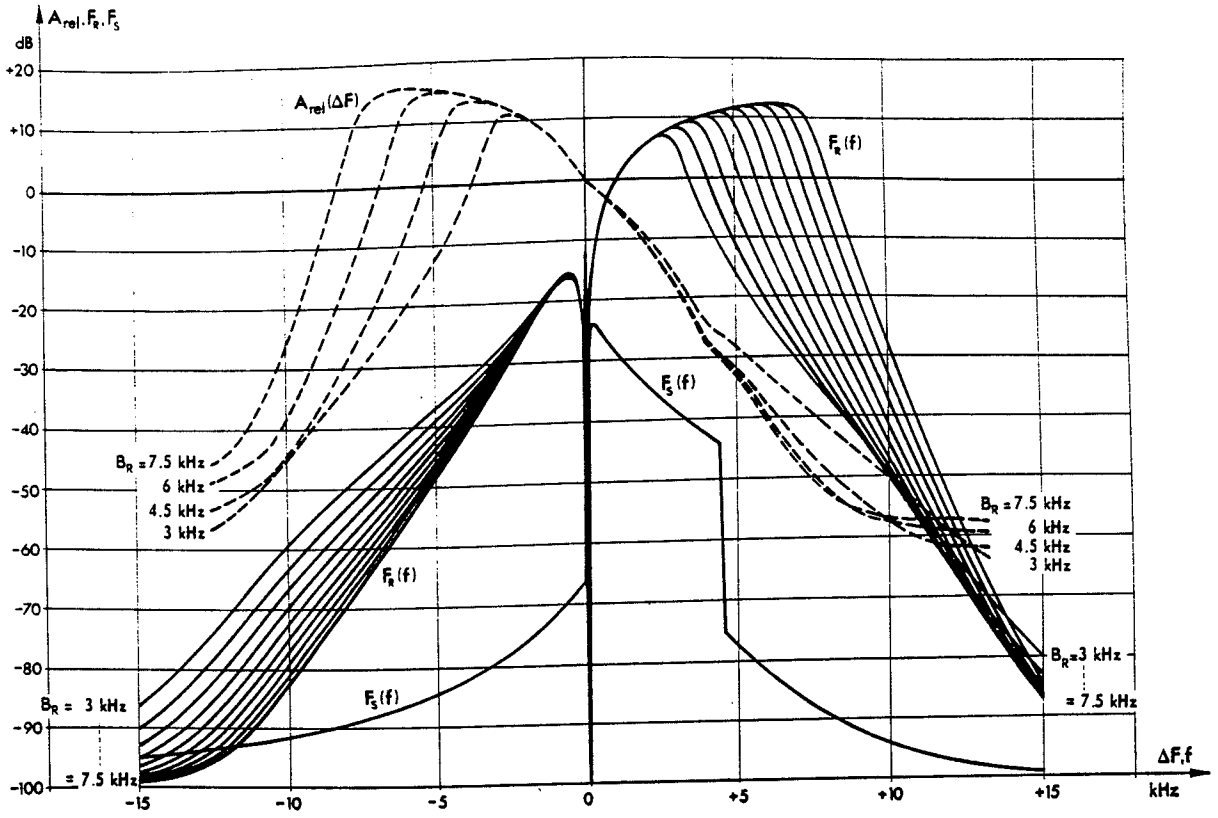

Fig. 13. — Influence of the receiver bandwidth.

Abscissa : relative frequency f or channel spacing ΔF (in kHz)
Ordinate : relative RF protection ratio A_{rel}; transmitter spectrum $F_S(f)$; weighted overall attenuation of the receiver $F_R(f)$ (in dB)
Parameter : bandwidth B_R of the receiver (in kHz).

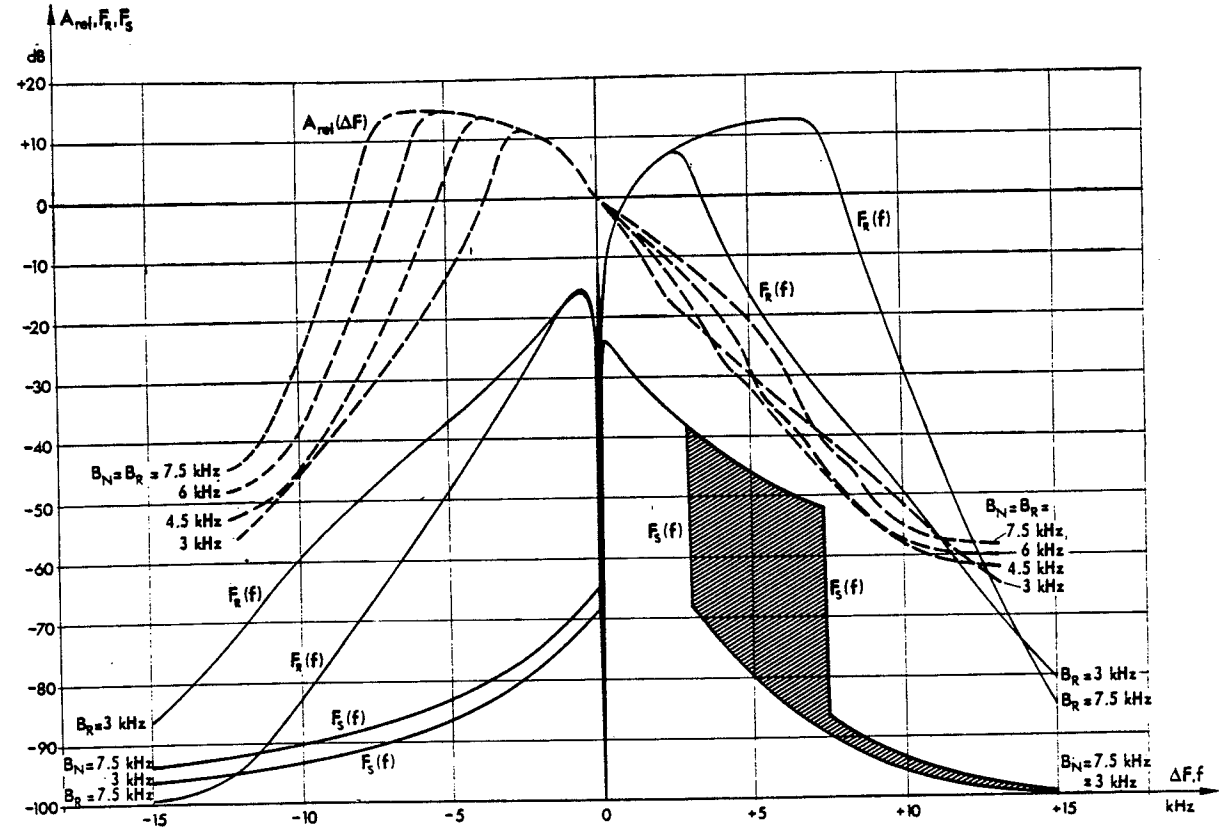

Fig. 14. — Influence of the system bandwidth.

Abscissa : relative frequency f or channel spacing ΔF (in kHz)
Ordinate : relative RF protection ratio A_{rel}; transmitter spectrum $F_S(f)$; weighted overall attenuation of the receiver $F_R(f)$ (in dB)
Parameter : system bandwidth $B_N = B_R$ (in kHz).

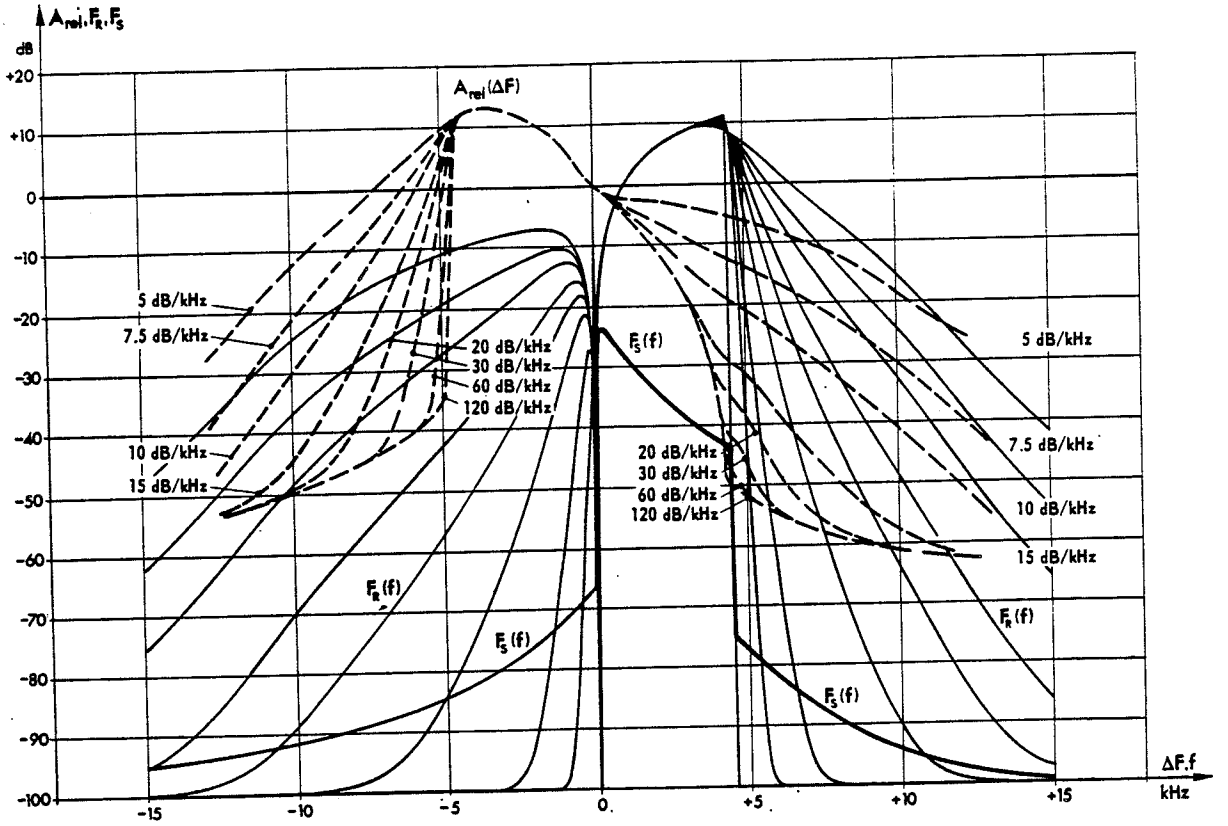

Fig. 15. — Influence of the steepnes of the receiver band limitation.

Abscissa : relative frequency f or channel spacing ΔF (in kHz)
Ordinate : relative RF protection ratio A_{rel}; transmitter spectrum $F_S(f)$; weighted overall attenuation of the receiver $F_R(f)$ (in dB)
Parameter : rate-of-cut α_R of the receiver filter (in dB/kHz).

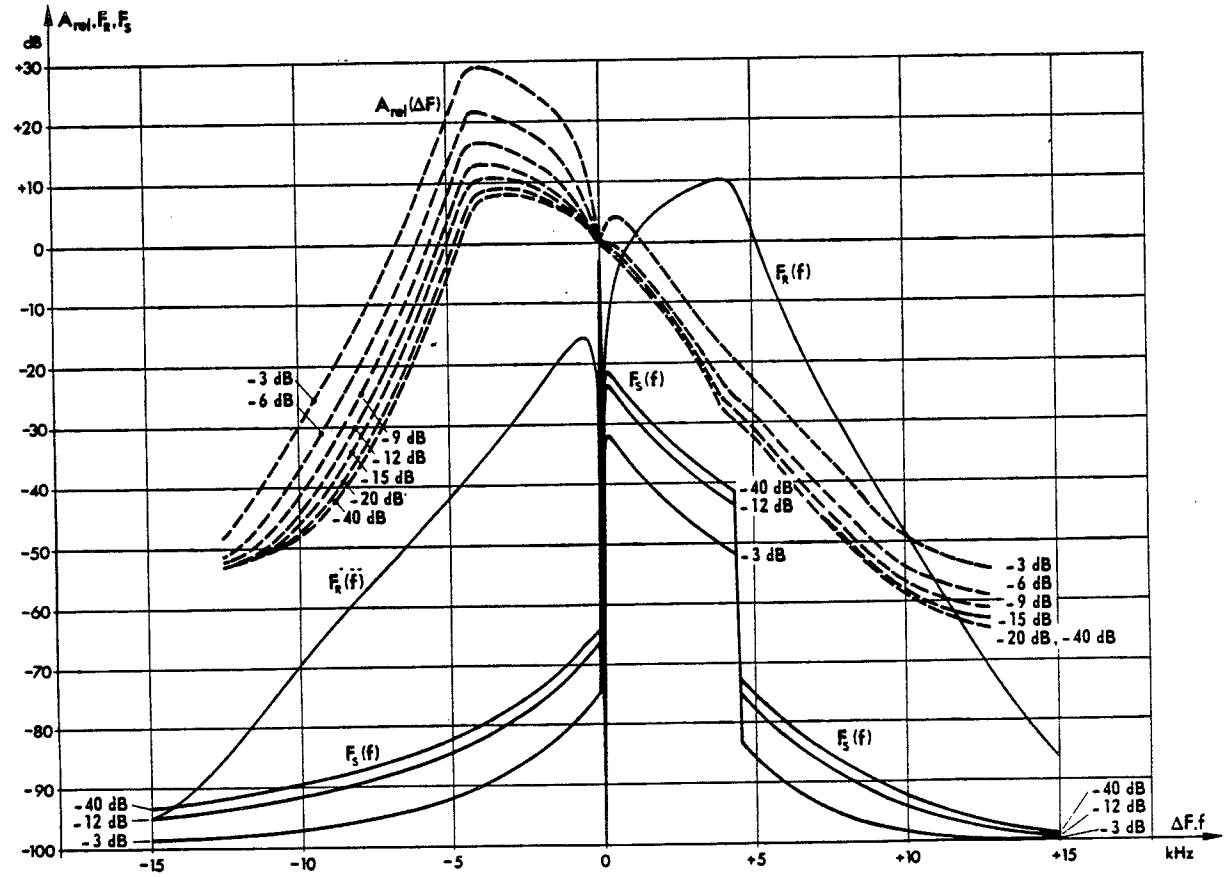

Fig. 16. — Influence of the carrier reduction.

Abscissa : relative frequency f or channel spacing ΔF (in kHz)
Ordinate : relative RF protection ratio A_{rel}; transmitter spectrum $F_S(f)$; weighted overall attenuation of the receiver $F_R(f)$ (in dB)
Parameter : carrier level T (in dB).

8.3. The influence of band-limitation with different slopes at the receiver

Fig. 15 depicts the dependence of the relative RF protection ratio on the slope of the band-limitation by the filters in the receiver with 4.5-kHz bandwidth, the other parameters remaining the same as in the preceding example. With a receiver bandwidth of 4.5 kHz and a channel spacing of 5 kHz, even with ideal band-limitation at the transmitter, an attenuation slope of the receiver filters of more than 60 dB/kHz would be necessary, in order to obtain an RF protection ratio against interference from the lower adjacent channel of —20 dB, a value which corresponds to favourable coverage in DSB sound-broadcasting networks [18]. A similarly steep slope would be required also, for example, when changing over from the DSB system in the MF band to SSB modulation by halving the channel spacing to 4.5 kHz and with a system bandwidth of 4 kHz, in order to obtain the value $A_{rel} = -20$ dB.

8.4. Influence of the carrier reduction

As would be expected, different degrees of carrier reduction have a more marked influence on the relative RF protection ratio, because if the transmitter peak envelope power is kept constant, any increase in the level of the residual carrier not only reduces the sideband power, but also increases the carrier interference, which is stronger in the lower adjacent channel and is directly proportional to the carrier level. A higher carrier level signifies a lower sideband power (see Sections 4.1 and 4.3). With $T = 3$ dB, for example, only about 30 % of the modulation range of the transmitter is available for the sidebands.

With the other parameters kept constant, the degree of the carrier reduction T was varied between 3 and 40 dB. The result is given in *Fig. 16*. As expected, the effect is more marked in the lower adjacent channel. For carrier levels below about —20 dB, there is only a negligible decrease in the relative RF protection ratio.

8.5. Influence of a notch filter

Notch filters in the AF amplifier of the receiver make possible the selective suppression of the interference with reception due to the carrier in the adjacent channel. On the basis of the present conditions in the HF bands, the effect of a notch filter having a centre frequency of 5 kHz and about 40 dB attenuation was examined in an assumed SSB system having the same bandwidth for the transmitter and for the receiver, $B_N = B_R = 4.5$ kHz, ideal band-limitation of the transmitter, and a slope attenuation $a_R = 15$ dB/kHz for the band-limiting filters of the receiver.

Fig. 17 shows that the notch filter has no influence on the relative RF protection ratio in the upper adjacent channel, because there the interference caused by the residual carrier is negligible compared with the interference caused by the sideband itself. In the lower adjacent channel, the relative RF protection ratio is improved selectively at $\Delta F = 5$ kHz by about 12 dB. The absolute value $A_{rel} = -7$ dB is, however, still very unfavourable for optimum network planning.

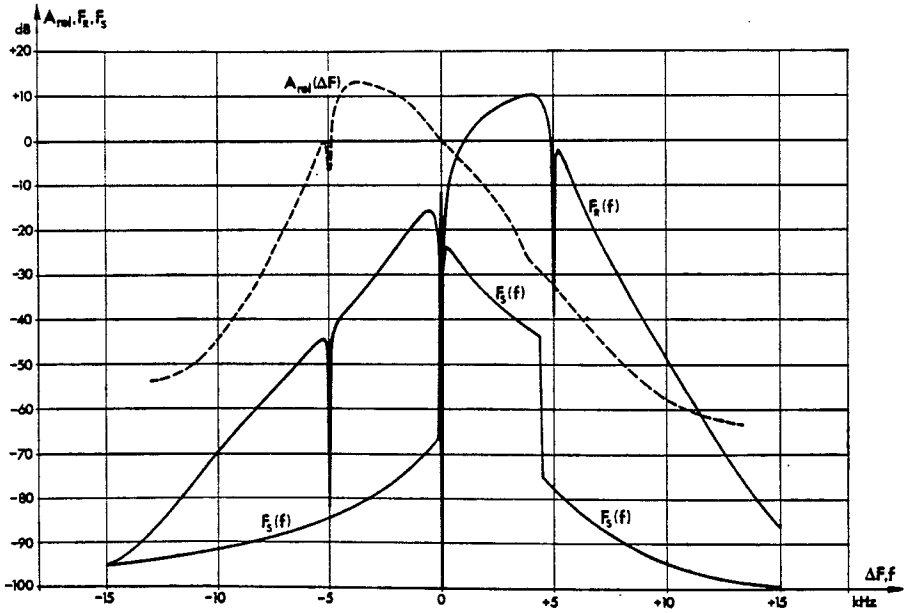

Fig. 17. — Influence of a notch filter.

Abscissa : relative frequency f or channel spacing ΔF (in kHz)

Ordinate : relative RF protection ratio A_{rel}; transmitter spectrum $F_N(f)$; weighted overall attenuation of the receiver $F_R(f)$ (in dB)

Resonant frequency of the notch filter : 5 kHz.

Magnification factor Q of the notch filter : 50.

L/C ratio of the notch filter : 2000.

Series resistance of the voltage-divider : 100 Ω.

9. Conclusions

The conclusion may be drawn from these results that the combination of parameters

$\Delta F = 5$ kHz	(channel spacing)
$B_N = B_R = 4.5$ kHz	(bandwidth)
$\alpha_S = \infty$	(maximum attenuation slope, transmitter)
$\alpha_R = 15$ dB/kHz	(maximum attenuation slope, receiver)
$T = 12$ dB	(carrier reduction)

despite the utilisation of a notch filter with a 40-dB attenuation in the lower adjacent channel, does not result in an adequate relative RF protection ratio. In order to retain the same attenuation slope of the receiver, the bandwidth would have to be reduced to about 3.5 kHz, or, if the bandwidth were retained, the attenuation slope would have to be increased to about 40-50 dB/kHz.

The greatly differing relative RF protection ratios in the upper and lower adjacent channels of an SSB system can probably also be taken into consideration when planning an optimum transmitter network. Appropriate planning methods have yet to be examined.

BIBLIOGRAPHICAL REFERENCES

[1] Gröschel, G.: *Ausserbandstrahlung und ihr Einfluss auf den Nachbarkanal beim AM Tonrundfunk* (Out-of-band radiation and its influence on the adjacent channel in AM sound broadcasting).
Nachrichtentechnische Fachberichte, Vol. 41, 1971, pp. 41-49.

[2] *Final Acts of the Regional Administrative LF/MF Broadcasting Conference (Regions 1 and 3), Geneva 1975.*
Published by the I.T.U., Geneva, 1976.

[3] *Sound broadcasting systems in bands 5 (LF), 6 (MF) and 7 (HF).*
C.C.I.R. Question 25/10, XIIIth Plenary Assembly, Geneva 1974, Vol. X, p. 239.

[4] Parreaux, D.: *A graphical method of determining protection ratios in the case of LF and MF amplitude-modulated transmissions.*
E.B.U. Review, No. 134, August 1972, pp. 163-167.

[5] Petke, G.: *Determination, by calculation, of the RF protection ratio for AM transmission systems.*
E.B.U. Review, No. 141, October 1973, pp. 216-223.

[6] *Amplitude modulation sound broadcasting. Objective two-signal methods for the determination of radio frequency protection ratios.*
C.C.I.R. Report 399-2, XIIIth Plenary Assembly, Geneva 1974, Vol. X, pp. 36-44.

[7] *Signal-to-interference ratios in amplitude-modulation sound broadcasting (Definitions).*
C.C.I.R. Recommendation 447, XIIIth Plenary Assembly, Geneva 1974, Vol. X, p. 21.

[8] *Amplitude-modulation sound broadcasting. Relative radio-frequency protection-ratio curves.*
C.C.I.R. Recommendation 449-2, XIIIth Plenary Assembly, Geneva 1974, Vol. X, pp. 22-24.

[9] *Power of radio transmitters.*
C.C.I.R. Report 531, XIIIth Plenary Assembly, Geneva 1974, Vol. I, pp. 336-337.

[10] Gröschel, G.: *The output power spectrum of an AM sound-broadcast transmitter modulated with a standard noise signal.*
E.B.U. Review, No. 123-A, October 1970, pp. 212-227.

[11] Wünsch, G.: *Theorie und Anwendung linearer Netzwerke. Teil II* (Theory and application of linear networks. Part II).
Akademische Verlagsgesellschaft Geest & Portig K.-G., Leipzig 1964.

[12] *Modulation processing techniques for AM sound broadcasting.*
E.B.U. document Tech. 3088, August 1971.

[13] *Spectra and bandwidths of emission.*
C.C.I.R. Recommendation 328-3, XIIIth Plenary Assembly, Geneva 1974, Vol. I, pp. 294-303.

[14] *Power of radio transmitters.*
C.C.I.R. Recommendation 326-2, XIIIth Plenary Assembly, Geneva 1974, Vol. I, pp. 270-287.

[15] *Measurement of audio-frequency noise in broadcasting, in sound-recording systems and on sound programme circuits.*
C.C.I.R. Recommendation 468-1, XIIIth Plenary Assembly, Geneva 1974, Vol. X, pp. 202-204.

[16] *Psophometers (Apparatus for the objective measurement of circuit noise).*
C.C.I.T.T. Recommendation P.53, Orange Book, Vol. V, 1977, pp. 63-66.

[17] Tüxen, O.: *Die Trennschärfe des Empfangsgleichrichters* (The selectivity of the reception detector).
Zeitschrift für technische Physik, No. 1, 1941, pp. 1-9.

[18] *Sound broadcasting in bands 5 (LF), 6 (MF) and 7 (HF). Factors limiting broadcasting coverage in band 6 (MF).*
C.C.I.R. Report 400-2, XIIIth Plenary Assembly, Geneva 1974, Vol. X, pp. 44-58.

Appendix E
Instructions for Operation of Program "ADJACENT"

Introduction

These instructions describe the operation of a computer program for the calculation of relative adjacent-channel protection ratio, A_{rel}.

Diskette description

The diskette is a double-density 5-1/4" 360 kb floppy. Protection ratio calculations require two BASIC programs, ADJACENT and ADJPRO. ADJACENT is a user-friendly data entry program; ADJACENT chains to ADJPRO, which is the program that does the calculations. Execution of the two programs may also generate other files.

The master diskette contains executable files (ADJACENT.EXE, ADJPRO.EXE) for both programs and contains three other related files (ADJPRO.DAT, NRSC.FSR, NRSC.OUT). The source code files (ADJACENT.BAS, ADJPRO.BAS) are available on a separate diskette from NAB upon request. Additional disk space is needed for program execution so the master diskette programs should be copied to a hard disk or separate floppy prior to use. The programs were compiled with Microsoft QuickBASIC v3.0 with coprocessor support and are designed to run on almost any PC-compatible computer.

Hardware requirements

A typically equipped PC with 256 kb or more is required. The program was designed to use the capabilities of the math coprocessor. The program contains emulation routines that will permit it to run without the coprocessor, but it will run extremely slowly (one run may take 30 minutes or more, compared to about 60 seconds with a coprocessor). A coprocessor-equipped machine is highly recommended.

A printer will provide a hard-copy of the output data, but the program will run without it (output data can be viewed on the screen). Plotting and graphics routines are not included as there is no standard plotting or graphics protocol for the PC.

Program setup

Users should familiarize themselves with the paper, "A mathematical model for the calculation of the adjacent-channel interference in single-sideband and double-sideband AM sound broadcasting systems," by G. Gröschel, published in the E.B.U. Review – Technical, June 1978. The computer program is modeled directly on the techniques described in the paper. During program setup, the user defines the subfunctions corresponding to each technical parameter that contributes to the overall transmitter and receiver response. These consist of:

- F0: the carrier (can be suppressed for single-sideband transmission)
- F1: spectral power density of the modulation signal
- F2: transmitter band limiting
- F3: transmitter preemphasis
- F4: transmitter out-of-band radiation
- F5: transmitter noise
- F6: receiver band limitation
- F7: psophometric curve
- F8: receiver deemphasis
- F9: receiver notch filter
- F10: receiver out-of-band selectivity.

In addition, the user specifies a "modulation factor," discussed in the Gröschel paper and below, which takes into account the depth of modulation and the amount of compression.

The program is run by typing "ADJACENT<ret>." The setup screen then appears; the help screen (press <F1>) explains how to use the setup screen. Once all fields are showing the correct information, typing "X" (no return) executes ADJPRO. Typing <Esc> exits the program. Typing either "X" or <Esc> will save the current setup screen data in the file ADJPRO.DAT.[1]

Following is a description of the fields in the setup screen:

Transmission mode. Select DSB/ISB (double sideband/independent sideband) or SSB (single sideband). Selection of mode automatically modifies the various subfunctions, and changes the setup screen, to match the mode requirements. This is discussed in detail below.

Type of study. Select SINGLE or SWEEP, and enter the difference frequency (dF) or difference frequency range and step size to be used. To obtain first- and second-adjacent-channel protection ratios, select SWEEP, with dF=10000 Hz to 20000 Hz every 10000 Hz.

FS/FR functions. Select COMPUTED, FROM DISK, or FROM KEYBOARD. Normal mode is COMPUTED, in which FS (the composite transmitter response) and FR (the composite receiver response) are calculated at the time of program execution from the transmitter and receiver subfunctions (F0 through F10) specified below. FROM DISK indicates that previously stored FS and FR values, if any, will be retrieved from disk. (The file name of the stored values will be requested at time of program execution.) FROM KEYBOARD permits FS and FR, from –25,000 Hz to +25,000 Hz in 100 Hz steps, to be manually entered. Use of FROM KEYBOARD is expected to be rare.

---

[1] As supplied on the master diskette, ADJPRO.DAT contains the settings for NRSC transmission and "Ideal" NRSC reception, as defined in Section V of the report.

Tabulate subfunctions. Select YES or NO. If YES, select frequency range from low to high. Selection of YES will print out FS, FR, and F0 through F10, at 100 Hz increments across the selected range.

Print FS/FR. Select YES or NO. Selection of YES will print out FS and FR from 0 Hz to ±25,000 Hz in 100 Hz increments.

Allow changes to FS/FR. Select YES or NO. Selection of YES will allow changes to FS and FR at any desired frequency to be manually entered from the keyboard. If FS/FR are COMPUTED, Print FS/FR is YES, and Allow changes to FS/FR is YES, then FS/FR will first be computed and printed for examination before the program asks for changes.

Save FS/FR to disk. Select YES or NO. Selection of YES will cause FS/FR values to be saved to a disk file for future use. At the time of execution, the program will ask for the filename to be used. FS/FR filenames will automatically be given the extension ".FSR".[2]

Modulation spectrum. Select USASI NOISE or CCIR NOISE. USASI noise has been recently used to characterize modern U.S. program material.

Modulation factor. Enter value from 0.01 to 2.00. An appropriate value for very highly compressed program material is 1.00. Modulation factor is related to "loudness." It affects the peak level of the sideband energy, A_m, but does not affect its shape, which is defined by F1, F2, and F3. While at first it might appear that the choice of modulation factor is critical, in fact it has a negligible effect on A_{rel}. Any overall change in sideband energy will indeed affect the adjacent-channel protection ratio, A, but its effect on the co-channel protection ratio, A_O, will be essentially equal. Since $A_{rel} = A - A_O$, A_{rel} will be affected little.[3]

TRANSMITTER DATA

Band limiting. Select LOW PASS, IDEAL, NRSC, or AK-5. If LOW PASS or IDEAL is selected, screen will also ask for filter parameters. Band limiting characteristic depends whether DSB/ISB or SSB transmission mode was selected. If SSB is selected, the screen will also prompt for carrier reduction and undesired sideband suppression. The filters have the following characteristics:

LOW PASS is an nth-order Butterworth filter of the selected attenuation rate and bandwidth. For DSB/ISB mode, the response is 3 dB down at ± the selected bandwidth, and attenuates at the specified rate above and below the passband. For SSB mode, the response has the same attenuation rate, but a lower 3 dB point of 0 Hz.

IDEAL is a filter with flat response within the selected bandwidth and, for DSB/ISB transmission, 100 dB attenuation at the ± cutoff frequencies and beyond. For SSB transmission, the filter is down by the selected amount of undesired sideband suppression from 0 Hz to the negative cutoff frequency, and is 100 dB down at that frequency and beyond.

NRSC is a 9th-order elliptic-function filter with a passband of ±9600 Hz (0.162 dB ripple) and a stopband of ±10,100 Hz (minimum attenuation 50 dB). NRSC is not available in SSB mode.

AK-5 is a 4500 Hz, 60 dB/octave filter characteristic used in Germany. It is not available in SSB mode.

Preemphasis. Select NONE, TC, or NRSC. If TC is selected, the screen will also prompt for time constant in microseconds.

Noise. Enter residual noise in dB below carrier. Typically assumed to be 100 dB down.

Out-of-band radiation. Select CCIR, NRSC MAX, or NRSC TEST. CCIR is the out-of-band radiation subfunction described in the Gröschel paper. If CCIR is selected, the screen will also prompt for intermodulation attenuation ("IM atten") in dB, which is typically assumed to be 30-40 dB. NRSC MAX and NRSC TEST are the maximum limits and test limits, respectively, of the emission limitation for AM broadcast transmission specified in NRSC Standard No. NRSC-2. This parameter has a significant effect on second-adjacent-channel protection ratios.

Carrier reduction. Only used with SSB transmission. Enter carrier reduction in dB below full carrier.

Undesired sideband suppression. Only used with SSB transmission. Used to specify undesired sideband suppression in ideal band limiting filter (see above).

RECEIVER DATA

Band limiting. Select LOW PASS, NRSC, or MBF. If LOW PASS is selected, the screen will also prompt for filter parameters. Band limiting characteristic depends whether DSB/ISB or SSB transmission mode was selected. The LOWPASS and NRSC filters are specified identically to those in the transmitter data. The MBF filter simulates an E.B.U. reference receiver. NRSC band limiting is not available in SSB mode.

Deemphasis. Select NONE, TC, or NRSC. If TC is selected, the screen will also prompt for time constant in microseconds.

Psophometric curve. Select CCIR–468 or CCITT–P53. CCIR–468 is most appropriate for medium-wave AM broadcasting. The psophometric curve represents the objectionability of sound as a function of frequency. It is needed in the calculations because, for adjacent-channel signals, the interfering frequencies are shifted by 10 kHz or 20 kHz

---

2 As supplied on the master diskette, NRSC.FSR contains FS for NRSC transmission and FR for "Ideal" NRSC reception.

3 This is true in the usual case where the adjacent-channel interference is dominated by the sideband energy, not by the carrier energy. If the carrier energy were the dominant contributor to adjacent-channel interference, a change in sideband energy would affect A_O and A_{rel}, not A.

and the energy contribution at each frequency must be properly weighted to correspond to the sensitivity of the ear.[4]

Out-of-band selectivity. Enter response in dB. Typically assumed to be 100 dB down.

Notch filter. Select NONE, IDEAL, or LC. If IDEAL or LC selected, the screen will prompt for resonant frequency Fr. IDEAL puts a 200 dB notch at exactly the selected frequency. If LC is selected, the screen will prompt for other LC notch filter parameters as described in the Gröschel paper.

Program execution

When all setup screen fields are as desired, pressing X will exit ADJACENT and execute ADJPRO. If FS/FR are to be retrieved from disk, the program will display all .FSR files and prompt for a selection. If FS/FR are to be input from the keyboard or changed, the program will prompt for the data. FS/FR will be printed if so specified. If FS/FR are to be saved to disk, the program will ask for a filename (extension .FSR will always be assigned).

When FS/FR calculations have been completed, the screen will display the following: a summary of input data; the three calculated Gröschel parameters of equivalent bandwidth Be, maximum power density Am, and out-of-band radiation factor Kr (if CCIR is selected); and a scrolling table of calculated protection ratios. If only a few frequency separations are being calculated, all input and output data will be simultaneously visible.

The program will ask whether output is to be printed, and then whether it is to be saved. Output can be saved in a user-specified filename and reviewed later at DOS level, using a TYPE command or other available file-examination utility.[5] After the two questions have been answered, the program returns to the ADJACENT setup screen for another run. If no other run is desired, type <Esc> to exit.

Output data

The program displays the relative adjacent-channel protection ratio Arel, and the contribution to Arel of the carrier (Atr) and the sidebands (Asb) of the adjacent-channel signal. Arel is a power summation of Atr and Asb. Users are encouraged to read the discussions in the Gröschel paper on interpretation of data and limitations of the numerical method. In particular, note that the relative adjacent-channel protection ratios calculated by the program are based on a determination of power. The numerical method does not take into account the additional 3 dB of co-channel noise suppression that results from coherent detection of the desired signal in the receiver. Therefore, values of A_{rel} calculated by the computer program must be corrected by –3 dB.

Program modification

Users with access to a QuickBASIC compiler are encouraged to modify the programs to meet their individual requirements, such as to include alternative subfunctions. Note that the program contains mathematical expressions that must be compiled on a coprocessor-equipped machine, using QuickBASIC with coprocessor support.

---

4 The psophometric curve is defined in equal 100 Hz increments, as are the other subfunctions. The program does not differentiate between a single tone and an equal-energy 100 Hz band of noise, even though the tone would be psychoacoustically more objectionable. Therefore, even though a protection ratio calculation may indicate that the interfering carrier does not contribute significant adjacent-channel interference, implying that a 10 kHz notch filter would make no audible improvement, a psychoacoustic test might show a notch filter to be effective.

5 As supplied on the master diskette, NRSC.OUT contains the output for calculations of A_{rel} at 10 kHz and 20 kHz under conditions of NRSC transmission and "Ideal" NRSC reception.

Appendix F

Anderson, H.R.: "Signal-to-Interference Ratio Statistics for AM Broadcast Groundwave and Skywave Signals in the Presence of Multiple Skywave Interferers."

SIGNAL-TO-INTERFERENCE RATIO STATISTICS FOR AM BROADCAST GROUNDWAVE AND SKYWAVE SIGNALS IN THE PRESENCE OF MULTIPLE SKYWAVE INTERFERERS

HARRY R. ANDERSON, P.E.
H.R. ANDERSON & ASSOCIATES, INC.
CONSULTING ENGINEERS
P.O. BOX 1547
EUGENE, OREGON 97440
(503) 687-0414

Abstract - **The development of a statistical description of the signal-to-interference ratio (SIR) for AM broadcast groundwave and skywave signals in the presence of multiple skywave interference signals is presented. The analysis assumes that the interfering signal envelope amplitudes are Rayleigh-distributed random variables with a lognormal distribution used to describe the long-term variations of the sum envelope amplitude. The resulting statistical description is used to evaluate the SIR degradation for a number of "interference exclusion" formulas under consideration for frequency allocation purposes.**

1.0 INTRODUCTION

Describing the statistics of the signal-to-interference ratio (SIR) of AM broadcast groundwave signals in the presence of multiple skywave interfering signals is important to understanding the reception and coverage possibilities of an AM broadcast station. Previously, the SIR has been calculated assuming the skywave fields were static; that is, not varying with time. With a constant desired groundwave signal amplitude, the resulting SIR was also a constant quantity.

It is the intent of this paper to consider the statistical variations of the combined skywave signals and to develop a statistical description of the SIR. This description is in the form of a probability density function (pdf) and associated cumulative distribution function (cdf). The cdf can be directly used to determine the percent time for which a given SIR is exceeded.

Following the analysis for a constant amplitude desired groundwave signal, the method will be extended for the case when the desired signal is a time-varying skywave signal.

2.0 SKYWAVE SIGNAL AMPLITUDE STATISTICS

AM broadcast skywave signals propagate primarily during nighttime hours by means of electromagnetic energy radiated from the transmitting antenna reflecting off the ionosphere and returning to earth at some distance from the transmitting antenna. AM broadcast signals reflect off both the E layer of the ionosphere at about 100 km above the earth and from the F layer at about 220 km above the earth. In North America, the dominant skywave propagation mechanism is via the E layer with an average altitude taken to be 100 km [1].

The amplitude of a skywave signal as received on earth varies primarily due to two mechanisms - the changing altitude and charged particle density in the reflecting layer and the fact that the skywave signal as received is actually the composite sum of several signals reflecting from different parts of the reflecting layer. The amplitude of each constituent part of the signal varies in amplitude and phase due to the changing layer characteristics. It can be shown [2] that with as few as six such reflecting signals, the amplitude variation of the sum is a gaussian-distributed random variable while the phase (relative to some arbitrary fixed reference) is a uniformly-distributed random variable.

For a signal with a gaussian-distributed total amplitude, the probability distribution of the envelope of that signal is Rayleigh-distributed. As the signal amplitude varies, the received signal appears to "fade" in and out, being louder and less noisy at times and weaker and more noisy at other times. Since the amplitude variation is Rayleigh-distributed, the term "Rayleigh-fading" has been used to describe this effect. The nature of the amplitude distribution of the skywave signal has been confirmed by measurements [3].

The pdf for the random variable v with a Rayleigh distribution is given by

$$p_V(v) = \frac{v}{\sigma^2} \exp\left[\frac{-v^2}{2\sigma^2}\right] \qquad (1)$$

The corresponding cdf is given by

$$P_V(v) = 1 - \exp\left[\frac{-v^2}{2\sigma^2}\right] \qquad (2)$$

The voltage amplitude which is exceeded 50 percent of the time (median) can be readily found by integrating the pdf as follows:

$$0.5 = \int_v^\infty p_V(v)\,dv = \exp\left[\frac{-v^2}{2\sigma^2}\right] \tag{3}$$

which yields a median value of 1.177σ. Similarly, the voltage exceeded 10 percent of the time is:

$$0.1 = \int_v^\infty p_V(v)\,dv \tag{4}$$

This gives a 10 percent time voltage of 2.146σ.

From this it is apparent that the voltage exceeded 10 percent of the time for a Rayleigh distribution is always about 5.2 dB higher than the median voltage. If the 10 percent time voltage is known or calculated using propagation curves, it can be used to find σ and thereby fully describe the distribution.

While measurements show that the short term (within an hour) variations in the signal envelope amplitude are Rayleigh-distributed, measurements taken over a longer period of time (from days to months) show a statistical variation in the median received field strength which is more closely described by a lognormal distribution [3,4].

The lognormal pdf is given by

$$p_V(v) = \frac{1}{v\sqrt{2\pi\sigma^2}} \exp\left[\frac{-(\ln v - a)^2}{2\sigma^2}\right] \tag{5}$$

where a is the mean value. The lognormal cdf is given by

$$P_V(v) = \frac{1}{2}\left[1 + \mathrm{erf}\left(\frac{(\ln v - a)}{\sigma\sqrt{2}}\right)\right] \tag{6}$$

where erf is the error function.

As shown above, the 10 percent time voltage for the Rayleigh distribution is only 5.2 dB above the median value. However, it is common in currently employed skywave field strength prediction methods to set the 10 percent time value at 8 dB [5] or 10 dB [1] above the median value, indicating that the lognormal distribution is the appropriate choice to describe the long term variations in the skywave signal strength.

3.0 COMPUTATION OF THE COMPOSITE INTERFERENCE PDF

In most situations, the total skywave interference at a given point in a station's coverage area is the sum of several co-channel interfering signals arriving from different stations with different power levels and transmitting antenna characteristics. Typically, the interfering signal from each is computed using the 10 percent time amplitude FCC propagation curves, and taking into account the interfering station's radiated power and antenna radiation characteristics at the appropriate vertical departure angle which results in an ionospheric reflection at the given point in the desired station's coverage area.

The total power in the composite interfering signal is the sum of the power of the contributing interfering signals. This power is given by the envelope voltage squared divided by the receiver input impedance. As shown above, for each interferer the 10 percent voltage can be used to find σ^2 which is then an indication of the power contributed by that interferer.

The problem of adding up the interfering signals can be easily solved by recognizing that each interfering envelope voltage can be resolved into quadrature voltage components, each of which is a gaussian random variable (r.v.). The gaussian quadrature components of all the interferers can then be added to yield a composite gaussian r.v. with σ^2 of the sum equal to the sum of the constituent σ^2 from each interferer and with a mean value equal to the sum of the mean values. If $N(a, \sigma^2)$ is used to indicate a normal or gaussian-distributed r.v., then the distribution of the sum of any M gaussian r.v.'s is given by:

$$N\left[\sum_{m=1}^{M} a_m\,,\ \sum_{m=1}^{M} \sigma_m^2\right] \tag{7}$$

Since all of the skywave signals have zero mean values (i.e., no d.c. component), the sum of the mean values a_m in (7) is zero.

Each of the individual σ_m^2 can be found from the predicted 10 percent time voltage as described above. By summing the σ^2 for both quadrature components, the quadrature components can then be used to find the Rayleigh distribution of the composite envelope voltage with

$$\sigma_T^2 = \sum_{m=1}^{M} \sigma_m^2 \tag{8}$$

This composite σ_T^2 can now be used to find the median value of the Rayleigh distribution which describes the total interference; that is, median $= 1.177\sigma_T$. This median value is then used for a in the lognormal distribution pdf equation given in (5). The standard deviation of the lognormal distribution as indicated by σ in (5) can be set to correspond to 8 or 10 dB as found in [5] or [1]. For FCC purposes, the upper decile value is 8 dB above the median, which corresponds to $\sigma = .72$ in equation (5).

The value of σ in the lognormal distribution given above produces the appropriate distribution when the voltage levels are around 1 mV/m or less. At higher voltage levels, the distribution is somewhat skewed.

It is recognized that this transition from the Rayleigh distribution to the lognormal distribution is a simplified, ad hoc approach. This ad hoc approach is not incorrect,

however, because the empirical data on skywave amplitudes generally falls between a Rayleigh distribution and a lognormal distribution. In other words, the distribution of amplitudes cannot be strictly characterized as Rayleigh or lognormal using some statistical-physical model of the ionospheric reflection mechanism. The distributions are approximate, empirical models which represent a reasonable match to the data. However, a more refined analysis of the interdependence of the two distributions can be done. This analysis is presented in the next section.

4.0 CONDITIONAL DISTRIBUTION OF RAYLEIGH SKYWAVE SIGNAL AMPLITUDES

In [4], the skywave amplitude is described as being Rayleigh-distributed over short periods (hours) with the median hourly value of this Rayleigh distribution itself a random variable (over long periods) with a lognormal distribution. The envelope voltage at any time, then, is a conditional Rayleigh probability density function which depends on lognormally-distributed median values.

If $p_V(v)$ represents the pdf over all time, then $p_V(v|z)$ represents the conditional pdf with median value z where z is a lognormally-distributed r.v. For a Rayleigh-distributed r.v., the median is proportional to the standard deviation ($z = 1.177\sigma$), so that one can write

$$p_V(v|z) = \frac{v}{(z/1.177)^2} \exp\left[\frac{-v^2}{2(z/1.177)^2}\right] \tag{9}$$

Our objective is the unconditional pdf $p_V(v)$ which is given by

$$p_V(v) = \int_0^\infty p_V(v|z)\, p_Z(z)\, dz \tag{10}$$

where $p_Z(z)$ is a lognormal pdf. Substituting the appropriate pdf's into (10) yields

$$p_V(v) = \int_0^\infty \frac{v}{(z/1.177)^2} \exp\left[\frac{-v^2}{2(z/1.177)^2}\right] \frac{1}{\sqrt{2\pi\sigma^2}} \exp\left[\frac{-(\ln z - a)^2}{2\sigma^2}\right] dz \tag{11}$$

Rearranging terms results in

$$p_V(v) = \int_0^\infty \frac{1.385v^2}{z^3\sqrt{2\pi\sigma^2}} \exp\left[\frac{-v^2}{2(z/1.177)^2} + \frac{-(\ln z - a)^2}{2\sigma^2}\right] dz \tag{12}$$

This somewhat cumbersome integral can be solved numerically to find the unconditional pdf for v over all time. The mean value of the lognormal distribution given by a in (12) would be found from the average of the hourly median values over a long period of time. As before, the value of σ can be chosen so that the voltage exceeded 10 percent of the time approximately matches the data.

5.0 COMPUTATION OF THE PDF FOR THE SIGNAL-TO-INTERFERENCE RATIO

The pdf for the SIR can be found by first converting the lognormal pdf from (5) in volts to a pdf in dBmW and doing the corresponding process for the desired signal amplitude in volts. The pdf of the SIR in dB is then found by subtracting the interference pdf in dBmW from the signal pdf in dBmW.

The signal amplitude in dBmW and the interference amplitude in dBmW are both random variables so that the SIR is also a random variable. The pdf of the sum (or difference) of two r.v.'s is given by the convolution of the pdf's, as follows:

$$p_Z(z) = p_X(x) * p_Y(-y) \tag{13}$$

For this case, z represents the SIR, x represents the desired signal level in dBmW, and y represents the interference level in dBmW.

The process of converting the envelope voltage pdf in volts (or mV/m) to dBmW across 1 ohm starts with the relationship:

$$S = 20\log(\text{mV}) - 30 \qquad \text{dBmW} \tag{14}$$

where S is power and mV is the voltage in millivolts. If the relationship between two quantities is known, the pdf for one can be found in terms of the pdf for the other using the following relationship:

$$p_S(s) = p_V(v)\left|\frac{dv}{ds}\right| \tag{15}$$

Starting with (14) and performing the operations indicated by (15), the resulting pdf for the power s in dBmW is

$$p_S(s) = p_V\left(10^{((s+30)/10)}\right)\, 10^{((s+30)/10)}\, \frac{\ln 10}{20} \tag{16}$$

The pdf for $p_V(v)$ is given by (5). To find $p_S(s)$, it is a matter of substituting the argument

$$10^{((s+30)/10)}$$

into equation (5) for v, and multiplying in the other components of (16), to arrive at the final equation for the pdf of s in dBmW.

The convolution in (13) can now be performed. Since this analysis was implemented on a computer, the convolution was done by a numerical method which is somewhat more efficient than the straight multiplication and summation approach. The technique goes as follows:

1. Take the Fast Fourier Transform (FFT) of each pdf

2. Multiply the two FFT's together

3. Take the inverse FFT of the result from step 2.

Since FFT's can be done very rapidly, this approach to a convolution is much faster than the straight multiplying method.

The convolution in (13) was performed using a constant desired signal amplitude of 1.0 mV/m (-30 dBmW across 1 ohm) and several different combinations of interfering signal amplitudes corresponding to various interference "exclusion" principles currently under consideration for frequency allocation purposes. Note that the pdf of the constant amplitude desired signal is simply a delta function at the signal level -30 dBmW.

Tables 1 through 5 show tabulations of various percent-time points for which the SIR is exceeded for the cases which were studied. The results show that for the addition of one interferer at the 50% exclusion level (that is; it would not be permitted if its amplitude were greater than 50% of the first interferer), that the SIR at the 50% time point is degraded by about 1 dB. This is found by comparing the 50% percent time points in Tables 1 and 2. For the 25% exclusion case, the degradation in SIR is about 0.27 dB (compare Tables 1 and 3). Similarly, for the four additional interferers and 50% exclusion, the SIR is degraded about 3 dB from the 1 interferer case. For 25% exclusion, the SIR is degraded by about 1 dB.

6.0 COMPUTATION OF THE PDF FOR THE SIR FOR A TIME-VARYING DESIRED SIGNAL

If the constant amplitude desired groundwave signal represented by x in (13) is replaced with a time-varying skywave signal (such as the 50% time secondary skywave service of Class I-A stations in the United States) the analysis in the last section can be repeated and a new set of SIR statistics produced for such skywave coverage areas. The lognormal pdf for the desired signal is established using the 50% time (median) value and the same σ value used before to set the upper decile point at 8 dB above the median. Convolving the resulting desired signal pdf in dBmW with the combined interference pdf in dBmW yields the SIR pdf.

The results of this process are shown in Tables 6 through 10. The tables show that the 50% time degradation in SIR is about what it was for the constant amplitude case. However, the standard deviation of the SIR is much greater owing to the spread in the desired signal amplitude. The 90% time point for the single interferer case (Table 6) is about 11 dB below the median value. The relative differences in the SIR statistics between the 50% exclusion and 25% exclusion cases are the same as for the constant amplitude desired signal case discussed in Section 5.0.

7.0 IMPACT ON SIR OF MULTIPLE INTERFERERS VERSUS A SINGLE INTERFERER

For frequency allocation purposes in the United States, it is common to use the root of the sum of the squares (RSS) of the amplitudes of multiple interferers to arrive at an indication of the signal-to-interference ratio. Currently, this RSS calculation is done using the 10 percent time signal amplitudes for each of the interferers as given by the appropriate propagation curve. This procedure suggests to some that a "worst case" assumption has been made that the 10 percent time signal level from each interferer is continuously present rather than present or exceeded only 10 percent of the time.

It is easy to show that the probability of multiple independent interferers all exceeding their 10 percent levels simultaneously at any given time is much smaller than 10 percent. However, only considering whether or not a 10 percent threshold is exceeded provides a very incomplete description of the sum voltage of multiple interferers since the contributing voltages involved are continuous, rather than discrete, random variables. To find the complete statistical description of the sum voltage, an approach like that taken in Section 3.0 of this paper must be used where the continuous statistical voltage variation of the constituent interferers is explicitly taken into account.

Consider the case of N interferers where the rms voltage of the i^{th} interferer is given by $\sqrt{2}\sigma_i$. From Section 2.0, for a Rayleigh distribution the 10 percent time voltage is $2.146\sigma_i$. The RSS of the 10 percent time voltages of this set of N interferers is then

$$\text{RSS} = \sqrt{\sum_{i=1}^{N} (2.146\sigma_i)^2} \tag{17}$$

$$\text{RSS} = \sqrt{4.605 \sum_{i=1}^{N} \sigma_i^2} \tag{18}$$

Now consider a single interferer with an rms voltage $\sqrt{2}\sigma_0$ and with a power level equal to the sum of the powers of the N individual interferers. The total power for the sum of the N interferers is the sum of the individual powers. The individual power for each (across 1 ohm) is given by the rms voltage squared, or $2\sigma_i^2$. The sum of these powers is then

$$\text{Total power} = P_T = \sum_{i=1}^{N} 2\sigma_i^2 \tag{19}$$

The equivalent single interferer will have a power equal to P_T. The power of this single interferer across 1 ohm is also equal to its rms voltage squared, or $2\sigma_0^2$.

TABLE 1

Constant desired signal amplitude: 1.00 mV/m

10% time amplitude of interferer 1: 0.0500 mV/m

Percent Time	Signal-to-Interference Ratio Exceeded:
90 %	26.11 dB
80	28.86
70	30.84
60	32.54
50	34.12
40	35.70
30	37.40
20	39.38
10	42.13

TABLE 2

Constant desired signal amplitude: 1.00 mV/m

10% time amplitude of interferer 1: 0.0500 mV/m
10% time amplitude of interferer 2: 0.0250 mV/m

Percent Time	Signal-to-Interference Ratio Exceeded:
90 %	25.09 dB
80	27.85
70	29.83
60	31.52
50	33.11
40	34.69
30	36.39
20	38.37
10	41.12

TABLE 3

Constant desired signal amplitude: 1.00 mV/m

10% time amplitude of interferer 1: 0.0500 mV/m
10% time amplitude of interferer 2: 0.0125 mV/m

Percent Time	Signal-to-Interference Ratio Exceeded:
90 %	25.83 dB
80	28.58
70	30.57
60	32.26
50	33.85
40	35.43
30	37.12
20	39.11
10	41.86

TABLE 4

Constant desired signal amplitude: 1.00 mV/m

10% time amplitude of interferer 1: 0.0500 mV/m
10% time amplitude of interferer 2: 0.0250 mV/m
10% time amplitude of interferer 3: 0.0250 mV/m
10% time amplitude of interferer 4: 0.0250 mV/m
10% time amplitude of interferer 5: 0.0250 mV/m

Percent Time	Signal-to-Interference Ratio Exceeded:
90 %	22.96 dB
80	25.71
70	27.69
60	29.39
50	30.97
40	32.55
30	34.25
20	36.23
10	38.98

TABLE 5

Constant desired signal amplitude: 1.00 mV/m

10% time amplitude of interferer 1: 0.0500 mV/m
10% time amplitude of interferer 2: 0.0125 mV/m
10% time amplitude of interferer 3: 0.0125 mV/m
10% time amplitude of interferer 4: 0.0125 mV/m
10% time amplitude of interferer 5: 0.0125 mV/m

Percent Time	Signal-to-Interference Ratio Exceeded:
90 %	25.09 dB
80	27.85
70	29.83
60	31.52
50	33.11
40	34.69
30	36.39
20	38.37
10	41.12

TABLE 6

50% time desired signal amplitude: 1.00 mV/m

10% time amplitude of interferer 1: 0.0500 mV/m

Percent Time	Signal-to-Interference Ratio Exceeded:
90 %	22.79 dB
80	26.68
70	29.49
60	31.88
50	34.12
40	36.36
30	38.76
20	41.56
10	45.45

TABLE 7

50% time desired signal amplitude: 1.00 mV/m

10% time amplitude of interferer 1: 0.0500 mV/m
10% time amplitude of interferer 2: 0.0250 mV/m

Percent Time	Signal-to-Interference Ratio Exceeded:
90 %	21.78 dB
80	25.67
70	28.47
60	30.87
50	33.11
40	35.35
30	37.74
20	40.55
10	44.44

TABLE 8

50% time desired signal amplitude: 1.00 mV/m

10% time amplitude of interferer 1: 0.0500 mV/m
10% time amplitude of interferer 2: 0.0125 mV/m

Percent Time	Signal-to-Interference Ratio Exceeded:
90 %	22.52 dB
80	26.41
70	29.21
60	31.61
50	33.85
40	36.09
30	38.48
20	41.29
10	45.17

TABLE 9

50% time desired signal amplitude: 1.00 mV/m

10% time amplitude of interferer 1: 0.0500 mV/m
10% time amplitude of interferer 2: 0.0250 mV/m
10% time amplitude of interferer 3: 0.0250 mV/m
10% time amplitude of interferer 4: 0.0250 mV/m
10% time amplitude of interferer 5: 0.0250 mV/m

Percent Time	Signal-to-Interference Ratio Exceeded:
90 %	19.64 dB
80	23.53
70	26.33
60	28.73
50	30.97
40	33.21
30	35.61
20	38.41
10	42.30

TABLE 10

50% time desired signal amplitude: 1.00 mV/m

10% time amplitude of interferer 1: 0.0500 mV/m
10% time amplitude of interferer 2: 0.0125 mV/m
10% time amplitude of interferer 3: 0.0125 mV/m
10% time amplitude of interferer 4: 0.0125 mV/m
10% time amplitude of interferer 5: 0.0125 mV/m

Percent Time	Signal-to-Interference Ratio Exceeded:
90 %	21.78 dB
80	25.67
70	28.47
60	30.87
50	33.11
40	35.35
30	37.74
20	40.55
10	44.44

$$2\sigma_0^2 = \sum_{i=1}^{N} 2\sigma_i^2 \tag{20}$$

The 2's cancel so

$$\sigma_0 = \sqrt{\sum_{i=1}^{N} \sigma_i^2} \tag{21}$$

The 10 percent time voltage for this single interferer is $2.146\sigma_0$ or

$$\text{10 percent time voltage} = 2.146 \sqrt{\sum_{i=1}^{N} \sigma_i^2} \tag{22}$$

The RSS of the 10 percent time voltage of this single interferer is just

$$\text{RSS} = \sqrt{\sum_{k=1}^{1} \left(2.146 \sqrt{\sum_{i=1}^{N} \sigma_i^2} \right)^2} \tag{23}$$

$$\text{RSS} = \sqrt{4.605 \sum_{i=1}^{N} \sigma_i^2} \tag{24}$$

Since the RSS value for the single interferer equals the RSS value for the sum (equation (18)), the variances are also the same and the Rayleigh distribution of the single interferer is the same as the Rayleigh distribution of the sum of the multiple interferers. It is clear, then, that regardless of the number or amplitude of the multiple interferers, the effect of the sum of interferers on the SIR is the same as the effect of a single interferer with equivalent power.

It should be noted that this analysis applies only to the ratio of the desired signal power to the total undesired signal power. It does not deal with the psychoacoustical effects, or listenability, of a single interferer versus multiple interferers. One might intuitively argue that a single interferer will more drastically degrade listenability than multiple interferers (though the SIR is the same), because the single loud interferer will cause more distraction from the desired program than will a "babble" of lower level interferers. Listenability tests of various interference circumstances will ultimately be needed to resolve this issue.

Since a Rayleigh distribution with $\sigma = \sigma_0$ provides a complete description of the statistical characteristics of the sum of N interferers, it is now possible to return to the earlier question of the probability that the sum voltage will be equal to or above some combination of 10 percent time voltage levels from the individual interferers. For example, assume that $N = 8$ and that each of the eight interferers has a 10 percent time amplitude of 2.146σ. The probability that the sum voltage will be, for instance, four times the 10 percent time voltage of one interferer is

$$\text{Probability} = \int_{4\times 2.146\sigma}^{\infty} \frac{v}{\sigma_0} \exp\left[\frac{-v^2}{2\sigma_0^2}\right] dv \tag{25}$$

From equation (21), and with $N = 8$, we have

$$\sigma_0 = \sqrt{\sum_{i=1}^{N} \sigma_i^2} = 2.828\sigma \tag{26}$$

Putting this value of σ_0 into (25) and performing the integration (from (3))

$$\text{Probability} = \exp\left[\frac{-(8.584\sigma)^2}{2(2.828\sigma)^2}\right] \tag{27}$$

This results in a probability of 0.009998 that the sum voltage will exceed 4 times the 10 percent time voltage of a single interferer.

For this case, the ratio of the 10 percent time voltage of the sum to the 10 percent time voltage of one of the eight constituent interferers (with all the σ_i's the same) is

$$\frac{2.146\sqrt{\sum_{i=1}^{N} \sigma_i^2}}{2.146\sigma_i} = \sqrt{N} = 2.828 \tag{28}$$

8.0 CONCLUSIONS

The foregoing analysis used statistical descriptions for the amplitude of a desired AM broadcast groundwave signal and multiple interfering skywave signals to develop a statistical description of the desired signal-to-interference ratio. The resulting probability density function was used to evaluate the percentage of time SIR's are exceeded with a variety of interfering signal combinations. The results show that adding four equal interferers, each at a level equal to 50% of a first interferer, degrades the 50% time SIR by a little more than 3 dB. If the four added interferers are all set at a level equal to 25% of the first interferer, the 50% time SIR is degraded by only 1 dB.

A similar analysis was conducted using a time-varying desired signal with a lognormal amplitude distribution. The results show that the spread of the SIR distribution increases so that the 90% time point is about 11 dB below the 50% time point. However, the relative changes in the SIR statistics between the various combinations of interference cases is the same as for the study with a constant amplitude desired signal.

A comparison of the impact on the SIR of multiple interferers with the impact on the SIR of a single interferer of equivalent power shows that the effect was the same in both cases.

9.0 REFERENCES

[1] CCIR, Geneva (1979). Report of IWP 6/4, "Sky-wave Field Strength Prediction Method for the Frequency Range 520 to 1600 kHz in Region 2."

[2] M. Schwartz, W.R. Bennett, and S. Stein. Communication Systems and Techniques. New York: McGraw-Hill Book Company, 1968, pp. 348-349.

[3] op. cit., M. Schwartz et al. pp. 381-382.

[4] CCIR, Dubrovnik (1986). Report 322-3 (draft), "Characteristics and Applications of Atmospheric Radio Noise Data."

[5] Federal Communications Commission, Rules and Regulations. Part 73.190(b)(2). October, 1986. (CFR 47 73.190(b)(2)).

ACKNOWLEDGEMENT

The work described in this paper was funded by the National Association of Broadcasters through a contract with Hammett & Edison, Inc., Consulting Engineers, of San Francisco, California.

Appendix G
Instructions for Operation of Program "SKYIN"

Introduction

These instructions describe the operation of a computer program to calculate signal-to-interference ratio statistics for AM broadcast groundwave and skywave signals in the presence of multiple skywave interferers.

Diskette description

The diskette is a double-density 5-1/4" 360 kb floppy. The master diskette contains the executable file SKYIN.EXE. The source code file SKYIN.FOR is available on a separate diskette from NAB upon request. The program may be copied, such as to a hard disk, but no additional disk space is necessary for program execution. The program was compiled with Microsoft FORTRAN v4.01 and is designed to run on almost any PC-compatible computer.

Hardware requirements

A typically equipped PC with 256 kb or more is required. The program was designed to use the capabilities of the math coprocessor. The program contains emulation routines that will permit it to run without the coprocessor, but it will run more slowly. A coprocessor-equipped machine is recommended.

All output data appears on the screen. Neither a printer nor graphics capability is required.

Program description

Users should familiarize themselves with the paper, "Signal-to-Interference Ratio Statistics for AM Broadcast Groundwave and Skywave Signals in the Presence of Multiple Skywave Interferers," by H. Anderson, which is Appendix F of this report. The paper describes the calculations made by the program and gives several examples.

Program execution

The program is run by typing "SKYIN<ret>". After a title screen appears, the user is asked to select a constant amplitude or lognormal-fading desired signal and to enter its amplitude. If a lognormal-fading signal is selected, there will be a delay while the computer calculates its probability density function (pdf).

The user is then asked for the number of interferers (up to 10) and their amplitudes, and the computer begins its calculations. When the calculation is complete, a results screen will be displayed which tabulates all of the input data and the signal-to-interference ratio exceeded from 10% to 90% of the time in steps of 10%. Results can be printed using the "PrtSc" keyboard command. The user can then select another run or exit from the program.

NRSC Document Improvement Proposal

If in the review or use of this document a potential change appears needed for safety, health or technical reasons, please fill in the appropriate information below and email, mail or fax to:

National Radio Systems Committee
c/o Consumer Electronics Association
Technology & Standards Department
1919 S. Eads St.
Arlington, VA 22202
FAX: 703-907-4190
Email: standards@ce.org

DOCUMENT NO.	DOCUMENT TITLE:
SUBMITTER'S NAME: COMPANY:	TEL: FAX: EMAIL:
ADDRESS:	
URGENCY OF CHANGE: _____ Immediate _____ At next revision	
PROBLEM AREA (ATTACH ADDITIONAL SHEETS IF NECESSARY): a. Clause Number and/or Drawing: b. Recommended Changes: c. Reason/Rationale for Recommendation:	
ADDITIONAL REMARKS:	
SIGNATURE:	DATE:

FOR NRSC USE ONLY

Date forwarded to NAB S&T: _____
Responsible Committee: _____
Co-chairmen: _____
Date forwarded to co-chairmen: _____


CEA
Consumer Electronics Association


NAB
NATIONAL ASSOCIATION OF BROADCASTERS